

N73-20615

NAS9-12392

NASA CR-128887

C.2

**DEVELOPMENT OF DESIGN ALLOWABLES DATA
FOR ADHESIVES FOR
ATTACHING REUSABLE SURFACE INSULATION**

**CASE FILE
COPY**

FINAL TECHNICAL REPORT

October 1972

~~FOR U.S. GOVERNMENT AGENCIES AND THEIR CONTRACTORS ONLY~~

Prepared Under Contract No. NAS 9-12392

GENERAL DYNAMICS
Convair Aerospace Division
Fort Worth, Texas

for

NATIONAL AERONAUTICS AND SPACE ADMINISTRATION

MANNED SPACECRAFT CENTER
Houston, Texas

Page Intentionally Left Blank

DEVELOPMENT OF DESIGN ALLOWABLES DATA
FOR ADHESIVES FOR ATTACHING
REUSABLE SURFACE INSULATION

H. P. Owen
M. T. Carroll
Convair Aerospace Division of General Dynamics
Fort Worth Operation

FINAL TECHNICAL REPORT

CONTRACT NO. NAS9-12392

October 1972

NATIONAL AERONAUTICS AND SPACE ADMINISTRATION
MANNED SPACECRAFT CENTER
HOUSTON, TEXAS

F O R E W O R D

This final report was prepared by General Dynamics' Convair Aerospace Division at Fort Worth for National Aeronautics and Space Administration, Manned Spacecraft Center (NASA, MSC) under contract NAS9-12392 including CCA No. 1, "Development of Design Allowables Data for Adhesives for Attaching Reusable Surface Insulation." Work reported herein was performed under the direction of the Materials Technology Branch of the Structures and Mechanics Division with I. K. Spiker as the Contracting Officer's technical monitor. Development work reported herein was conducted between 17 January 1972 and 30 September 1972.

The authors wish to acknowledge the contributions of the following individuals who were directly responsible for performing the program tasks and preparing this final report: J. E. Halkias, E. W. Turns, J. D. Reynolds, and H. J. Weltman (Engineering Test Laboratories), R. V. Wolff and M. S. Howeth (Structures and Materials) and E. W. Gomez (Stress Analysis).

T A B L E O F C O N T E N T S

<u>Section</u>		<u>Page</u>
1	INTRODUCTION AND SUMMARY	1
2	TEST MATERIALS AND METHODS	5
	2.1 Specified Adhesives	6
	2.2 Selection of Adherends and Primers	6
	2.2.1 Adherends (Substrates)	11
	2.2.2 Primers	12
	2.3 Processing	13
	2.3.1 Mixing and Handling Character- istics	13
	2.3.2 Uniformity of Lots	15
	2.4 Vendor Quality Control Certificates	16
	2.4.1 Selection of RTV Silicone for Modification	16
	2.4.2 Selection of Microballoon Fillers	16
	2.4.3 Selection of Closed-Cell Silicone Rubber Sponge	18
3	DEVELOPMENT OF REDUCED MODULUS AND LOWER DENSITY ADHESIVE SYSTEM	19
	3.1 Modification of Dow Corning's 77-137 RTV Silicone Material	20
	3.2 Modification of GE RTV-560 Using Microballoons as Fillers	21
	3.3 Raybestos-Manhattan's Closed-Cell Sili- cone Rubber Sponge, RL-1973, Bonded Between GE RTV-560	25
	3.3.1 Effect of Reduced Pressure on RL-1973 Sponge	28
	3.3.2 Selection of RL-1973/GE RTV-560 as the Fourth Adhesive System in the Program	28
	3.4 Density of Adhesives	30

TABLE OF CONTENTS (Continued)

<u>Section</u>	<u>Page</u>
4 MECHANICAL PROPERTIES	33
4.1 Adhesion in Tension	34
4.1.1 Test Method	34
4.1.2 Results and Discussion	35
4.1.3 Data Analysis	36
4.2 Adhesion in Shear	55
4.2.1 Test Method	55
4.2.2 Results and Discussion	55
4.2.3 Data Analysis	58
4.3 Tensile Modulus and Poisson's Ratio	70
4.3.1 Test Method	70
4.3.2 Results and Discussion	74
4.4 Shear Modulus	85
4.4.1 Test Method	85
4.4.2 Results and Discussion	86
4.5 Compression Modulus	102
4.5.1 Test Method	102
4.5.2 Results and Discussion	104
4.6 Poisson's Ratio	112
4.6.1 Results	112
4.6.2 Discussion	112
4.7 Constant Strain-Stress Relaxation	122
4.7.1 Test Method	123
4.7.2 Results and Discussion	127

TABLE OF CONTENTS (Continued)

<u>Section</u>		<u>Page</u>
5	THERMAL PROPERTIES	131
	5.1 Thermal Expansion	132
	5.1.1 Test Method	132
	5.1.2 Results and Discussion	134
	5.2 Thermal Conductivity	146
	5.2.1 Test Method	146
	5.2.2 Results and Discussion	148
	5.3 Specific Heat	153
	5.3.1 Test Method	153
	5.3.2 Results and Discussion	156
	5.4 Thermal Cycling	157
	5.4.1 Band-Shaped Specimens	157
	5.4.2 Torsional Shear Specimens	159
	5.4.3 Shear Strength at Failure	161
	5.4.4 Tensile (Spool) Specimens	163
6	BEHAVIOR OF SILICONE RUBBER ADHESIVES AT AND BELOW THEIR GLASS TRANSITION TEMPERA- TURES	165
	6.1 Observation of Specimens at and Below Glass-Transition Temperature	166
	6.2 Literature Survey Regarding Low Tem- perature Properties of Silicone Rubber	167
	6.3 Stress Relaxation of Polymers at Low Temperature	168
7	CONCLUSIONS AND RECOMMENDATIONS	171
	7.1 Conclusions	172
	7.2 Recommendations	173

TABLE OF CONTENTS (Continued)

<u>Section</u>		<u>Page</u>
APPENDIX I	Quality Control Documents Received for Test Candidate Materials	177
APPENDIX II	Summary of Regression Analysis and Tolerance Limit Techniques Used in Data Reduction	189
APPENDIX III	Compilation of Stress-Strain Calculations	195
APPENDIX IV	Summary of Strain Confidence Limits for Best Fitting Regression Equation to Stress-Strain Data	215
APPENDIX V	Summary of Strength Confidence Limits for Best Fitting Regression Equation to Strength-Temperature Data	233
APPENDIX VI	Tensile Modulus, Poission's Ratio Least Square Computations	237
REFERENCES		241

L I S T O F I L L U S T R A T I O N S

<u>Figure</u>		<u>Page</u>
1	Program Overview	7
2	Tensile Specimen	8
3	Shear Specimen	8
4	Tensile Modulus Specimen	8
5	Shear Modulus Specimen	8
6	Compression Specimen	9
7	Density and Specific Heat Specimen	9
8	Thermal Expansion Specimen	9
9	Thermal Conductivity Specimen	9
10	Band-Shaped Specimen	10
11	Constant Strain Tension Adhesive Specimen	10
12	Tensile Stress-Strain of Aluminum to Aluminum Bonded Butt Joints 0.064" Glue Lines (approx.) Tests at 75 ^o F	27
13	Shear Stress-Strain of Aluminum to Aluminum Bonded Single Overlap Joints 0.064" Glue Lines (approx.) Tests at 75 ^o F	27
14	Volume Change Vs. Time at Vacuum and Pressure: RM RL-1973 Sponge	29
15	Cylinder Adhesion Test Setup	35
16	Tensile Strength Vs. Temperature	38
17	Ultimate Elongation Vs. Temperature	38
18	Average Flatwise Tensile Strength of Adhesive Materials	45

LIST OF ILLUSTRATIONS (Continued)

<u>Figure</u>		<u>Page</u>
19	Tensile Strength Vs. Temperature - RTV-560 Material	46
20	Tensile Strength Vs. Temperature - SLA-561 Material	46
21	Tensile Strength Vs. Temperature DC 93-046 Material	46
22	Tensile Strength Vs. Temperature RTV 560/ RL-1973	46
23	Tensile Stress-Strain RTV-560 (-270 ^o F)	47
24	Tensile Stress-Strain RTV-560 (-200 ^o F)	47
25	Tensile Stress-Strain RTV-560 (-175 ^o F)	47
26	Tensile Stress-Strain RTV-560 (-150 ^o F)	47
27	Tensile Stress-Strain RTV-560 (-65 ^o F)	48
28	Tensile Stress-Strain RTV-560 (80 ^o F)	48
29	Tensile Stress-Strain RTV-560 (300 ^o F)	48
30	Tensile Stress-Strain RTV-560 (350 ^o F)	48
31	Tensile Stress-Strain SLA-561 (-150 ^o F)	49
32	Tensile Stress-Strain SLA-561 (-65 ^o F)	49
33	Tensile Stress-Strain SLA-561 (80 ^o F)	49
34	Tensile Stress-Strain SLA-561 (300 ^o F)	49
35	Tensile Stress-Strain SLA-561 (350 ^o F)	50
36	Tensile Stress-Strain DC-93-046 (-270 ^o F)	50
37	Tensile Stress-Strain DC-93-046 (-200 ^o F)	50

LIST OF ILLUSTRATIONS (Continued)

<u>Figure</u>		<u>Page</u>
38	Tensile Stress-Strain DC-93-046 (-175 ^o F)	50
39	Tensile Stress-Strain DC-93-046 (-150 ^o F)	51
40	Tensile Stress-Strain DC-93-046 (-65 ^o F)	51
41	Tensile Stress-Strain #1 DC-93-046 (80 ^o F)	51
42	Tensile Stress-Strain #2 DC-93-046 (80 ^o F)	51
43	Tensile Stress-Strain DC-93-046 (300 ^o F)	52
44	Tensile Stress-Strain DC-93-046 (350 ^o F)	52
45	Tensile Stress-Strain RTV 560/RL-1973 (-270 ^o F)	52
46	Tensile Stress-Strain RTV 560/RL-1973 (-200 ^o F)	52
47	Tensile Stress-Strain RTV 560/RL-1973 (-175 ^o F)	53
48	Tensile Stress-Strain RTV 560/RL-1973 (-150 ^o F)	53
49	Tensile Stress-Strain RTV 560/RL-1973 (-65 ^o F)	53
50	Tensile Stress-Strain RTV 560/RL-1973 (80 ^o F)	53
51	Tensile Stress-Strain RTV 560/RL-1973 (300 ^o F)	54
52	Tensile Stress-Strain RTV 560/RL-1973 (350 ^o F)	54
53	Shear Strength Vs. Temperature	57
54	Average Overlap Shear Strength of Adhesive Materials	63
55	Shear Strength Vs. Temperature RTV-560 Material	63
56	Shear Strength Vs. Temperature SLA-561 Material	63
57	Shear Strength Vs. Temperature DC 93-046 Material	63

LIST OF ILLUSTRATIONS (Continued)

<u>Figure</u>		<u>Page</u>
58	Shear Strength Vs. Temperature RTV-560/ RL-1973	64
59	Shear Stress-Strain Curve RTV-560 (-175 ^o F)	64
60	Shear Stress-Strain Curve RTV-560 (-150 ^o F)	64
61	Shear Stress-Strain Curve RTV-560 (80 ^o F)	64
62	Shear Stress-Strain Curve RTV-560 (300 ^o F)	65
63	Shear Stress-Strain Curve RTV-560 (350 ^o F)	65
64	Shear Stress-Strain Curve SLA-561 (-150 ^o F)	65
65	Shear Stress-Strain Curve SLA-561 (-65 ^o F)	65
66	Shear Stress-Strain Curve SLA-561 (80 ^o F)	66
67	Shear Stress-Strain Curve SLA-561 (300 ^o F)	66
68	Shear Stress-Strain Curve SLA-561 (350 ^o F)	66
69	Shear Stress-Strain Curve DC 93-046 (-65 ^o F)	66
70	Shear Stress-Strain Curve DC 93-046 (80 ^o F)	67
71	Shear Stress-Strain Curve DC 93-046 (300 ^o F)	67
72	Shear Stress-Strain Curve DC 93-046 (350 ^o F)	67
73	Shear Stress-Strain RTV 560/RL-1973 (-270 ^o F)	67
74	Shear Stress-Strain RTV 560/RL-1973 (-200 ^o F)	68
75	Shear Stress-Strain RTV 560/RL-1973 (-175 ^o F)	68
76	Shear Stress-Strain RTV 560/RL-1973 (-150 ^o F)	68
77	Shear Stress-Strain RTV 560/RL-1973 (-65 ^o F)	68
78	Shear Stress-Strain RTV 560/RL-1973 (80 ^o F)	69

LIST OF ILLUSTRATIONS (Continued)

<u>Figure</u>		<u>Page</u>
79	Shear Stress-Strain RTV 560/RL-1973 (300°F)	69
80	Shear Stress-Strain RTV 560/RL-1973 (350°F)	69
81	Poisson's Ratio for GE's RTV 560 at Room Temperature	71
82	35mm Veritron Camera Mounted on CRE/2K Scott Tester	71
83	Tensile Modulus Setup	73
84	Tensile Modulus Vs. Temperature RTV-560, 0.4 In./In./Min Strain Rate	76
85	Tensile Modulus of RTV-560 Vs. Strain Rate	76
86	Tensile Modulus Vs. Temperature DC 93-046, 0.4 In./In./Min Strain Rate	80
87	Tensile Modulus of DC 93-046 Vs. Strain Rate	80
88	Tensile Modulus Vs. Temperature SLA-561 0.4 In./In./Min Strain Rate	82
89	Tensile Modulus of SLA-561 Vs. Strain Rate	82
90	Tensile Modulus Vs. Temperature RTV-560/RL-1973	84
91	Tensile Modulus of RTV-560/RL-1973 Vs. Strain Rate	84
92	Shear Modulus Test Setup	86
93	Shear Modulus of GE-560 at Various Strain Rates, Bondline Thicknesses and Temperatures	98
94	Shear Modulus of DC 93-046 at Various Strain Rates, Bondline Thicknesses and Temperatures	99
95	Shear Modulus of SLA-561 at Various Strain Rates, Bondline Thicknesses and Temperatures	100

LIST OF ILLUSTRATIONS (Continued)

<u>Figure</u>		<u>Page</u>
96	Shear Modulus of GE 560/RL-1973 at Various Strain Rates, Bondline Thickness and Temperatures	101
97	Compression Modulus Test Setup	103
98	Effect of -200 ^o F on DC 93-046 Compression Specimens	105
99	Effect of 550 and 600 ^o F on Compression Specimens	105
100	Compression Modulus of GE RTV-560 Vs. Temperature	111
101	Compression Modulus of DC 93-046 Vs. Temperature	111
102	Compression Modulus of SLA-561 Vs. Temperature	111
103	Compression Modulus of RM/RL-1973 Vs. Temperature	111
104	Constant Strain Test Fixture	124
105	Stacked Specimen Constant Strain Test Setup	124
106	Stress Relaxation at Constant Strain, GE RTV-560, Band Specimens	128
107	Stress Relaxation at Constant Strain, SLA-561, Band Specimens	128
108	Stress Relaxation at Constant Strain, R/M RL-1973, Band Specimens	128
109	Stress Relaxation at Constant Strain, GE RTV-560, Stacked Disc Specimens	129
110	Stress Relaxation at Constant Strain, SLA-561, Stacked Disc Specimens	129

LIST OF ILLUSTRATIONS (Continued)

<u>Figure</u>		<u>Page</u>
111	Stress Relaxation at Constant Strain, R/M RL-1973, Stacked Disc Specimens	129
112	Thermophysics Corp. Model TE-3000L Linear Thermal Expansion Unit	133
113	Perkin Elmer Differential Scanning Calorimeter/ Thermomechanical Analyzer Unit	133
114	Linear Thermal Expansion Vs. Temperature, RTV-560	138
115	Linear Thermal Expansion Vs. Temperature, DC 93-046	140
116	Linear Thermal Expansion Vs. Temperature, SLA-561	142
117	Linear Thermal Expansion Vs. Temperature, RM/RL-1973	142
118	Linear Thermal Expansion Vs. Temperature	143
119	Liquid Nitrogen Being Flowed Through ASTM-C- 177 Thermal Conductivity Tester	147
120	Thermal Conductivity Vs. Mean Temperature, RTV-560	147
121	Thermal Conductivity Vs. Mean Temperature, DC 93-046	151
122	Thermal Conductivity Vs. Mean Temperature, SLA-561	151
123	Thermal Conductivity Vs. Mean Temperature, R/M RL-1973 Sponge	155
124	Thermal Conductivity Vs. Mean Temperature	155
125	Band-Shaped Specimen in Test on CRE-2K Bendix Scott Test Machine	159

LIST OF ILLUSTRATIONS (Continued)

<u>Figure</u>		<u>Page</u>
126	Test Area for Tensile Modulus and Poisson's Ratio	237
127	Least Squares Elastic Modulus and Poisson's Ratio	239

L I S T O F T A B L E S

<u>Table</u>		<u>Page</u>
I	Adhesive Advantage and Disadvantage Summary	4
II	Adhesive Properties of Various Lots of GE-560 Using GE 4004 and 4155 Primers	17
III	Properties of Dow Corning's RTV Silicone 77-137 Formulations	22
IV	Dow Corning 77-158 Single Overlap Shear Data	23
V	Dow Corning X3-6000 Tensile and Lap Shear Adhesion Data	24
VI	Tensile and Shear Strength of Formulated GE-560 and Raybestos-Manhattan RL-1973 Closed Cell Sponge in Bonded Aluminum to Aluminum Lap and Butt Joints	26
VII	Density at Room Temperature ASTM-D-297, 17(C)	31
VIII	Ultimate Tensile Strength and Elongation Average Values	37
IX	Summary of Tensile Stress-Strain Conditions Regression Analysis	40
X	Results of Tensile Stress-Strain Regression	41
XI	Results of Flatwise Tensile Strength - Temperature Regression	43
XII	Single Overlap Shear Strength Average	56
XIII	Summary of Shear Stress-Strain Conditions for Regression Analysis	59
XIV	Results of Shear Stress-Strain Regression	60
XV	Results of Shear Strength-Temperature Regression	62
XVI	Poisson's Ratio for GE's RTV-560 at Room Temperature	72

LIST OF TABLES (Continued)

<u>Table</u>		<u>Page</u>
XVII	Tensile Modulus of GE's RTV-560	75
XVIII	Tensile Modulus of GE RTV-560 Determined from Cylinder Adhesion Specimen	77
XIX	Tensile Modulus of DC 93-046	79
XX	Tensile Modulus of SLA-561	81
XXI	Tensile Modulus of RTV-560/RL-1973	83
XXII	Shear Modulus (Double Lap Torsion Test) of GE-560	87
XXIII	Shear Modulus (Double Lap Torsion Test) of DC 93-046	90
XXIV	Shear Modulus (Double Lap Torsion Test) of SLA-561	92
XXV	Shear Modulus (Double Lap Torsion Test) of GE RTV-560/RL-1973 System	95
XXVI	Compression Modulus of GE RTV-560	107
XXVII	Compression Modulus of DC 93-046	108
XXVIII	Compression Modulus of MMC SLA-561	109
XXIX	Compression Modulus of RM/RL-1973	110
XXX	Poisson's Ratio in Tension	113
XXXI	Poisson's Ratio in Compression	114
XXXII	Tensile Modulus	115
XXXIII	Compression Modulus	117
XXXIV	Poisson's Ratio Computed from Shear and Tension Modulus	119

LIST OF TABLES (Continued)

<u>Table</u>		<u>Page</u>
XXXV	Poisson's Ratio Computed from Shear and Compression Modulus	120
XXXVI	Summary of Constant Strain Tests on Band Specimens	125
XXXVII	Summary of Constant Strain Tests on Stacked Disc Specimens	126
XXXVIII	Summary of Linear Thermal Expansion Data, RTV-560	136
XXXIX	Summary of Linear Thermal Expansion Data, RTV-560	137
XL	Summary of Linear Thermal Expansion Data, DC 93-046	139
XLI	Summary of Linear Thermal Expansion Data, MMC SLA-561	141
XLII	Summary of Linear Thermal Expansion, RM/RL-1973 Sponge	144
XLIII	Thermal Conductivity Test Results, RTV-560	149
XLIV	Thermal Conductivity Test Results, DC 93-046	150
XLV	Thermal Conductivity Test Results, MMC-SLA-561	152
XLVI	Thermal Conductivity Test Results, RL-1973 Sponge	154
XLVII	Summary of Specific Heat Vs. Temperature, Space Shuttle Adhesives	158
XLVIII	Ultimate Shear Strength and Elongation After Environmental Conditioning of Band Shaped Specimens	160

LIST OF TABLES (Continued)

<u>Table</u>		<u>Page</u>
XLIX	Ultimate Shear Strength and Torsional Shear Modulus After Environmental Conditioning of Double Lap Shear Specimens	162
L	Adhesion in Tension After Environmental Conditioning of Cylindrical Flatwise Tension Specimens	164
LI	Tensile Stress-Strain Results , -270 ^o F	196
LII	Tensile Stress-Strain Results , -200 ^o F	197
LIII	Tensile Stress-Strain Results , -175 ^o F	198
LIV	Tensile Stress-Strain Results , -150 ^o F	199
LV	Tensile Stress-Strain Results , -65 ^o F	200
LVI	Tensile Stress-Strain Results , 80 ^o F	201
LVII	Tensile Stress-Strain Results , 300 ^o F	202
LVIII	Tensile Stress-Strain Results , 350 ^o F	203
LIX	Ultimate Tensile Strength and Elongation at 550 ^o and 600 ^o F	204
LX	Shear Stress-Strain Results , -270 ^o F	205
LXI	Shear Stress-Strain Results , -200 ^o F	206
LXII	Shear Stress-Strain Results , -175 ^o F	207
LXIII	Shear Stress-Strain Results , -150 ^o F	208
LXIV	Shear Stress-Strain Results , -65 ^o F	209
LXV	Shear Stress-Strain Results , 80 ^o F	210
LXVI	Shear Stress-Strain Results , 300 ^o F	211
LXVII	Shear Stress-Strain Results , 350 ^o F	212

LIST OF TABLES (Continued)

<u>Table</u>		<u>Page</u>
LXVIII	Single Overlap Shear Strength at 550° and 600°F	213
LXIX	Summary of Tensile Strain Confidence Limits at -270°F	216
LXX	Summary of Tensile Strain Confidence Limits at -200°F	217
LXXI	Summary of Tensile Strain Confidence Limits at -175°F	218
LXXII	Summary of Tensile Strain Confidence Limits at -150°F	219
LXXIII	Summary of Tensile Strain Confidence Limits at -65°F	220
LXXIV	Summary of Tensile Strain Confidence Limits at 80°F	221
LXXV	Summary of Tensile Strain Confidence Limits at 300°F	222
LXXVI	Summary of Tensile Strain Confidence Limits at 350°F	223
LXXVII	Summary of Shear Strain Confidence Limits at -270°F	224
LXXVIII	Summary of Shear Confidence Limits at -200°F	225
LXXIX	Summary of Shear Strain Confidence Limits at -175°F	226
LXXX	Summary of Shear Strain Confidence Limits at -150°F	227
LXXXI	Summary of Shear Strain Confidence Limits at -65°F	228
LXXXII	Summary of Shear Strain Confidence Limits at 80°F	229

LIST OF TABLES (Continued)

<u>Table</u>		<u>Page</u>
LXXXIII	Summary of Shear Strain Confidence Limits at 300°F	230
LXXXIV	Summary of Shear Strain Confidence Limits at 350°F	231
LXXXV	Summary of Tensile Strength Confidence Limits and Strength Allowables	234
LXXXVI	Summary of Shear Strength Confidence Limits and Strength Allowables	235

SECTION 1

INTRODUCTION AND SUMMARY

S E C T I O N 1

I N T R O D U C T I O N A N D S U M M A R Y

The work performed on NASA, MSC contract NAS9-12392, Development of Design Allowables for Adhesives for Attaching Reusable Surface Insulation, is described in this report. The overall objective of this program was to test and establish design allowables data for the following room temperature vulcanizing (RTV) silicone rubber based adhesives, (1) General Electric's RTV-560, (2) Dow Corning's 93-046, and (3) Martin Marietta's SLA-561. These adhesives are being evaluated for attaching reusable surface insulation (RSI) to space shuttle structure.

General Electric's PD-200 adhesive system was originally scheduled for testing in this program, but it was deleted per CCA No. 1 early in the program.

A further objective was to modify existing RTV silicone adhesive formulations to impart reduced modulus and density as compared to the adhesives specified above. In this portion of the program, development work was confined to modifications of GE RTV-560 and Dow Corning's unfilled RTV 77-137 and development of an adhesive system comprised of Raybestos Manhattan's RL-1973 closed-cell silicone sponge sandwiched between bond lines of GE RTV-560.

Glass and phenolic microballoons were added to GE RTV-560 and DC-77-137 formulations to reduce density and possibly reduce modulus. This approach was successful in reducing density, but the high modulus of the microballoons caused the modulus of the formulations to increase rather than decrease. The addition of microballoons to the formulations also created shelf aging and processing problems.

The system comprised of RL-1973 sponge bonded with GE RTV-560 proved to be quite successful. Its density is less than half that of the solid adhesives tested, and it has a very low modulus. The system possesses adequate strength to compete with the other adhesives. Based on these findings, the RL-1973/GE RTV-560 system was selected for design allowable testing along with the three contract specified adhesives.

The three specified adhesives and the RL-1973/GE RTV-560 developed system were tested for adhesion in tension and shear;

tensile, shear, and compression modulus along with Poisson's ratio; constant-strain/stress-relaxation; thermal expansion, thermal conductivity, and specific heat; and effects of thermal cycling. Test methods used and data obtained are reported herein. Design allowables curves were developed for adhesion in tension and shear to failure at temperatures above the glass transition points of the four adhesive systems.

A summary of the advantages and disadvantages of the four adhesive systems is presented in Table I. Difficulties were encountered in determining the modulus of the four adhesives at temperatures below their glass transition points. These difficulties arose because the test methods for determining deformation of specimens under increasing loads were designed to accommodate high elongations. As the adhesives become stiff and brittle at temperatures below their glass transition points, deformation under the relatively low loads become so small that minute measurement inaccuracies caused extreme fluctuations in calculated values of modulus.

Poisson's ratio values obtained on the adhesives at temperatures below their glass-transition points were also extremely variable for the same reason as the modulus values. In addition, it was discovered, unexpectedly, that specimens exhibited shrinkage when initially subjected to load at these low temperatures. Initial application of load produced negative rather than positive elongations. Under these low loading conditions, Poisson's ratio could not be determined. Because of this unforeseen problem at low temperatures and due to the fact that values for the adhesives in their rubbery state are approximately 0.5, utilization of these data in analysis techniques based on theories of elasticity is inadvisable.

Under amendment 2S to this contract, a fifth adhesive, Dow Corning's X3-6004, was tested the same as the four covered in this report. In addition, tensile modulus of X3-6004, along with GE RTV-560 as a control, was tested using a new procedure. Molded "dog bone" shaped specimens, 10 inches long with 0.5-inch-diameter throats, were fitted with a 2-inch Instron extensometer and tested in an environmental chamber on an Instron test machine. This method gave significantly higher tensile modulus values than the strap specimens described in paragraph 4.3.1.2 of this report. Details of the test and data obtained are presented in an addendum to this report.

TABLE I ADHESIVE ADVANTAGE AND DISADVANTAGE SUMMARY

Adhesive	Advantages	Disadvantages
GE RTV-560	<ul style="list-style-type: none"> . Easy processing . Best low temperature properties . Highest strength at intermediate temperature 	<ul style="list-style-type: none"> . Highest thermal conductivity . Highest density . Highest modulus . Thick sections blister internally at 550°F
DC 93-046	<ul style="list-style-type: none"> . Second lowest modulus 	<ul style="list-style-type: none"> . Viscous, difficult to process . Highest glass transition temperature . Cracks on thermal shock at -200°F . Thick sections revert and blister internally at 550°F
SLA-561	<ul style="list-style-type: none"> . Best high temperature strength . Easy processing, easiest to degas 	<ul style="list-style-type: none"> . Weak in shear strength . Thick sections crack at 550°F . Fresh SLA-561 has low adhesion to cured SLA-561
RL-1973/GE RTV-560	<ul style="list-style-type: none"> . Lowest density . Lowest modulus . Lowest thermal conductivity 	<ul style="list-style-type: none"> . Volume sensitive to pressure change . Lowest strength . Must be sliced to desired thickness . Compatibility with base adhesive must be determined

SECTION 2

TEST MATERIALS AND METHODS

S E C T I O N 2

T E S T M A T E R I A L S A N D M E T H O D S

Candidate adhesives and tests conducted are shown in Figure 1, Program Overview. Tests were generally conducted in triplicate, using identical specimens. Specimen configurations were as shown in Figures 2 through 11. When thermal conditioning or testing at low or elevated temperature was involved, the required environment was maintained for five minutes following stabilization of the specimen at ambient conditions.

2.1 SPECIFIED ADHESIVES

Originally the program called for testing of the following materials:

1. GE RTV-560
2. GE PD-200
3. Dow Corning 93-046
4. Martin MMC SLA-561

The GE PD-200 was deleted from the program when it became impractical for NASA, MSC to obtain fabricated specimens from GE. A further contract objective was to conduct investigations leading to development of a lower modulus and density adhesive system. The effort was not considered to be a major formulation of adhesives but rather a modification of existing adhesives. As a result of this effort in the program, the GE RTV-560/RL-1973 system evolved as the most promising material, the technical monitor agreed to include it in the program as the fourth test adhesive system.

2.2 SELECTION OF ADHERENDS AND PRIMERS

Selection of these materials was based on the most recent information available relative to space shuttle technology.

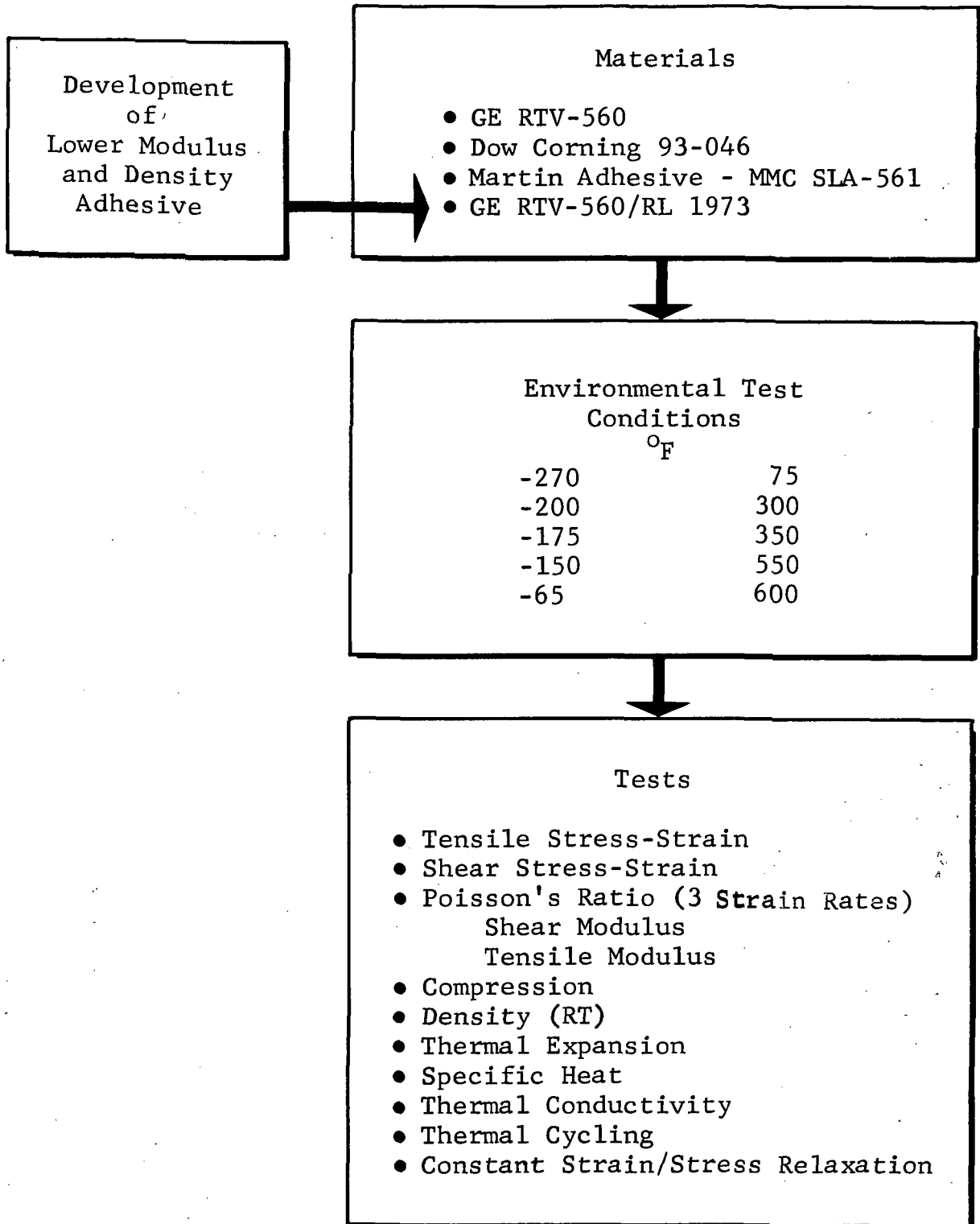


Figure 1 Program Overview

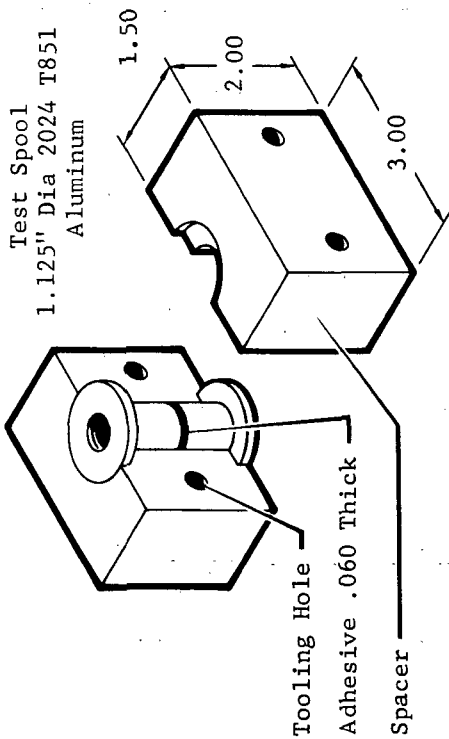


Figure 2 Tensile Specimen

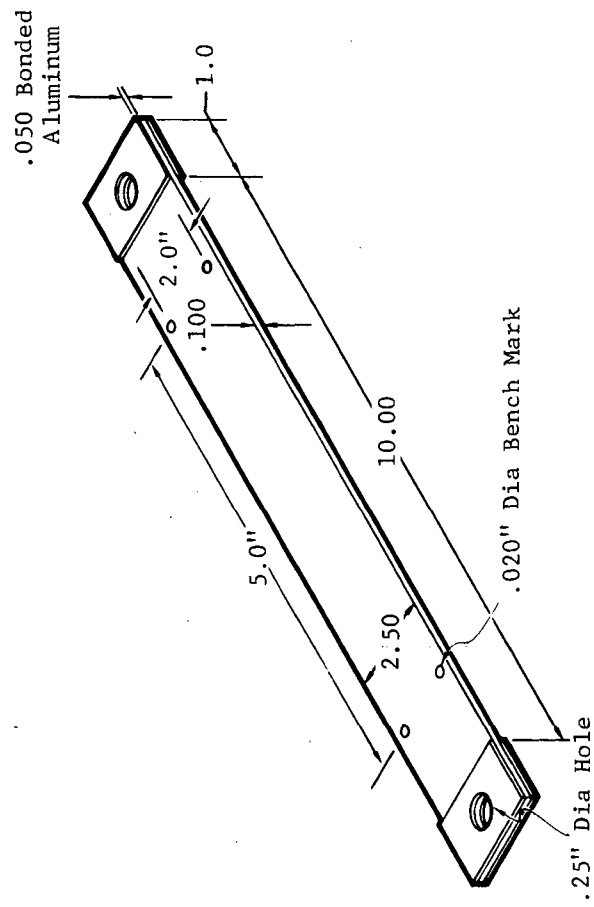


Figure 4 Tensile Modulus Specimen

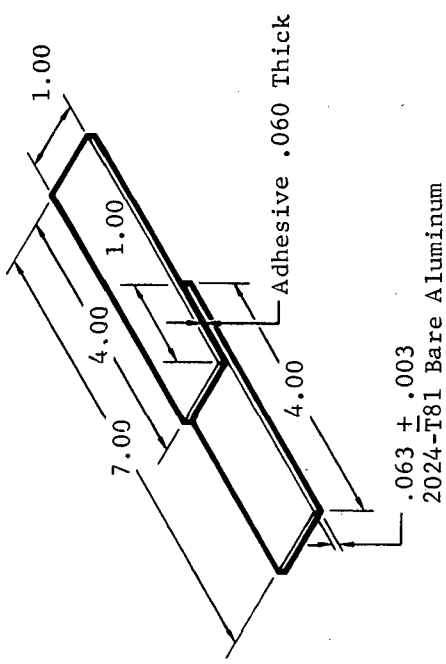


Figure 3 Shear Specimen

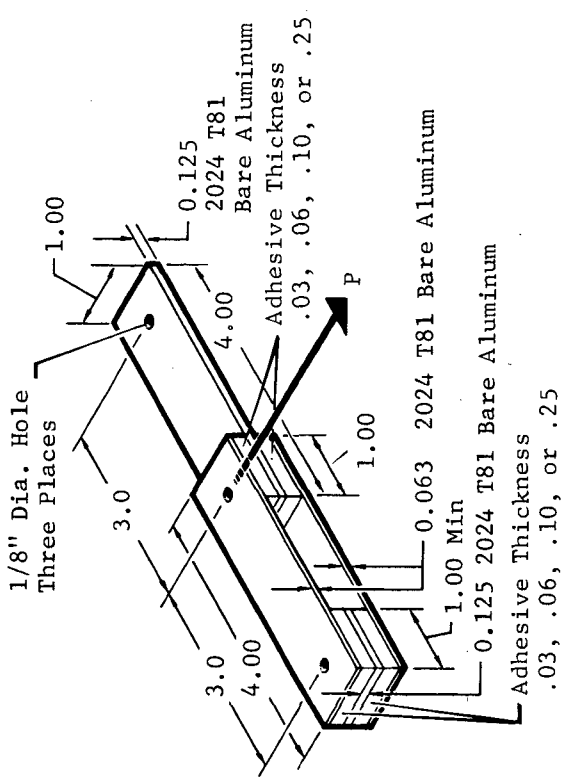


Figure 5 Thorsion Shear Modulus Specimen

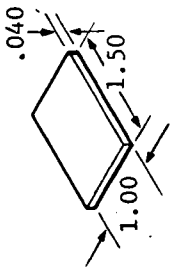


Figure 7 Density and Specific Heat Specimen

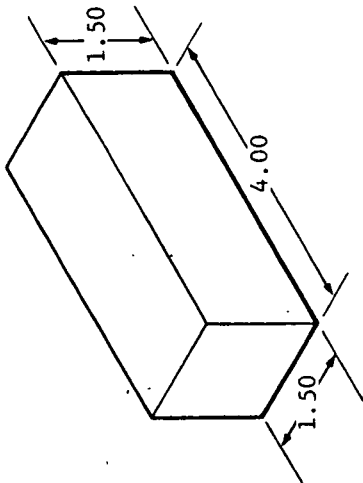


Figure 6 Compression Specimen

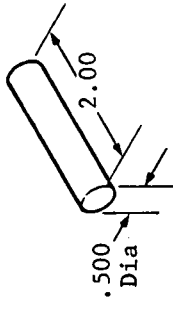


Figure 8 Thermal Expansion Specimen

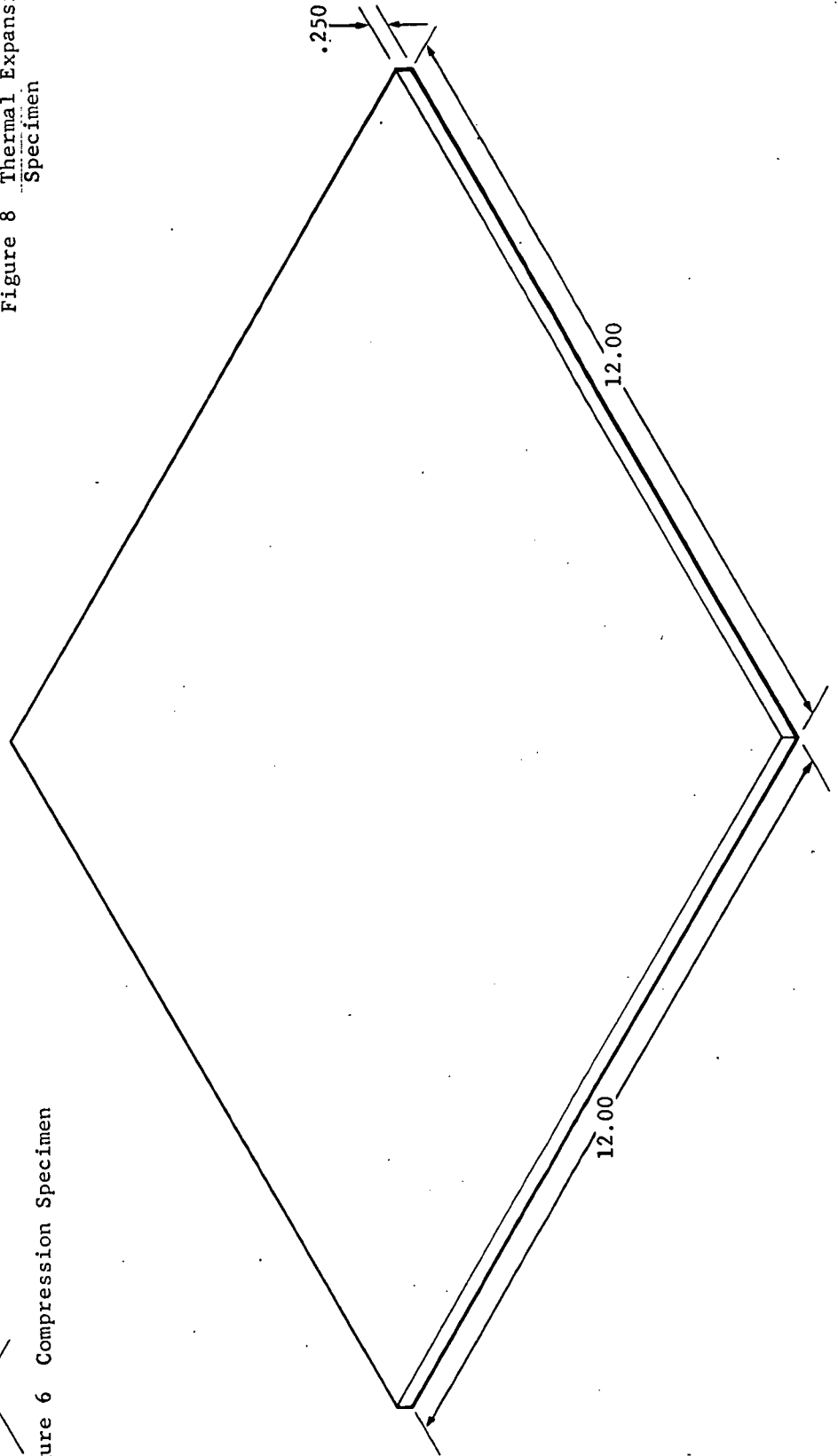


Figure 9 Thermal Conductivity Specimen

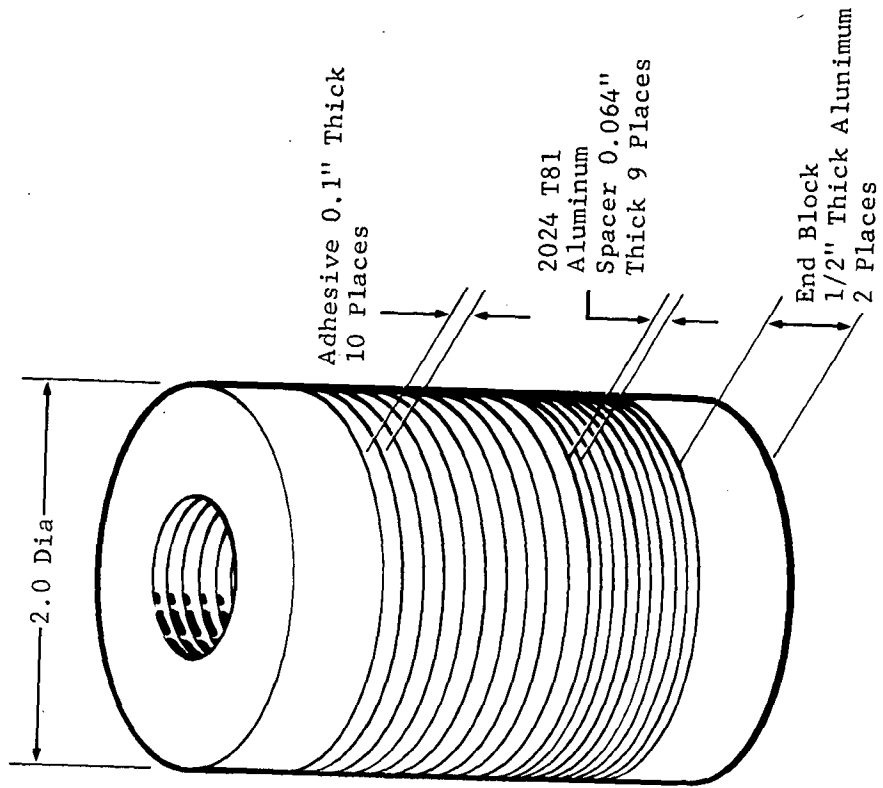


Figure 11 Constant Strain Tension Adhesion Specimen

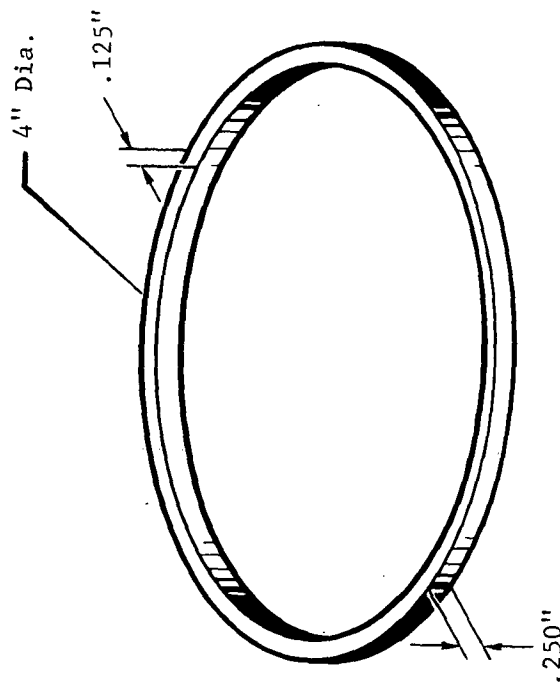


Figure 10 Band-Shaped Specimen

2.2.1 Adherends (Substrates)

Bare aluminum alloy sheet 2024T81 and rod 2024T851 were used as the substrate for all the adhesive systems tested. All substrates were uniformly cleaned by the following technique:

1. All surface soils, oil, and grease were removed by wiping with cheesecloth moistened with methyl ethyl ketone (MEK).
2. Specimen substrates were then vapor degreased in a trichloroethylene vapor degreaser.
3. Pre-etch cleaning was accomplished by immersion for 9 to 15 minutes in a solution of the following composition maintained at room temperature:

69% Nitric Acid Fed. Spec. (O-N-350)	10 to 22% by Volume
70 Hydrofluoric Acid	0.4 to 0.8% by Volume
Chromium Trioxide Fed. Spec. (O-C-303B)	3.5 to 4.5 oz (Dry Wt.)
Tap Water	Balance to make 1 gal.

4. Adherends were rinsed in clean, running tap water at room temperature for 6 to 12 minutes.
5. Adherends were then immersed from 9 to 15 minutes in a solution of the following composition, which was maintained at $155 \pm 15^{\circ}\text{F}$.

(66 ^o Be) Sulfuric Acid Fed. Spec. (O-S-809A)	10 Parts/Wt.
Sodium Dichromate Fed. Spec. (O-S-595)	4 Parts/Wt.
Water (Tap)	30 Parts/Wt.

6. Specimen substrates (adherends) were rinsed in clean tap water at room temperature and then spray rinsed thoroughly with room temperature demineralized water.

7. Drying was accomplished in a 160°F ± 10°F oven for 30 minutes.

NOTE: During all degreasing, cleaning, rinsing, and drying operations the specimens were individually separated in aluminum racks to provide identical, uniform treatment.

2.2.2 Primers

Based on either vendors data and recommendations, or previously obtained data from room temperature lap shear tests of primer, adhesive, and adherend combinations, the following adhesive primer systems were selected.*

1. GE RTV-560 with GE SS4004 or GE SE4155 prime
2. DC 93-046 with DC 1200 prime
3. MMC SLA-561 with DC 1200 prime
4. GE RTV-560/RL 1973 with GE SE4155 prime

* Cure time for all specimens was 7 days.

The fundamental consideration in selecting primers was the ability to promote adhesion sufficient to provide cohesive failures of the adhesive rather than adhesive failure to the substrate. Practically all of the specimens in the program did fail cohesively.

In the application of primers it is Convair's experience and observation that a very thin but uniform coating of primers is required. Thicker coatings of the silane-based primers form loosely adhering powders on the surface when they hydrolyze. Therefore, in this effort all primers were applied with a clean camel's hair artist's brush to cover the surface completely. The primed surface was then immediately wiped with clean cheesecloth or lint free "Kim-Wipes" removing all excess prime. The remaining very thin film was allowed to air dry for 30 minutes before application of the subsequent required adhesive.

Initially, the vendor recommended that SS4004 primer be used with the GE RTV-560 adhesive. Difficulties developed with the use of this primer (paragraph 2.3.2.1), however, and the vendor

later suggested that SE4155 be evaluated for use in place of SS4004. The SE4155 primer is a silane-type primer, while the SS4004 is a silicone resin type. The SE4155 presents fewer problems in application; i.e., it makes a more uniform coating on the aluminum substrates. Also, current tests of lap shear and flatwise tension adhesion specimens made with SE4155 primer and tested up to 600°F show 100 percent cohesive failures in the RL-1973. Hence, there appears to be no problem with the SE4155 primer at elevated temperature. Based on these findings, GE primer SE4155 was used to prepare the remaining specimens under the contract. A new lot of GE RTV-560 was ordered for use in CCA No. 1 and was tested before use in preparing the required specimens.

2.3 PROCESSING

The techniques used were based on Convair Aerospace's previous experience with sealing and potting compounds. All pertinent details are supplied in the following sections.

2.3.1 Mixing and Handling Characteristics

Adhesive components were mixed as described below. All mixing and curing were performed in a room with a controlled temperature of $77 \pm 2^\circ\text{F}$ and a relative humidity of 50 ± 5 percent.

2.3.1.1 Weighing

Base materials and their corresponding catalysts were weighed on a torsion balance. Batch sizes of 100 grams or more were used to provide additional uniformity.

2.3.1.2 GE RTV-560

The weight ratio of the base to the catalyst for this candidate material is 100:0.5. The desired quantity was weighed out in a new clean mixing container, and the exact required quantity of catalyst was added to the base. The material then was hand blended with a spatula for a minimum of five minutes. The completely blended GE RTV-560 was then transferred to new plastic Semco centrifuge-dispensing tubes. Most of entrapped air bubbles was expelled by

centrifuging the material at 1500 RPM for 10 minutes. The GE RTV-560 was immediately piston dispensed from the tube into the various types of specimen molds or applied in adhesive joints. Work life of GE RTV-560 was approximately 2 hours.

2.3.1.3 DC 93-046

DC 93-046 is a black thixotropic material and requires special techniques to achieve uniform blends. The weight ratio of the base to the catalyst is 10:1. It was also batch size limited; i.e., when batches larger than 500 grams were attempted a reduced pot life resulted and the material tended to gel and become more viscous and tacky. Consequently, 300 to 400 gram batches were utilized. Mixing was accomplished by one of the two methods listed below:

1. The base and catalyst were partially mixed. The premixed material was then vacuum degassed (28 in. Hg. min.) followed by final mixing in a pneumatic operated Pyles Industries mixer. With this device, mixed material was hydraulically forced into plastic Semco tubes. Filled tubes were then immediately utilized to inject the DC 93-046 into the required specimen molds or adhesive joints.
2. The 10:1 weighed DC 93-046 was thoroughly mixed for at least 5 minutes in a new throw-away container. It was then evacuated (28 in. Hg. min.) for 5 minutes. The material was transferred to plastic Semco tubes and centrifuged at 1500 RPM for 10 minutes. It was immediately injected to form the required specimens. This evolved method was the final preferred method of mixing and degassing since it eliminated the laborious, time consuming task of cleaning the Pyles mixer immediately after each batch.

The work life of DC 93-046 was approximately 1 hour.

2.3.1.4 MMC SLA-561

This material is a transparent blend of a base-catalyst ratio of 10:1 by weight. Viscosity is ideal for uniform mixing; however, air bubble entrapment was a problem. Bubbles were eliminated by evacuation (28 in. Hg. min.) for 5 minutes, followed by centrifugation in a Semco plastic tube for 10 minutes at 1500

RPM. The material was immediately injected into the required specimen molds or adhesive joints. The work life of MMC SLA-561 was approximately 1 hour.

2.3.1.5 GE RTV-560/RL-1973

This was a composite material composed of GE RTV-560 blended as described in 2.3.1.2 and slices of RM/RL-1973 closed-cell silicone sponge. The required thickness of sponge for the various specimens was cut to specimen configuration. The surfaces of the sponge were washed with methyl ethyl ketone and blotted dry with cheesecloth several times. After a 30 minute air dry, RTV-560 was trowelled onto the sponge faying surfaces with a spatula. After brief experimentation, it was learned the surface thickness of 0.005 to 0.010 inch RTV-560 coating could be controlled by scraping off the excess leaving just enough material to fill the surface cells and maintain a continuous, uniform surface coating.

2.3.2 Uniformity of Lots

2.3.2.1 Variability of Different Lots of GE RTV-560

The majority of tests of GE RTV-560 in this program were conducted using a 50-pound shipment of lot number 592. A 10-pound shipment of lot 618 was received to complete the tests.

In the interim between use of these two lots, Convair was notified by NASA, MSC technical monitor that General Electric was having adhesion problems with some later lots of GE RTV-560, particularly when used to bond silicone rubber sponge to substrates.

Convair Aerospace immediately tested lot 618 in conjunction with Raybestos-Manhattan's RL-1973 closed-cell silicone rubber sponge. GE primer SS4004 was used in the test specimens. Test failures were mostly adhesive failures between the GE RTV-560 and the SS4004 primer; with lots 592 and 608, failures were 100 percent cohesive in the RL-1973 sponge.

Convair Aerospace notified General Electric Silicone Division of the problem, and General Electric replaced lot 618 with lot 619 and suggested that GE primer SE4155 be used in lieu of SS4004. Lot 619 was tested in the same manner as described above.

Lot 619 shows some of the same tendency as lot 618 to fail adhesively at the SS4004 primer interface; however, tests with SE4155 primer show 99 percent cohesive failure in the RL-1973 sponge. Data obtained are tabulated in Table II. Based on these data, the few remaining GE RTV-560/RL-1973 sponge specimens were made using SE 4155 primer in lieu of SS4004 primer.

2.3.2.2 Vendor Quality Control Certificates

Vendor quality control certifications accompanying materials used in this program are included in Appendix I.

2.4 SELECTION OF MATERIALS FOR DEVELOPMENT OF REDUCED MODULUS AND DENSITY ADHESIVE

Two approaches were selected for modifying available silicone RTV adhesives to reduce modulus and density. One approach was to fill suitable RTV silicone adhesives with extremely low density glass or phenolic microballoons. The other approach was to obtain a low-density, low-temperature, commercially available silicone rubber sponge that can be sliced into any desired thickness. Selected thicknesses can then be bonded between substrates to provide low-modulus, low-density bond lines.

2.4.1 Selection of RTV Silicone for Modification

GE RTV-560 and Dow Corning 77-137 were selected for modification. Both are copolymers containing phenyl groups in the polymer chain to impart low-temperature properties. GE RTV-560 was selected for its low viscosity. It was reasoned that a greater percent of low-density fillers could be incorporated; hence, a lower density of the cured adhesive bond line would result. DC 77-137 was selected because of its inherent low modulus and absence of fillers. Here again it was reasoned that DC 77-137 would accept a greater volume of low-density fillers and result in a considerably reduced modulus and density adhesive.

2.4.2 Selection of Microballoon Fillers

The following microballoons were selected for use in this program:

TABLE II ADHESIVE PROPERTIES OF VARIOUS LOTS OF GE-560
USING GE SS 4004 & SE 4155 PRIMERS

(Lap Shear Specimens, 1 in. ² joints, 2024 T81, .064", Load Rate 0.03"/min.)						
Without sponge in Glue Line				With RL-1973 sponge (0.050") in Glue Line		
Lot No.	Shear, psi	Percent Cohesive	Bondline Thickness	Shear, psi	Percent Cohesive	Bondline Thickness
592	288	100	0.06	91	100	0.07
	270	100	0.06	89	100	0.07
	<u>286</u>	<u>100</u>	0.05	<u>95</u>	<u>100</u>	0.07
	281	100		92	100	
608	282	100	0.05	94	100	0.08
	277	100	0.05	79	100	0.07
	<u>276</u>	<u>100</u>	0.05	<u>92</u>	<u>100</u>	0.07
	277	100		88	100	
618				77	60	0.07
				76	40	0.06
				78	60	0.06
				48	0	0.07
				49	0	0.07
				57	0	0.06
619	287	99	0.04	101	85	0.06
	279	98	0.05	92	95	0.06
	<u>272</u>	<u>90</u>	0.05	<u>83</u>	<u>85</u>	0.06
	279	96		92	88	
				60	50	0.06
				61	10	0.06
				<u>80</u>	<u>90</u>	0.06
				67	50	
				87	60	0.06
				73	50	0.06
				<u>91</u>	<u>80</u>	0.06
				84	73	
				*With SE 4155 rather than SS 4004 Primer		
				99	100	0.07
				99	100	0.07
				<u>94</u>	<u>98</u>	0.07
			97	99		

Note: All specimens made with GE SS 4004 primer except as noted.

1. 3M's B-22A glass
2. Emerson Cumming's IG-101 glass
3. Union Carbide's BJO-0930 phenolic

These three fillers were selected for their low density (less than 0.33g./cc), availability, and relatively low cost.

2.4.3 Selection of a Closed-Cell Silicone Rubber Sponge

Raybestos-Manhattan's RL-1973 silicone sponge was selected for use in the program because of its closed-cell structure, low density (0.30g./cc), and low-temperature properties. Convair Aerospace uses this sponge in certain F-111 airplane applications and it has proved to be uniform in quality and density from lot to lot. It can be obtained from the vendor in most any thickness desired down to 0.03 inch.

SECTION 3

DEVELOPMENT OF REDUCED MODULUS
AND LOWER DENSITY ADHESIVE SYSTEM

S E C T I O N 3

D E V E L O P M E N T O F R E D U C E D M O D U L U S A N D L O W E R D E N S I T Y A D H E S I V E S Y S T E M

Decreasing the modulus and density of the adhesive would effect a substantial weight savings in the space shuttle thermal protection system (TPS). Therefore, the objective for this portion of the program was to modify existing adhesives to reduce both modulus and density yet retain sufficient strength properties to provide reliable attachment of the RSI to the space shuttle structure. Approaches taken were:

1. Formulation of Dow Corning's low modulus silicone material 77-137 using fillers as well as phenolic and glass microballoons to make a low-density syntactic foam.
2. Formulation of GE RTV-560 with the same phenolic and glass microballoons to reduce density.
3. Utilization of Raybestos-Manhattan's closed-cell silicone sponge with thin glue lines of GE RTV-560 on either side and GE primer SE4155 on the adherends.

3.1 MODIFICATION OF DOW CORNING'S 77-137 RTV SILICONE MATERIAL

Dow Corning's 77-137 mixed with accompanying catalyst cures at room conditions. Preliminary tests of the material showed it to have extremely low modulus but unexpected low strength properties. Dow Corning's technical service personnel were contacted to discuss the need for a low-modulus RTV silicone adhesive and the deficiencies of 77-137. Dow Corning suggested incorporating 5 micron-particle-size Minusil (Pennsylvania Sand and Glass' ground silica) to improve tensile strength and elongation. Small batches of 77-137, one with 30 and another with 40 parts per hundred of rubber (phr) 5-micron Minusil, were prepared. Two additional batches were mixed; one had 18 phr phenolic microballoons and the other had 15 phr phenolic microballoons plus 30 phr 5-micron Minusil.

Sheets of the four batches were cast. Small dumbbell specimens were cut from these sheets and tested for ultimate tensile strength and elongation. Lap shear specimens using both DC 92-019 and

DC 1200 primer on 0.064 gauge 2024-T81 adherends were also prepared. Formulations and data obtained are shown in Table III. Analysis of these data indicated that more work was needed to improve the strength, adhesion, and processing properties of the 77-137.

Reinforcement of the 77-137 with 30 to 40 phr of 5-micron Minusil increased tensile strength from 18 psi to 153 psi, but its tear strength was still low. Viscosity of the formulated 77-137 was low, which made it difficult to confine it in a bond line. Further discussions were held with Dow Corning personnel regarding low strength and viscosity of the formulated 77-137. Dow Corning responded by reformulating the 77-137 to produce a more workable viscosity material. The new formulation was designated 77-158.

Exploratory tests consisting of lap shear strength of the 77-158 to 2024-T81 aluminum showed the adhesive to have excellent shear strength after 11 days cure and it still exhibited the desirable low modulus as shown in Table IV. Observations during the fabrication of these lap shear specimens revealed that the 77-158 was too viscous for easy processing. The tests also show that DC 92-019 primer did not develop full shear strength of the 77-158. Failures were 100 percent adhesive to the aluminum substrates.

Following further deliberation with Dow Corning representatives, a third formulation, designated X3-6000 and based on the same polymer precursor system, was submitted to Convair Aerospace. Flatwise tension and lap shear specimens were prepared with the X3-6000. Test data obtained is shown in Table V. The X3-6000 has excellent strength in both tension and shear as well as high elongation and low modulus. Although X3-6000 shows highly desirable properties, the base component of the two-component system thickens prematurely during shelf storage. Dow Corning determined that this is due to hydrogen bonding between one of the fillers and the liquid copolymer. This condition has now been corrected by substitution of another filler. The fourth reformulation is designated X3-6004, but its development came too late for it to be considered as a candidate adhesive in this contract work.

3.2 MODIFICATION OF GE RTV-560 USING MICROBALLOONS AS FILLERS

General Electric's RTV-560 has the lowest viscosity of the three silicone adhesives included in this program; therefore, it

TABLE III PROPERTIES OF DOW CORNING'S RTV
SILICONE 77-137 FORMULATIONS

FORMULA NO.	1	2	3	4	5
<u>Ingredients</u>	<u>PARTS BY WEIGHT</u>				
77-137 Base	100	100	100	100	100
5 μ Minusil	-	30	30	40	-
Phenolic Microballoons	18	15	-	-	-
77-137 Catalyst	<u>10</u>	<u>10</u>	<u>10</u>	<u>10</u>	<u>10</u>
	128	155	140	150	110
Tensile Strength, psi	7 day cure				
1	57	66	125	171	20
2	58	66	137	154	16
3	<u>63</u>	<u>66</u>	<u>125</u>	<u>133</u>	-
Avg.	59	66	129	153	18 (22) ¹
Ultimate Elongation, percent					
1	30	80	160	170	70
2	20	90	180	160	70
3	<u>35</u>	<u>105</u>	<u>160</u>	<u>140</u>	-
Avg.	28	92	167	157	70 (55) ¹
Lap Shear Strength, psi	.064" 2024-T81, 1" overlaps, .063" glue line				
With DC-92-019 primer	not tested	not tested	no bond	100% adh.	19
			failure	Avg.	19 (2)
With DC-RTV-1200 primer	not tested	not tested	49	40	
			48	39	
			<u>49</u>	<u>43</u>	
			Avg. 49(2)	41 (3)	Avg.

1. Vendor brochure data
2. 100 percent cohesive failures
3. 90 to 95 percent cohesive failures

TABLE IV DC 77-158 SINGLE OVERLAP SHEAR

Substrate 2024-T81 Bare Aluminum
 Acid Cleaned, Primer DC 92-019
 Tests at Room Temperature

Specimen	Bond Thickness, Inch	Bond Area, in ²	Shear Strength PSI	Modulus, Initial PSI	Modulus, 2/3 Load PSI	Mode of Failure Percent Adhesion
3 Day cure @ RT	0.06	0.86	88	22	19	100
3 Day cure @ RT	0.06	0.85	94	23	20	100
Average			91	22.5	19.5	100
11 Day cure @ RT	0.06	0.85	200	31	34	100
11 Day cure @ RT	0.06	0.87	228	28	38	100
Average			214	29.5	36	100

TABLE V

DOW CORNING X3-6000

Tensile & Lap Shear Adhesion Data, 2024 T81 Bare Aluminum, Acid Cleaned
 Primer RTV-1200, Cure 6 Days at R.T.
 Tested at 75°F

Specimen	Bond Thickness, Inch	Bond Area, in ²	Tensile Strength PSI	Lap Shear Strength PSI	Percent Elong.	P	Δ	Modulus*, Initial PSI	Mode of Failure Percent Adhesion
Tensile #1	0.02	1.0	181		380				100
Tensile #2	0.08	1.0	245		527				100
Lap Shear #1	0.05	1.0		222		40	0.044	50	95
#2	0.05	1.0		228		50	0.052	50	95

$$*\text{Modulus} = \frac{(P)}{(A)} \frac{(t)}{(\Delta)}$$

was selected for modification with glass and phenolic microballoons. It was reasoned that the lower viscosity material would accommodate the largest volume loading of microballoons; thus it would produce the lowest density syntactic foam adhesive. Three types of microballoons, 3M's B-22A, Emerson Cumming's IG-101, and Union Carbide's BJO-0930, were obtained for use in the program. Work with the latter two was soon abandoned because they caused the GE RTV-560 to cure without the addition of catalyst. It was surmised that moisture on the large surface area of these two types of microballoons caused the cure. Attempts were made to dry the IG-101 and BJO-0930 microballoons, but this did not completely mitigate the problem with the IG-101 microballoons and at the 350°F drying temperature the phenolic microballoons began to smoulder.

Formulation work was continued with the B-22-A microballoons and tested along with the Raybestos Manhattan RL-1973/GE RTV-560 system discussed in paragraph 3.3. In Table VI, formulas 7 and 8 are GE RTV-560 filled with 14 and 7 parts by weight of B-22-A microballoons, respectively. Formula 7 contains equal volumes of GE RTV-560 and B-22-A microballoons while formula 8 contains a ratio of 100 to 50 parts by volume of the two materials. Density of the resulting formulations were reduced by 50 and 25 percent, respectively. In contrast, modulus of formulas 7 and 8 as compared to the control (100 percent GE RTV-560) are increased by over 100 percent. This is to be expected when one considers the high modulus of the glass microballoons as compared to the low modulus of the silicone rubber based GE RTV-560. In view of this fact; i.e., the increased modulus imparted by glass microballoons, work on modifying the GE RTV-560 with glass microballoons stopped in favor of the more promising development of the RL-1973 closed cell silicone rubber sponge. Data on adhesion in tension and shear are tabulated in Table VI and are shown graphically in Figures 12 and 13.

3.3 RAYBESTOS MANHATTAN'S CLOSED-CELL SILICONE RUBBER SPONGE, RL-1973, BONDED BETWEEN GE RTV-560

Silicone RTV liquid polymers are available as foam-in-place materials. These were considered only briefly in this program because it would be almost impossible to obtain uniform density glue lines in any kind of production process. Convair Aerospace has used Raybestos Manhattan's RL-1973 (a low-density, low-modulus

TABLE VI TENSILE AND SHEAR STRENGTH OF FORMULATED GE RTV-560 AND RAYBESTOS-MANHATTAN
 RL-1973 CLOSED CELL SPONGE IN BONDED ALUMINUM TO ALUMINUM
 LAP AND BUTT JOINTS

		.064" Glue Lines, Tested at 75°F				
Formula No.	Z	8	Sponge	Control	Control	(Dumbbell Specimens)
Material	PARTS BY WEIGHT					
GE RTV-560	100	100		100		-
3M's B-22-A Glass spheres	14	7		-		-
Eccospheres - IG - 101	-	-		-		-
RL 1973 Sponge	-	-	100*	-		100
1 sq. in. butt joints - SS - 4004 Prime, 2024 T851	452	409	107	276		W/L direction 48/56
Tensile Adhesion, psi	67	64	95	40		180/220
Ultimate Elong., %	100	100	100 (in sponge)	97		
% Cohesive Failure						
Tensile Modulus, psi	486	427	103	469		
Initial	934	854	103	858		
Final						
1 sq. in. single overlap joints - SS - 4004 Prime, 2024 T81	280	250	92	281		
Shear, psi	100	100	97	100		
% Cohesive failure			(in sponge)			
Shear Modulus, psi	187	173	31	75		
Initial	307	273	64	225		
Final	0.73	0.085	0.46**	1.42		0.29
Density, gm./cc						

* 0.06 sponge with 5-mil bond lines of GE RTV-560 on either side
 ** Calculated using densities of sponge and GE 560

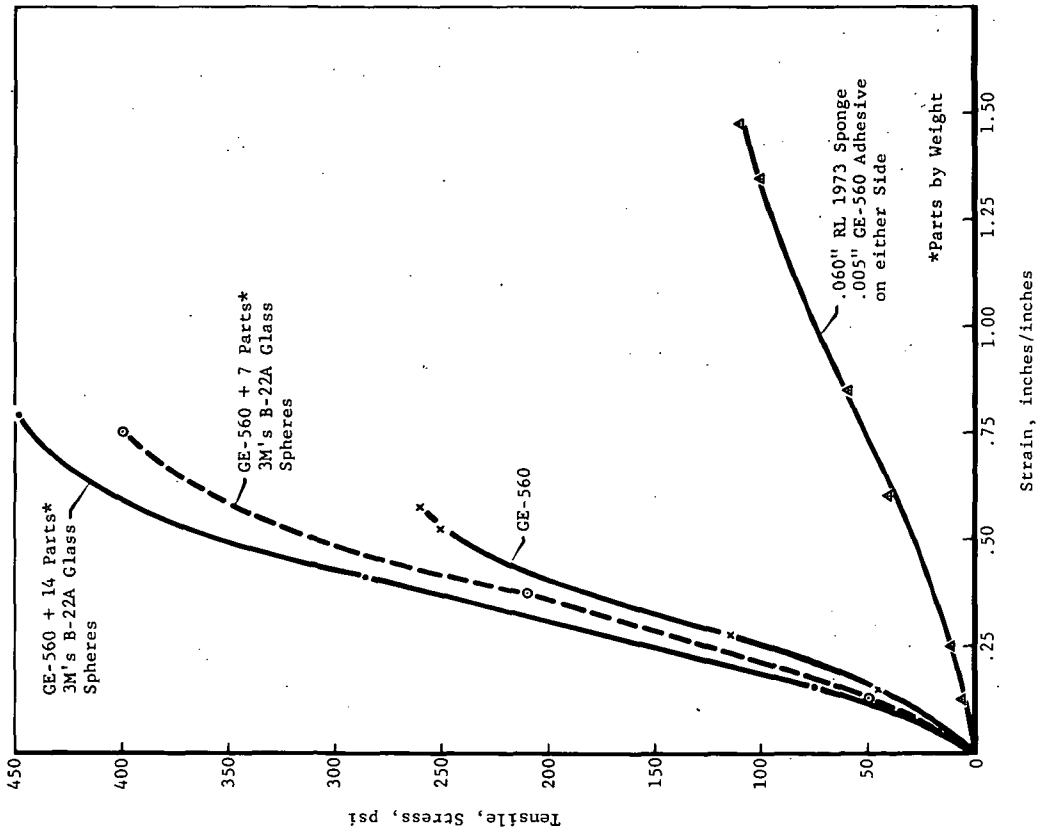


Figure 12 Tensile Stress-Strain of Aluminum to Aluminum Bonded Butt Joints 0.064" Glue Lines (Approx.) Tests at 75°F

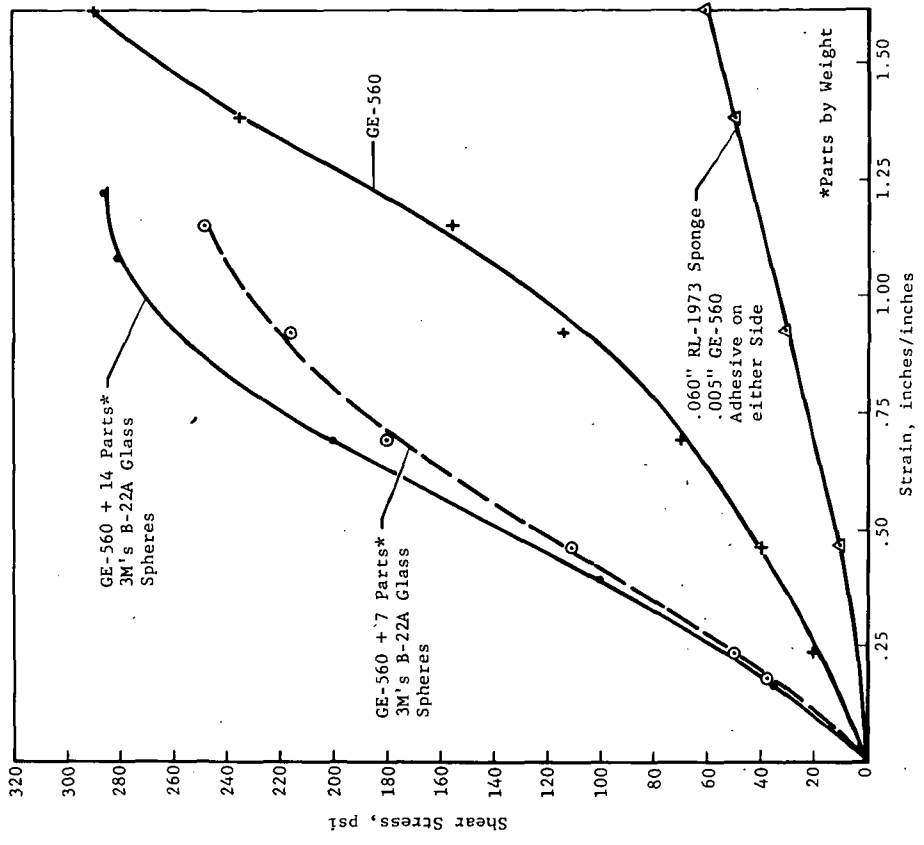


Figure 13 Shear Stress-Strain of Aluminum to Aluminum Bonded Single Overlap Joints 0.064" Glue Lines (Approx.) Tests at 75°F

sponge) in numerous applications on airplanes and found it to be a highly reliable material. Therefore, it was brought into this program. RL-1973 can be sliced to any desired thickness and bonded in place with most any RTV silicone adhesive. Since GE RTV-560 was one of the adhesives to be fully evaluated and characterized in this program, it was selected as the adhesive to be used in combination with the RL-1973 sponge.

Preliminary data on RL-1973/GE RTV-560 is shown in Table VI in direct comparison to GE RTV-560 alone and GE RTV-560 filled with 100 and 50 percent by volume glass microballoons. It is quite obvious that the RL-1973/GE RTV-560 system possesses the lowest modulus and has about one-third the density of GE RTV-560. As mentioned in paragraph 3.2, these data are shown graphically in Figures 12 and 13. In adhesion in tension and shear, the RL-1973/GE RTV-560 shows about one-third the strength of GE RTV-560 alone, but this (approximately 100 psi) should be adequate for the intended application.

3.3.1 Effect of Reduced Pressure on RL-1973 Sponge

The RL-1973 sponge exhibits linear and volumetric changes when exposed to variations in pressure. The magnitude of change has been estimated by placing specimens of known dimensions upon standard grids in a variable pressure chamber and noting dimensional changes versus time at pressure. The sponge expands immediately when subjected to a mechanical pump vacuum of 29.5 in. Hg. (Figure 14), but it begins returning to its original dimensions as evacuation of the cells continues. On release of the vacuum, the sponge immediately contracts and again begins returning to its original dimensions as pressure in the cells returns to atmospheric. This characteristic may or may not be a drawback. Comparable data on the solid RTV adhesives was not determined.

3.3.2 Selection of RL-1973/GE RTV-560 As the Fourth Adhesive System in the Program

Since the RL-1973/GE RTV-560 adhesive system proved to be the lowest in density and modulus of all those investigated, the NASA, MSC technical monitor and Convair Aerospace agreed that it would be the fourth adhesive system to be tested for establishment of complete design allowables data.

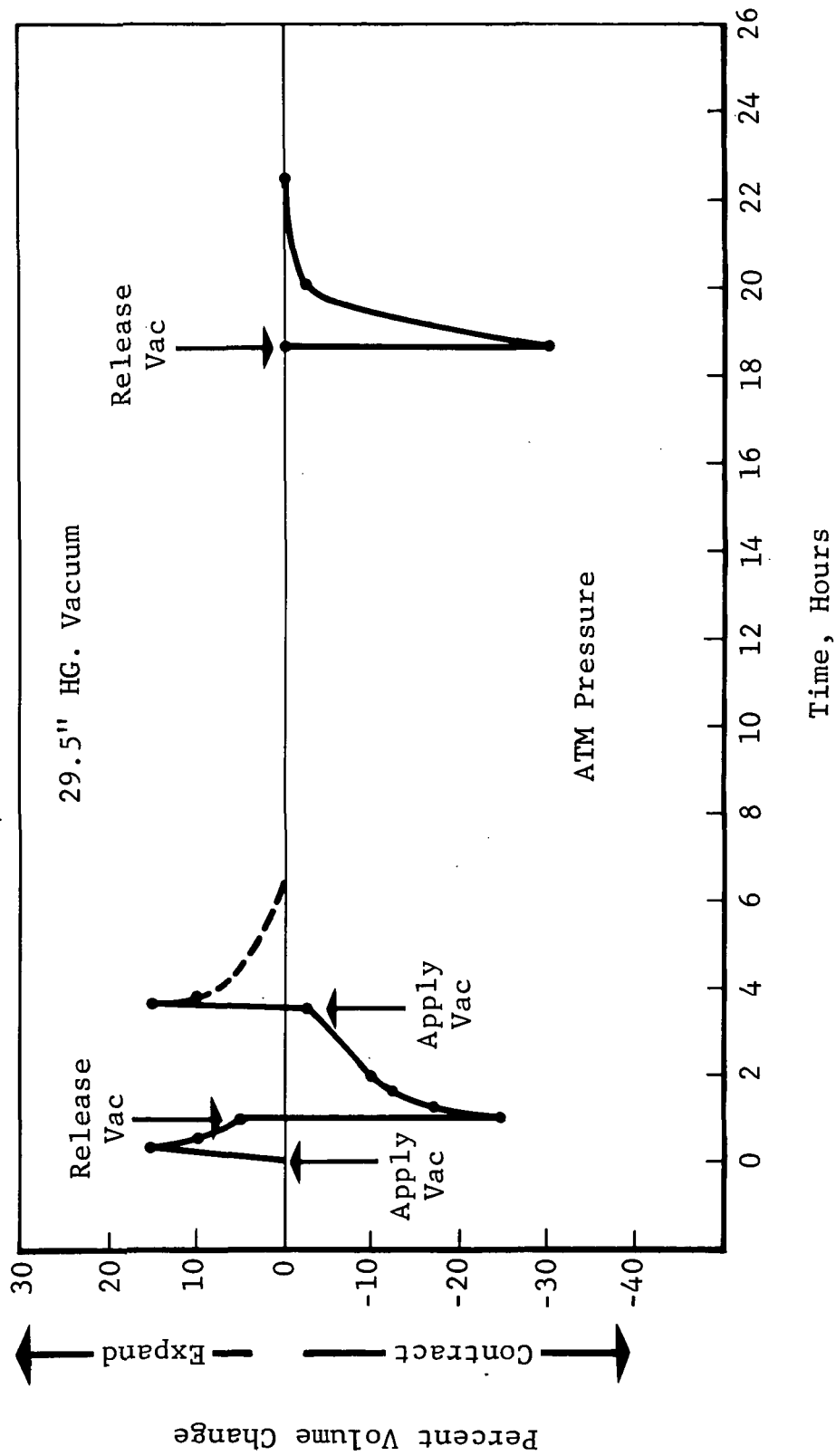


Figure 14 Volume Change Vs. Time at Vacuum and Pressure: RM RL-1973 Sponge

3.4 DENSITY OF ADHESIVES

Density at room temperature was determined using the hydrostatic method described in ASTM-D-297 Section 17(C). Essentially this involves weighing the specimen in air and water, deducting tare (hanging wire), etc. This calculation was as follows:

$$\text{Density} = \frac{A}{A-(B-C)}$$

Where A = weight of specimen

B = weight of specimen and supporting wire in water

C = weight of supporting wire in water

Data for the specified adhesives and modified formulations are shown in Table VII.

TABLE VII DENSITY AT ROOM TEMPERATURE ASTM-D-297, 17(C)
FIVE SPECIMENS PER TEST

RTV-560 Standard	Density, Grams/cc 1.4044 1.3997 1.4018 1.3984 1.4004 Average 1.4009
GE RTV-560 Vacuum Deaerated	Density, Grams/cc 1.4211 1.4208 1.4184 1.4194 1.4192 Average 1.4198
DC 93-046	Density, Grams/cc 1.0845 1.0846 1.0845 1.0847 1.0845 Average 1.0846
MMC SLA 561	Density, Grams/cc 1.0501 1.0472 1.0476 1.0507 1.0474 Average 1.0486
RM/RL-1973 Silicone Sponge Thickness (Avg.) = 0.059"	Density, Grams/cc 0.3065 0.2997 0.2998 0.2999 0.2992 Average 0.3010

SECTION 4
MECHANICAL PROPERTIES

SECTION 4
MECHANICAL PROPERTIES

4.1 ADHESION IN TENSION

The intended adhesive application dictated that tensile properties should be determined using flatwise adhesion specimens. These specimens were two solid metal cylinders bonded with an 0.060-inch-thick layer of the test adhesive. Properties determined were ultimate tensile strength, ultimate elongation, and percent cohesive failure to metal. The load deflection curves obtained with each specimen were used to develop stress-strain curves.

4.1.1 Test Method

Test specimens consisted of two 1.125-inch-diameter 2024-T81 solid aluminum cylinders bonded with an adhesive glue line thickness of 0.060 inch (Figure 2, Section 2). The lay-up fixture shown in this figure was used to ensure uniform bond line thicknesses and parallel surfaces of the test cylinders. After the adhesive was cured, the specimens were tested by loading the specimen normal to the cylinder faces, Figure 15, in a Scott CRE 2K or Instron test machine.

Actual bond line thicknesses were measured before testing. Deformation during testing was recorded autographically and percent elongation was calculated as follows:

$$\%E = \frac{\text{deformation of adhesive}}{\text{original thickness}} \times 100.$$

To ensure that only deformation of the adhesive was used in the determination of ultimate elongation, a solid cylinder was loaded at each test temperature and a load deformation curve determined. This curve represented the extraneous extensions inherent in the test set-up in addition to the deformation of the cylinder. This value was subtracted from the deformation recorded for each test specimen before calculation of ultimate elongation or development of stress-strain curves.

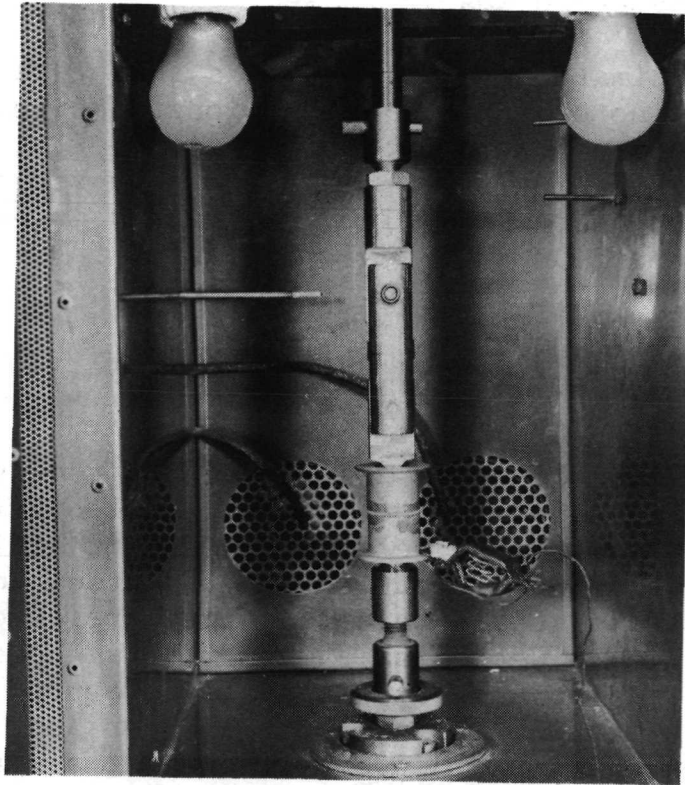


Figure 15 Cylinder Adhesion Test Setup

Since the bonded area was 1 square inch, load in psi was read directly from the load deflection curves. Strain rate was 0.4 inch/inch/minute.

4.1.2 Results and Discussion

Average tensile and ultimate elongation values are shown in Table VIII and Figures 16 and 17. These values are averages of three specimens. The average percent cohesive failures of the specimens at each temperature are also shown. Individual specimen values are shown in Appendix II.

In general, the data show that the tensile strengths increase as the test temperature decreases. Also the percent cohesive failure decreases with decrease in test temperature with the exception of the RTV-560/RL-1973 specimens, which generally exhibit 100 percent cohesive failure. At temperatures above 350°F, rapid deterioration of all materials occurs (Figure 16). It was also

noted during the tensile tests that MMC SLA 561 emitted dense white fumes at approximately 450°F. These fumes soon dissipated as the temperature was increased.

A plot of ultimate elongation versus temperature is shown in Figure 17. As noted, the ultimate elongation increases as the temperature decreases to a point just above the brittle point of the material followed by a rapid decrease in elongation as the temperature decreases below the brittle point. This corresponds to a maximum shear value as shown in Section 4.2.

4.1.3 Data Analysis

Flatwise tension data was analyzed using regression and tolerance limit techniques to give statistical confidence limits and allowables. Statistical relationships were derived for stress versus strain and ultimate strength versus temperature test results. Stress-strain relationships were developed using regression analysis to determine a mathematical model which best represented the test data at each test temperature. In addition to the "best-fitting" relationship, upper and lower confidence limits were determined for the relationship at a statistical confidence limit of 95 percent. Thus, if the sample tested were an accurate representation of the adhesive stress-strain characteristics, then 95 percent of all additional samples tested may be expected to have "best-fitting" stress-strain relationships which would be contained by the established confidence limits. Data analysis also included establishment of a best-fitting relationship and confidence limits for ultimate strength as a function of absolute temperature. In addition, strength allowables were established using the lower confidence limit of the mathematical model as a baseline and calculating one-sided tolerance limits for 90 percent and 99 percent confidence levels. The strength allowables at 90 and 99 percent confidence levels reduced from a "typical" value based on a 95 percent confidence level are analogous to the definitions of B- and A-basis allowables, respectively, as given in MIL-HDBK-5A, and have been denoted as B' and A' allowables in this report.

4.1.3.1 Methodology

The methodology associated with regression and tolerance limit calculations is summarized in Appendix II.

Table VIII ULTIMATE TENSILE STRENGTH AND ELONGATION AVERAGE VALUES

Test Temp. °F	GE RTV-560			DC 93-046			MMC SLA-561			RTV-560/RL-1973		
	psi	%E	% Coh. Failure	psi	%E	% Coh. Failure	psi	%E	% Coh. Failure	psi	%E	% Coh. Failure
-270	1997	51	55	2218	41	50	7620	39	30	933	45	100
-200	1708	55	60	2692	43	65	5235	59	15	642	53	100
-175	1034	44	30	2470	45	80	1430	29	0	390	82	100
-150	579	136	65	1513	43	85	357	46	0	281	124	100
- 65	387	56	85	259	175	80	232	32	0	164	142	100
RT	276	31	95	121	153	80	126	11	100	99	99	97
300	191	19	100	57	102	100	130	25	100	48	62	100
350	177	23	100	52	82	100	105	18	100	48	62	100
550	26	7	100	0	0	sponged	47	15	100	15	54	100
600	2	26	90	0	0	sponged	31	20	100	3	22	100

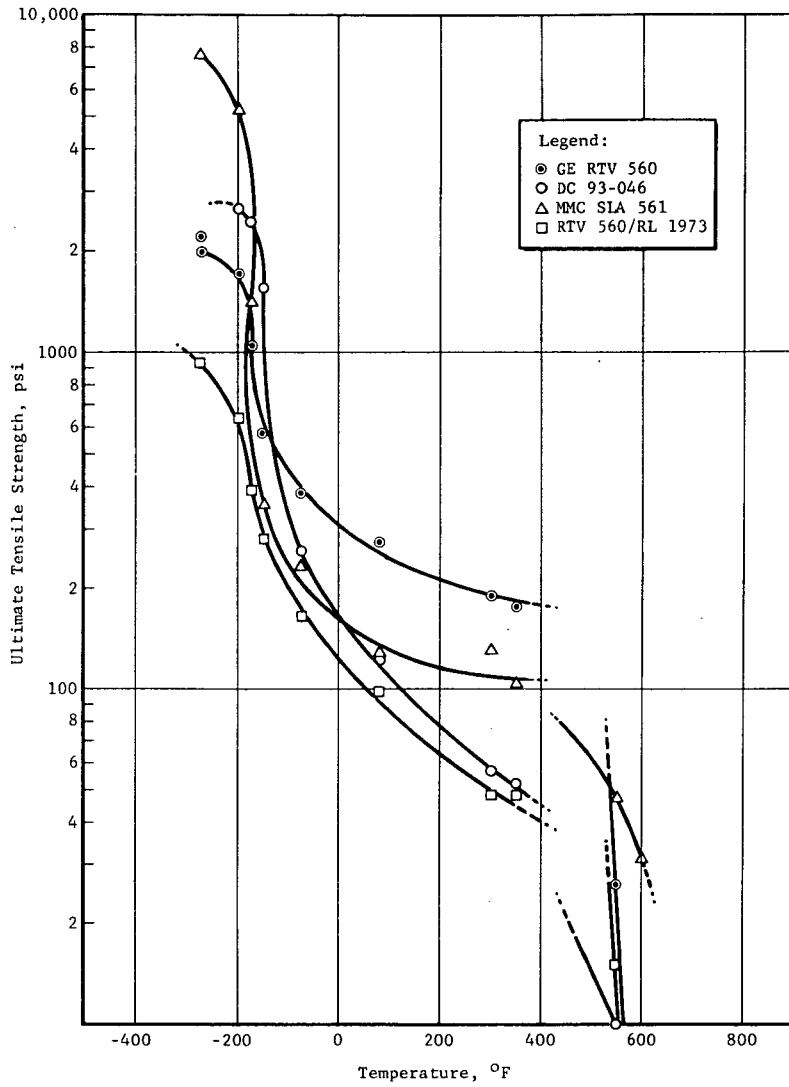


Figure 16 Tensile Strength Vs. Temperature

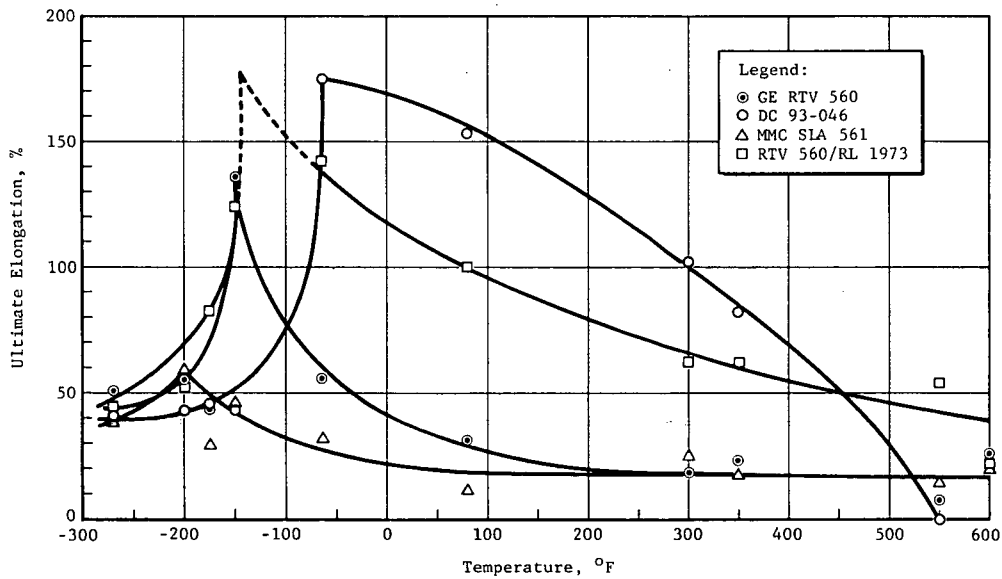


Figure 17 Ultimate Elongation Vs. Temperature

4.1.3.2 Compilation of Test Data

Continuous load-versus-deflection curves through ultimate load were obtained autographically for each specimen tested in flatwise tension. Values of deflection were read from each curve for several values of load including ultimate load. Strain and stress were calculated for each pair of load-deflection data read for each specimen tested. The calculations are summarized in Appendix III.

The deflection data read directly from load-deflection curves was corrected by subtracting empirical correction factors before calculating values of strain. The empirical correction factors were determined by loading solid metal details of the same gauge and configuration used in flatwise tensile specimens on the same test machines and temperatures used in the bonded specimen tests. The correction factors are summarized below:

Test Machine	Method	Material	Temperature Range (°F)	Correction Factor (in/lb)
Scott Tester	Tensile	RTV-560 only	+350 to -175	0.0000346
Instron	Tensile	RTV-560 only	-200 & -270	0.000012
Instron	Tensile	SLA-561, DC93046, and RTV-560/RL-1973	+350 to -270	0.000012

Test results for 550°F and 600°F conditions were not analyzed. The results at these temperatures indicate the materials do not have sufficient/reliable strength characteristics to justify statistical calculations.

Test results for low temperatures (less than -150°F) are generally highly erratic and in most cases have not been analyzed.

A summary of the test conditions studied for stress-strain regression analyses is given in Table IX.

4.1.3.3 Tensile Stress-Strain Data

The regression coefficients, standard deviations, and correlation coefficients determined for each strain-strain test condition are summarized in Table X. Regression analyses of tensile stress-strain data gave a wider range of "r" (correlation coefficient) values than for shear data (Reference paragraph 4.2.3); however, it was possible to perform the analyses

Table IX SUMMARY OF TENSILE STRESS-STRAIN CONDITIONS
REGRESSION ANALYSIS

Material	TEST TEMPERATURE °F (3)									
	-270	-200	-175	-150	-65	80	300	350	550 &	600
RTV-560	0.95	0.96	0.79	0.83	0.98	0.98	0.79	0.75		
SLA-561	(1)	(1)	(1)	0.94	0.90	0.96	0.90	0.80	(2)	
DC 93-046	0.90	0.88	0.92	0.72	0.96	0.65	0.83	0.90		
RTV-560/RL-1973	0.51	0.88	0.94	0.99	0.998	0.99	0.95	0.91		

Notes:

- (1) No analysis conducted - strain data included negative results or decreases in strain for increases in stress.
- (2) No analysis conducted - strength data either too low or not obtained because specimens degraded too severely to test.
- (3) Numerical values in Table are values of correlation coefficient.

Table X RESULTS OF TENSILE STRESS-STRAIN REGRESSION

MATERIAL	TEMP (°F)	n	ln A	B	S $\epsilon \cdot \sigma$	r	r _{upper}	r _{lower}
RTV-560	-270	19	-4.87	0.558	0.13797	0.95	0.98	0.86
	-200	19	-0.716	0.167	0.03631	0.96	0.98	0.89
	-175	21	-0.363	0.102	0.06205	0.79	0.91	0.53
	-150	21	-5.55	0.833	0.50409	0.83	0.93	0.60
	-65	21	-4.64	0.648	0.12602	0.87	1.0	0.95
	80	21	-4.61	0.591	0.10089	0.98	1.0	0.95
	300	15	-4.25	0.472	0.43687	0.79	0.93	0.45
350	15	-3.35	0.346	0.36028	0.75	0.91	0.37	
SLA-561	-150	20	-3.58	0.452	0.16731	0.94	0.97	0.85
	-65	18	-3.98	0.491	0.21756	0.90	0.96	0.73
	80	12	-5.08	0.605	0.15067	0.96	0.99	0.83
	300	12	-3.28	0.391	0.15917	0.90	0.98	0.62
	350	11	-3.89	0.470	0.28307	0.80	0.94	0.37
DC-93-046	-270	19	-6.94	0.799	0.32269	0.90	0.96	0.74
	-200	21	-5.70	0.620	0.28572	0.88	0.95	0.73
	-175	21	-5.05	0.547	0.18994	0.92	0.96	0.80
	-150	16	-3.57	0.351	0.26862	0.72	0.89	0.32
	-65	11	-7.27	1.34	0.27661	0.96	0.99	0.81
	80	27	-0.688	0.319	0.39246	0.65	0.83	0.35
	300	17	-2.71	0.638	0.43835	0.83	0.93	0.58
	350	27	-3.17	0.736	0.26578	0.90	0.95	0.75
RTV-560/RL-1973	-270	21	-2.66	0.269	0.50266	0.51	0.76	0.10
	-200	18	-2.36	0.257	0.14430	0.88	0.96	0.76
	-175	21	-1.49	0.00312	0.15753	0.94	0.96	0.86
	-150	21	-1.64	0.00681	0.09128	0.99	1.0	0.97
	-65	10	-2.17	0.473	0.03261	0.998	1.0	0.96
	80	14	-3.95	0.853	0.05316	0.99	1.0	0.96
	300	18	-3.65	0.782	0.17068	0.95	0.97	0.86
	350	22	-3.09	0.659	0.17720	0.91	0.96	0.77

for all test temperatures $\leq 350^{\circ}\text{F}$ for all materials except SLA-561. Data for SLA-561 for temperatures $< -150^{\circ}\text{F}$ was too erratic to be characterized by a math model and was not analyzed. In the case of tensile loading, data at temperatures below the glass-transition temperature gave values of "r" similar to those observed for data at higher temperatures. Glass-transition temperatures are characterized by abrupt changes in thermal properties. Based on results given previously, approximate glass-transition temperatures are listed below.

Material	Approximate Glass Transition	Abrupt Changes in
DC-93-046	-50°F	Specific heat, thermal conductivity, and expansion
SLA-561	-175°F	Thermal conductivity and expansion
RTV-560	-175°F	Thermal conductivity and expansion
RTV-560/RL-1973	$-100^{\circ}\text{F}/-175^{\circ}\text{F}$	Thermal conductivity and expansion

4.1.3.4 Tensile-Strength-Temperature Data

Ultimate strength and strain results for each specimen are included in Appendix III.

Regression analyses were also conducted for ultimate strength-temperature data from tests in flatwise tension for RTV-560, DC 93-046, SLA-561, and RTV-560/RL-1973. The results are summarized in Table XI.

The analyses used temperature (degrees R) as the independent variable and ultimate strength as the dependent variable. Temperature range included in the analyses was 260°R to 810°R (-200°F to 350°F). Data outside this range at test temperatures of 190°R (-270°F), 1010°R (550°F), and 1060°R (600°F) was deleted from the analysis. These results were not compatible with the results at the other temperature conditions.

General observations relative to tensile strength are

1. When strength-temperature data is plotted on semi-logarithmic graph paper (Figure 18) two straight lines can be fitted to the data. The lines are distinct for RTV-560/RL-1973, SLA-561, and RTV-560 adhesive and intersect approximately at the glass-transition temperature. Fitting the lines to

Table XI RESULTS OF FLATWISE TENSILE STRENGTH-TEMPERATURE REGRESSION

MATERIAL	n	TEMP RANGE (°R)	ln A	B	S σ·T ln (psi)	r	r _{upper}	r _{lower}
RTV-560	9	260-310	13.01	-0.0214	0.17369	0.95	0.97	0.75
RTV-560	12	395-810	6.66	-0.00186	0.06431	0.98	0.99	0.90
DC-93-046	12	260-395	13.16	-0.01938	0.42210	0.94	0.97	0.78
DC-93-046	13	395-810	6.76	-0.00360	0.40790	0.85	0.95	0.55
SLA-561	9	260-310	22.21	-0.05262	0.28660	0.98	1.0	0.92
SLA-561	12	395-810	5.90	-0.00152	0.19302	0.83	0.95	0.48
RTV-560/RL-1973	12	190-310	8.79	-0.00981	0.15881	0.95	0.97	0.81
RTV-560/RL-1973	13	395-810	6.21	-0.00289	0.10814	0.98	0.99	0.91

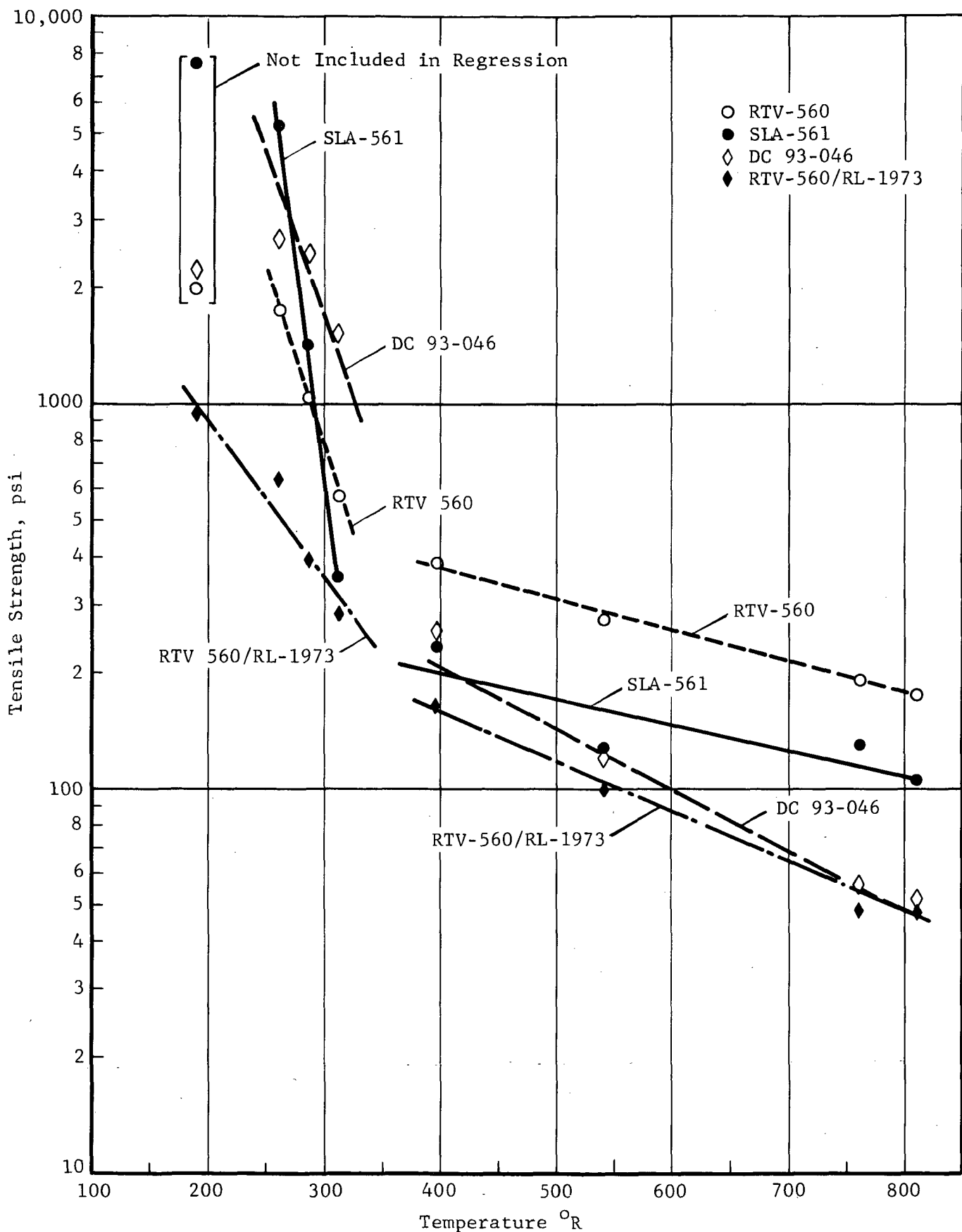


Figure 18 Average Flatwise Tensile Strength of Adhesive Materials

DC 93-046 material data was less straightforward; the lines fitted to this data were based on the trend observed on the other materials using the glass-transition temperature to approximate the intersection point.

2. SLA-561 specimens generally failed adhesively at sub-zero test conditions and cohesively for room and elevated temperature conditions.
3. RTV-560 specimens generally failed cohesively at temperatures of 395^oR (-65^oF) and above. Failures below 395^oR were mixed.
4. DC 93-046 specimens generally failed cohesively at all test temperatures.

4.1.3.5 Data Reduction and Presentation

Regression analyses were conducted using Convair Aerospace computer program AON to calculate the values of ln A, B, [C], Sy.x, and r. These values (except the C matrix) were presented in Tables X and XI. The tables also include the 95 percent confidence limits for r.

Confidence limits on the best-fitting regression line were calculated on a Hewlett-Packard desk computer. The desk computer was also used to calculate B' and A' allowables in the case of ultimate strength-temperature data reduction. The tensile strain confidence limits for specific values of tensile stress are summarized in Appendix IV. Ultimate strength confidence limits and allowables for specific test temperatures are summarized in Appendix V.

Data is presented graphically as follows:

- o Figures 19 through 22 Tensile Strength - Temperature
- o Figures 23 through 52 Tensile Stress-Strain

In the case of stress-strain data, the regression analysis stress is the independent variable, but the variables were reversed in the graphs to allow plotting the data in the manner familiar to engineers.

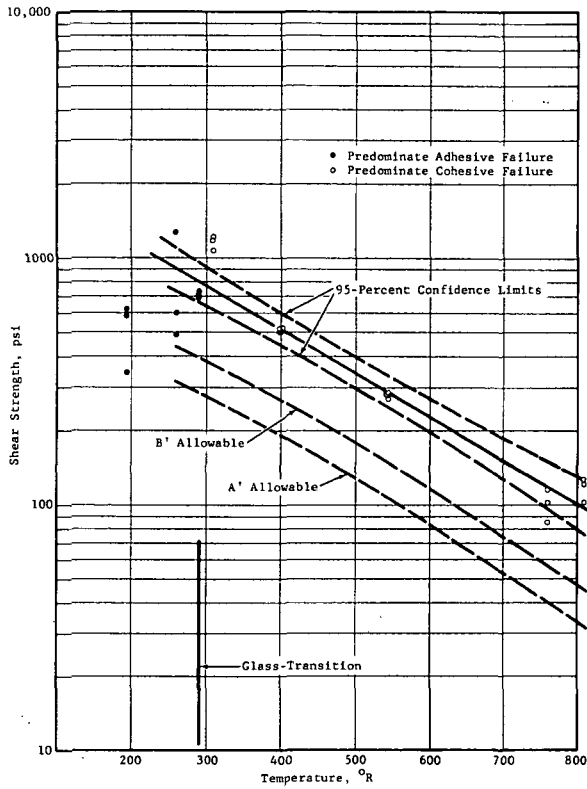


Figure 19 Tensile Strength Vs. Temperature
RTV-560 Material

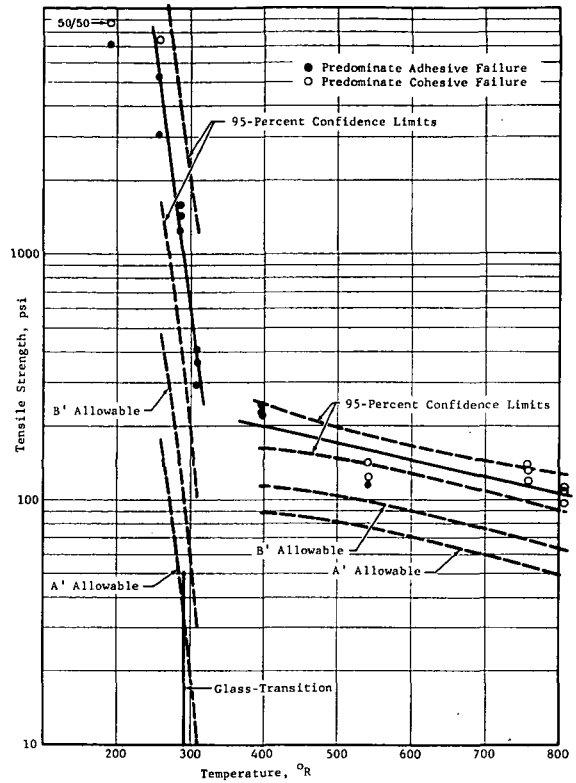


Figure 20 Tensile Strength Vs. Temperature
SIA-561 Material

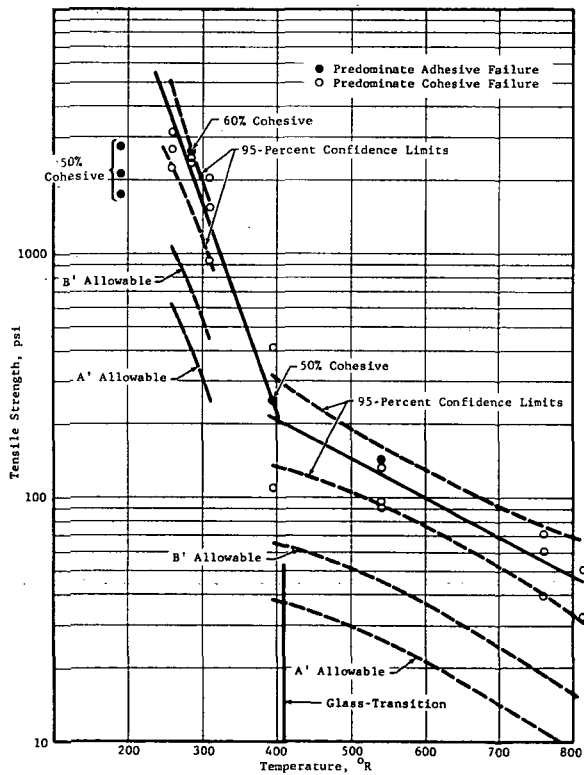


Figure 21 Tensile Strength Vs. Temperature
DC 93-046 Material

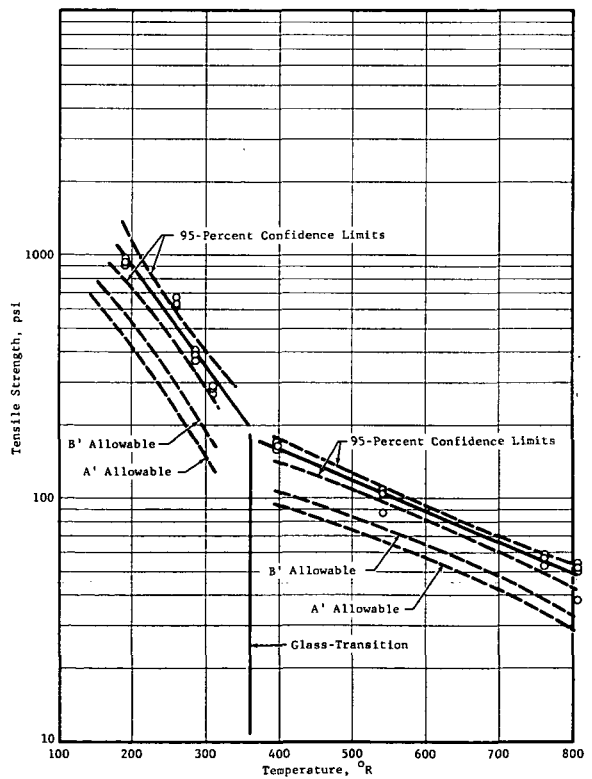


Figure 22 Tensile Strength Vs. Temperature
RTV 560/RL-1973

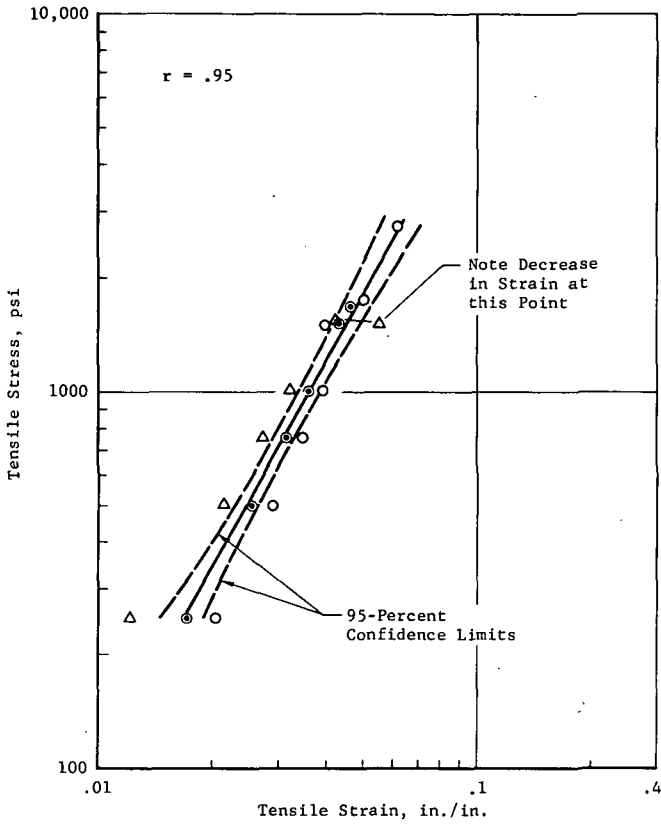


Figure 23 Tensile Stress-Strain RTV-560 (-270°F)

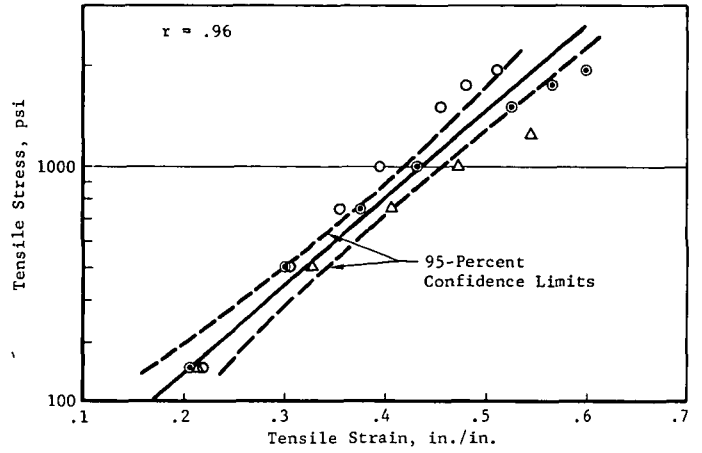


Figure 24 Tensile Stress-Strain RTV-560 (-200°F)

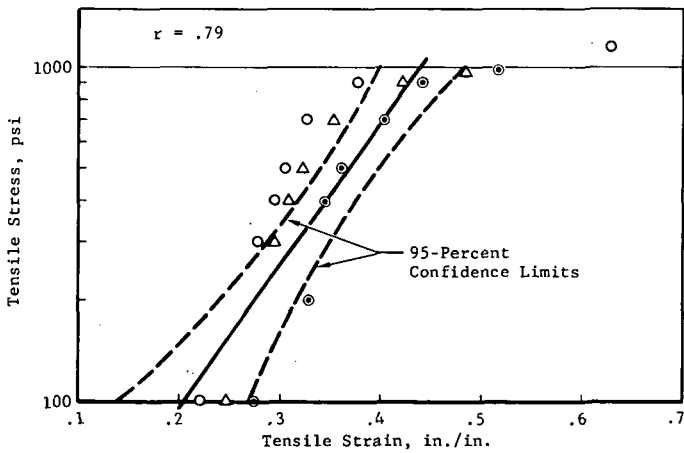


Figure 25 Tensile Stress-Strain RTV-560 (-175°F)

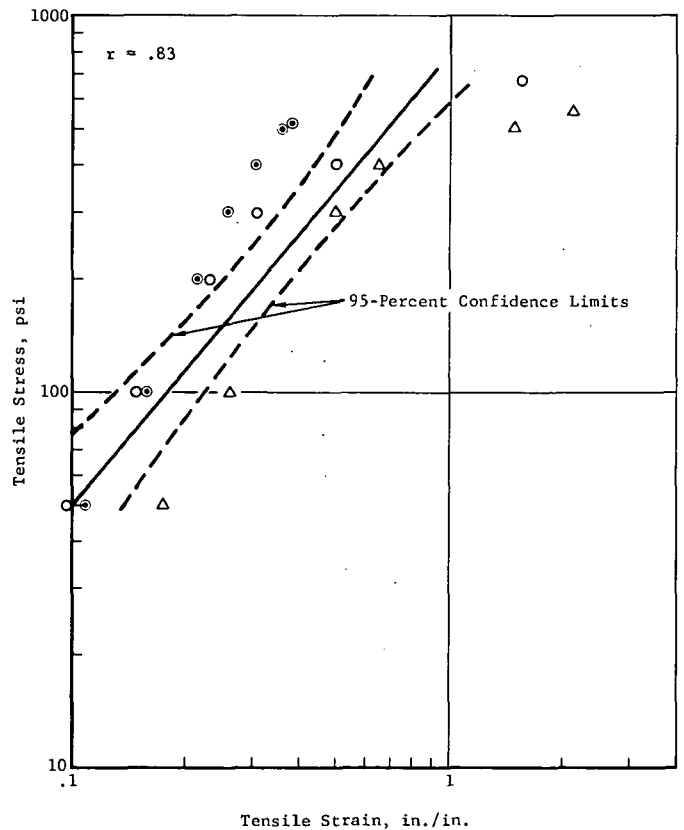


Figure 26 Tensile Stress-Strain RTV-560 (-150°F)

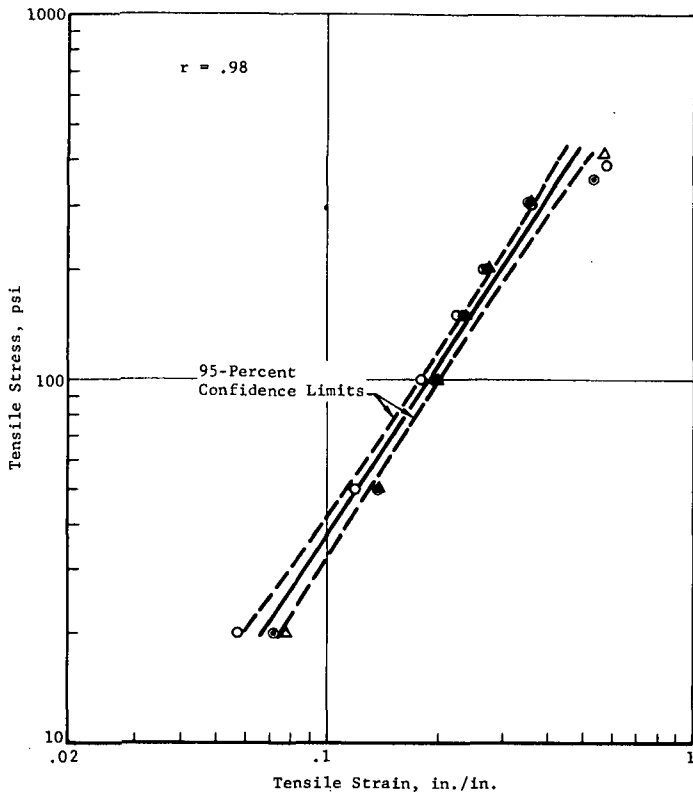


Figure 27 Tensile Stress-Strain RTV-560 (-65°F)

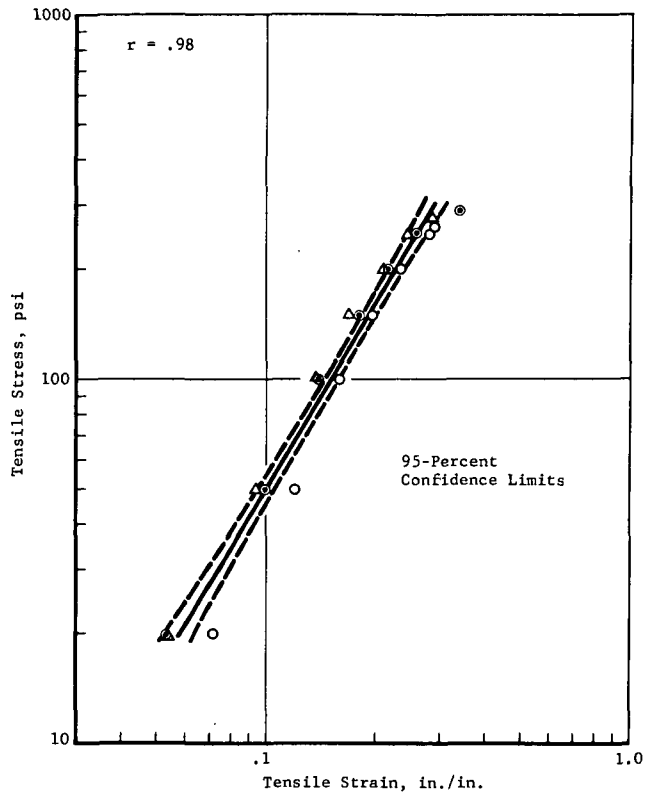


Figure 28 Tensile Stress-Strain RTV-560 (80°F)

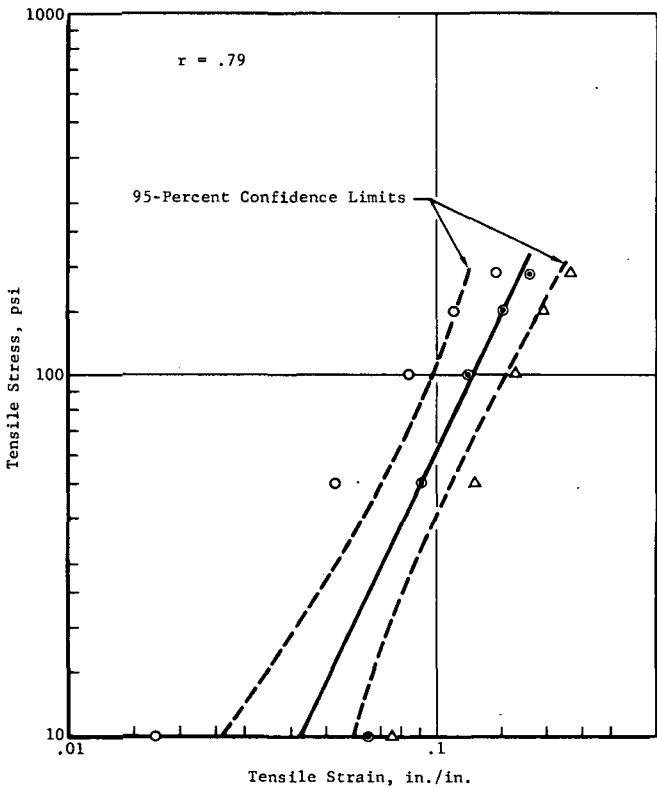


Figure 29 Tensile Stress-Strain RTV-560 (300°F)

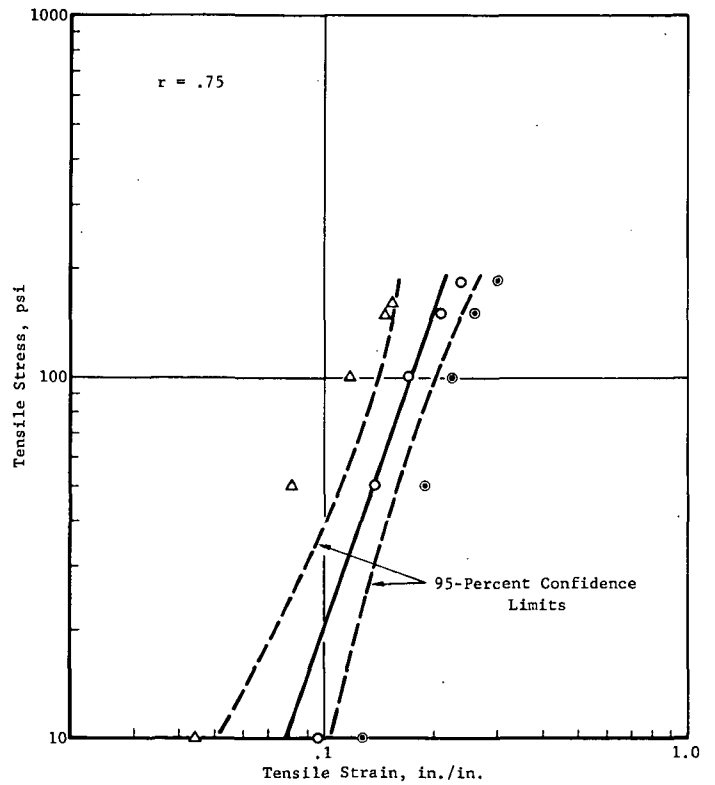


Figure 30 Tensile Stress-Strain RTV-560 (350°F)

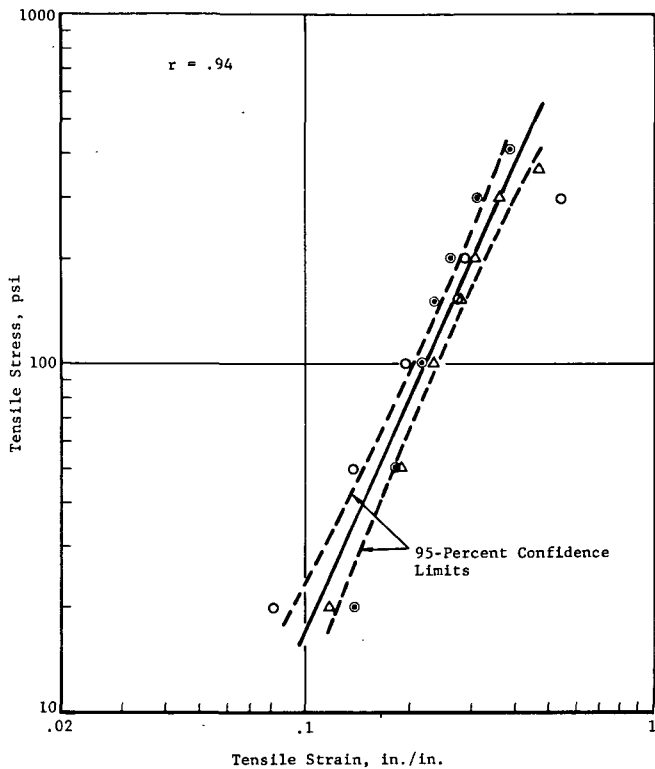


Figure 31 Tensile Stress-Strain SLA-561
(-150°F)

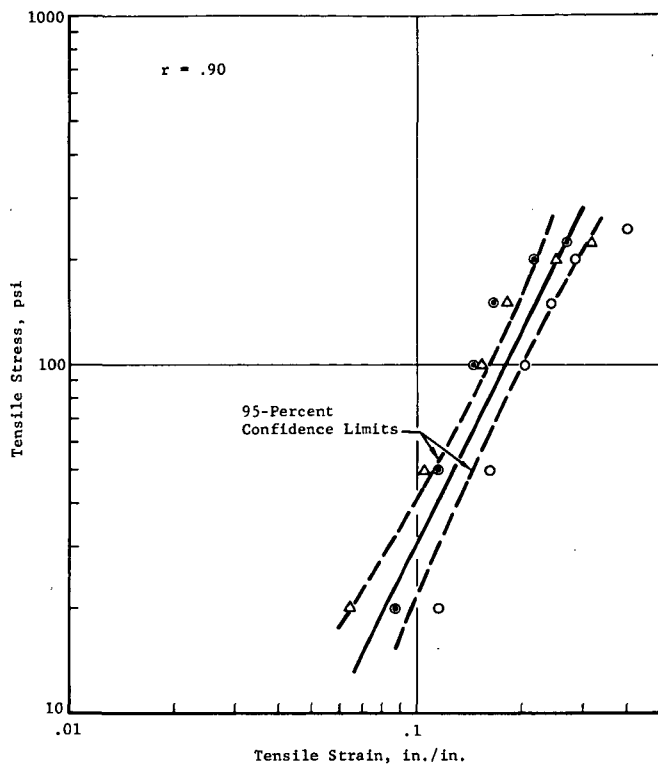


Figure 32 Tensile Stress-Strain SLA-561
(-65°F)

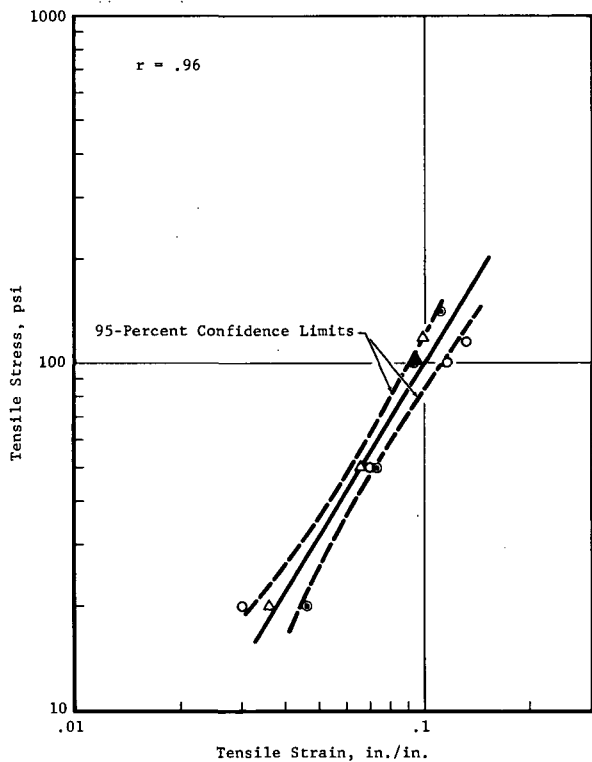


Figure 33 Tensile Stress-Strain SLA-561
(80°F)

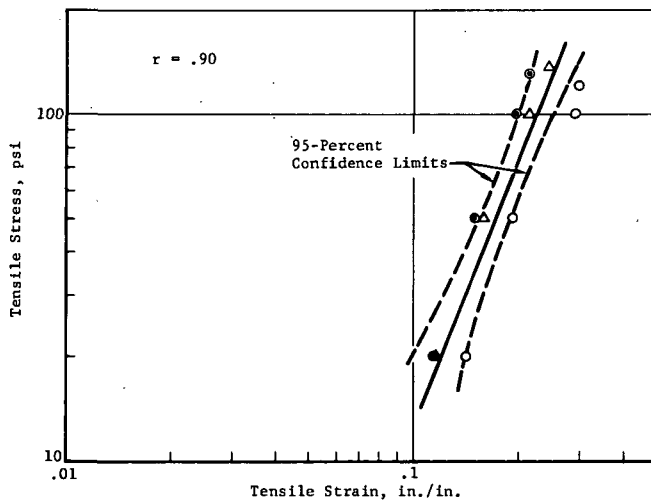


Figure 34 Tensile Stress-Strain SLA-561
(300°F)

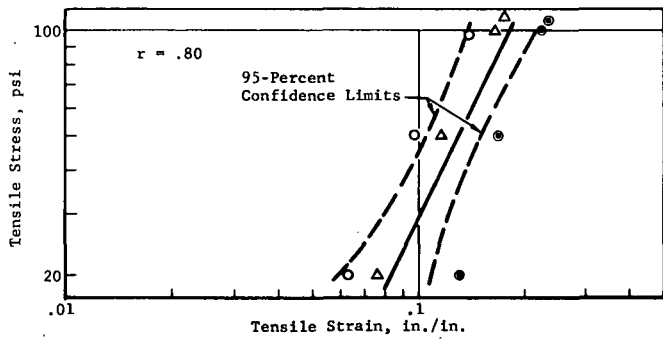


Figure 35 Tensile Stress-Strain SLA-561 (350°F)

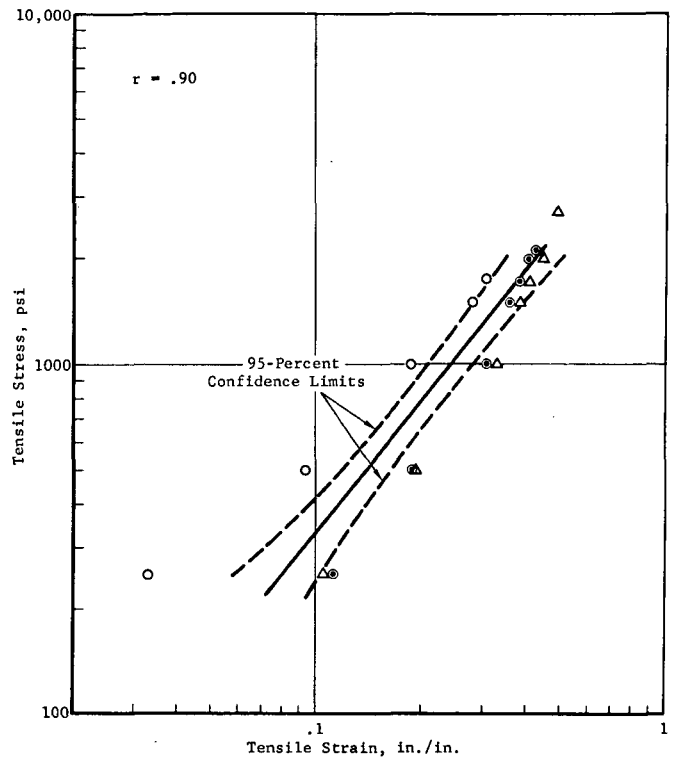


Figure 36 Tensile Stress-Strain DC 93-046 (-270°F)

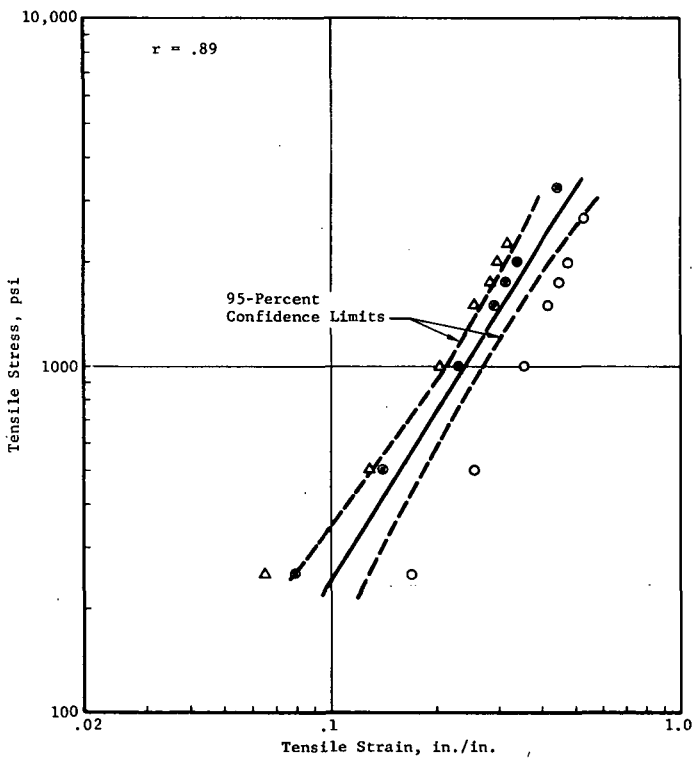


Figure 37 Tensile Stress-Strain DC-93-046 (-200°F)

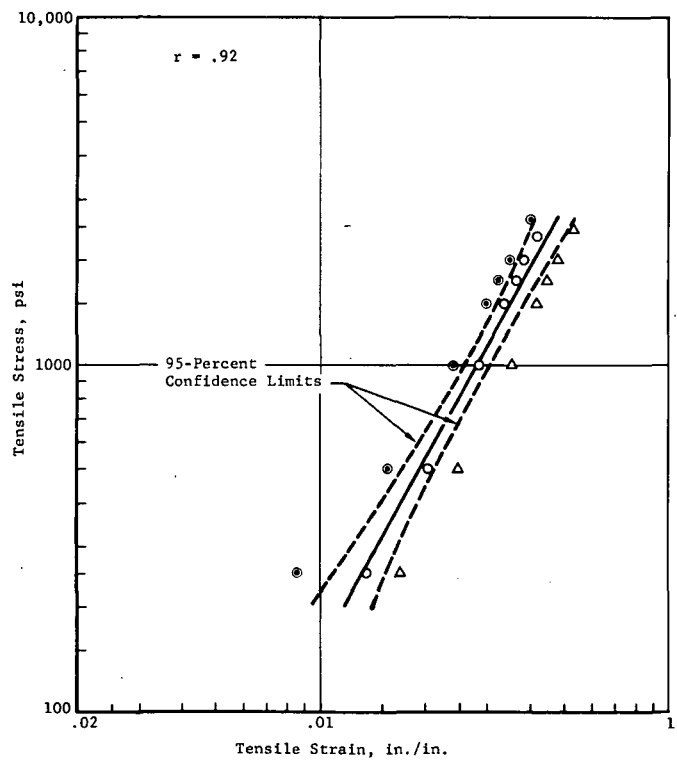


Figure 38 Tensile Stress-Strain DC-93-046 (-175°F)

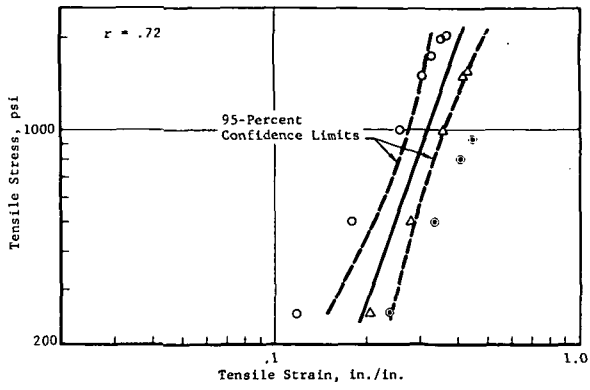


Figure 39 Tensile Stress-Strain DC-93-046 (-150°F)

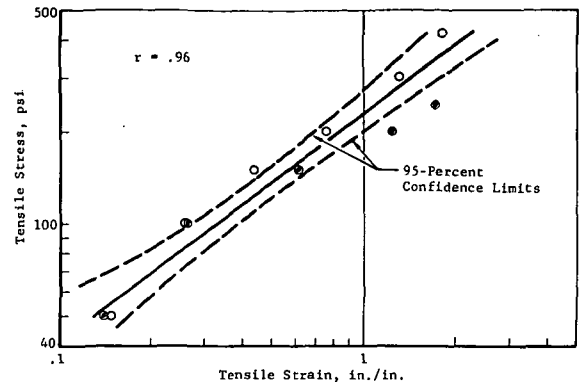


Figure 40 Tensile Stress-Strain DC-93-046 (-65°F)

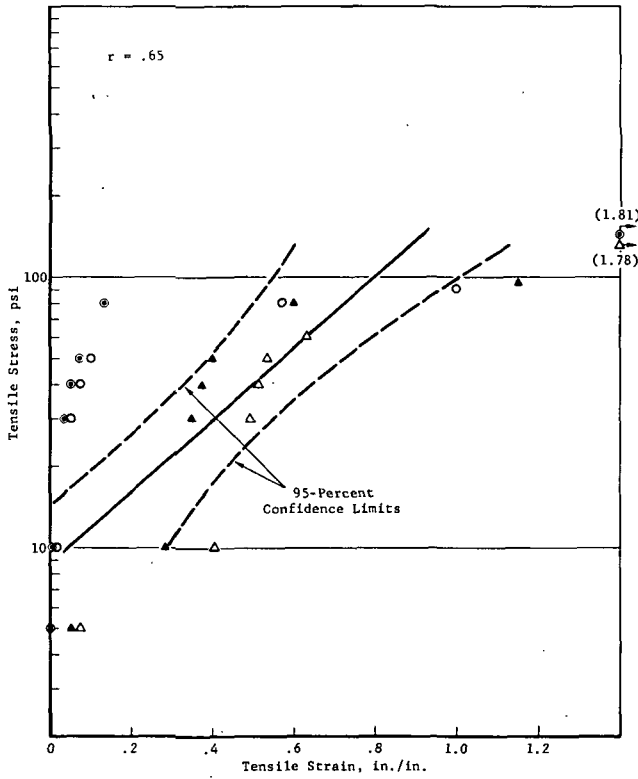


Figure 41 Tensile Stress-Strain #1 DC-93-046 (80°F)

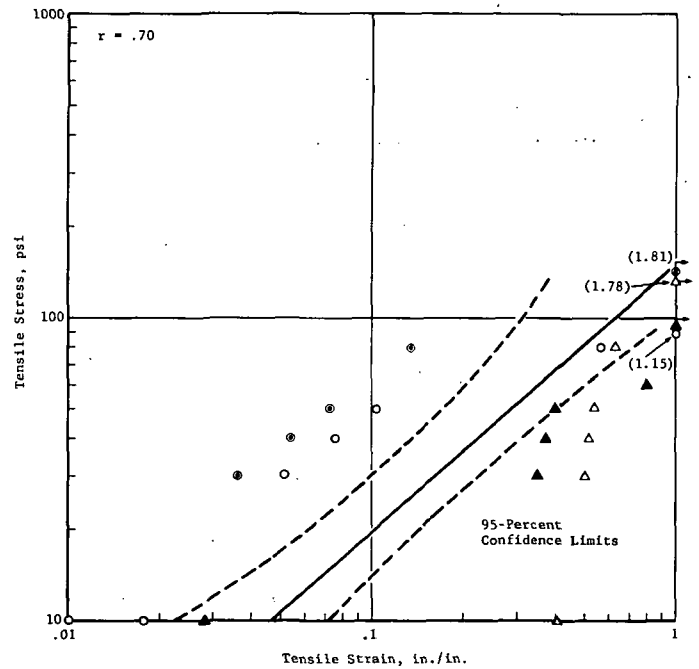


Figure 42 Tensile Stress-Strain #2 DC-93-046 (80°F)

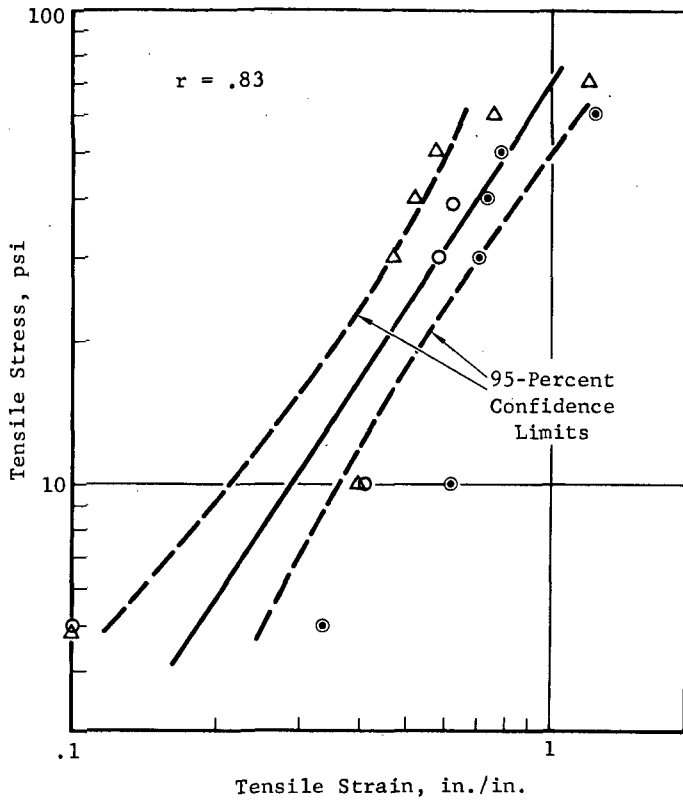


Figure 43 Tensile Stress-Strain DC-93-046 (300°F)

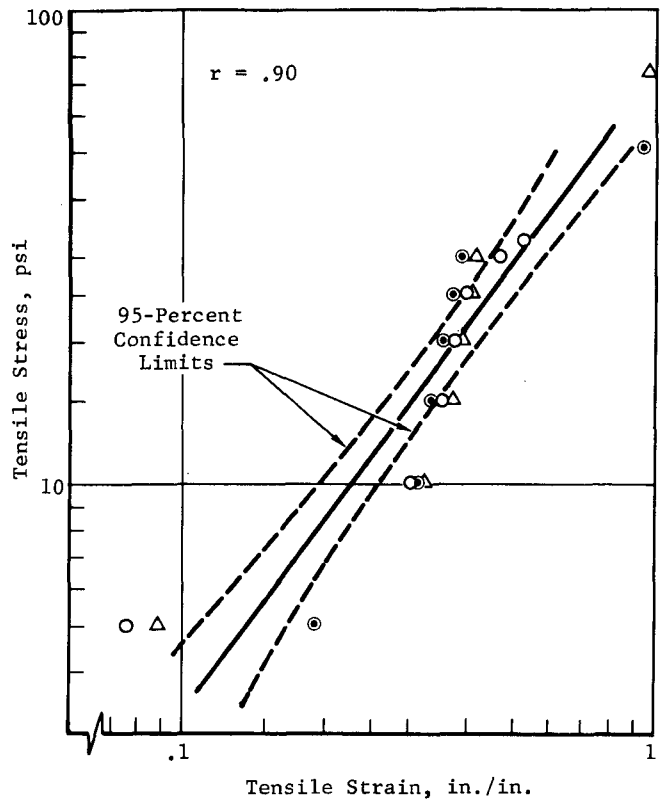


Figure 44 Tensile Stress-Strain DC-93-046 (350°F)

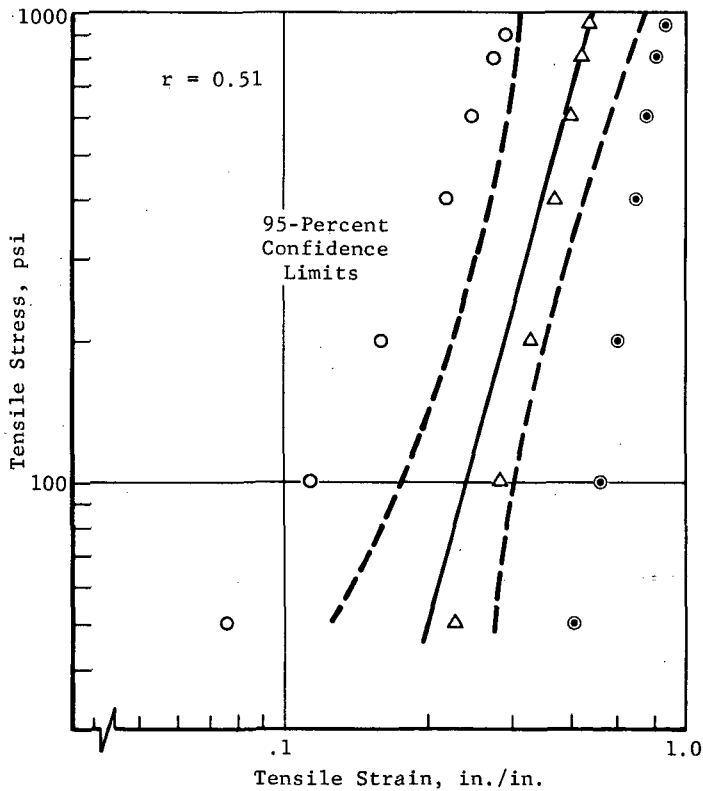


Figure 45 Tensile Stress-Strain RTV 560/RL-1973 (-270°F)

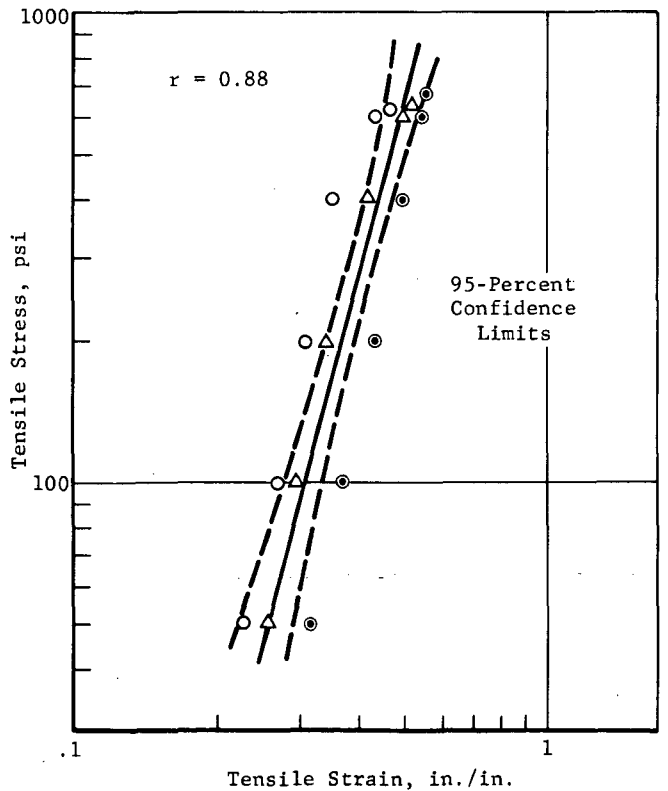


Figure 46 Tensile Stress-Strain RTV 560/RL-1973 (-200°F)

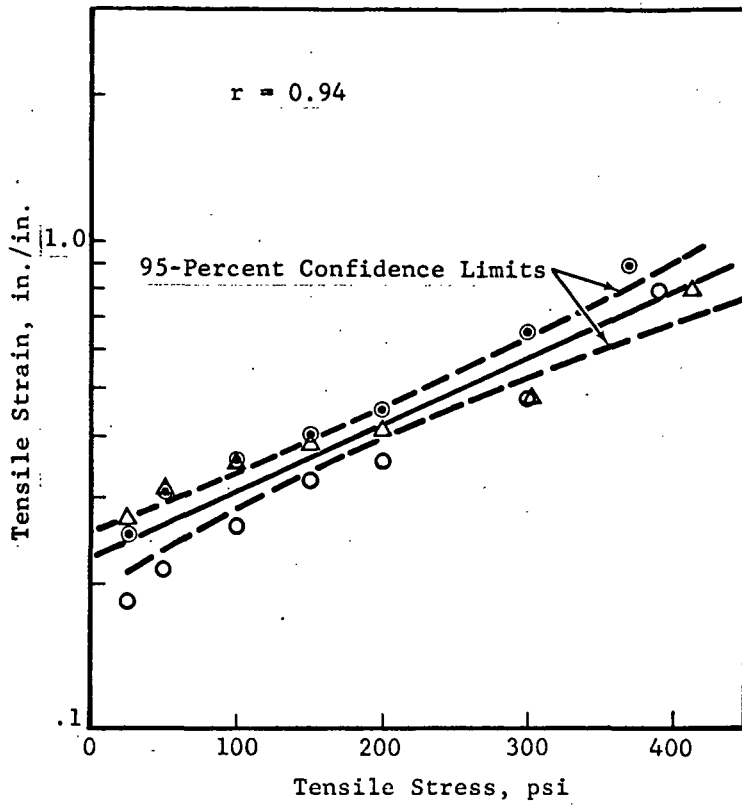


Figure 47. Tensile Stress-Strain
RTV 560/RL-1973 (-175°F)

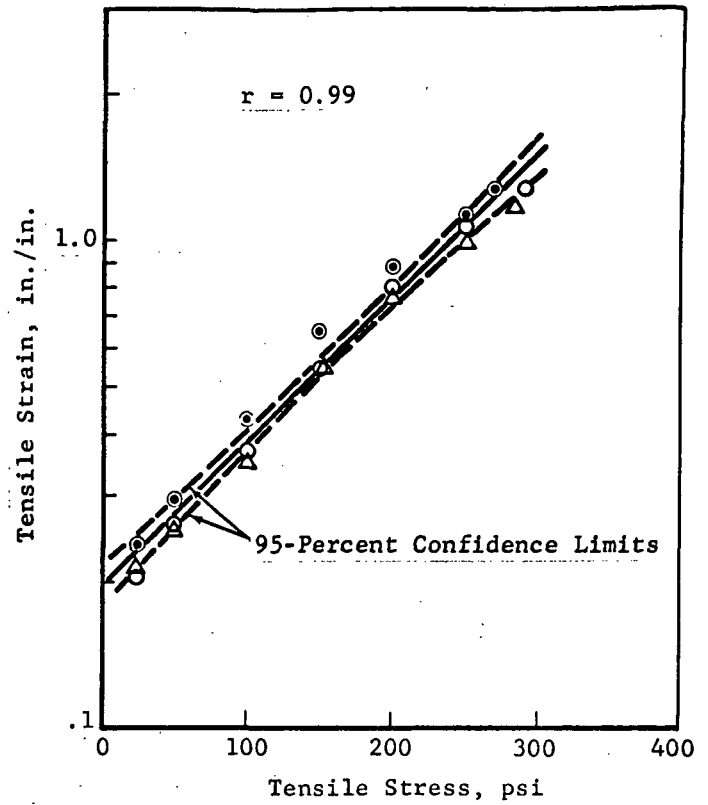


Figure 48. Tensile Stress-Strain
RTV 560/RL-1973 (-150°F)

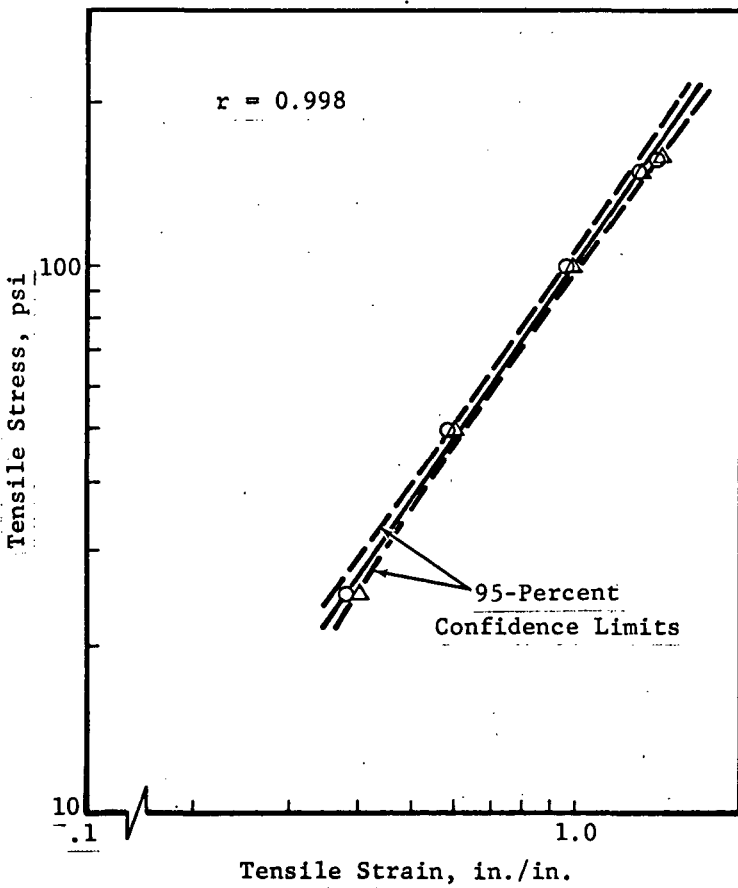


Figure 49. Tensile Stress-Strain
RTV 560/RL-1973 (-65°F)

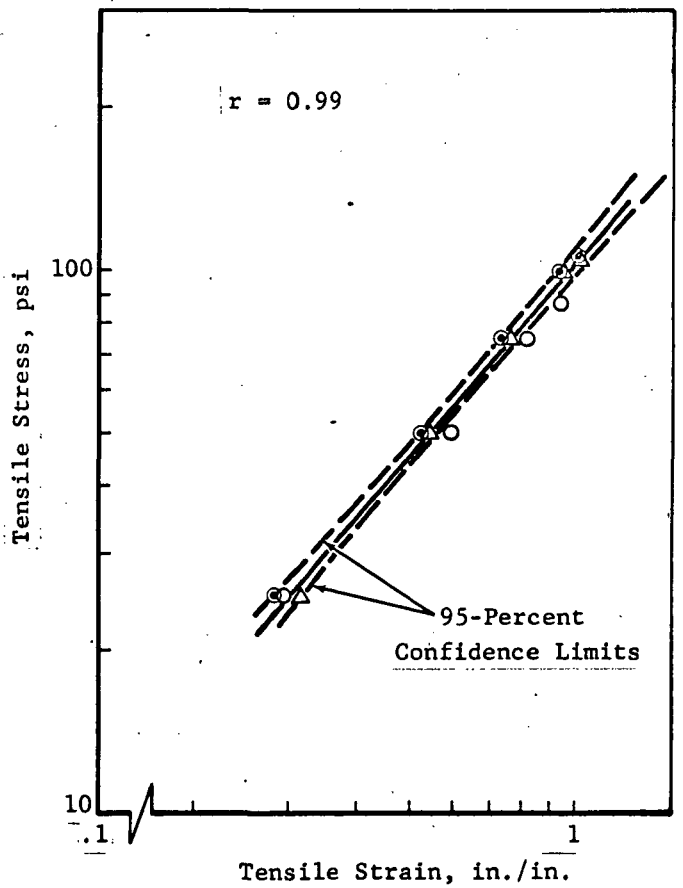


Figure 50. Tensile Stress-Strain
RTV 560/RL-1973 (80°F)

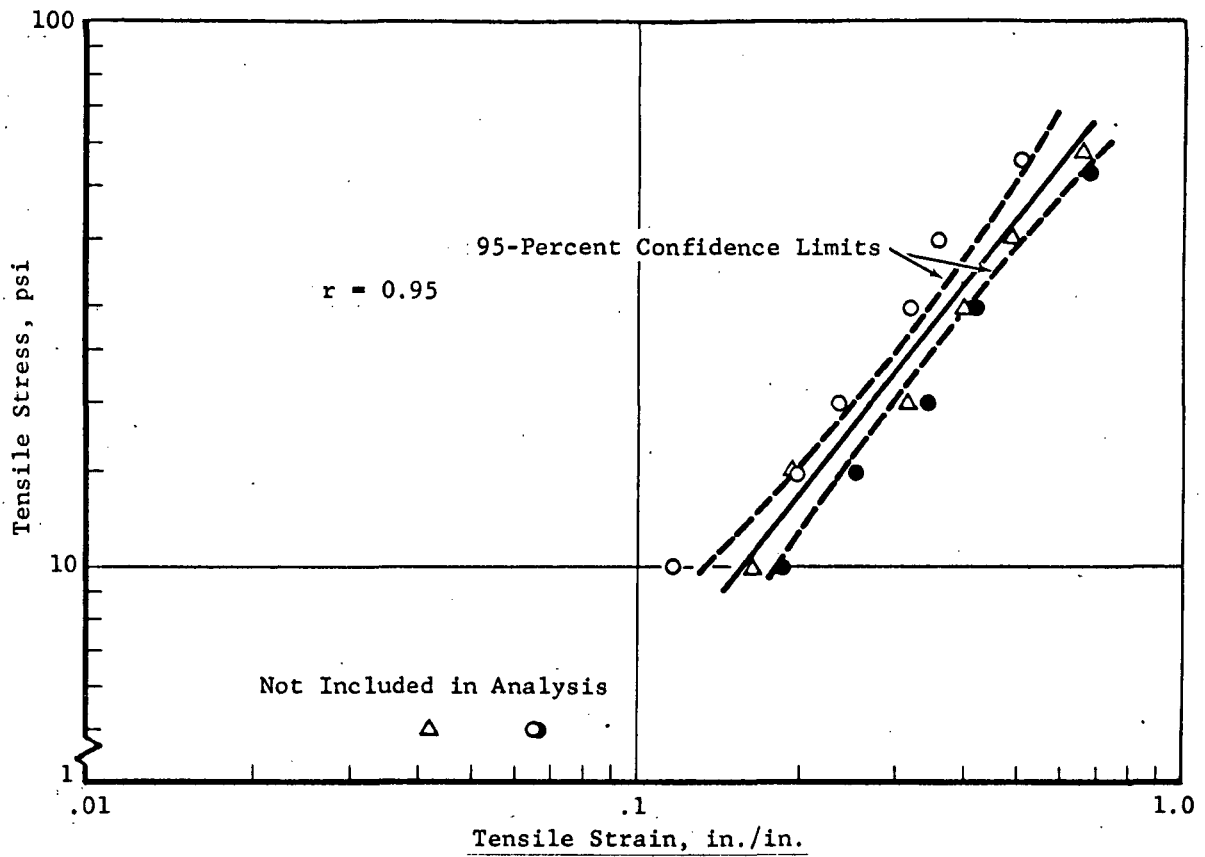


Figure 51 Tensile Stress-Strain RTV 560/RL-1973 (300°F)

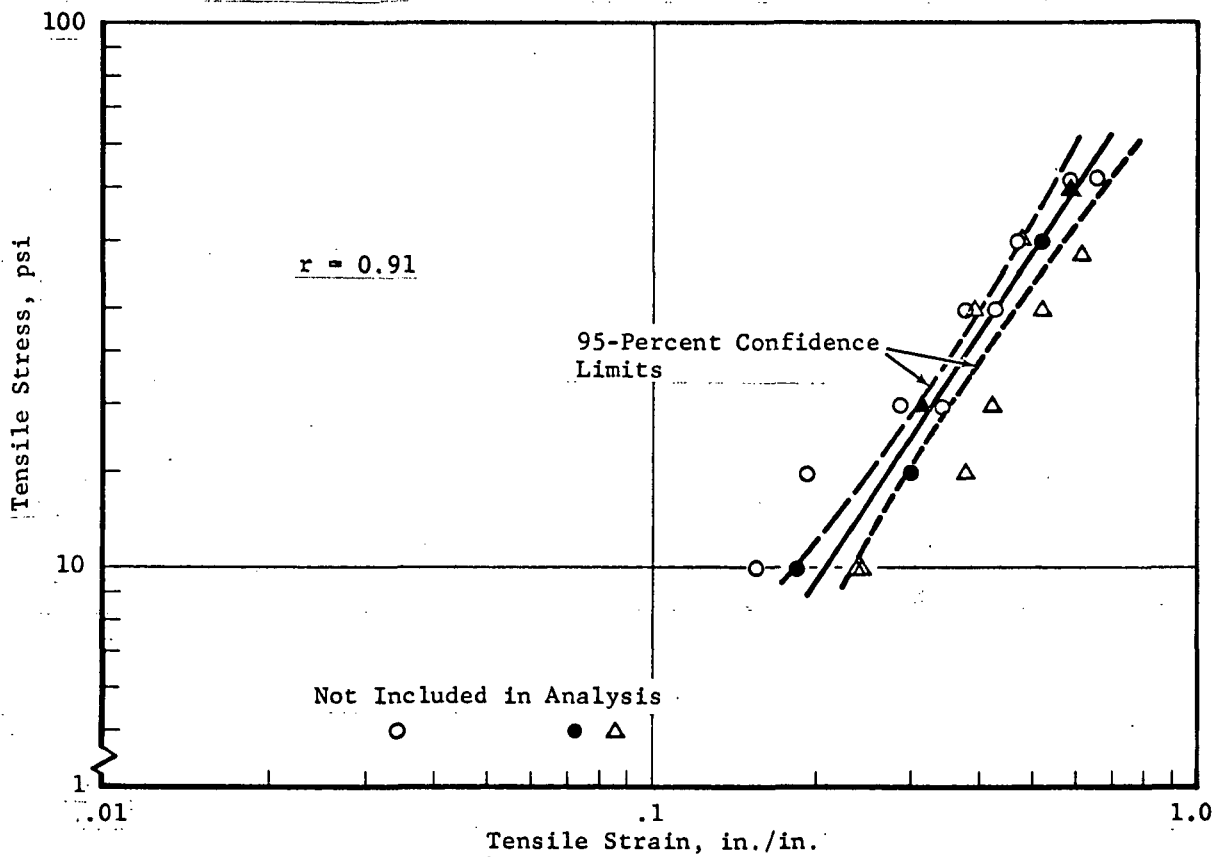


Figure 52 Tensile Stress-Strain RTV 560/RL-1973 (350°F)

4.2 ADHESION IN SHEAR

Shear properties were determined using single overlap shear specimens. The properties determined were shear strength, percent cohesive failure, and shear stress-strain curves.

4.2.1 Test Method

Shear specimens consisted of a standard 1-inch-wide single overlap shear specimen with a 1-inch overlap and 0.060-inch bond line (Figure 3, Section 2). The adherends were 2024-T81 aluminum. Specimens were tested at ten different temperatures from -270°F to 600°F using a strain rate of 0.4 inch/inch/minute. Individual specimen bond thickness and overlap area were measured and recorded before testing. Shear strength was calculated as follows:

$$\text{Shear, psi} = \frac{\text{Load at Failure (pounds)}}{\text{Over Lap Area (in.}^2\text{)}} .$$

Load-deformation curves were determined for each specimen, and these curves were used to develop the shear stress-strain curves. A solid metal specimen was loaded and the data used to correct for extraneous extensions inherent in the test setup. Specimens were tested in tension in a Scott CRE 2K or Instron test machine.

4.2.2 Results and Discussion

Average shear strengths and percent cohesive failure are shown in Table XII and Figure 53. Individual specimen data is shown in Appendix III.

As noted in Figure 53, the shear strength of the materials tested increases with decrease in temperature to a point slightly above the brittle point of the material and then decreases with further decrease in temperature. The percent cohesive failure increases with increase in temperature with the exception of RTV-560/RL-1973, which shows 100 percent cohesive failure at all test temperatures. The materials exhibit rapid deterioration at temperatures above 350°F (300°F for DC 93-046).

Table XII SINGLE OVERLAP SHEAR STRENGTH AVERAGE

Test Temp., °F	GE RTV-560		DC 93-046		MMC SLA-561		RTV-560/RL-1973	
	psi	% Coh. Failure	psi	% Coh. Failure	psi	% Coh. Failure	psi	% Coh. Failure
-270	520	0	488	0	1264	0	621	100
-200	795	0	912	0	2240	Al. Failure*	584	100
-175	717	0	1068	0	1219	0	415	100
-150	1160	95	1278	70	380	0	279	100
- 65	518	100	553	5	81	0	140	100
RT	281	100	184	100	54	10	90	100
300	101	75	84	100	58	100	47	100
350	122	95	57	100	50	100	41	100
550	22	100	Deteriorated		22	100	4.3	100
600	8	100	Deteriorated		14	100	Not Tested	

*Attachment hole failed.

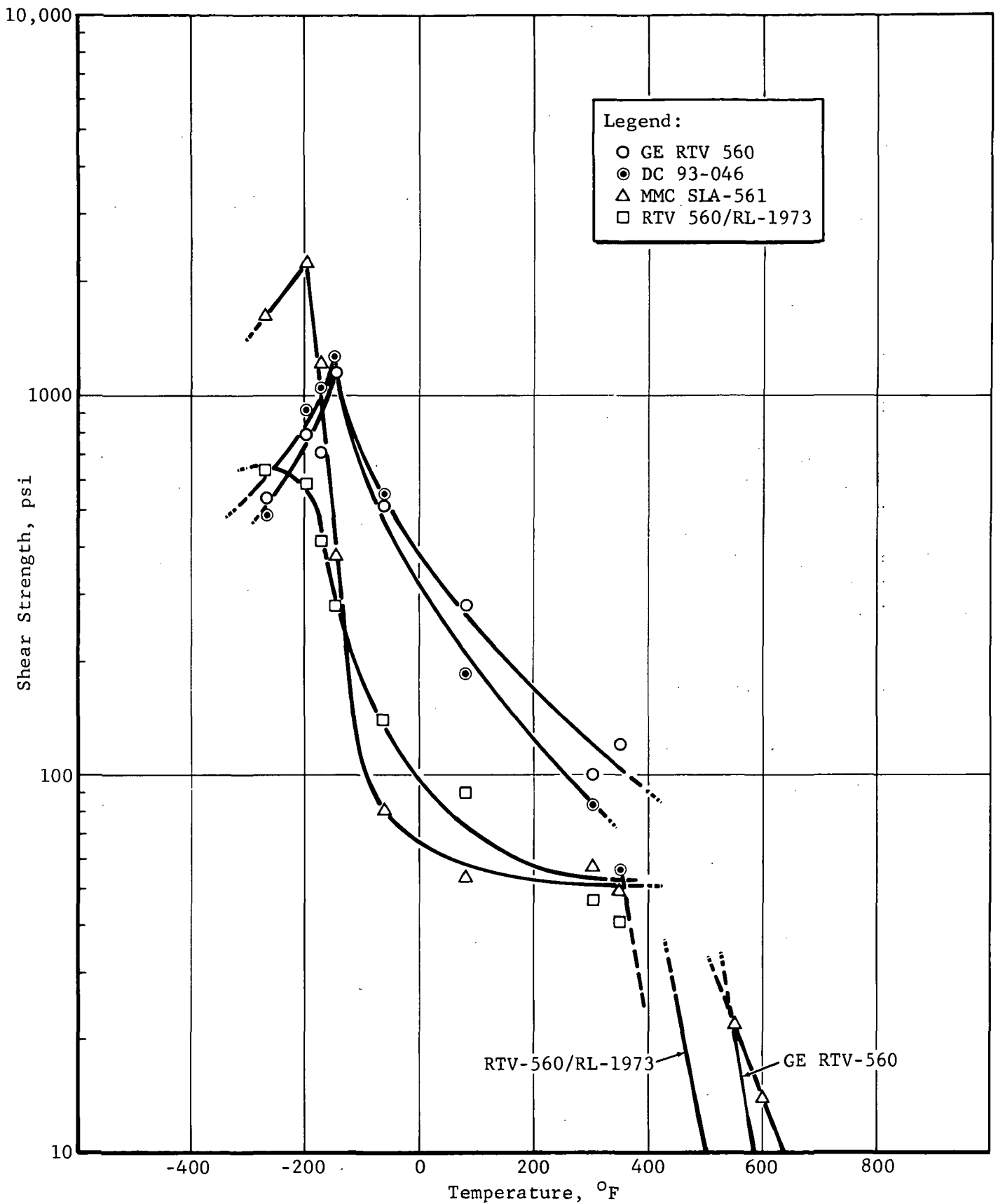


Figure 53 Shear Strength Vs. Temperature

4.2.3 Data Analysis

Single overlap shear data was analyzed using regression and tolerance limit techniques similar to those used to analyze the flatwise tension data (Reference paragraph 4.1.3). The same statistical values were developed for shear data, i.e., stress-strain and strength-temperature, as were developed for tensile data.

4.2.3.1 Methodology

The methodology used in analyzing shear data is summarized in Appendix II.

4.2.3.2 Compilation of Test Data

Continuous load-deflection curves through ultimate load were also obtained for shear specimens. The load-deflection readings were converted to stress-strain exactly as was done in the case of tensile specimens (Reference paragraph 4.1.3.2) except the correction factor used was 0.00004 inch/pound for all four adhesive materials. The calculations of stress-strain for shear specimens are summarized in Appendix III.

A summary of the test conditions studied for stress-strain regression analyses is given in Table XIII.

4.2.3.3 Shear Stress-Strain Data

Regression analysis of shear stress-strain data gave high (>0.9) values of "r," the sample correlation coefficient, for all test temperature conditions except those near the glass-transition temperature. The stress-strain regression results are summarized in Table XIV.

Shear data for temperatures below the glass-transition temperatures were generally too erratic to be used in a regression analysis. Negative values of strain were calculated for DC93-046 at -150° and -175° F, and negative values of strain were calculated for SLA-561 at -200° and -270° F. Test specimens within a temperature condition were too dissimilar to select a common math model for the regression analysis for RTV-560 at -200° and -270° F and SLA-561 at -175° F. Tests on DC93-046 specimens at -200° F and -270° F yielded stress-strain curves that included decreases in strain level for corresponding increases in stress level. Regression analyses were conducted for the modified adhesive RTV-560/RL-1973 at -200° and -270° F to illustrate that such data gives poor

Table XIII SUMMARY OF SHEAR STRESS-STRAIN CONDITIONS FOR REGRESSION ANALYSIS

Material	Test Temperature °F (4)									
	-270	-200	-175	-150	-65	80	300	350	550	600
RTV-560	(1)	(1)	0.78	0.997	0.997	0.93	0.96	0.97		
SLA-561	(2)	(2)	(1)	0.98	0.998	0.991	0.91	0.987	(3)	
DC-93-046	(2)	(2)	(2)	(2)	0.81	0.955	0.96	0.97		
RTV-560/RL-1973	0.27	0.79	0.94	0.98	0.997	0.997	0.96	0.98		

NOTES:

- (1) No analysis conducted - scatter in results prevents selection of suitable math model to represent all specimen results.
- (2) No analysis conducted - strain data included negative results or decreases in strain for increases in stress.
- (3) No analysis conducted - strength data either too low or not obtained because specimens degraded too severely to test.
- (4) Numerical values in Table are values of correlation coefficient.

Table XIV RESULTS OF SHEAR STRESS-STRAIN REGRESSION

Material	Temp (°F)	n	ln A	B	S ϵ . σ	r	r _{upper}	r _{lower}
RTV-560	-175	21	-1.05	0.275	0.20853	0.78	0.91	0.53
	-150	21	-2.84	0.535	0.04970	0.997	1.0	0.96
	-65	21	-2.17	0.473	0.03261	0.997	1.0	0.96
	80	21	-2.47	0.552	0.21216	0.93	0.97	0.83
	300	13	-3.51	0.752	0.12467	0.96	0.98	0.86
	350	15	-4.44	0.926	0.15244	0.97	0.99	0.90
SLA-561	-150	15	-2.48	0.582	0.09476	0.98	1.0	0.96
	-65	12	-3.91	0.962	0.03619	0.998	1.0	0.95
	80	9	-4.48	1.11	0.08433	0.991	1.0	0.93
	300	9	-2.90	0.714	0.19248	0.91	0.97	0.58
	350	9	-2.93	0.713	0.05455	0.987	0.99	0.95
DC-93-046	-65	21	-1.39	0.338	0.21820	0.81	0.91	0.55
	80	10	-3.44	0.911	0.08665	0.995	1.0	0.97
	300	12	-3.20	0.977	0.19855	0.96	0.98	0.80
	350	9	-3.60	1.13	0.15924	0.97	0.98	0.80
RTV-560/RL-1973	-270	21	-2.52	0.169	0.57466	0.27	0.63	-0.21
	-200	21	-2.03	0.158	0.11249	0.79	0.90	0.54
	-175	20	-7.12	1.16	0.31376	0.94	0.97	0.85
	-150	18	-3.22	0.699	0.08142	0.98	0.99	0.91
	-65	15	-1.61	0.495	0.02747	0.997	1.0	0.97
	80	21	-2.19	0.644	0.03720	0.997	1.0	0.97
	300	18	-2.315	0.700	0.01639	0.96	0.98	0.89
	350	17	-1.79	0.570	0.06470	0.98	1.0	0.93

correlation results (note the low value of "r" in Table XIV). The modified adhesive data did exhibit good correlation at two test temperatures below its glass-transition temperature; this was inconsistent with the behavior of the other materials.

4.2.3.4 Shear Strength-Temperature Data

Ultimate strength and strain results for each specimen are included in Appendix III.

Regression analysis was also conducted for ultimate strength-temperature data from overlap shear tests for all four adhesives. The results are summarized in Table XV.

The analyses for shear was similar to that used for tension as discussed in paragraph 4.1.3.4.

General observations relative to shear strength include

1. When strength-temperature data is plotted on semi-logarithmic graph paper (Figure 54), only one straight line is required to represent test data for DC 93-046 and RTV-560 materials, but two straight lines are necessary for SLA-561 and RTV-560/RL-1973. The intersection point of these lines is near the glass-transition temperature.
2. Specimens tested at sub-zero conditions generally failed adhesively; those tested at room and elevated temperature generally failed cohesively.

4.2.3.5 Data Reduction and Presentation

Regression analyses and confidence limits were conducted using the computer program AON and the desk computer as discussed in paragraph 4.1.3.5.

Strain confidence limits for specific values of shear stress are summarized in Appendix IV. Ultimate strength confidence limits and allowables for specific test temperatures are summarized in Appendix V.

Data is presented graphically as follows:

Figures 55 through 58 Shear Strength-Temperature

Figures 59 through 80 Shear Stress-Strain

Table XV RESULTS OF SHEAR STRENGTH-TEMPERATURE REGRESSION

Material	n	Temp Range (°R)	ln A	B	S $\sigma \cdot T$ ln (psi)	r	r _{upper}	r _{lower}
RTV-560	21	260-810	7.86	-0.00404	0.29773	0.95	0.97	0.87
DC-93-046	21	260-810	8.48	-0.00550	0.25429	0.98	1.0	0.96
SLA-561	9	260-310	20.53	-0.04706	0.02452	0.9998	1.0	0.97
SLA-561	12	395-810	4.63	-0.00085	0.13474	0.78	0.93	0.36
RTV-560/RL-1973	9	260-310	10.22	-0.01478	0.05814	0.988	1.0	0.92
RTV-560/RL-1973	12	395-810	6.11	-0.00297	0.02149	0.999	1.0	0.96

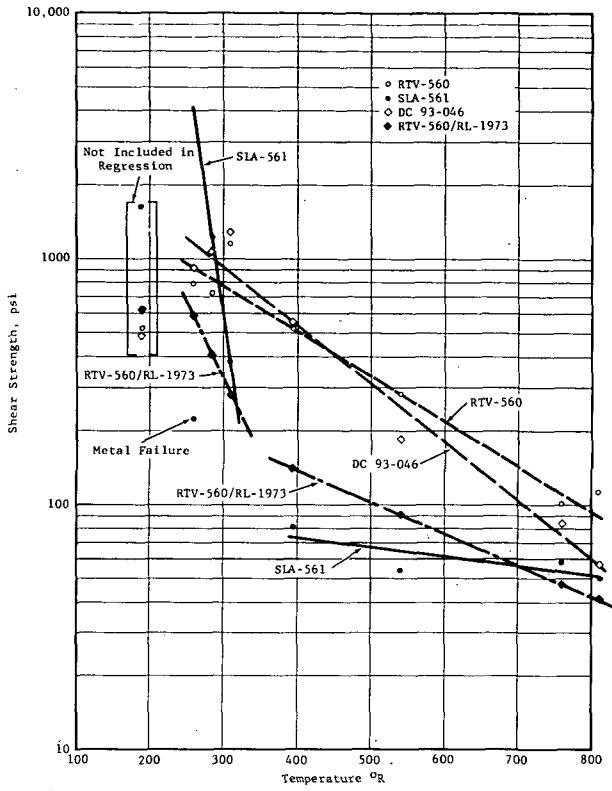


Figure 54 Average Overlap Shear Strength Adhesive Materials

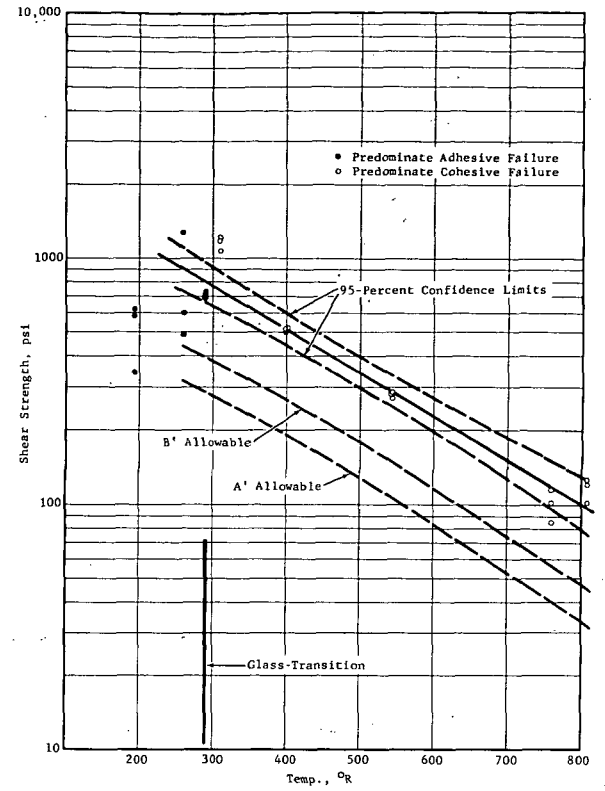


Figure 55 Shear Strength Vs. Temperature RTV-560 Material

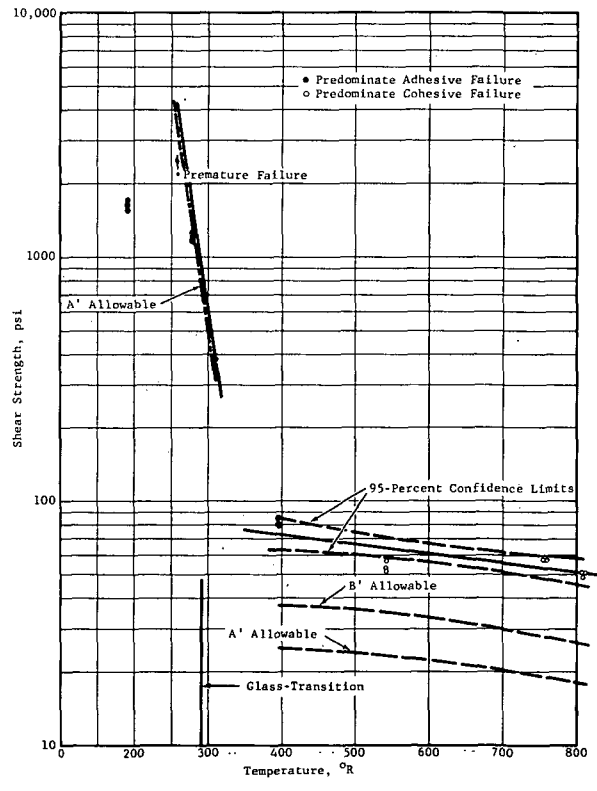


Figure 56 Shear Strength Vs. Temperature SLA-561 Material

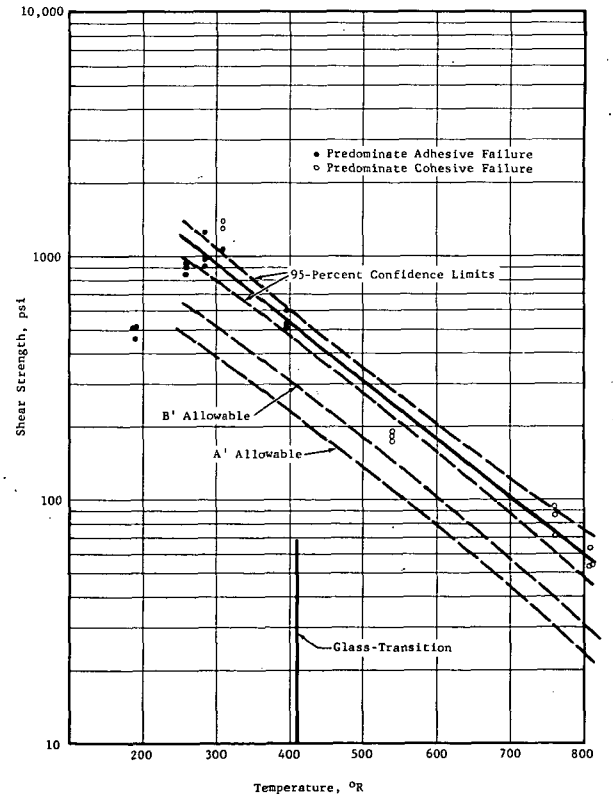


Figure 57 Shear Strength Vs. Temperature DC 93-046 Material

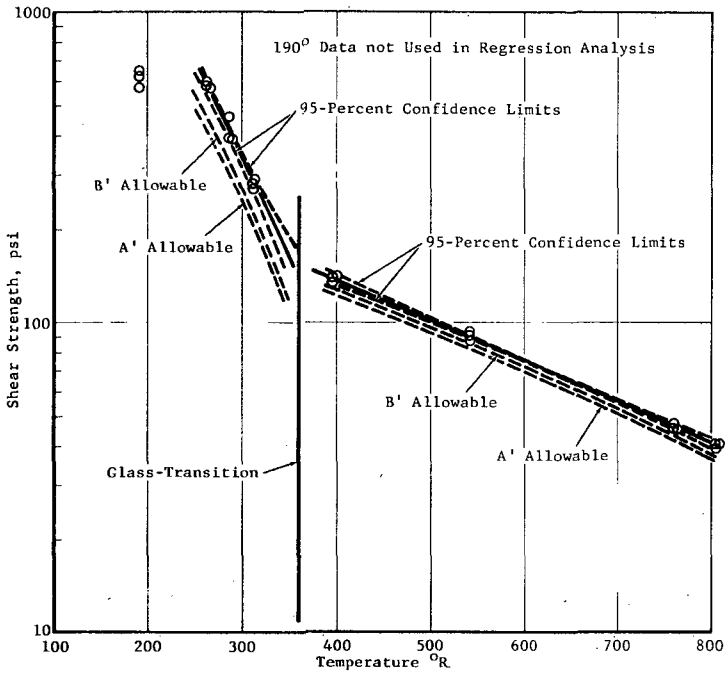


Figure 58 Shear Strength Vs. Temperature RTV 560/RL-1973

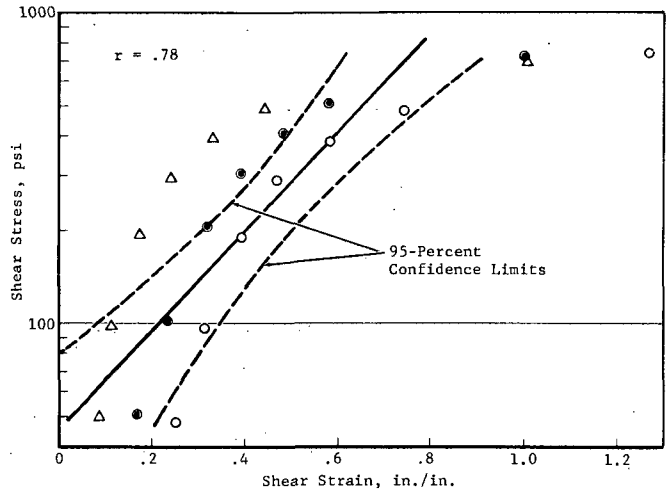


Figure 59 Shear Stress-Strain Curve RTV-560 (-175°F)

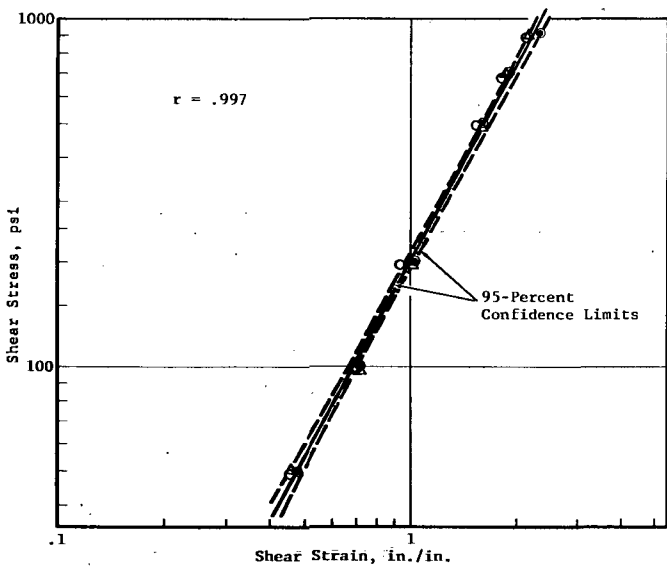


Figure 60 Shear Stress-Strain Curve RTV-560 (-150°F)

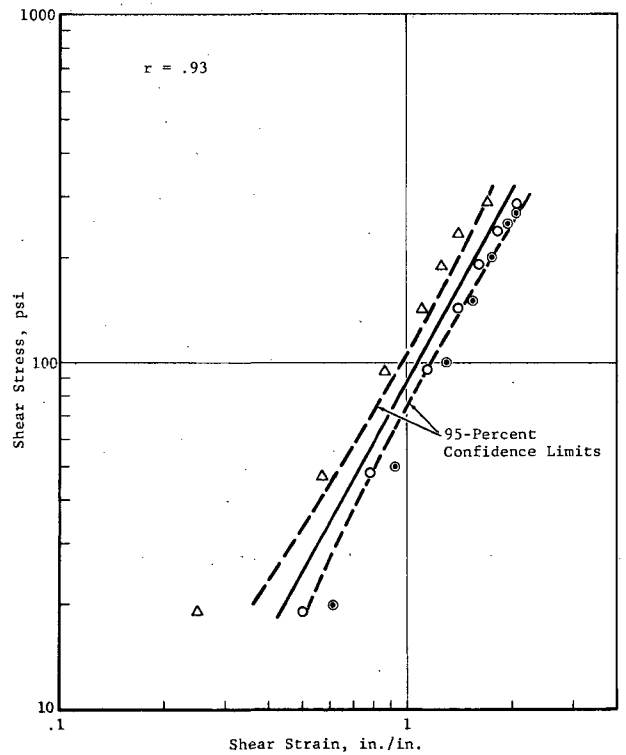


Figure 61 Shear Stress-Strain Curve RTV-560 (80°F)

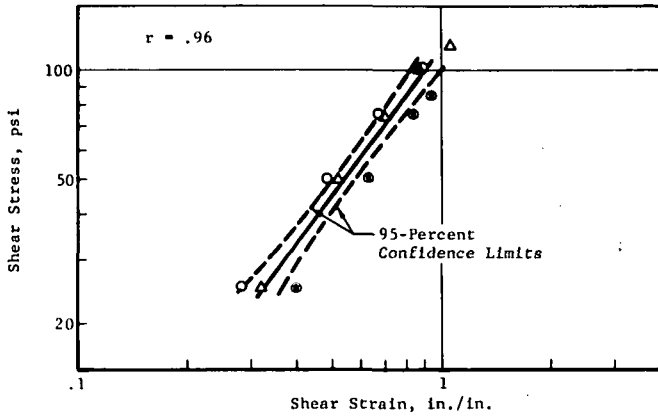


Figure 62 Shear Stress-Strain Curve RTV-560 (300°F)

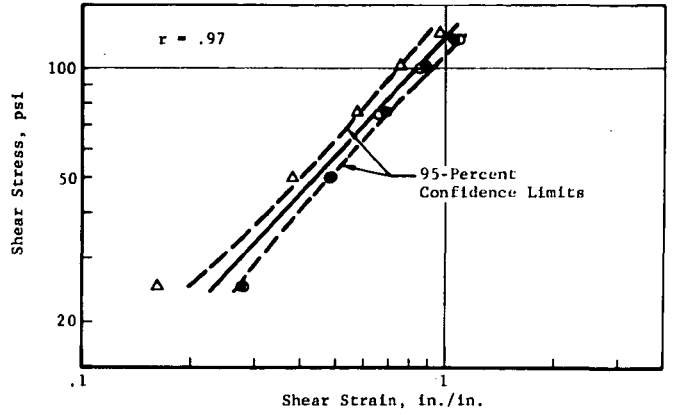


Figure 63 Shear Stress-Strain Curve RTV-560 (350°F)

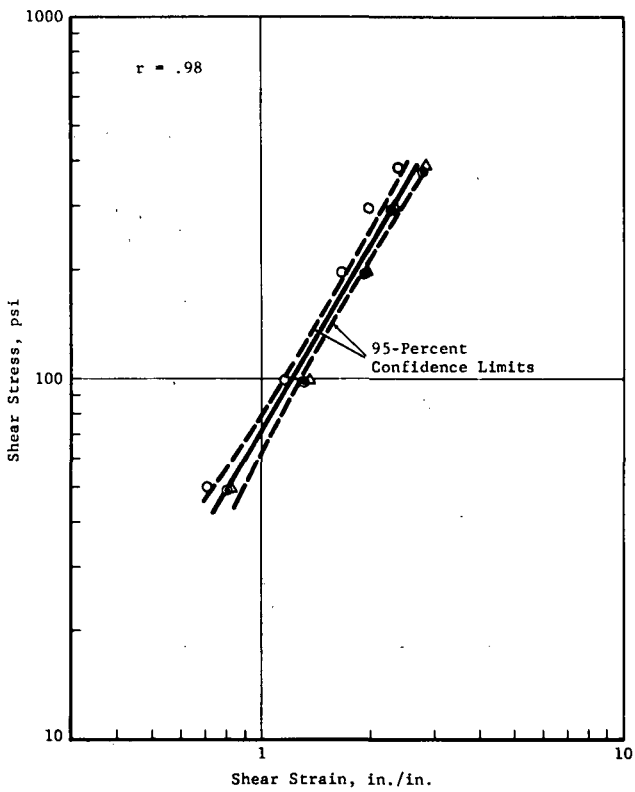


Figure 64 Shear Stress-Strain Curve SLA-561 (-150°F)

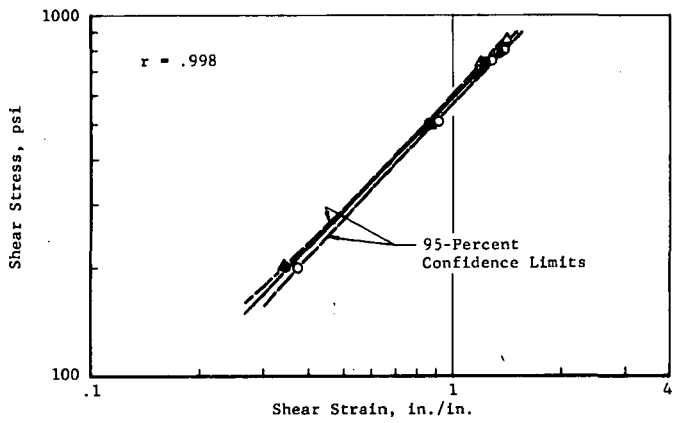


Figure 65 Shear Stress-Strain Curve SLA-561 (-65°F)

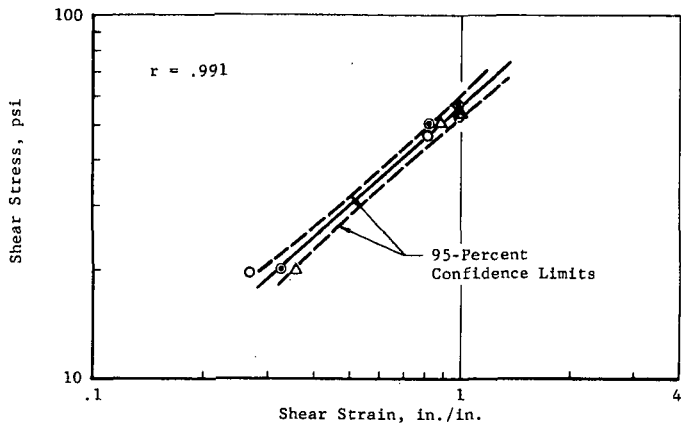


Figure 66 Shear Stress-Strain Curve SLA-561 (80°F)

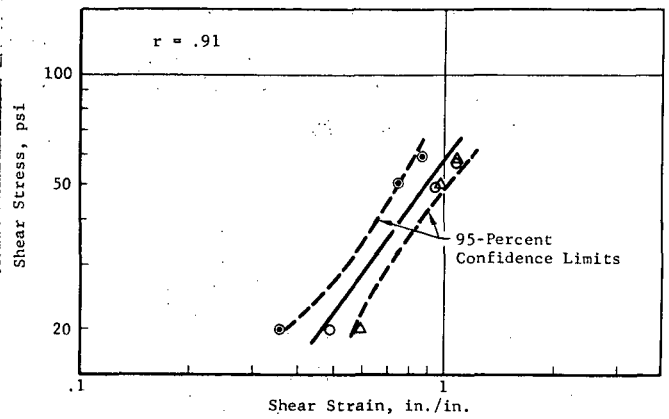


Figure 67 Shear Stress-Strain Curve SLA-561 (300°F)

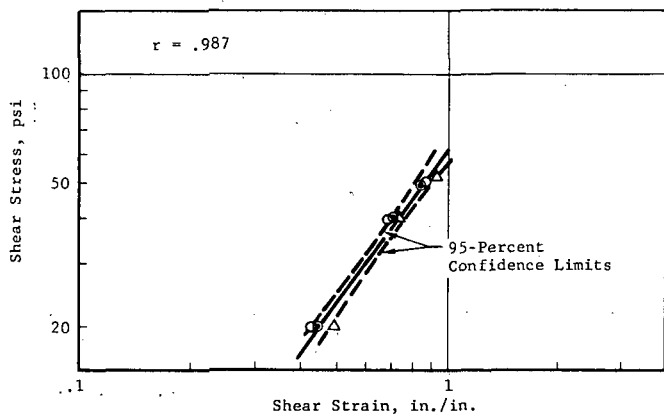


Figure 68 Shear Stress-Strain Curve SLA-561 (350°F)

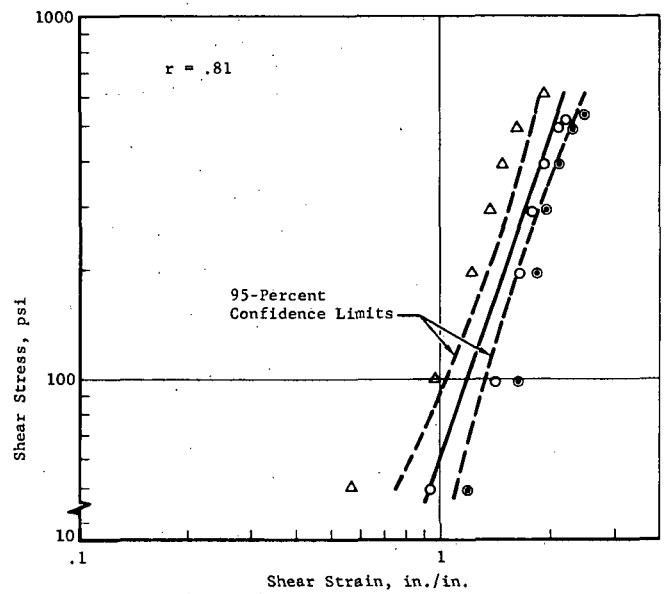


Figure 69 Shear Stress-Strain Curve DC 93-046 (-65°F)

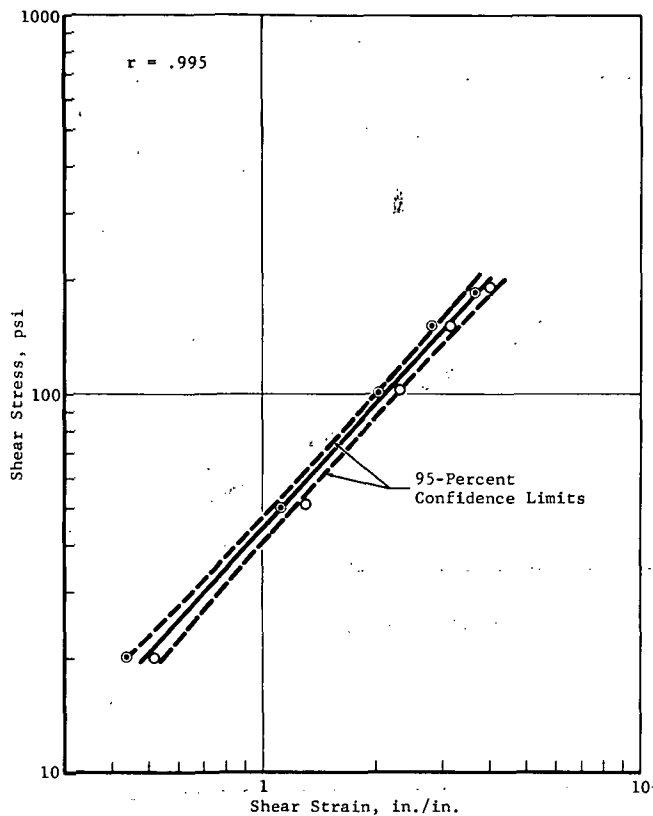


Figure 70 Shear Stress-Strain Curve
DC 93-046 (80°F)

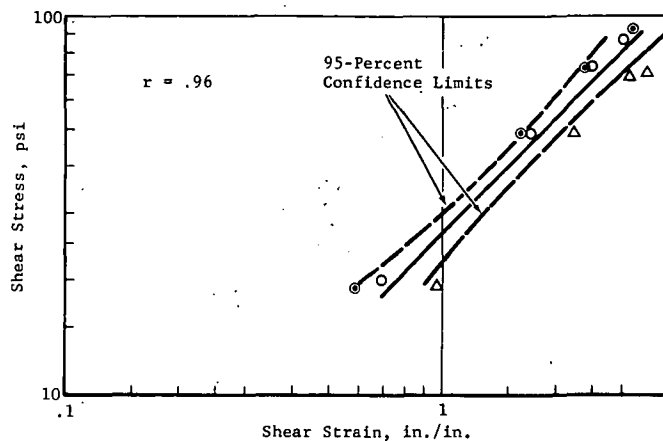


Figure 71 Shear Stress-Strain Curve
DC 93-046 (300°F)

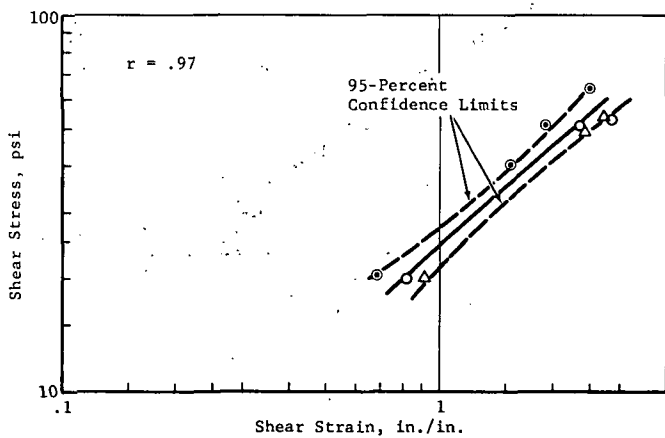


Figure 72 Shear Stress-Strain Curve
DC 93-046 (350°F)

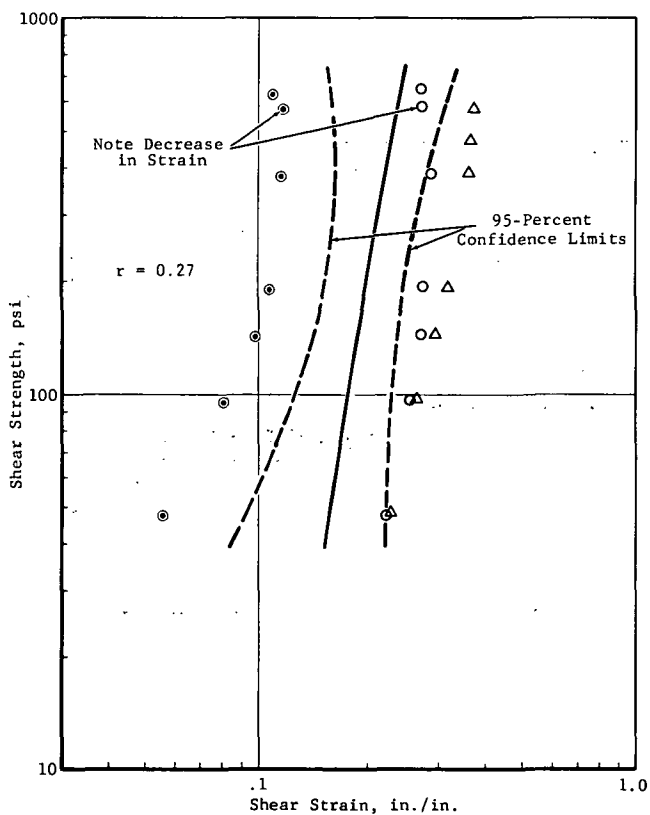


Figure 73 Shear Stress-Strain RTV
560/RL-1973 (-270°F)

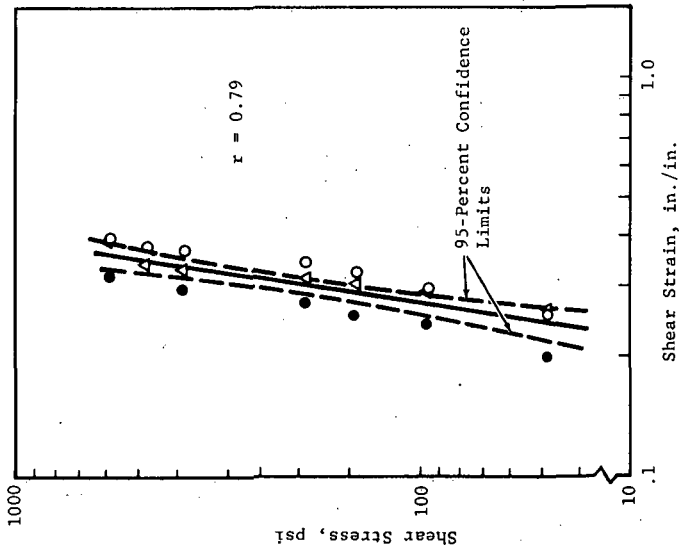


Figure 74 Shear Stress-Strain RTV
560/RL-1973 (-200°F)

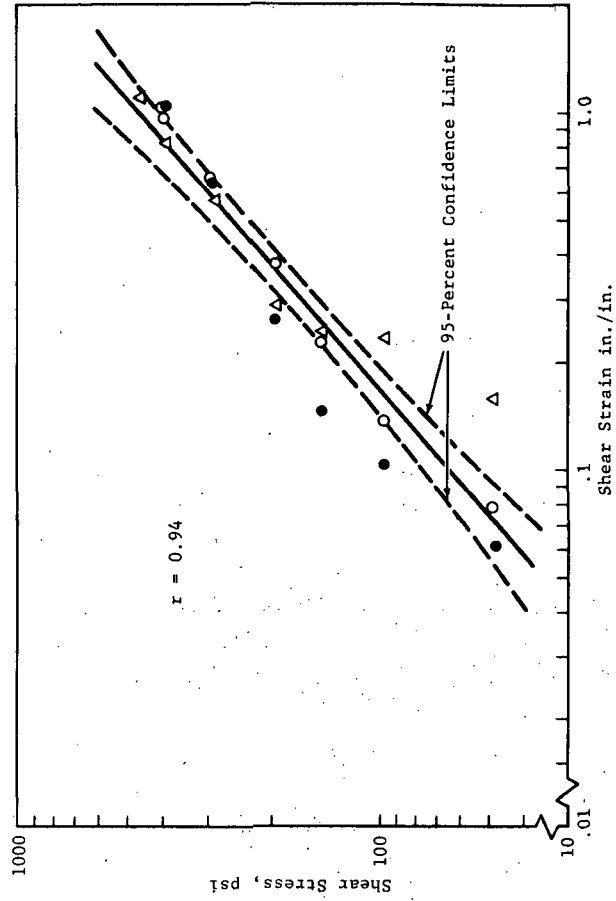


Figure 75 Shear Stress-Strain RTV 560/RL-1973 (-175°F)

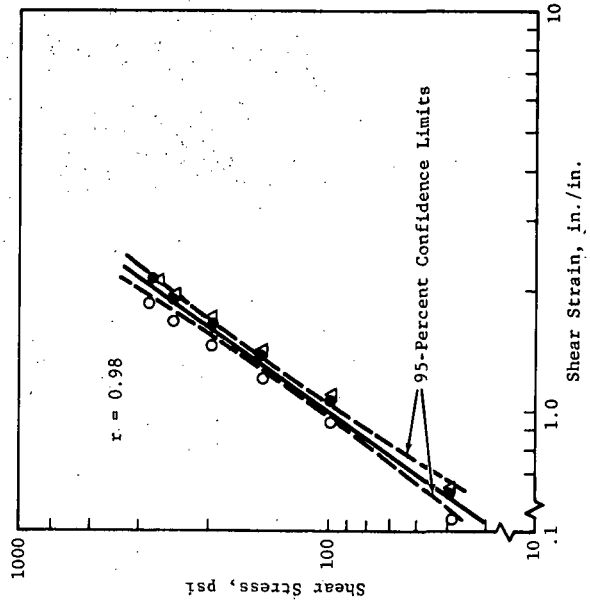


Figure 76 Shear Stress-Strain RTV
560/RL-1973 (-150°F)

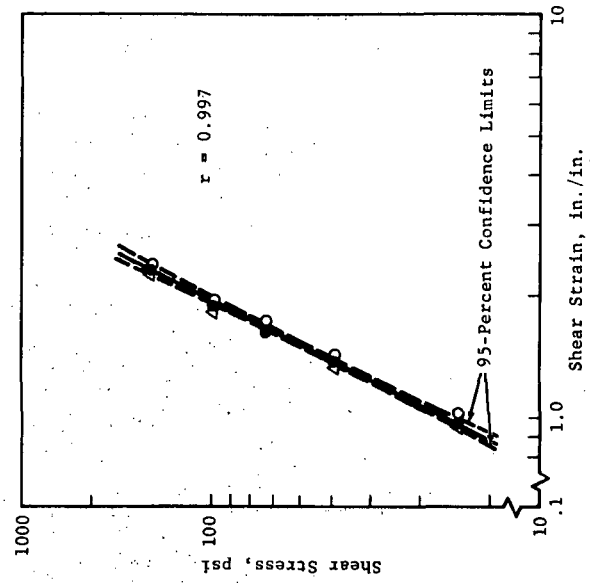


Figure 77 Shear Stress-Strain RTV
560/RL-1973 (-65°F)

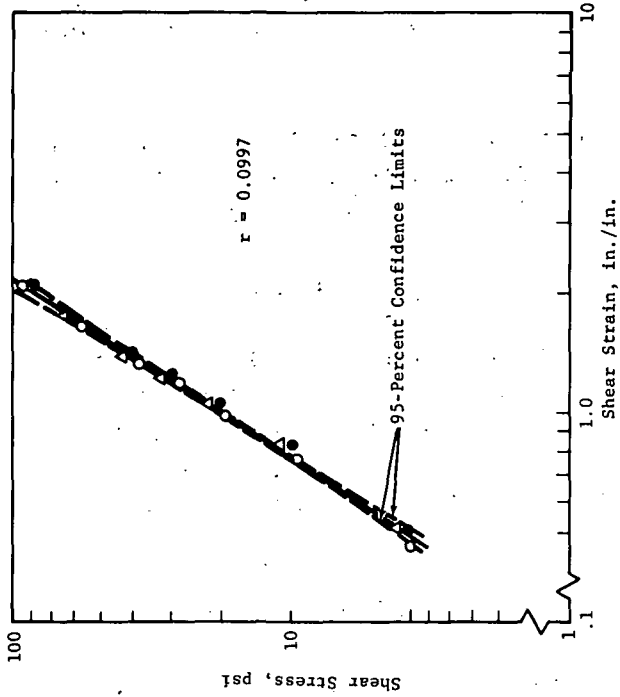


Figure 78 Shear Stress-Strain RTV 560/RL-1973 (80°F)

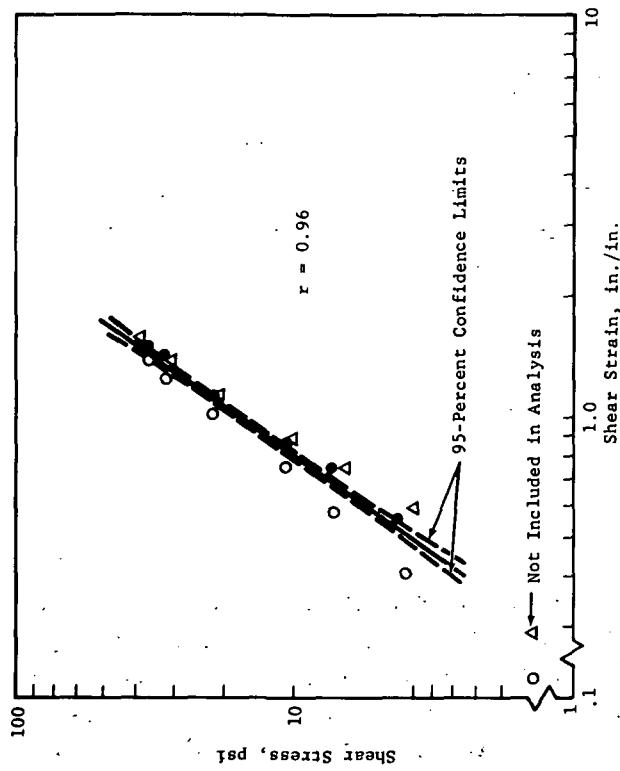


Figure 79 Shear Stress-Strain RTV 560/RL-1973 (300°F)

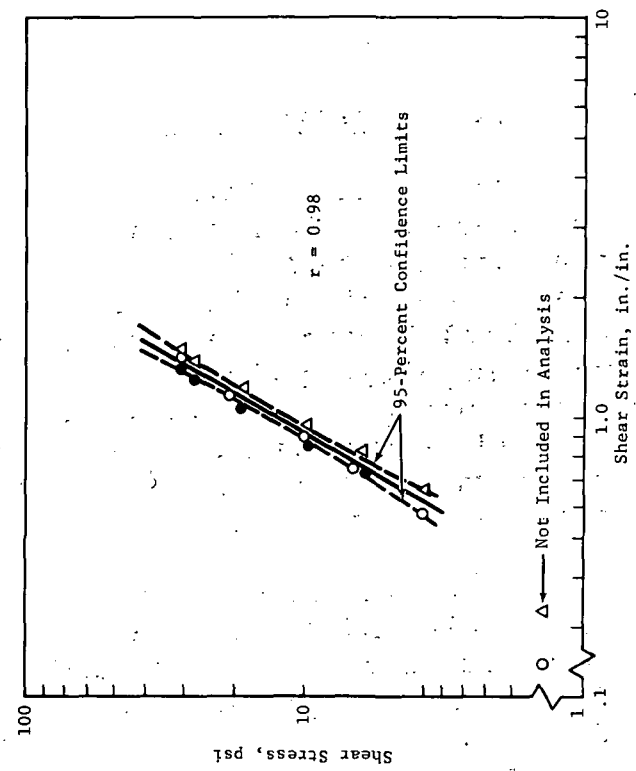


Figure 80 Shear Stress-Strain RTV 560/RL-1973 (350°F)

In the case of stress-strain data, stress is the independent variable; however, the variables were reversed for plotting purposes.

4.3 TENSILE MODULUS AND POISSON'S RATIO

Tensile modulus and Poisson's ratio values were determined from measurements made on flat specimens loaded in tension. The properties reported in this section are "least squares" modulus and Poisson's ratio values.

4.3.1 Test Method

4.3.1.1 Development of Test Method

During the development of a test method to determine Poisson's ratio and tensile modulus, several determinations were made using dead weights to load a GE RTV-560 specimen in tension up to approximately 40 psi and 11.5 percent elongation. Measurements at incremental loadings were taken using a millimeter scale and a two-power magnifying glass. Even though changes in ΔL and ΔW are small (using one to two pound incremental loading) and difficult to read, fairly uniform values for Poisson's ratio were obtained as shown in Table XVI and Figure 81, Test Number 6. Values ranged between 0.4 and 0.45.

Since it would be impossible to make measurements with a hand held scale and the eye during dynamic loading and at low and high temperature environmental conditions, a camera was set up on the Scott tester as shown in Figure 82. The 35mm Beattie-Colman Veritron camera was tied in electrically with the device on the tester that makes specific load indicating "blips" on the chart paper. With this setup, sequence photographs can be made of the specimen as it is being loaded. Later, the loading charts and photographs can be read and related directly by the sequence of "blips" on the chart paper. Measurements of ΔL and ΔW can be taken directly from the photographs and Poisson's ratio calculated.

In checking the photographic method, several enlargement methods were investigated to read ΔL and ΔW as shown in Tests 1, 2, 3, 4, and 5 in Table XVI. Note that the Poisson's ratio values obtained using the photographs and recorded in Table XVI and plotted in Figure 81 appear to be reasonable at 20 psi loads and above but not at lower loadings. These apparent errors were

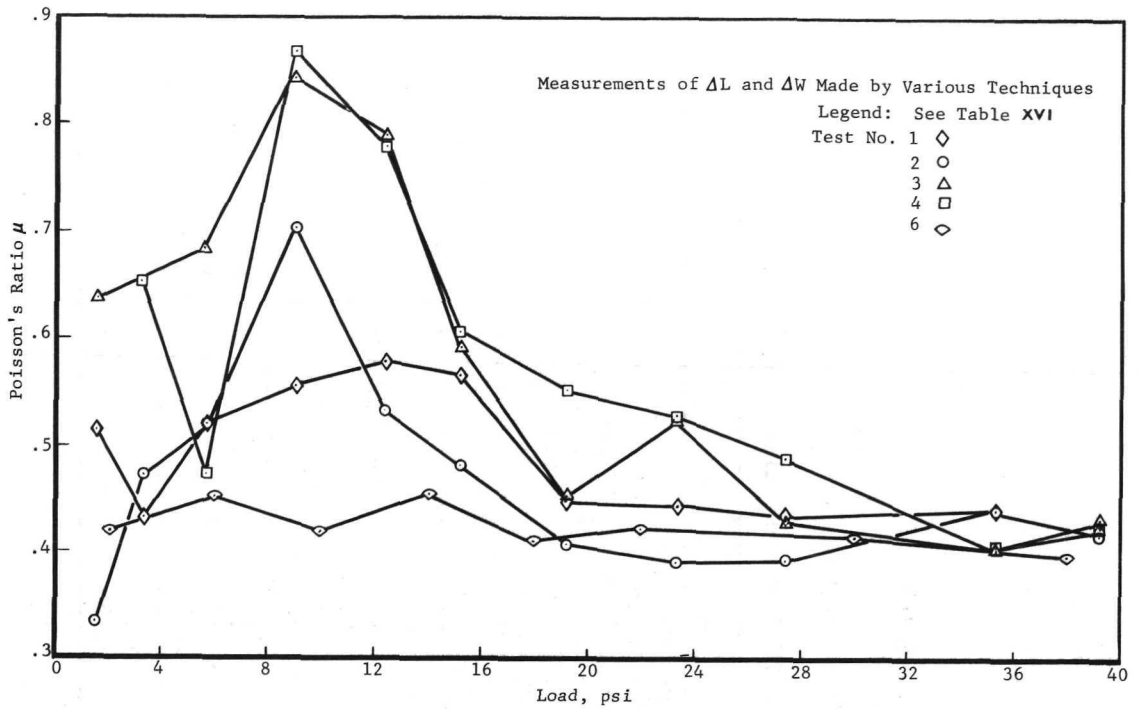


Figure 81 Poisson's Ratio for GE's RTV 560 at Room Temperature

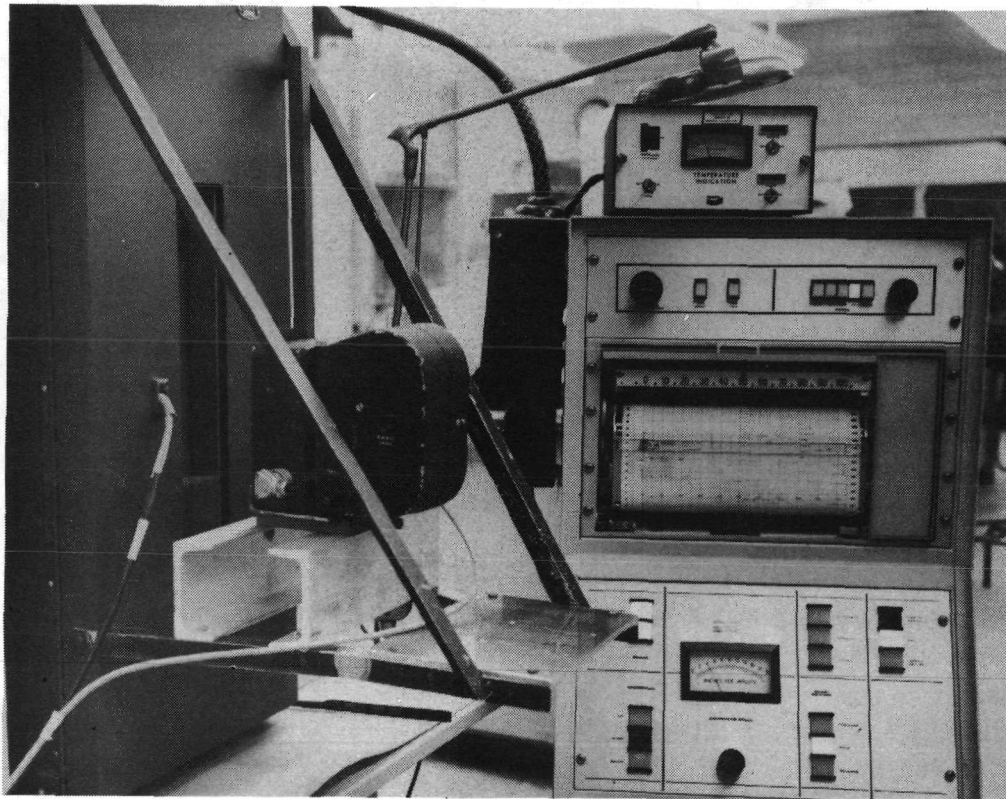


Figure 82 35mm Veritron Camera Mounted on CRE/2K Scott Tester

Table XVI POISSON'S RATIO FOR GE'S RTV-560
AT ROOM TEMPERATURE

(Measurements of ΔL and ΔW Made by Various Techniques)

Specimen 10" x 2.5" x .10" - Measurements Taken on 5" x 2" Center Section $\frac{\Delta W}{\Delta L} \cdot \mu = \mu$

TEST NO.	1	2	3	4	5	6
Type Measure- ment and Magnification	Eye Measure with 100th Scale - No. Magnification Operator (A)	Eye Measure of Photos with 100th Scale 1.85 Mag. Operator (A)	Computer Measurement- Operator Sets on 4 Corners 0.9 Mag. Operator (A)	Eye Measure of Photos with 100th Scale 1.39 Mag. Operator (A)	Eye Measure with mm Scale 10 Mag. with Photo Pro- jector Operator (B)	Eye Measure with mm Scale 2 Mag. Operator (B)
Type Loading	Deadweight Using CRE/2K Scott Tester					
Load, psi	Hanging Dead Weights					
1.6	0.5198	0.3240	0.6387	-	Lines of 10X	2.1
3.3	0.4332	0.4713	-	0.6506	Photo are	6.1
5.7	0.5198	0.5184	0.6844	0.4731	Too Fuzzy	10.0
9.0	0.5569	0.7070	0.8434	0.8674	for	-
12.4	0.5775	0.5337	0.7902	0.7807	Accurate	-
15.2	0.5650	0.4823	0.5929	0.6072	Measurements.	14.0
19.2	0.4481	0.4093	0.4507	0.5520		18.0
23.3	0.4455	0.3928	0.5233	0.5323		22.0
27.4	0.4332	0.3937	0.4310	0.4909		30.0
35.3	0.4413	0.4407	0.4059	0.4089		-
39.2	0.4332	0.4204	0.4388	0.4345		38.0

Total
Elongation
approx.
11.5 percent

due to the "fuzziness" of the bench mark lines on the specimens and the magnification of the photographs. To mitigate these problems, the camera was refocused and moved closer to the specimen and a bench mark method utilizing 0.02-inch-diameter dots was devised.

4.3.1.2 Tensile Modulus and Poisson's Ratio Test Method

Flat strips of molded adhesive (except RL-1973 sponge) 0.1 inch thick, 12 inches long, and 2.5 inches wide (Figure 4, Section 2, and Figure 83) were tested for determination of tensile modulus and Poisson's ratio. One-inch-wide aluminum doublers were bonded on each end to distribute the applied load to the entire specimen. A two- by five-inch test section was bench marked with 0.02-inch-diameter dots in the center of the specimen face. The bench marks were applied using a template and GE RTV-102. For temperatures below room temperature, the GE RTV-102 was pigmented black for marking GE RTV-560, MMC SLA-561, and RTV-560/RL-1973 specimens. Unpigmented GE RTV-102 was used to mark all DC 93-046 (a black material) specimens. The black dots used to mark specimens tested below room temperature assisted in distinguishing the bench marks from frost in the photographs.

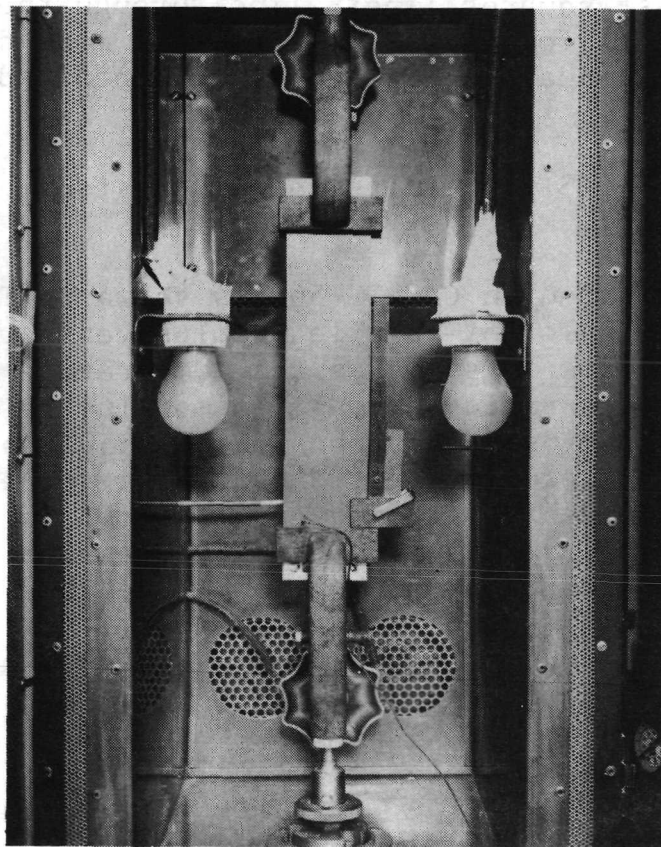


Figure 83 Tensile Modulus Test Setup

The RL-1973 sponge specimens were cut from flat sheets 0.1 inch thick. A 0.005- to 0.010-inch-thick coating of GE RTV-560 was applied to each face of the specimen and cured before bench marking as described above. In addition, one RL-1973 specimen without the GE RTV-560 coating was tested at -200°F .

Specimens were tested at six temperatures ranging from -65°F to 600°F using a strain rate of 0.4 inch/inch/minute. Specimens also were tested at additional strain rates of 0.25 and 0.003 inch/inch/minutes at -65°F , RT, and 300°F . At temperatures below -65°F , the strain rate selected for each material provided a load rate consistent with the response of the test machine. These strain rates are shown in the tables of data.

During testing, photographs were made at incremental loadings; these were later measured for calculating tensile modulus and Poisson's ratio. Transverse and axial measurements from the photographs were fed directly into a Hewlett-Packard 2116A computer programmed to give a printout of Poisson's ratio and moduli values along with "least squares" values for the two properties. The "least squares" value is the slope of the least squares linear line through the stress-strain points for tensile modulus and the slope of the least squares linear line through the transverse-axial strain points for Poisson's ratio. A more detailed discussion of the least squares computation is contained in Appendix VI.

4.3.2 Results and Discussion

The data obtained on GE RTV-560 is shown in Table XVII and Figure 84. In the plot of tensile modulus versus temperature, a decrease in modulus is shown as the temperature decreases from 350°F to -65°F and a rapid increase in modulus is shown from -150°F to -175°F . The modulus values obtained at 550°F and 600°F show a rapid deterioration of the material at these temperatures. A plot of strain rate versus tensile modulus is shown in Figure 85. As noted, a slight decrease in modulus occurs as the strain rate is decreased from 0.4 to 0.003 inch/inch/minute.

An additional modulus test was conducted using a cylinder adhesion specimen in which the deflection was measured using an extensometer. These tests were conducted at -175°F , -200°F , and -270°F . The data obtained is shown in Table XVIII. The specimen configuration, thin glue line, and difficulties encountered in determining deflections with the extensometer at low temperatures can account for the difference in the values obtained between the strap and cylinder specimens.

Table XVII TENSILE MODULUS OF GE'S RTV-560,
PSI

Strain Rate, In./In./Min.	Temperature, °F									
	-270	-200	-175	-150	-65	RT	300	350	550	600
0.4			38,975	385	295	341	402	391	326	222
0.4			28,816	447	303	335	440	408	320	225
0.4			13,964	400	323	335	485	435	304	196
0.4			32,662	398						
0.4			32,967	656						
Avg.			29,477	457	307	337	442	411	317	214
0.25					293	356	402			
0.25					297	368	424			
0.25					302	359	409			
0.01	59,675	202,472								
0.01	149,490	108,656								
0.01	94,852	123,188								
Avg.	101,333	144,772			297	361	412			
0.003					277	341	418			
0.003					273	354	427			
0.003					265	319	406			
Avg.					272	338	417			

NOTE: Data from strap specimens elongated only up to approximately 10 percent.

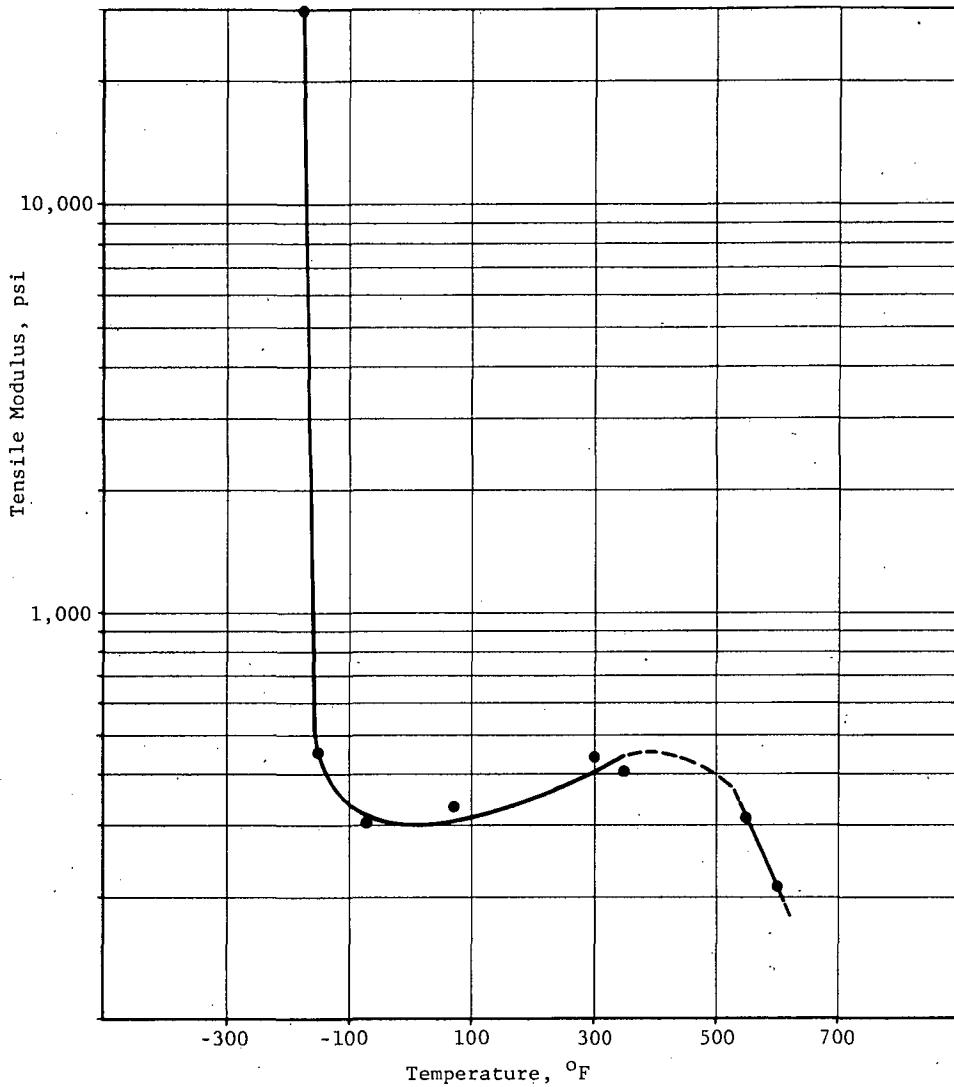


Figure 84 Tensile Modulus Vs. Temperature RTV 560, 0.4 in./in./min. Strain Rate

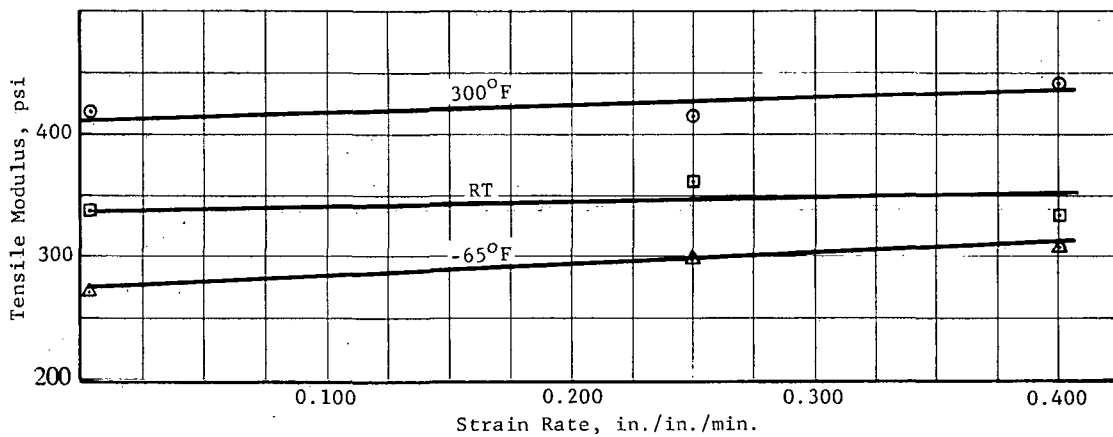


Figure 85 Tensile Modulus of RTV-560 Vs. Strain Rate

Table XVIII TENSILE MODULUS OF GE RTV-560
DETERMINED FROM CYLINDER ADHESION SPECIMEN

Spec. No.	Temp., °F	Tensile Str., psi	Elongation, %	Initial Modulus, psi	Modulus @ 400 psi,	Cohesive Failure, %
1	-175	1800	15.8	92,308	92,308	70
2	-175	1160	>18.2	36,000	14,118	60
Avg.		1480	>17.0	64,154	53,213	65
1	-200	2100	1.7	95,000	95,000	40
2	-200	1150	2.2	46,857	82,000	0
Avg.		1625	2.0	70,928	88,500	20
1	-270	1675	4.3	21,875	28,571	70
2	-270	1050	1.1	71,429	71,429	10
Avg.		1362	2.7	46,652	50,000	40

NOTE: Deformations measured with extensometer.

The tensile modulus data for DC 93-046 is shown in Table XIX and Figure 86. As can be seen, the plot of tensile modulus versus temperature is of the same general shape as that obtained for GE RTV-560. Softening of DC 93-046 begins at 300°F and rapid increase in modulus begins at -65°F. As noted, the material deteriorated and could not be tested at 550°F and 600°F. Also, the strains developed in the material while being cooled to -270°F caused the specimens to crack and no data could be obtained.

Figure 87 is a plot of tensile modulus versus strain rate. As shown, the modulus values obtained are independent of strain rate at room temperature and 300°F and appear to be independent at -65°F except for the value obtained at 0.003 inch/inch/minute strain rate (Table XIX). The high value obtained at -65°F at the low strain rate is believed to be due to the long soak time at temperature this specimen received. Normally, the specimens are brought to test temperature in about 20 minutes then soaked at temperature 5 minutes before testing. The time required for testing is approximately 3 minutes. At the low strain rate, however, the time required to test the specimen is 30 minutes, which results in a longer soak time. DC 93-046 appears to be extremely time-temperature dependent at temperatures approaching its brittle point.

The tensile modulus data for MMC SLA-561 is shown in Table XX and Figure 88. The plot of tensile modulus versus temperature is similar to the other two materials and shows a decrease in modulus as the temperature decreases from 350°F to -65°F and a rapid increase in modulus from -150°F to -270°F. The values obtained at 550°F and 600°F show a rapid deterioration of the material at these temperatures. A plot of load rate versus tensile modulus is shown in Figure 89. As noted, the tensile modulus values are essentially the same in the strain rate range of 0.003 to 0.4 inch/inch/minute.

Tensile modulus values for RM/RL-1973 sponge are shown in Table XXI and Figure 90. With the exception of one specimen tested at -200°F, the specimens were coated on each face with 0.005- to 0.010-inch thickness of GE RTV-560. This coating of GE RTV-560 was applied to simulate the actual bond conditions. At -200°F, the specimen without a coating exhibits a modulus approximately one tenth that of the coated specimens.

Figure 90 is a graph of tensile modulus versus temperature. As shown, this curve is similar to the other materials tested. A minimum modulus is reached at approximately 200°F and a maximum modulus is reached at -200°F. The rapid increase in modulus begins at approximately -100°F. Softening of the material is shown at temperatures above 350°F.

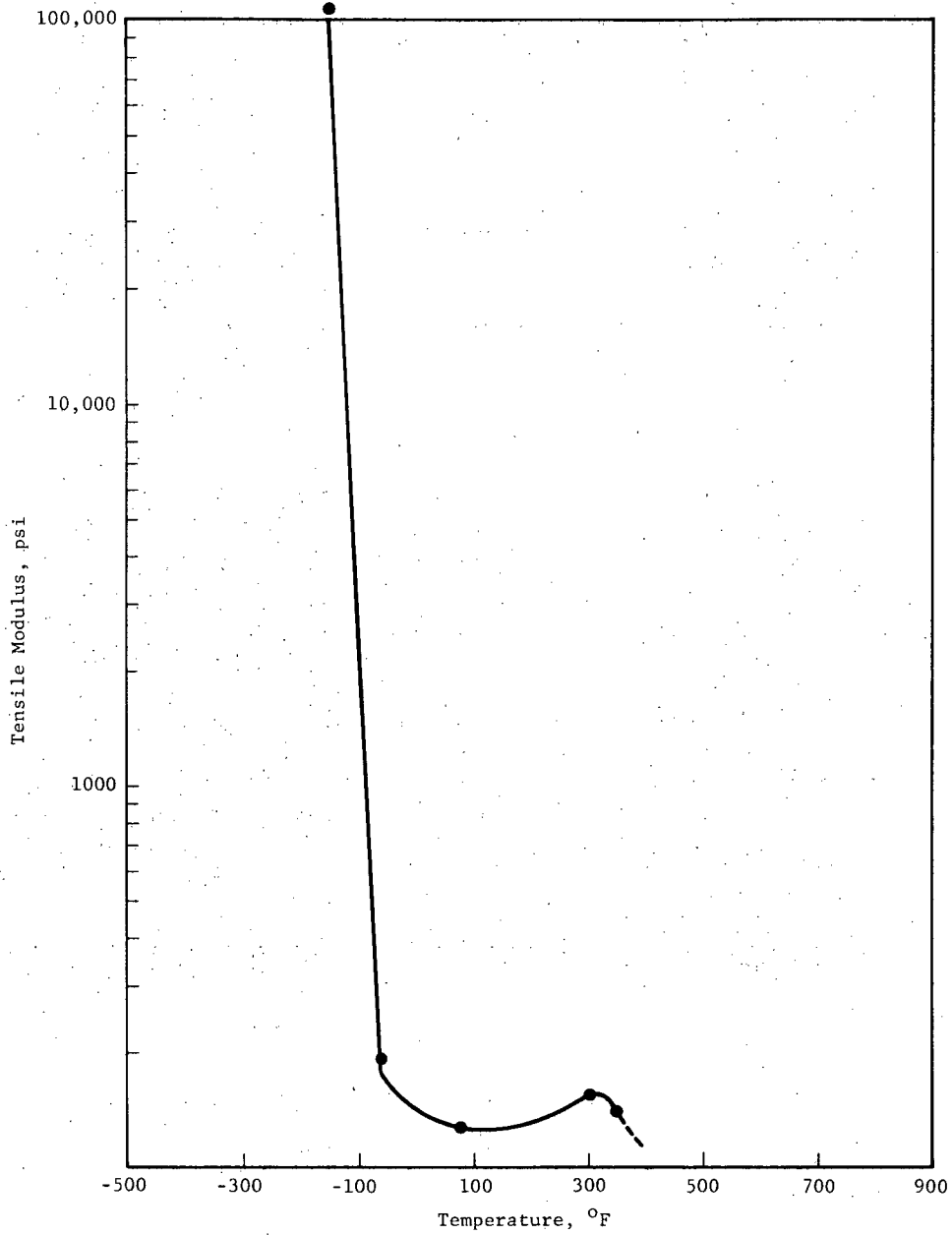


Figure 86 Tensile Modulus Vs. Temperature DC 93-046, 0.4 in./in./min. Strain Rate

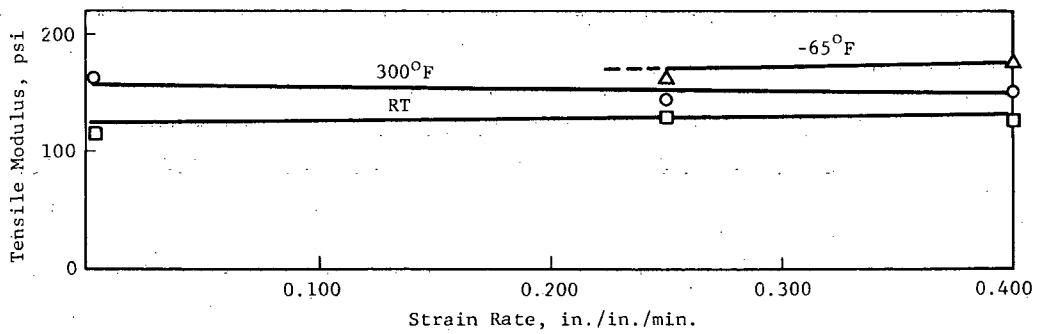


Figure 87 Tensile Modulus of DC 93-046 Vs. Strain Rate

Table XX TENSILE MODULUS OF SLA-561, PSI

Strain Rate, In./In./Min.	Temperature, °F									
	-270	-200	-175	-150	-65	RT	300	350	550	600
0.4				331	176	248	339	347	295	203
0.4				392	178	248	339	393	258	198
0.4				356	193	235	397	334	276	196
Avg.				360	182	244	358	358	276	199
0.25					194	244	323			
0.25					194	248	367			
0.25					178	247	335			
Avg.					189	246	342			
0.015	114,178	91,447	7,504							
0.015	91,487	102,236	7,945							
0.015	70,614	104,642	13,834							
Avg.	92,093	99,442	9,761							
0.003				186	251	340				
0.003				170	246	373				
0.003				165	245	346				
Avg.				174	247	253				

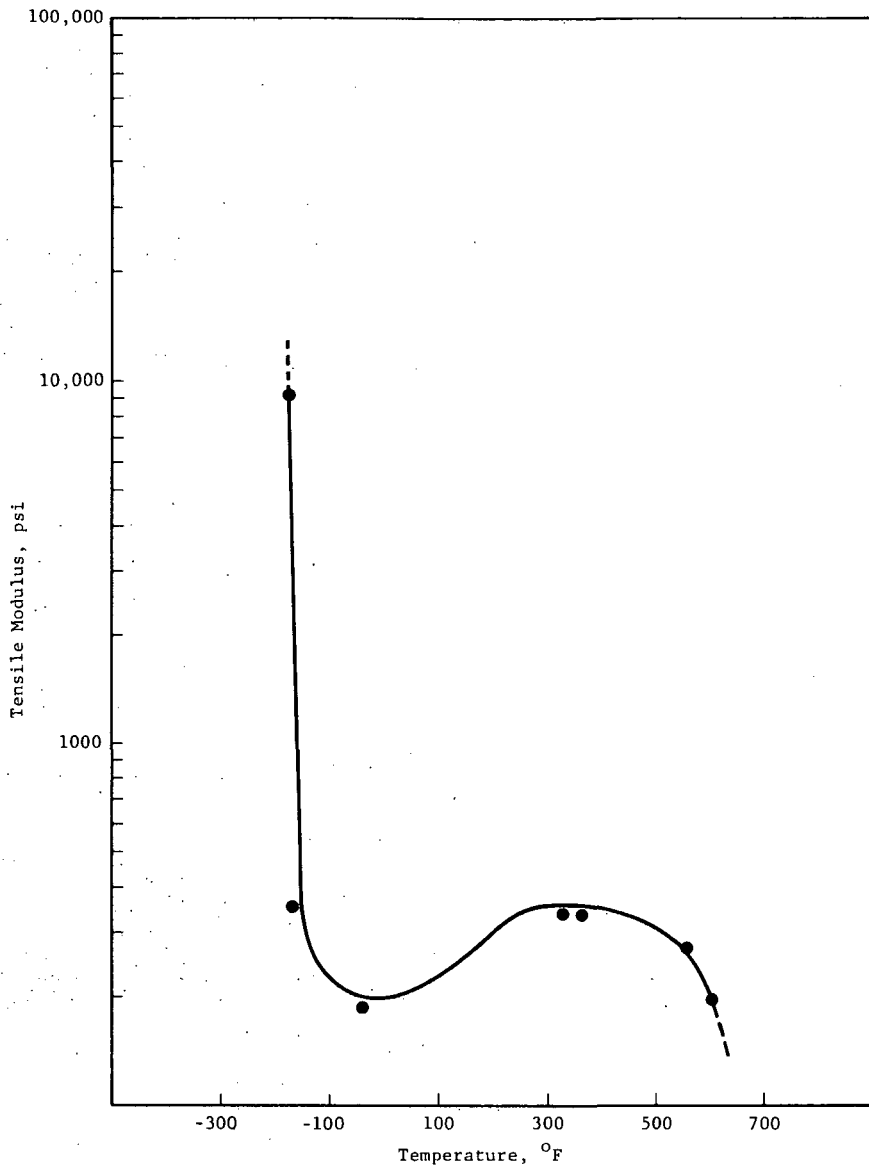


Figure 88 Tensile Modulus Vs. Temperature SLA 561 0.4 in./in./min. Strain Rate

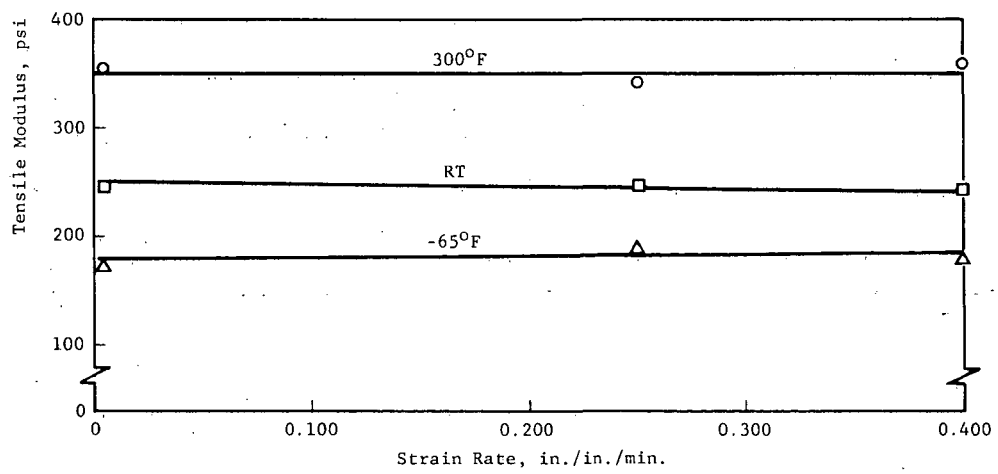


Figure 89 Tensile Modulus of SLA 561 Vs. Strain Rate

Table XXI TENSILE MODULUS OF RTV-560/RL-1973, PSI

Strain Rate, In./In./Min.	Temperature, °F										
	-270	-200*	-200	-175	-150	-65	RT	300	350	550	600
0.4					663	161	139	141	132	111	
0.4					534	154	133	128	156	111	
0.4					722	170	172	168	188	102	
Avg.					640	162	148	146	159	108	
0.25						160	134	120			
0.25						160	139	123			
0.25						155	139	133			
Avg.						158	137	125			
0.10						1,545					
0.10						1,524					
0.10						1,411					
Avg.						1,493					
0.05						182,401					
0.05						62,061					
0.05						122,231					
Avg.						110,548					
0.05						70,167					
0.05						125,395					
Avg.						74,519					
0.003						7,472					
0.003						7,472					
0.003						90,358					
Avg.						168	117	140			

*Specimen was not coated with GE RTV-560.

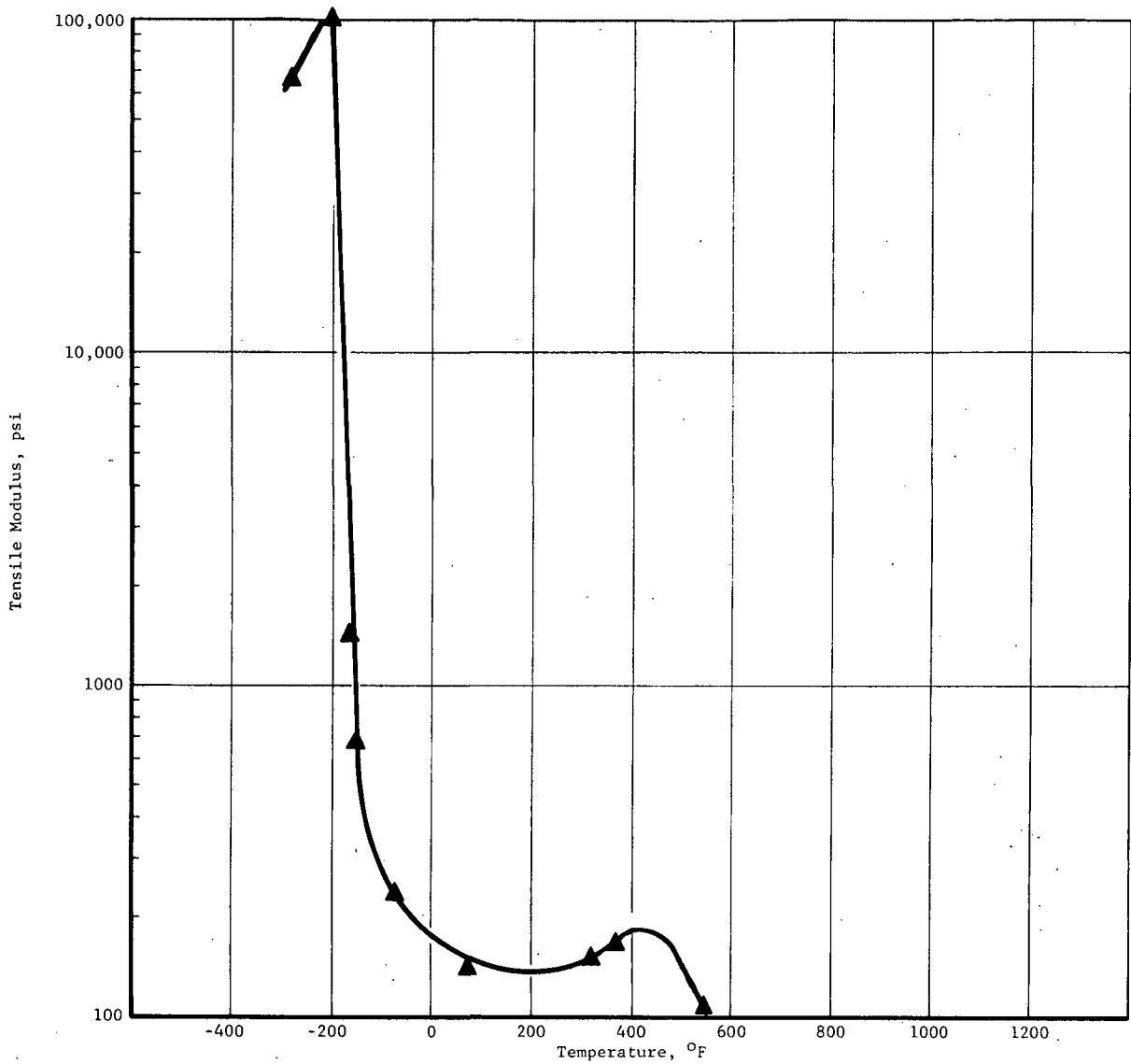


Figure 90 Tensile Modulus Vs. Temperature RTV 560/RL-1973

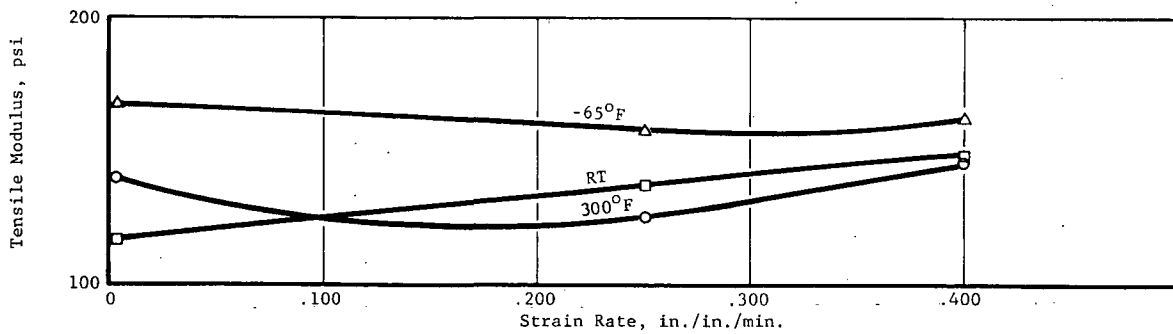


Figure 91 Tensile Modulus of RTV 560/RL-1973 Vs. Strain Rate

Tensile modulus as a function of strain rate is shown in Figure 91. The modulus decreases slightly as the strain rate is decreased at room temperature, but it is essentially constant at all strain rates at 300°F and -65°F.

As noted in the tables of data, large variations in values are obtained when the materials are tested below their brittle point. This variation is partly due to inaccuracies in measurement of these low deformations. A further discussion of this problem is contained in Section 6.

4.4 SHEAR MODULUS

4.4.1 Test Method

Shear modulus tests were conducted on double overlap shear specimens as shown in Figure 5 of Section 2 and Figure 92 loaded in torsion. The specimens were 1 inch wide with a 1-inch overlap. Bond thicknesses were 0.03, 0.06, 0.10, and 0.25 inch. Three specimens were tested for each data point. Strain rates were 0.4, 0.25, and 0.02 inch/inch/minute at -65°F, room temperature, and 300°F and 0.4 inch/inch/minute at 350°F, 550°F, and 600°F. At temperatures below -65°F, a strain rate was selected for each material which would provide a load rate consistent with the response of the test machine. These load rates are shown in the tables of data.

Load-deformation curves were obtained for each specimen tested. An initial slope was obtained from these curves and used to calculate the shear modulus as follows:

$$\text{Shear Modulus, psi} = \frac{2.66 \times P \times t}{\text{Arc sin } (\Delta/3.0)}$$

where: p/Δ = initial slope of load deformation curve
 t = average bondline thickness

The shear modulus test fixture was designed so that the specimen could be pinned with 0.125-inch-diameter pins at each end, and the load was applied at the center of the specimen through another 0.125-inch-diameter pin (Figure 92 and inserts in Figure 93 through 96). The fixture arm clevises holding each end were free to swivel and the cross arm holding the arm clevises was also free to swivel at the center. This allowed the specimen and fixture to be in alignment under all load conditions.

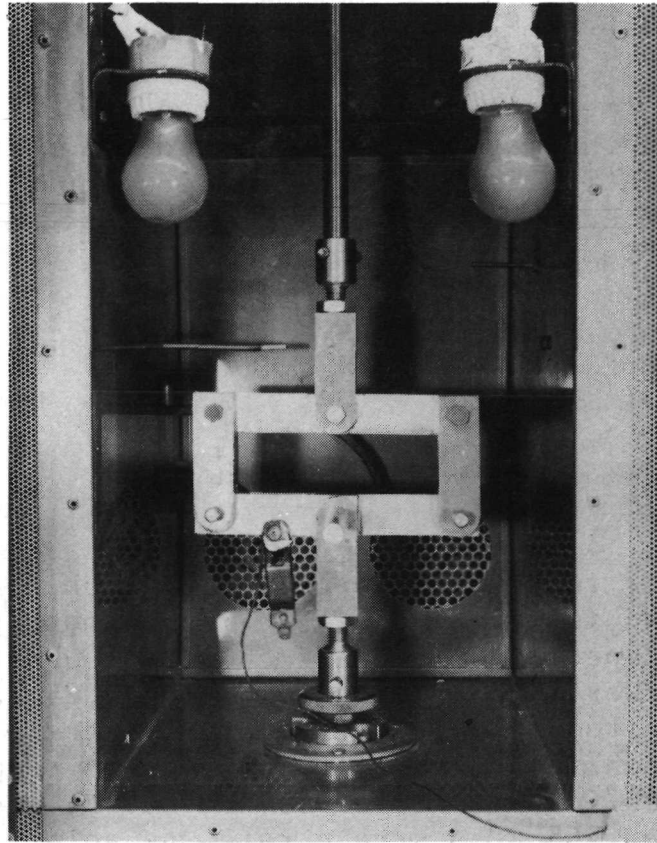


Figure 92 Shear Modulus Test Setup

4.4.2 Results and Discussion

Testing of shear modulus in torsion of the four adhesive materials was accomplished as described above. Effects of bondline thickness (0.03, 0.06, 0.10, and 0.25-inch), strain rates (0.4, 0.25, and 0.02 inch/inch/minute), and temperatures from -270°F to 600°F were determined.

Generally the modulus of all four adhesives vary directly with load rate and inversely with thickness of bond lines and temperature. There are individual exceptions to this generalization, however, as shown in Tables XXII, XXIII, XXIV, and XXV and graphically in Figures 93 through 96.

Table XXII SHEAR MODULUS (DOUBLE LAP TORSION TEST)
OF GE RTV-560

Bondline Test Temp. °F	Thickness Strain Rate in/in/min.	0.030 Inch		0.060 Inch		0.10 Inch		0.25 Inch	
		Spec. No.	Modulus PSI	Spec. No.	Modulus PSI	Spec. No.	Modulus PSI	Spec. No.	Modulus PSI
75	0.4	1-1	263	1-1	136	1-1	119	1-7	126
		1-2	166	1-2	146	1-2	137	2-1	158
		1-3	181	1-3	140	1-3	115	2-2	121
		Avg.	203	Avg.	141	Avg.	124	Avg.	135
		1-4	156	1-4	125	1-4	127	1-4	144
		1-5	122	1-5	146	1-5	120	1-5	144
	0.02	1-6	113	1-6	134	1-6	135	1-6	141
		Avg.	130	Avg.	135	Avg.	127	Avg.	143
		1-7	150	1-7	119	1-7	124	1-1	142
		2-1	196	2-1	113	2-1	117	1-2	126
		2-2	141	2-2	105	2-2	124	1-3	146
		Avg.	162	Avg.	112	Avg.	122	Avg.	138
300	0.4	2-3	315	2-6	170	2-3	175	2-3	138
		2-4	168	2-7	199	2-4	173	2-4	170
		2-5	166	3-1	175	2-5	170	2-5	151
		Avg.	216	Avg.	181	Avg.	173	Avg.	153
		2-6	215	3-2	200	2-6	160	2-6	142
		2-7	178	3-4	223	2-7	138	2-7	163
	0.02	3-1	168	3-5	200	3-1	160	3-1	150
		Avg.	187	Avg.	208	Avg.	153	Avg.	152
		3-2	121	2-3	179	3-2	150	3-2	155
		3-3	153	2-4	180	3-3	163	3-3	151
		3-4	135	2-5	186	3-4	166	3-4	164
		Avg.	136	Avg.	155	Avg.	159	Avg.	156
350	0.4	3-5	119	3-6	179	3-5	150	3-5	219
		3-6	175	3-7	147	3-6	159	3-6	213
		3-7	167	4-1	149	3-7	160	3-7	188
		Avg.	154	Avg.	158	Avg.	156	Avg.	206

Table XXII SHEAR MODULUS (DOUBLE LAP TORSION TEST)
OF GE RTV-560 (Continued)

Bondline Test Temp. °F	Thickness Strain Rate in/in/min.	0.030 Inch		0.060 Inch		0.10 Inch		0.25 Inch	
		Spec. No.	Modulus PSI	Spec. No.	Modulus PSI	Spec. No.	Modulus PSI	Spec. No.	Modulus PSI
550	0.4	4-1	55	4-2	33	4-1	48	4-1	71
		4-2	54	4-3	30	4-2	46	4-2	75
		4-3	57	4-4	34	4-3	50	4-3	110
		Avg.	55	Avg.	32	Avg.	37	Avg.	86
600	0.4	4-4	23	4-5	17	4-4	25	Not Tested	
		4-5	32	4-6	17	4-5	24		
		5-1	26	4-7	15	4-6	24		
		Avg.	27	Avg.	16	Avg.	24		
-65	0.4	5-6	110	5-1	132	4-7	78	4-4	137
		5-7	94	5-2	152	5-1	86	4-5	108
		6-1	87	5-3	137	5-2	83	4-6	122
		Avg.	97	Avg.	140	Avg.	82	Avg.	122
		5-3	107	5-4	133	5-3	102	4-7	93
		5-4	105	5-5	128	5-4	102	5-1	99
		5-5	102	5-6	145	5-5	100	5-2	101
		Avg.	105	Avg.	135	Avg.	101	Avg.	98
		4-6	92	5-7	153	5-6	99	5-3	115
		4-7	95	6-1	117	5-7	99	5-4	124
		5-2	97	6-2	110	6-1	78	5-5	118
Avg.	95	Avg.	127	Avg.	92	Avg.	119		
-150	0.4	6-2	160	6-3	223	6-2	170	5-6	226
		6-3	221	6-4	204	6-3	137	5-7	134
		6-4	250	6-5	253	6-4	131	6-1	181
		Avg.	210	Avg.	226	Avg.	146	Avg.	180
-175	0.02	6-5	1094	6-6	2740	6-5	3028	6-2	63,840*
		6-6	1683	6-7	2016	6-6	1805	6-3	5,389
		6-7	857	7-1	2640	6-7	1882	6-4	4,402
		Avg.	1212	Avg.	2465	Avg.	2238	Avg.	4,895

Table XXII SHEAR MODULUS (DOUBLE LAP TORSION TEST)
OF GE RTV-560 (Continued)

Bondline Test Temp. °F	Thickness Strain Rate in/in/min.	0.030 Inch		0.060 Inch		0.10 Inch		0.25 Inch	
		Spec. No.	Modulus PSI	Spec. No.	Modulus PSI	Spec. No.	Modulus PSI	Spec. No.	Modulus PSI
-200	0.02	7-1	1276	7-2	2020	7-1	Neg.	6-5	6869
		7-2	1216	7-3	2576	7-2	22,200	6-6	8291
		7-3	1134	7-4	3707	7-3	19,600	6-7	9617
		Avg.	1209	Avg.	2770	Avg.	20,911	Avg.	8259
-270	0.02	7-4	5054	7-5	7600	7-4	3224	7-1	4772
		7-5	Neg.	7-6	15,600	7-5	4879	7-2	2778
		7-6	Neg.	7-7	13,800	7-6	1654	7-3	2080
		Avg.	5054	Avg.	12,333	Avg.	3252	Avg.	3210

*Not included in average.

Table XXIII SHEAR MODULUS (DOUBLE LAP TORSION TEST)
OF DC 93-046

Bondline Test Temp. °F	Thickness Strain Rate in/in/min.	0.030 Inch		0.060 Inch		0.10 Inch		0.25 Inch	
		Spec. No.	Modulus PSI	Spec. No.	Modulus PSI	Spec. No.	Modulus PSI	Spec. No.	Modulus PSI
75	0.04	6-1	59	B1-1	63	1-1	65	2-3	72
		6-2	64	B1-2	50	1-2	74	2-4	75
		6-3	58	B1-3	50	1-3	79	2-5	79
		Avg.	60	Avg.	54	Avg.	73	Avg.	76
		6-4	60	B1-4	58	1-4	66	1-7	91
		6-5	62	B1-5	54	1-5	59	2-1	77
	0.02	6-6	61	B1-6	51	1-6	64	2-2	87
		Avg.	61	Avg.	54	Avg.	63	Avg.	85
		6-7	52	B1-7	48	1-7	60	1-1	68
		7-1	52	B2-1	54	2-1	70	1-2	76
		7-2	60	B2-2	63	2-2	76	1-6	83
		Avg.	55	Avg.	55	Avg.	69	Avg.	76
300	0.4	7-3	40	B3-2	64	3-2	71	2-6	85
		7-4	40	B3-3	65	3-3	87	2-7	84
		7-5	48	B3-4	62	3-4	64	3-1	88
		Avg.	43	Avg.	64	Avg.	74	Avg.	86
		7-6	47	B2-6	59	2-6	68	3-5	72
		7-7	63	B2-7	59	2-7	71	3-6	86
	0.25	A4-1	55	B3-1	76	3-1	72	Avg.	79
		Avg.	55	Avg.	64	Avg.	70	3-7	69
		A4-2	54	B2-3	67	2-3	64	4-1	50
		A4-3	49	B2-4	60	2-4	68	4-2	52
		A4-4	46	B2-5	59	2-5	63	Avg.	57
		Avg.	50	Avg.	62	Avg.	65	4-4	65
350	0.4	A4-5	44	B3-5	55	3-5	55	4-6	71
		A4-6	46	B3-6	58	3-6	69	5-1	111
		A4-7	46	B3-7	57	3-7	55	Avg.	82
		Avg.	45	Avg.	57	Avg.	60		

Table XXIV SHEAR MODULUS (DOUBLE LAP TORSION TEST)
OF MMC SLA-561

Bondline Test Temp. °F	Thickness Strain Rate in/in/min.	0.030 Inch		0.060 Inch		0.10 Inch		0.25 Inch	
		Spec. No.	Modulus PSI	Spec. No.	Modulus PSI	Spec. No.	Modulus PSI	Spec. No.	Modulus PSI
75	0.4	1-1	89	1-1	100	1-7	95	1-7	56
		1-2	109	1-2	82	2-1	85	2-1	63
		1-3	82	1-3	74	2-2	86	2-2	65
		Avg.	94	Avg.	85	Avg.	89	Avg.	62
		1-4	82	1-4	87	1-4	90	1-4	64
		1-5	82	1-5	97	1-5	73	1-5	67
	0.25	1-6	77	1-6	106	1-6	80	1-6	75
		Avg.	81	Avg.	97	Avg.	81	Avg.	69
		1-7	87	1-7	95	1-1	93	1-1	67
		2-1	87	2-1	91	1-2	91	1-2	69
		2-2	83	2-2	98	1-3	84	1-3	71
		Avg.	86	Avg.	95	Avg.	89	Avg.	69
300	0.04	3-2	116	3-2	124	2-3	110	2-3	103
		3-3	115	3-3	124	2-4	108	2-4	98
		3-4	120	3-4	128	2-5	126	2-5	89
		Avg.	117	Avg.	125	Avg.	115	Avg.	97
		2-6	121	2-6	158	2-6	116	2-6	79
		2-7	110	2-7	136	2-7	114	2-7	80
	0.25	3-1	216	3-1	124	3-1	143	3-1	87
		Avg.	119	Avg.	140	Avg.	124	Avg.	82
		2-3	123	2-3	126	3-2	136	3-2	88
		2-4	135	2-4	140	3-3	132	3-3	76
		2-5	113	2-5	132	3-4	138	3-4	96
		Avg.	124	Avg.	133	Avg.	135	Avg.	87
350	0.4	3-5	116	3-5	120	3-5	146	3-5	94
		3-6	112	3-6	126	3-6	142	3-6	70
		3-7	119	3-7	132	3-7	154	3-7	78
		Avg.	116	Avg.	126	Avg.	147	Avg.	81

Table XXIV SHEAR MODULUS (DOUBLE LAP TORSION TEST)
OF MMC SLA-561 (Continued)

Bondline Test Temp. °F	Thickness Strain Rate in/in/min.	0.030 Inch		0.060 Inch		0.10 Inch		0.25 Inch	
		Spec. No.	Modulus PSI	Spec. No.	Modulus PSI	Spec. No.	Modulus PSI	Spec. No.	Modulus PSI
550	0.4	4-1	86	4-1	68	4-1	93	4-1	76
		4-2	71	4-2	84	4-2	102	4-2	67
		4-3	78	4-3	83	4-3	91	4-3	67
		Avg.	78	Avg.	78	Avg.	96	Avg.	70
600	0.4	4-4	81	4-4	59	4-4	68	No Test	
		4-5	64	4-5	65	4-5	75		
		4-6	62	4-6	66	4-6	79		
		Avg.	68	Avg.	64	Avg.	74		
-65	0.4	5-6	56	4-7	77	4-7	80	4-4	67
		5-7	76	5-1	79	5-1	74	4-5	242
		6-1	92	5-2	78	5-2	77	4-6	203
		Avg.	75	Avg.	78	Avg.	77	Avg.	171
0.25	0.25	5-3	82	5-3	86	5-3	76	4-7	46
		5-4	86	5-4	141	5-4	77	5-1	53
		5-5	80	5-5	83	5-5	74	5-2	52
		Avg.	83	Avg.	103	Avg.	75	Avg.	50
0.02	0.02	4-7	89	5-6	75	5-6	78	5-3	55
		5-1	71	5-7	80	5-7	74	5-4	62
		5-2	77	6-1	105	6-1	63	5-5	64
		Avg.	79	Avg.	87	Avg.	72	Avg.	60
-150	0.25	6-2	319	6-2	1861	6-2	99	5-6	74
		6-3	336	6-3	1549	6-3	98	5-7	72
		6-4	326	6-4	282	6-4	103	6-1	69
		Avg.	327	Avg.	1216	Avg.	100	Avg.	72
-175	0.2	6-5	4166	6-5	Neg.	6-5	Neg.	6-2	604
		6-6	25,200	6-6	32,562	6-6	Neg.	6-3	13,210
		6-7	349,000	6-7	Neg.	6-7	20,703	6-4	65,170
		Avg.	126,122	Avg.	32,562	Avg.	20,703	Avg.	26,328

Table XXIV SHEAR MODULUS (DOUBLE LAP TORSION TEST)
OF MMC SLA-561 (Continued)

Bondline Thickness Test Temp. °F	Strain Rate in/in/min.	0.030 Inch		0.060 Inch		0.10 Inch		0.25 Inch	
		Spec. No.	Modulus PSI	Spec. No.	Modulus PSI	Spec. No.	Modulus PSI	Spec. No.	Modulus PSI
-200	0.2	7-1	4118	7-1	2792	7-1	9744	6-5	8575
		7-2	8268	7-2	18,311	7-2	3413	6-6	13,577
		7-3	33,800	7-3	Neg.	7-3	5822	6-7	5871
		Avg.	11,266	Avg.	10,551	Avg.	6326	Avg.	9341
-270	0.2	7-4	6259	7-4	2993	7-4	5362	7-1	13,300
		7-5	2389	7-5	3512	7-5	7656	7-2	3179
		7-6	2780	7-6	2770	7-6	2618	7-3	3767
		Avg.	3809	Avg.	3091	Avg.	5178	Avg.	6749

Table XXV SHEAR MODULUS (DOUBLE LAP TORSION TEST)
OF GE RTV-560/RL-1973 SYSTEM

Bondline Test Temp. °F	Thickness Strain Rate in/in/min.	0.030 Inch		0.060 Inch		0.10 Inch		0.25 Inch	
		Spec. No.	Modulus PSI	Spec. No.	Modulus PSI	Spec. No.	Modulus PSI	Spec. No.	Modulus PSI
75	0.4	1-7	78	1-7	45	1-7	39	1-7	18
		2-1	70	2-1	51	2-1	64	2-1	15
		2-2	108	2-2	55	2-2	57	2-2	16
		Avg.	85	Avg.	50	Avg.	53	Avg.	16
		1-4	61	1-4	35	1-4	36	1-4	16
		1-5	62	1-5	37	1-5	36	1-5	20
	0.25	1-6	67	1-6	32	1-6	40	1-6	20
		Avg.	63	Avg.	35	Avg.	37	Avg.	18
		1-1	54	1-1	35	1-1	38	1-1	16
		1-2	57	1-2	36	1-2	39	1-2	18
		1-3	48	1-3	33	1-3	39	1-3	17
		Avg.	53	Avg.	34	Avg.	39	Avg.	17
300	0.4	6-2	83	6-3	44	6-2	32	2-3	17
		6-3	98	6-4	43	6-3	39	2-4	18
		6-4	102	6-5	41	6-4	30	2-5	16
		Avg.	94	Avg.	43	Avg.	34	Avg.	17
		5-6	76	5-7	37	5-6	30	2-6	12
		5-7	74	6-1	36	5-7	29	2-7	12
	0.25	6-1	84	6-2	36	6-1	32	3-1	11
		Avg.	78	Avg.	36	Avg.	30	Avg.	12
		5-3	89	5-3	45	5-3	34	3-2	6
		5-4	89	5-4	41	5-4	28	3-3	7
		5-5	88	5-5	60	5-5	35	3-4	8
		Avg.	89	Avg.	49	Avg.	32	Avg.	7
350	0.4	6-5	101	6-6	45	6-5	40	3-5	8
		6-6	128	6-7	46	6-6	42	3-6	10
		6-7	93	7-1	63	6-7	45	3-7	10
		Avg.	107	Avg.	51	Avg.	42	Avg.	9

Table XXV SHEAR MODULUS (DOUBLE LAP TORSION TEST)
OF GE RTV-560/RL-1973 SYSTEM (Continued)

Bondline Test Temp. °F	Thickness Strain Rate in/in/min.	0.030 Inch		0.060 Inch		0.10 Inch		0.25 Inch	
		Spec. No.	Modulus PSI	Spec. No.	Modulus PSI	Spec. No.	Modulus PSI	Spec. No.	Modulus PSI
550	0.4	7-1	79	7-2	18	7-1	30	4-1	6
		7-2	55	7-3	17	7-2	27	4-2	6
		7-3	68	7-4	21	7-3	25	4-3	6
		Avg.	67	Avg.	19	Avg.	27	Avg.	6
-65	0.4	2-3	102	2-3	38	2-3	78	4-4	21
		2-4	93	2-4	51	2-4	77	4-5	16
		2-5	76	2-5	47	2-5	69	4-6	14
		Avg.	90	Avg.	46	Avg.	75	Avg.	17
		2-6	93	2-6	28	2-6	54	4-7	8
		2-7	74	2-7	35	2-7	51	5-1	13
		3-1	87	3-1	40	3-1	55	5-2	12
Avg.	85	Avg.	35	Avg.	53	Avg.	11		
-150	0.02	3-2	55	3-2	33	3-2	35	5-3	12
		3-3	79	3-3	41	3-3	41	5-4	11
		3-4	78	3-4	36	3-4	48	5-5	11
		Avg.	71	Avg.	37	Avg.	41	Avg.	11
		3-5	1451	3-5	248	3-5	650	5-6	756
		3-6	945	3-6	151	3-6	475	5-7	353
		3-7	1888	3-7	251	3-7	667	6-1	463
Avg.	1428	Avg.	217	Avg.	597	Avg.	524		
-175	0.4	4-1	17,977	4-1	Neg.	4-1	1411	6-2	3282
		4-2	17,538	4-2	31,569	4-2	1391	6-3	2424
		4-3	47,381	4-3	13,173	4-3	2748	6-4	2414
		Avg.	27,632	Avg.	22,371	Avg.	6023	Avg.	2707
-200	0.4	4-4	16,622	4-4	17,822	4-4	31,920	6-5	4293
		4-5	46,134	4-5	4875	4-5	30,856	6-6	2552
		4-6	16,223	4-6	1834	4-6	21,382	6-7	5623
		Avg.	26,340	Avg.	8177	Avg.	28,053	Avg.	4156

Table XXV SHEAR MODULUS (DOUBLE LAP TORSION TEST)
OF GE RTV-560/RL-1973 SYSTEM (Continued)

Bondline Test Temp. °F	Thickness Strain Rate in/in/min.	0.030 Inch		0.060 Inch		0.10 Inch		0.25 Inch	
		Spec. No.	Modulus PSI	Spec. No.	Modulus PSI	Spec. No.	Modulus PSI	Spec. No.	Modulus PSI
-270	0.25	4-7	5953	4-7	1919	4-7	72,200	7-1	3278
		5-1	15,561	5-1	2245	5-1	14,980	7-2	5911
		5-2	22,167	5-2	105,888	5-2	41,895	7-3	2712
		Avg.	14,560	Avg.	36,684	Avg.	43,026	Avg.	3967

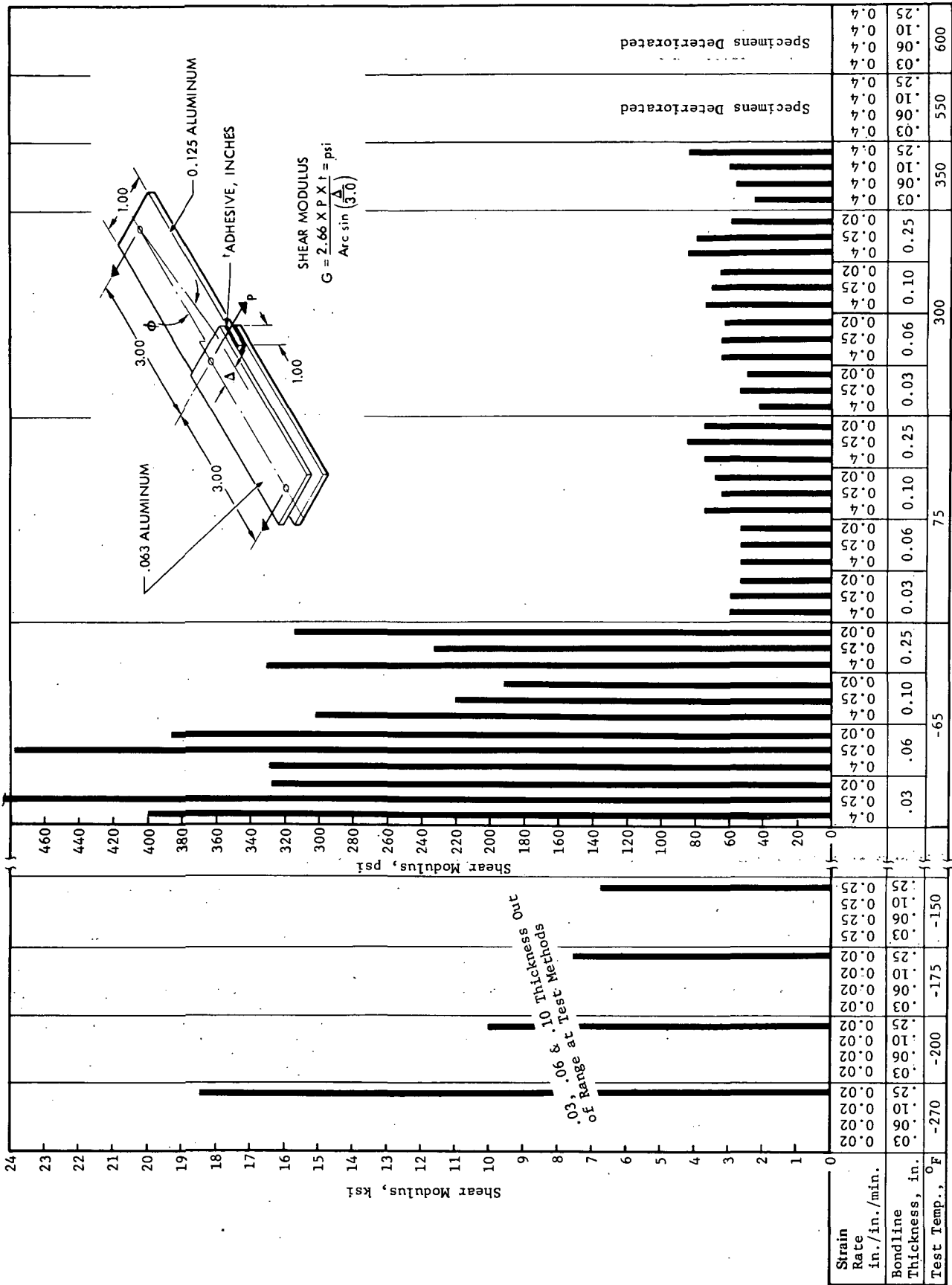


Figure 94 Shear Modulus of DC 93-046 at Various Strain Rates, Bondline Thicknesses, and Temperatures

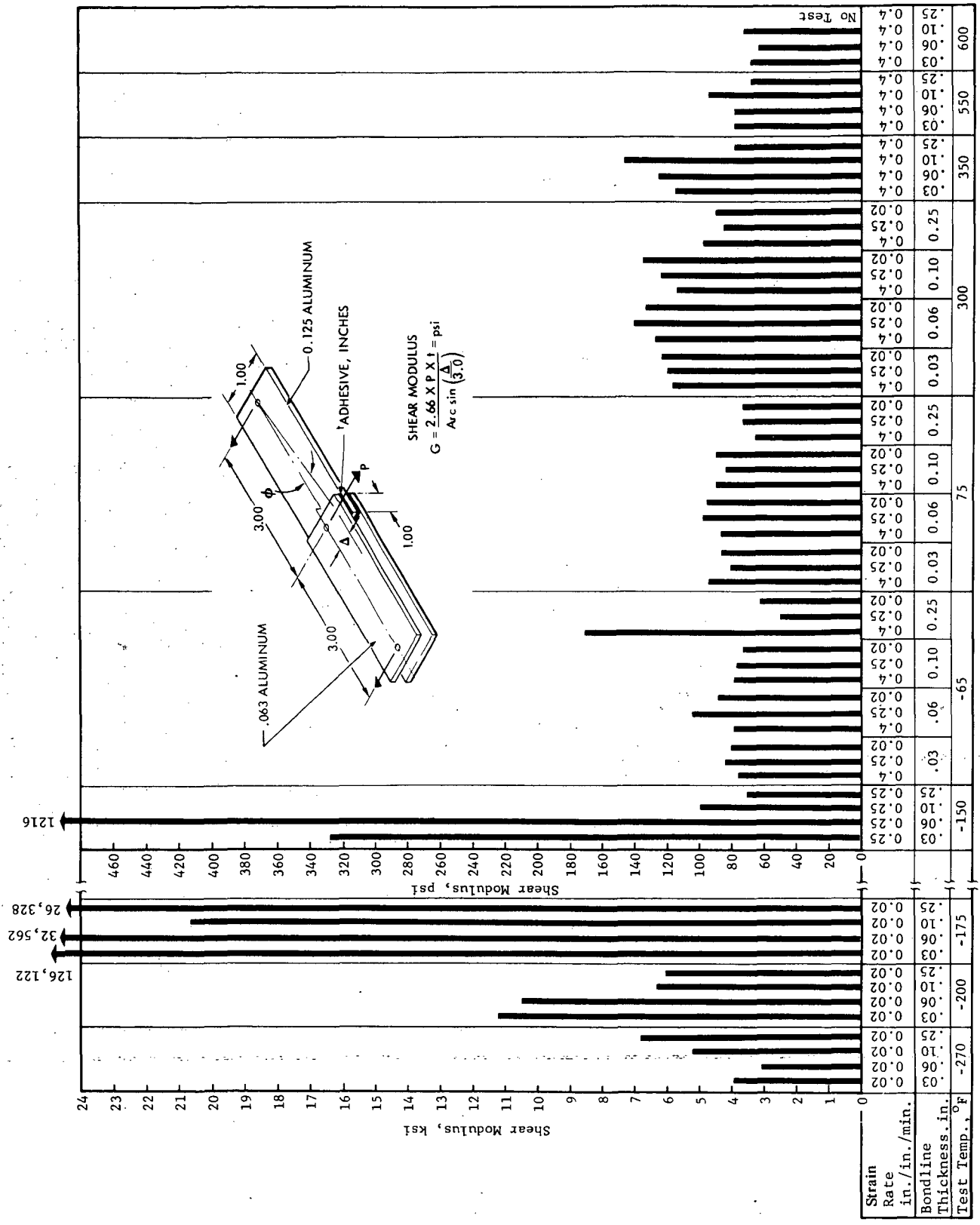


Figure 95 Shear Modulus of SLA-561 at Various Strain Rates, Bondline Thicknesses, and Temperatures

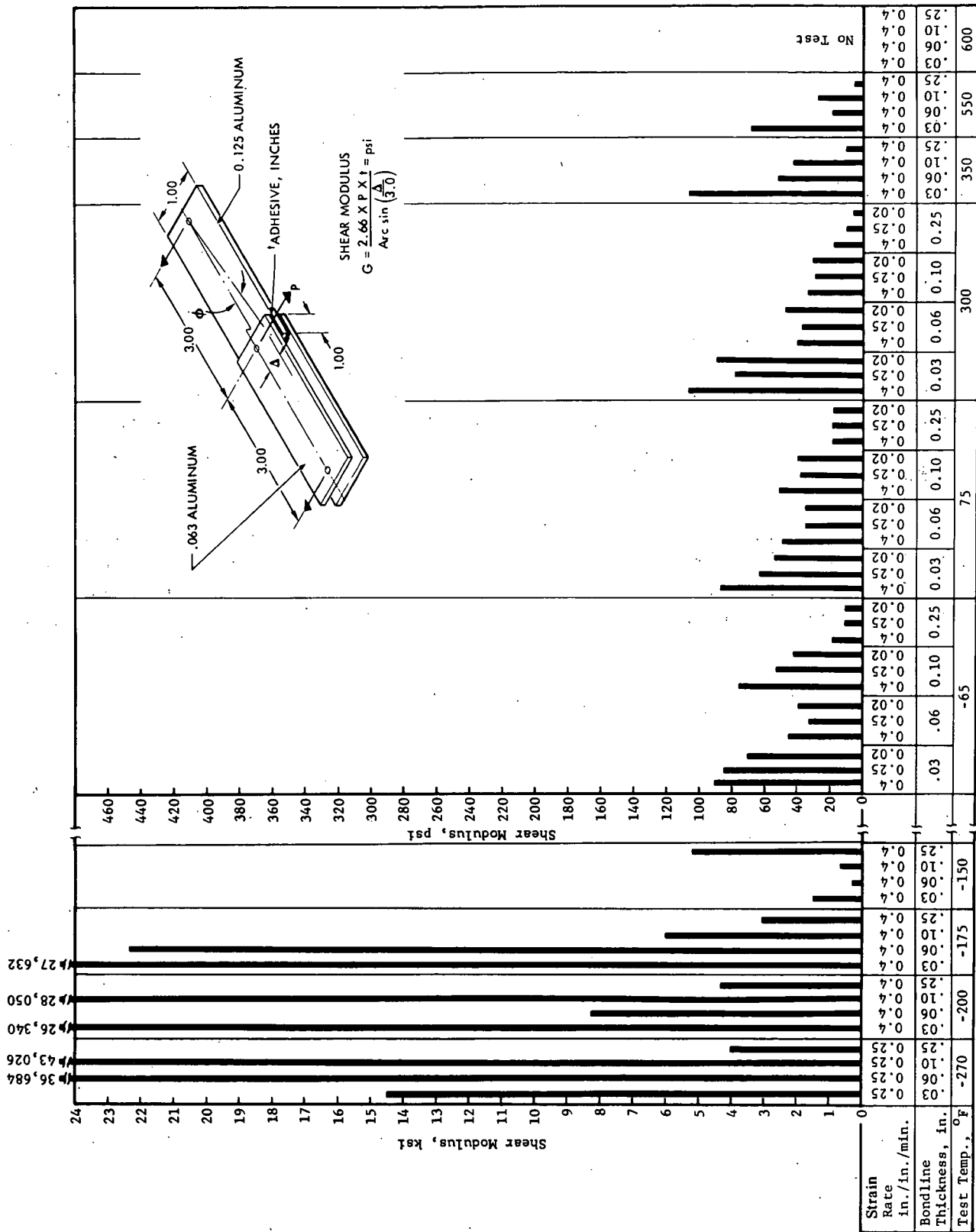


Figure 96 Shear Modulus of GE-560/RL-1973 at Various Strain Rates, Bondline Thicknesses, and Temperatures

The RTV-560/RL-1973 system has the lowest shear modulus of the four adhesives in the temperature range of -65°F to 550°F , while the GE RTV-560 has the lowest modulus values below -65°F . This difference may or may not be real. The lower values for GE RTV-560 at -175°F , -200°F , and -270°F may be due to polymer structure slippage rather than actual lower modulus. In crude shock tests (striking lap shear specimens at -200°F), the RL-1973 specimens appear to be the toughest of the four adhesives at this low temperature.

The large decrease in shear modulus of the 0.25-inch bond line RTV-560/RL-1973 as compared with the 0.1 inch and thinner bond line specimens is believed to be due to smaller percentages of GE RTV-560 contained in the bond line. When using the GE RTV-560 as an adhesive for the RM/RL-1973 sponge, the outer layer of sponge cells are filled with the adhesive. This in addition to the bond line comprises a high percentage of the total bond line in the specimens with thin bond lines but only a small percentage of the total bond line in specimens with thicker bond lines.

As noted in the tables of data, large variations in values are obtained when the materials are tested at temperatures below their brittle point. These variations are partly due to inaccuracies in measurements, which is discussed further in Section 6.

4.5 COMPRESSION MODULUS

Molded parallelepipeds were subjected to compressive loads, and their longitudinal and transverse deformations were monitored. The data obtained was used to determine compression modulus and Poisson's ratio in compression.

4.5.1 Test Method

Parallelepipeds 1.5 inches square by 4 inches high were molded from the three two-component adhesives (Figures 6, and 97). The RM RL-1973 sponge specimens were cut from sheets of sponge 1.5 inches thick. GE RTV-560 was applied to each end of the sponge specimens to provide ends that were closer to being parallel than could be cut from the sponge sheets.

One face of each specimen was bench marked with four 0.02-inch-diameter dots using a template and procedure as described under tensile modulus testing. During testing, 35mm photographs

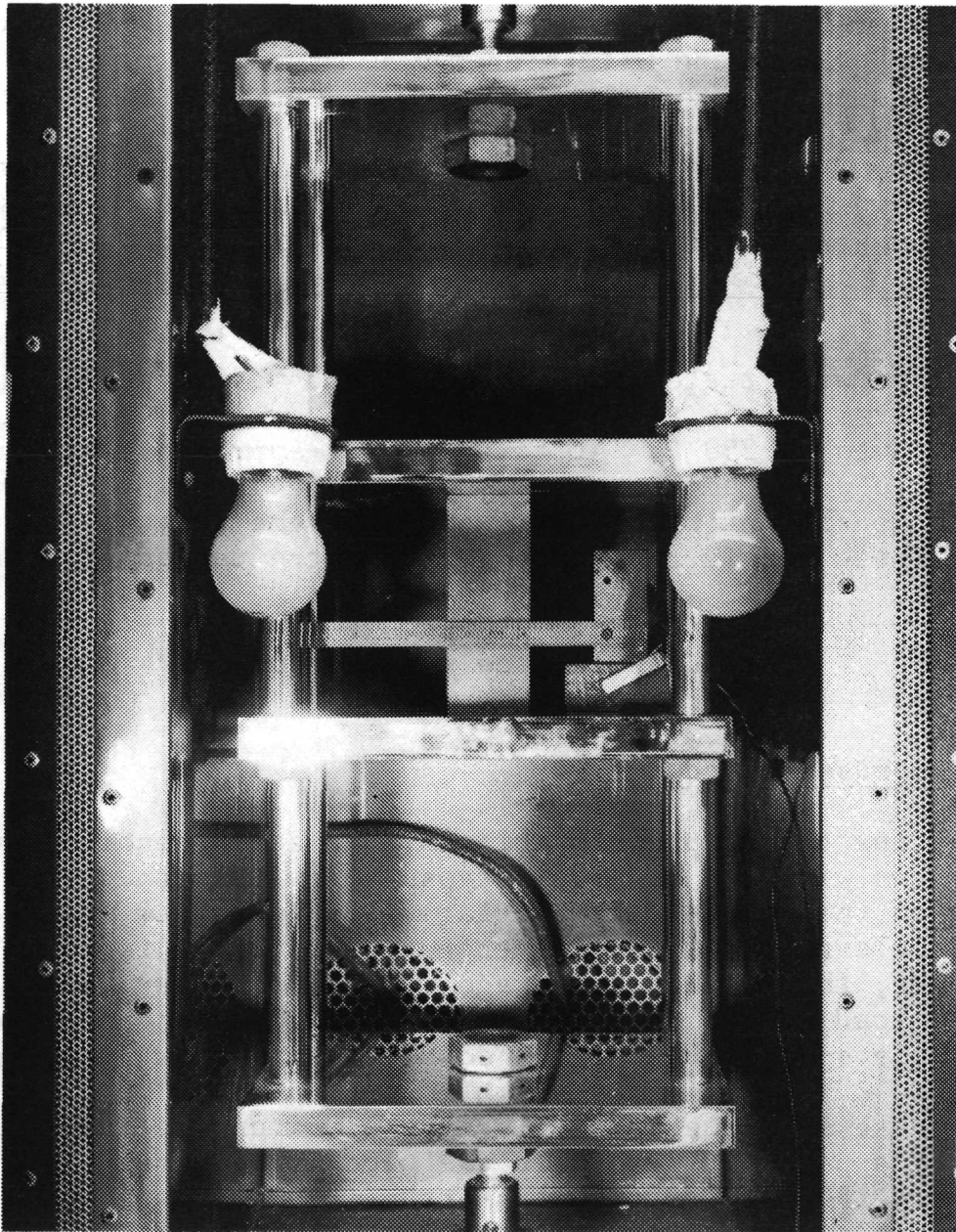


Figure 97 Compression Modulus Test Setup

(Figure 82) were taken at incremental loadings; these were later developed and measured. The camera and techniques used to relate an individual photograph with a specific load were the same as those used during the tensile modulus testing. Two dots, one at the top and one at the bottom of the specimen, were used to monitor longitudinal strain, and two dots, one on each edge of the specimen 2 inches from the ends, were used to monitor transverse strain. The computer program described in Appendix V was slightly modified to calculate compression modulus and Poisson's ratio in compression.

Specimens were tested at 0.4, 0.25, and 0.007 inch/inch/minute strain rates at -65°F , room temperature, and 300°F and at 0.4 inch/inch/minute at 350°F . At temperatures approaching the material's brittle point and below, a strain rate that would provide a load rate consistent with the response of the test machine was selected. These strain rates are shown in the tables of data.

4.5.2 Results and Discussion

4.5.2.1 Compression Modulus

In testing the compression blocks, the same phenomenon was encountered as with the tensile straps at low temperatures. For example, when the blocks were initially loaded at temperatures below their glass-transition temperature they began to shrink. In some cases, the rate of shrinkage was greater than the loading rate; hence load on the machine chart would go up and then return to zero as the specimen being tested began to shrink (Section 6).

When these silicone materials freeze, extensive internal stresses are apparently set up in the block specimens. At -200°F , approximately 150°F below the glass-transition temperature of DC 93-046, stresses were so great that the slight thermal shock caused by opening the door to the environmental chamber fractured the specimen as shown pictorially in Figure 98.

Elevated temperatures were extremely detrimental to the 1.5 x 1.5 x 4.0-inch compression blocks, particularly since 30 minutes to 1 hour was required to bring the centers of the specimens to ambient temperature. At 350°F and above, the DC 93-046 sponged internally. At 550° and 600°F the GE-560 also sponged internally while the SLA-561 cracked. These effects are shown in Figure 99. At temperatures above 350°F , the RL-1973 closed-cell silicone sponge expanded and buckled under load. Because of these effects, data on compression at temperatures above 350°F were unobtainable.

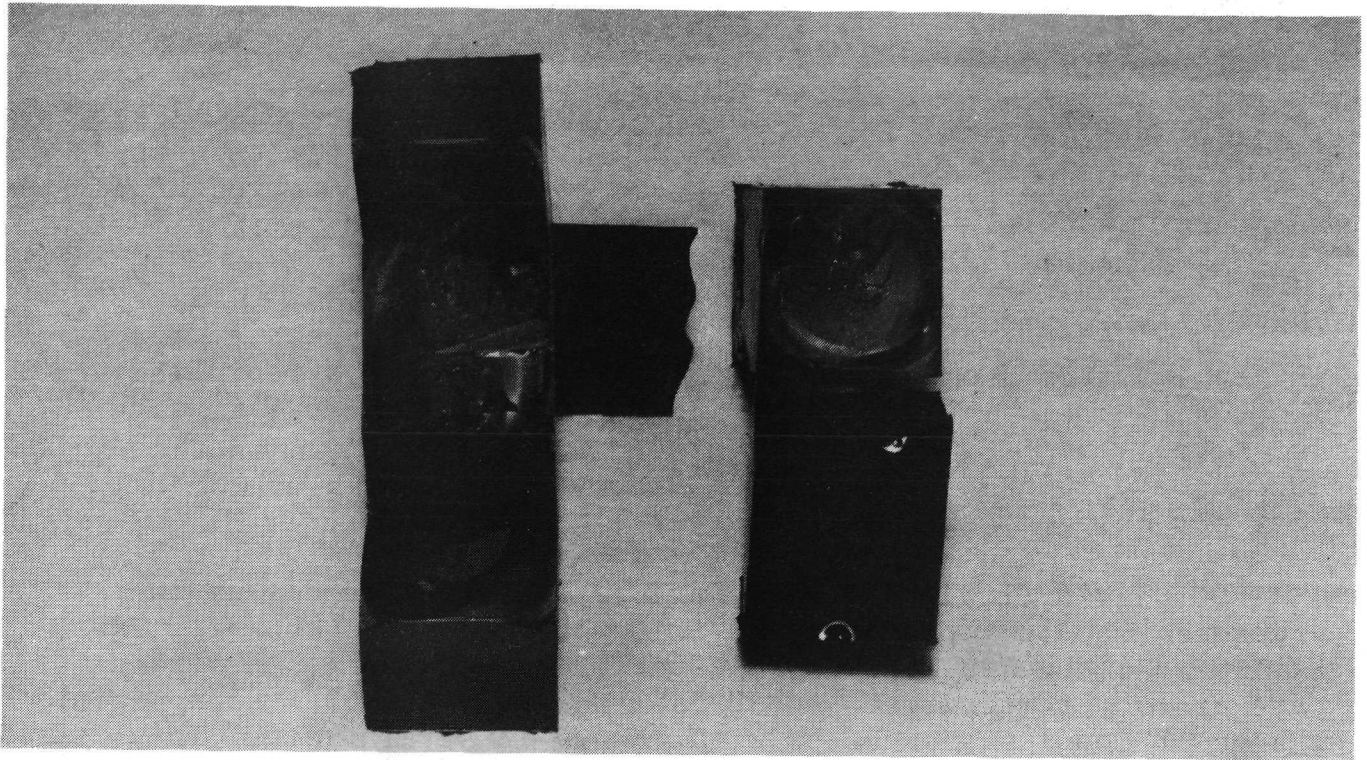


Figure 98 Effect of -200°F on DC 93-046 Compression Specimens

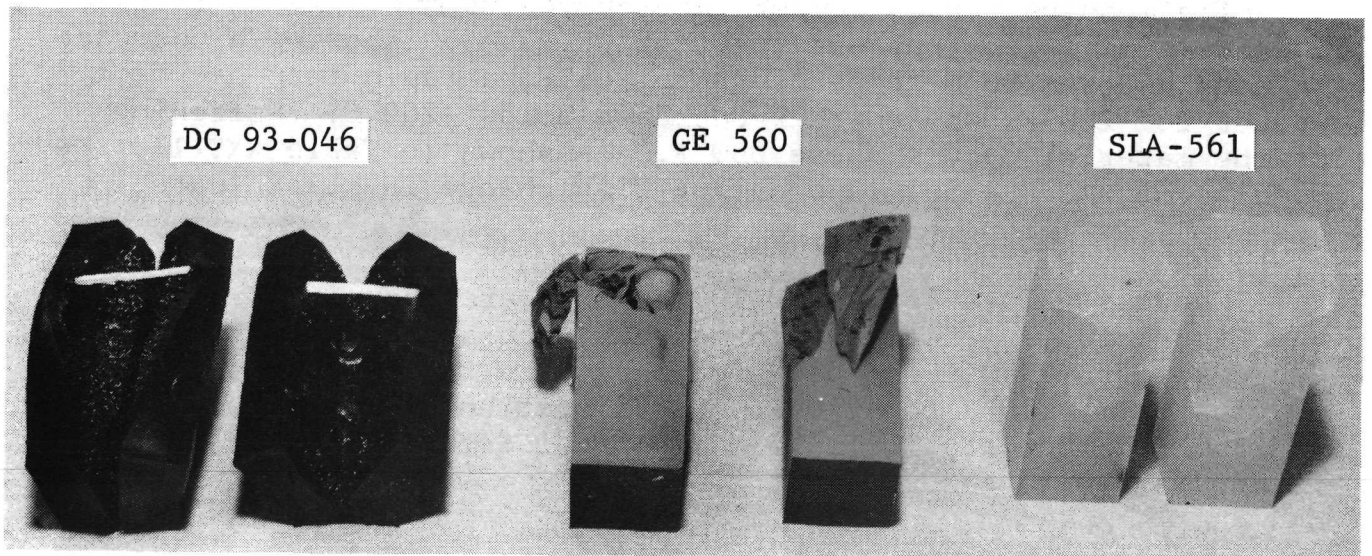


Figure 99 Effect of 550°F & 600°F on Compression Specimens

One effort to heat a GE-560 specimen faster by placing it in a dielectric oven resulted in rupture and partial depolymerization of the specimen.

The compression modulus data on individual specimens is shown in Tables XXVI through XXIX, and the relationship between compression modulus and temperature is shown in Figures 100 through 103. As can be seen in these figures, the curve obtained is similar to that obtained for tensile modulus.

GE RTV-560 (Table XXVI and Figure 100) experiences a decrease in modulus from room temperature to -65°F and then a rapid increase in modulus from -150°F to -200°F followed by a decrease in modulus below -200°F . Softening of the material is shown in the curve above 300°F . As noted in Table XXVI, compression modulus does not change with change in strain rate.

DC 93-046 (Table XXVII and Figure 101) experiences an increase in modulus with decrease in temperature. As shown in Table XXVII, no change in modulus is associated with change in strain rate at room temperature and 300°F . However, at -65°F an apparent change in modulus does occur with change in strain rate. This is believed to be due to the time at temperature tolerance allowed with these specimens. As discussed previously, DC 93-046 is extremely time-temperature dependent, and slight variations in time at temperature greatly affect the test results.

The modulus versus temperature curve for MMC SLA-561 (Figure 102) is similar to that obtained for GE RTV-560 showing a decrease in modulus from room temperature to -65°F , a rapid increase from -150°F to -200°F , and another decrease below -200°F . Softening of the material occurs above 350°F . As shown in Table XXVIII, the modulus of MMC SLA-561 is constant with change in strain rate.

Modulus values for RM/RL-1973 sponge are shown in Table XXIX and Figure 103. A decrease in modulus occurs as the temperature decreases from 350°F to -65°F followed by a rapid increase in modulus from -150°F to -270°F . Deterioration begins between 350°F and 550°F . The data in Table XXIX also indicate that the modulus is constant with change in strain rate.

Table XXVI COMPRESSION MODULUS OF GE RTV-560, PSI

Strain Rate, In./In./Min.	Temperature, Of									
	-270	-200	-175	-150	-65	RT	300	350	525	
0.4				840	397	446	381	270	172	
0.4				836	382	446	417	287		
0.4				808	377	452	407	278		
Avg.				828	385	448	402	278	172	
0.25					395	449	347			
0.25					418	458	388			
0.25					410	469	396			
Avg.					408	459	377			
0.007	37,221	55,396	10,030		403	442	395			
0.007	119,218	170,049	99,737		398	448	333			
0.007	56,531	284,010	230,681		408	442	356			
Avg.	70,990	169,818	113,483		403	444	361			

Table XXVII COMPRESSION MODULUS OF DC 93-046, PSI

Strain Rate, In./In./Min.	Temperature, °F							
	-270	-200	-175	-150	-65	RT	300	350
0.4					327	236	121	
0.4					2151	229	104	
0.4					411	228	126	
Avg.					963	231	117	
0.25					344	235	134	
0.25					682	221	106	
0.25					298	214	107	
Avg.					441	223	116	
0.007				78,375	1017	207	77	
0.007					288	237	97	
0.007					409	207	152	
Avg.					571	217	107	
								Specimens Deteriorated

Table XXVIII COMPRESSION MODULUS OF
MMC SLA-561, PSI

Strain Rate, In./In./Min.	Temperature, °F							
	-270	-200	-175	-150	-65	RT	300	350
0.4				283	252	321	407	391
0.4				305	263	326	412	415
0.4				304	262	322	405	392
Avg.				207	259	323	408	399
0.25					261	337	414	
0.25					251	331	400	
0.25						321	405	
Avg.					256	330	406	
0.007	10,349	134,220	44,387		245	332	397	
0.007	6,258	136,499	22,306		236	318	385	
0.007	79,114	185,273	24,899		239		384	
Avg.	31,916	151,997	30,531		240	325	387	

Table XXIX COMPRESSION MODULUS OF
RM/RL-1973, PSI

Strain Rate, In./In./Min.	Temperature, °F							
	-270	-200	-175	-150	-65	RT	300	350
0.4				269	36	56	50	92
0.4				371	42	52	45	84
0.4				270	41	46	43	
AVG.				303	40	51	46	88
0.25					57	50	47	
0.25					63	43	44	
0.25					54	40	44	
AVG.					58	44	45	
0.007	76,706	17,443	16,794		53	62	42	
0.007					63	66	49	
0.007					57	59	48	
AVG.					58	62	47	

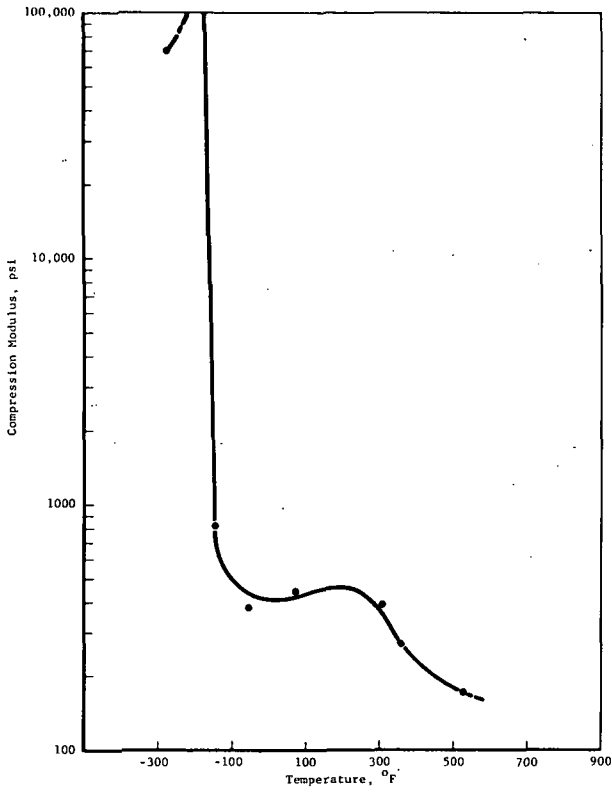


Figure 100 Compression Modulus of GE RTV 560 Vs. Temperature

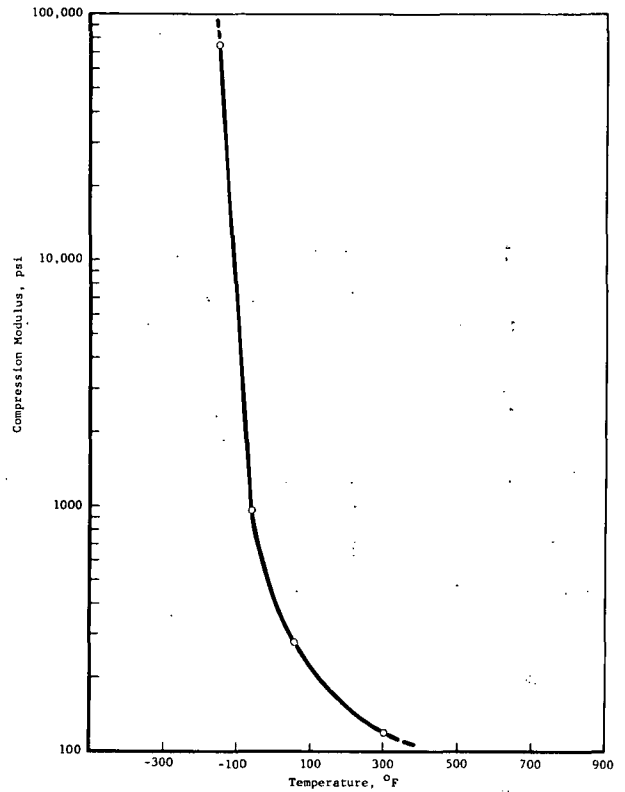


Figure 101 Compression Modulus of DC 93-046 Vs. Temperature

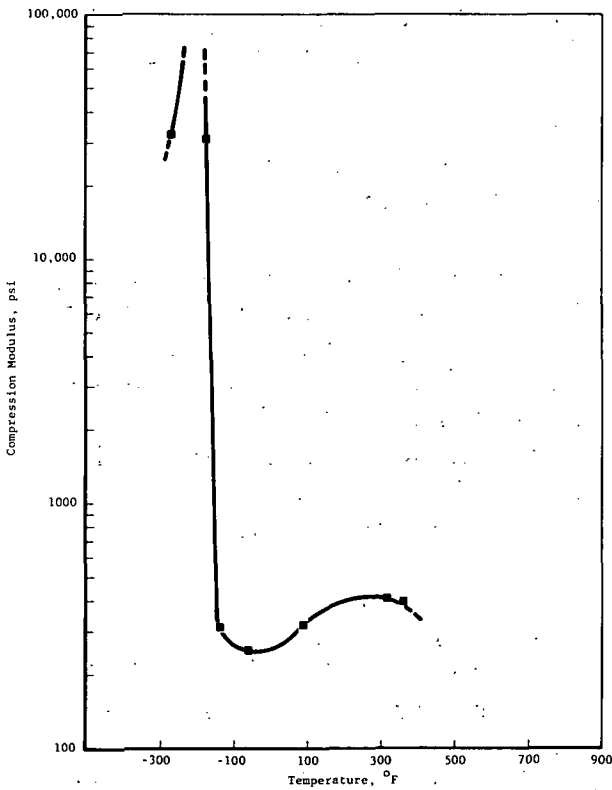


Figure 102 Compression Modulus of SLA 561 Vs. Temperature

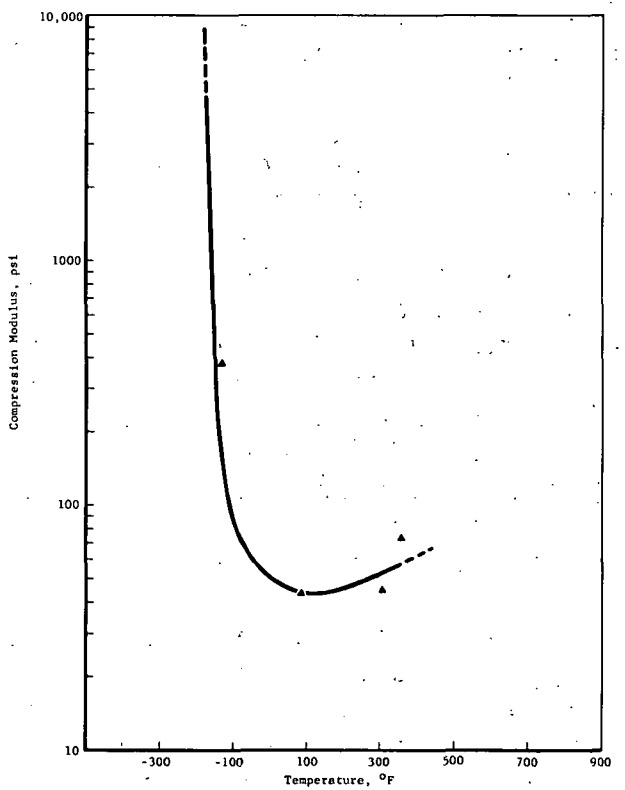


Figure 103 Compression Modulus of RM/RL-1973 Vs. Temperature

4.6 POISSON'S RATIO

4.6.1 Results

Maximum and minimum values of measured Poisson's ratio are shown in Tables XXX and XXXI, as obtained from strap tension tests and block compression tests.

Values of tension and compression modulus of elasticity are shown in Tables XXXII and XXXIII. Strain rate, which was a test variable, is disregarded in this tabulation. The closeness of values at each temperature justifies this omission. Averages of these and shear modulus are used to obtain calculated values of Poisson's ratio shown in Tables XXXIV and XXXV.

4.6.2 Discussion

The minimum and maximum measured values of Poisson's ratio shown in Tables XXX and XXXI generally indicate that all the materials tested exhibit a Poisson's ratio close to 0.5. A rubber-like material that strains easily and without volume change would be expected to have a value of Poisson's ratio slightly smaller than 0.5.

Further examination of the data indicates that the various materials tested exhibit some rather unusual behavior.

At very low temperatures (indicated by * in Tables XXX through XXXV), the apparent stiffness increases suddenly by several orders of magnitude and volume decreases (strain of negative magnitude in both length and width). This behavior suggests that the materials are complex and that residual stresses in part of the material, caused by freezing, are released when load is applied. The observed strains are a composite of the strains caused by the externally applied loads and the strains caused by release of internal (thermal) stresses.

There is also evidence that the materials are complex at temperatures above freezing. The data in Tables XXXII and XXXIII indicate that the materials are stiffer in compression than they are in tension. This behavior is analogous to that of a reinforced material where tension is carried by the reinforcement and compression is carried by all the parts of the material. Since there is more material effective in compression, the stiffness is

Table XXX POISSON'S RATIO IN TENSION

Temp., °F	Material									
	GE RTV-560		DC 93-046		MMC SLA-561		GE RTV-560/ RL-1973			
	(Min)	(Max)	(Min)	(Max)	(Min)	(Max)	(Min)	(Max)	(Min)	(Max)
-270	0.741*	1.118*	0.315*	(One Value)	0.851*	1.059	*	*	*	*
-200	0.737*	1.197*	0.402*	1.186*	0.840*	1.116*	*	*	*	*
-175	0.349*	0.621*	0.757*	1.189*	0.626*	0.909*	0.385*	0.462*		
-150	0.431	0.470	0.438*	1.193*	0.556	0.568	0.372	0.408		
-65	0.439	0.540	0.511	2.876*	0.517	0.626	0.425	0.482		
+75	0.420	0.503	0.501	0.543	0.501	0.609	0.409	0.491		
+300	0.294	0.558	0.506	0.604	0.603	0.759	0.411	0.495		
+350	0.376	0.448	0.475	0.505	0.599	0.823	0.482	0.500		
+550	0.568	0.667	-	-	0.589	0.645	0.401	0.458		
+600	0.501	0.676	-	-	0.506	0.538	-	-		

*Strains too small for accurate measurement of Poisson's ratio.

Table XXXI POISSON'S RATIO IN COMPRESSION

Temp., °F	Material												
	GE RTV-560		DC 93-046		MMC SLA-561		GE RTV-560/ RL-1973						
	(Min)	(Max)	(Min)	(Max)	(Min)	(Max)	(Min)	(Max)					
-270	*	*											
-200	*	*											
-175	*	*			*	*							
-150	0.748	0.758	*	*	0.780	0.810	*	*				*	*
-65	0.549	0.710	0.620	0.980	0.618	0.702	0.158	0.300					
+75	0.599	0.652	0.667	0.726	0.669	0.722	0.271	0.499					
+300	0.547	0.668	0.636	0.747	0.613	0.669	0.308	0.463					
+350	0.698	0.745	-	-	0.700	0.731	0.408	0.415					
+550	0.433	(One Value)	-	-	-	-	-	-					
+600	-	-	-	-	-	-	-	-					

*Strains too small for accurate measurement of Poisson's ratio.

Table XXXII TENSILE MODULUS (SLOPES OF LEAST SQUARES STRESS-STRAIN CURVES)

Material	Temperature, °F									
	600	550	350	300	75	-65	-150	-175	-200	-270
GE RTV-560	222 225 196	326 320 304	391 408 435	402 440 485 402 424 409 418 427 406	341 335 356 368 359 341 341 354 319	295 303 323 293 297 302 277 273 265	385* 447* 400* 398* 656*	*		
Average	<u>214</u>	<u>317</u>	<u>411</u>	<u>424</u>	<u>346</u>	<u>292</u>	<u>457</u>			
DC 93-046	-	-	137 141 139	148 156 150 147 148 143 161	135 110 132 127 134 133 118	*	*	*	*	*
Average		<u>139</u>		<u>150</u>	<u>127</u>					
MMC SLA-561	203 198 196	295 258 276	347 393 334	339 339 397 323 367 335 340 373 346	248 248 235 244 248 247 251 246 245	176 178 193 194 194 178 165 170 186	331* 392* 356*	*	*	*
Average	<u>199</u>	<u>276</u>	<u>358</u>	<u>351</u>	<u>246</u>	<u>182</u>	<u>360</u>			

Table XXXII TENSILE MODULUS (SLOPES OF LEAST SQUARES STRESS-STRAIN CURVES)
(Continued)

Material	Temperature, °F									
	600	550	350	300	75	-65	-150	-175	-200	-270
GE RTV-560/ RL-1973		111	132	141	139	161	663	1545		
		111	156	128	133	154	534	1524*	*	
		102	188	168	172	170	722	1411*		*
				120	134	160				
Average		<u>108</u>	<u>159</u>	<u>136</u>	<u>139</u>	<u>161</u>	<u>640</u>	<u>1493</u>		

*Strains too small for accurate measurement of modulus.

Table XXXIII COMPRESSION MODULUS (SLOPES OF LEAST SQUARES STRESS-STRAIN CURVES)

Material	Temperature, °F									
	600	550	350	300	75	-65	-150	-175	-200	-270
GE RTV-560		172	270	381	446	397	840	*	*	*
			287	417	446	382	836			
			278	407	452	377	808			
				347	449	395				
				388	458	418				
				396	469	410				
				395	442	403				
				333	448	398				
				356	442	408				
	Average		<u>172</u>	<u>278</u>	<u>380</u>	<u>450</u>	<u>399</u>	<u>828</u>		
DC 93-046		-	-	121	236	344	*			
				104	229	682*				
				126	228	298				
				134	235	1017				
				106	221	288				
				107	214	327				
				77	207	2151				
				97	237	411				
				152	207	209*				
	Average			<u>114</u>	<u>224</u>	<u>657</u>				
MMC SLA-561			391	407	321	252	283	*		
			415	412	326	263	305			
			392	405	322	262	304			
				414	337	261				
				400	331	251				
				405	321	245				
				397	332	236				
				385	318	239				
				384						
	Average		<u>399</u>	<u>401</u>	<u>326</u>	<u>251</u>	<u>297</u>			

Table XXXVIII COMPRESSION MODULUS (SLOPES OF LEAST SQUARES STRESS-STRAIN CURVES) (Continued)

Material	Temperature, °F										
	600	550	350	300	75	-65	-150	-175	-200	-270	
GE RTV-560/ RL-1973			92	50	56	36	269*	*	*		
			84	45	52	42	371				
				43	46	41	270				
				47	50	57					
				44	43	63					
				44	40	54					
				42	62	53					
				49	66	63					
				48	59	57					
	Average		88	46	53	52	303				

*Strains too small for accurate measurement of modulus.

Table XXXIV POISSON'S RATIO COMPUTED FROM SHEAR
AND TENSION MODULUS**

Temp., °F	GE RTV-560 Average			DC 93-046 Average			MMC SLA-561 Average			GE RTV-560/ RL-1973 Average		
	G	E	u	G	E	u	G	E	u	G	E	u
-270	*	*					*	*		*	*	
-200	*	*					*	*		*	*	
-175	*	*					*	*		*	*	
-150	191	457	0.20		*		547	360*		692	640	-
-65	109	292	0.34		*		84	182	0.08	48	161	0.68
+75	139	346	0.25	65	127	-0.02	83	246	0.48	42	139	0.65
+300	169	424	0.26	64	150	0.18	117	351	0.50	43	136	0.58
+350	169	411	0.22	61	139	0.14	118	358	0.51	52	159	0.53
+550	53	317	1.99	-	-	-	81	276	0.70	30	108	0.80
+600	22	214	3.86	-	-	-	69	199	0.44	-	-	-

*Strains too small for accurate measurement of Poisson's ratio.

** $G = \frac{E}{2(1 + u)}$, for elastic isotropic material

where: G = Shear modulus
E = Tensile modulus
u = Poisson's ratio

Table XXXV POISSON'S RATIO COMPUTED FROM SHEAR AND COMPRESSION MODULUS**

Temp., °F	Material											
	GE RTV-560 Average			DC 93-046 Average			MMC SLA-561 Average			GE RTV-560/RL-1973 Average		
	G	E	u	G	E	u	G	E	u	G	E	u
-270												
-200												
-175		*						*			*	
-150	191	828	1.16		*		547	297	-0.73	692	303	-0.78
-65	109	399	0.38		657		84	251	0.50	48	52	-0.49
+75	139	450	0.62		65	224	83	326	0.96	42	53	-0.37
+300	169	380	0.12		64	114	117	401	0.72	43	46	-0.47
+350	169	278	-0.18		61		118	399	0.69	52	88	-0.15
+550	53	172	0.62				81			30		
+600	22						69					

*Strains too small for accurate measurement of Poisson's ratio.

** $G = \frac{E}{2(1+u)}$, for elastic isotropic material

where: G = Shear modulus
 E = Tensile modulus
 u = Poisson's Ratio

greater in compression than tension. The tested values of the moduli are remarkably consistent.

Values of Poisson's ratio computed using measured moduli and the assumption of perfectly elastic behavior in an isotropic continuum, $G = \frac{E}{2(1 + \nu)}$ (Ref. 1), are shown in Tables XXXIV and XXXV.

The resulting calculations indicate that either the testing capability was inadequate or the materials are not perfectly elastic, isotropic, and homogeneous.

The calculated values for GE RTV-560/RL-1973 appear quite consistent when calculated from the shear modulus and one of the other moduli. Using compression modulus, the average result is 0.65. Using tension modulus, the average result is -0.45. The consistency of results in each type of calculation indicates that the test techniques were probably adequate. This material is a mechanical arrangement of membranes, which is probably the reason for its mechanical behavior.

The calculated values for the other materials indicate that the materials may not be perfectly elastic, isotropic, and homogeneous.

In summary, the more pertinent observations are

1. The measured modulus of elasticity in tension is different from the modulus in compression for the materials tested.
2. There is a drastic change in the behavior of each of the materials at temperatures below their glass-transition points.
3. The measured, average values of Poisson's ratio for these materials is generally close to 0.50, except at cryogenic temperatures where reasonable measurements were not obtainable.
4. The preceding observations indicate that the materials tested are complex arrangements or mechanisms affected by thermal stressing.

The apparent complexity of the materials, the drastic change in properties at cryogenic temperatures, and, particularly, the apparent closeness of Poisson's ratio to 0.5 indicate that analysis techniques based on theories of elasticity are not advisable.

This last point is illustrated by solving for stresses along three axes using Hooke's Law for strain-stress relationships in elastic, homogeneous, and isotropic materials.

Unit strains are shown as e and subscripted for each axis. Stresses, S , are subscripted similarly. Poisson's ratio is shown as u and modulus of elasticity as E .

$$e_x = \frac{S_x}{E} - \frac{uS_y}{E} - \frac{uS_z}{E}$$

$$e_y = \frac{S_y}{E} - \frac{uS_x}{E} - \frac{uS_z}{E}$$

$$e_z = \frac{S_z}{E} - \frac{uS_x}{E} - \frac{uS_y}{E}$$

Algebraic solution of these expressions results in

$$S_x = \frac{Ee_x (1-u) + uEe_y + uEe_z}{(1+u)(1-2u)}$$

$$S_y = \frac{Ee_y (1-u) + uEe_x + uEe_z}{(1+u)(1-2u)}$$

$$S_z = \frac{Ee_z (1-u) + uEe_x + uEe_y}{(1+u)(1-2u)}$$

It can be seen that solutions for stress involving values of Poisson's ratio approaching 0.5 become undefined.

4.7 CONSTANT STRAIN-STRESS RELAXATION

The four adhesive materials were tested to determine stress relaxation under constant strain conditions as a function of time.

4.7.1 Test Method

Determination of stress relaxation using a test fixture as shown in Figure 104 was initially planned. Specimens would be elongated to the specified strain and the relaxation would be periodically monitored using load rings connected to a recording system. However, initial tests revealed that most of the stress relaxation occurred during the first few minutes following loading, which necessitated continuous recording of stress values. Also, the wide variation in stress developed by the different adhesives precluded the use of a single load cell arrangement to monitor stress. Therefore, the data contained in this report was obtained from specimens that were individually tested in a Scott or Instron test machine in which the stress was continuously recorded.

Two types of specimens were tested--a molded band specimen (Figure 10) with an inside diameter of 4.0 inches and a cross section dimension of 0.125 inch thickness x 0.25 inch width and a stacked specimen as shown in Figures 11 and 105. The band RL-1973 sponge specimens were cut from a flat sheet of sponge 0.25 inch thick. The stacked specimen consisted of alternate layers of aluminum and adhesive to provide a total adhesive thickness of approximately 1 inch. This specimen was selected to simulate actual installation conditions and to provide correlation with previously determined data.

Initial plans were to subject the band specimens to strains of 0.10, 0.04, and 0.02 inch per inch at temperatures of -270°F , -175°F , -125°F , and room temperature and to monitor the stress over a 6-hour period. The stacked specimens were to be tested at 0.10 inch per inch strain. During preliminary testing, it was determined that the stacked specimens failed before the required strain was obtained and that at temperatures below the brittle point of the materials the band specimens failed at strains below 0.01 inch per inch. In addition, the low stresses developed in the band specimens at the low strain levels coupled with the difficulty encountered in obtaining an exact zero stress-strain point precluded obtaining useful information at these low strain levels.

These results were discussed with the NASA, MSC project monitor, and as a result of this discussion the original test plan was modified. The test temperatures and strain values decided upon are listed in Tables XXXVI and XXXVII with the tabulated data. Also, stress relaxation was monitored until stress was constant.

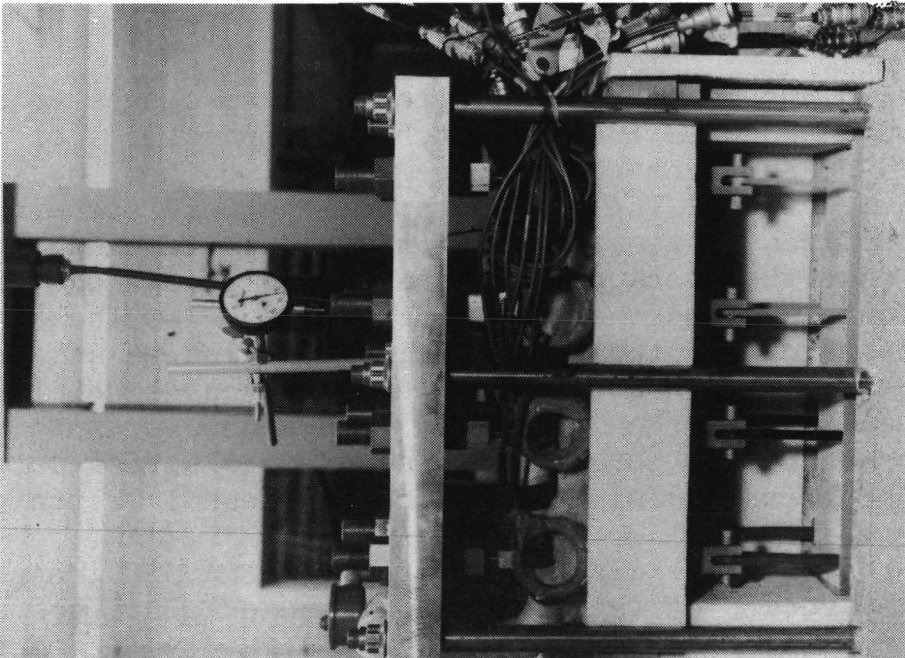


Figure 104 Constant Strain Test Fixture

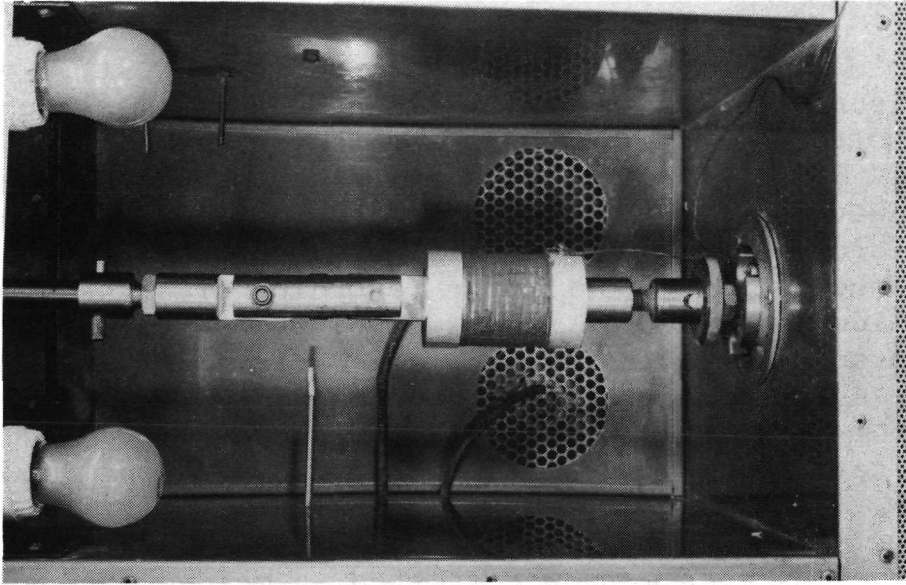


Figure 105 Stacked Specimen Constant Strain Test Setup

Table XXVI SUMMARY OF CONSTANT STRAIN TESTS ON BAND SPECIMENS
Load/Pounds Per Sq. In.

ELAPSED TIME AFTER % ELONGATION WAS ACHIEVED	GE RTV-560				DC 93-046				MMC STA-561				RM/RL-1973											
	10% @-175°F		0.4% @-200°F		10% @-175°F		0.4% @-200°F		10% @-175°F		0.4% @-270°F		10% @-175°F		0.4% @-200°F		0.4% @-270°F							
	B-1	B-2	B-3	B-4	B-1	B-2	B-3	B-6	B-1	B-2	B-1	B-2	B-3	B-6	B-7	B-8	B-1	B-2	B-3	B-4	B-5	B-6	B-7	
Initial Load	23.7	31.0	949	1007	2035	1842	2421	2193	15.1	14.9	500	259	1474	1750	1614	1293	2.20	2.93	75.9	144	358	328	435	312
15 Sec.	23.6	30.9	525	572	1895	1693	2333	2184	14.4	14.2	267	168	1360	1643	1535	1276	2.03	2.59	48.3	91.2	288	267	435	312
30 Sec.	23.6	30.7	441	486	1860	1649	2325	2175	14.2	13.8	230	146	1316	1589	1526	1267	2.03	2.59	43.1	82.5	277	253	432	312
45 Sec.	23.6	30.5	398	431	1842	1614	2325	2175	14.2	13.8	208	132	1281	1554	1526	1267	2.41		41.4	78.9	268	246	432	312
60 Sec.	23.6	30.5	373	405	1825	1579	2325	2167	14.2	13.6	192	125	1246	1527	1259	1267			36.2	75.4	256	233		
75 Sec.	23.4	30.5	342	379	1789	1544	2325	2158	14.0	13.6	175	116	1202	1491	1250	1241			34.5	71.9	251	228		
90 Sec.	23.4	30.5	339	359	1772	1526	2325	2149	13.8	13.6	155	107	1175	1464	1216	1216			68.4	68.4	218	218		
105 Sec.	23.2	30.5	332	336	1737	1482	2325	2149	13.3	13.1	155	107	1175	1464	1216	1216			25.9	36.8	179	191		
120 Sec.	22.7	30.0	144	179	1386	1175	2316	2105	13.1	12.9	91.7	57.1	877	1107	1216	1216			24.1	26.3	160	154		
15 Min.	22.4	29.5	115	147	1246	1061	2316	2070	13.1	12.9	80.0	44.6	781	982	1216	1216			22.8		149	147		
30 Min.	22.4	29.3	98.3	129	1158	1018	2281	2035	12.7		75.0	42.9	719	911	1216	1216					144	137		
45 Min.			84.7		1105	974	2254	2000					684	875	1216	1216					137	133		
60 Min.			78.0		1053	921	2219	1991					667	830	1207	1207								
75 Min.					1035		2211	1991					632	804	1207	1207								
90 Min.					1018		2193						614	786	1198	1198								
105 Min.					1000		2184						596	777	1190	1190								
120 Min.					991		2167								1181	1181								
135 Min.					991		2158								1172	1172								
150 Min.							2158																	
165 Min.																								
180 Min.																								
195 Min.																								
210 Min.																								
225 Min.																								
240 Min.																								
300 Min.																								
360 Min.																								
Type Failure	NF	NF	NF	NF	NF	NF	NF	NF	NF	NF	NF	NF												
% Stress Relaxation	5	5	92	87	51	50	11	9	13	15	2	3	85	83	60	57	5	8	18	68	84	62	59	1

N.F. - NO FAILURE
C - COHESIVE FAILURE
A.M. - ADHESIVE FAILURE TO PREVIOUSLY CURED MATERIAL
A.X. - ADHESIVE FAILURE TO METAL
P.A. - PARTIAL ADHESIVE FAILURE

Table XXXVII SUMMARY OF CONSTANT STRAIN TESTS ON STACKED DISC SPECIMENS
Load/Pounds Per Sq. In.

ELAPSED TIME AFTER % ELONGATION WAS ACHIEVED	GE RTV-560			DC 93-046			MMC SLA-561			RTV-560/RL-1973												
	4% @ R.T. S-1 S-2	4% @-125°F S-5 S-6	4% @-175°F S-3 S-4	10% @ R.T. S-1 S-2	10% @-125°F S-5 S-6	10% @-175°F S-3 S-4	2% @ R.T. S-1 S-2	2% @-125°F S-5 S-6	2% @-175°F S-3 S-4	10% @ R.T. S-1 S-2	10% @-125°F S-3 S-4	10% @-175°F S-5 S-6	0.4% @-270°F S-7 S-8									
Initial Load	176	146	119	130	622	503	42.3	58.9	89.1	71.6	155	69.4	17.5	11.1	18.5	41.1	47.1	141	141	166	102	
15 Sec.	143	113	125	573	457	37.6	55.7	78.9	63.0	68.4	146	67.2	11.1	8.6	18.5	38.2	44.6	121	118	166	100	
30 Sec.	142	111	124	560	455	37.2	55.1	77.0	61.8	68.4	143	66.8	10.2	7.6	18.5	37.6	43.3	110	114	166	99.6	
45 Sec.	141	111	124	547	455	37.1	54.7	75.8	61.1	68.4	143	66.8	9.2	7.0	18.5	37.2	42.7	104	111	166	99.0	
60 Sec.	141	111	124	540	454	36.9	54.1	74.8	60.5	68.4	142	66.8	8.6	6.4	18.5	36.9	42.0	100	109	165	98.7	
75 Sec.	140	110	124	532	452	36.8	53.5	74.2	59.8	68.4	141	66.8	8.3	6.0	18.5	36.9	41.7	97.1	107	165	98.0	
90 Sec.	140	110	124	522	450	36.7	53.2	73.8	59.5	68.4	139	66.8	8.0	5.7	18.5	41.4	94.9	105	165	97.4		
105 Sec.	140	110	124	516	450	36.6	52.8	73.2	58.6	68.4	138	66.8	7.3	5.5	18.5	41.2	92.3	103	165	96.8		
120 Sec.	139	110	124	508	449	36.3	52.5	72.2	58.6	68.4	137	66.8	7.0	5.4	18.5	41.1	89.8	102	165	96.1		
15 Min.	131	108	124	388	393	30.9	40.7	67.2	54.1	68.4	106	65.9	3.2	0	12.7	8.2	10.0	39.8	64.6	87.2	157	79.3
30 Min.	125	108	118	334	334	26.7	36.0	65.3	52.5	68.4	57.9	2.2	2.2	2.5	2.2	7.8	9.5	55.1	77.3	139	60.5	
45 Min.	123	108	111	296	301	23.2	33.4	64.3	51.6	68.4	55.1	2.2	2.2	2.2	2.2	7.6	9.2	51.7	73.8	131	51.9	
60 Min.	102	267	283	19.7	31.5	63.7	50.9	Specimens not Tested		68.4	54.1	1.9	1.9	1.9	0.9	7.5	9.0	51.7	72.3	122	43.9	
75 Min.	99.3	250	274	16.6	29.9	63.0	50.3			68.4	54.1	1.9	1.9	1.9	0.9	7.5	9.0	51.7	72.3	122	43.9	
90 Min.	98.0	240	266	14.6	28.3	62.4	50.0			68.4	54.1	1.9	1.9	1.9	0.9	7.5	9.0	51.7	72.3	122	43.9	
105 Min.	98.0	221	259	11.5	26.1	62.1	49.7			68.4	54.1	1.9	1.9	1.9	0.9	7.5	9.0	51.7	72.3	122	43.9	
120 Min.	212	253	212	10.2	22.9	61.4	49.3			68.4	54.1	1.9	1.9	1.9	0.9	7.5	9.0	51.7	72.3	122	43.9	
135 Min.	202	247	202	9.2	20.7	61.1	49.0			68.4	54.1	1.9	1.9	1.9	0.9	7.5	9.0	51.7	72.3	122	43.9	
150 Min.	197	244	197	9.2	20.7	60.8	48.7			68.4	54.1	1.9	1.9	1.9	0.9	7.5	9.0	51.7	72.3	122	43.9	
165 Min.	193	239	193	8.4	19.3	60.8	48.4			68.4	54.1	1.3	1.3	1.3	0.9	7.3	8.7	51.7	72.3	122	43.9	
180 Min.	189	234	189	8.1	18.9	60.8	48.1			68.4	54.1	1.3	1.3	1.3	0.9	7.3	8.6	51.7	72.3	122	43.9	
195 Min.	185	232	185	8.1	18.5	60.8	47.7			68.4	54.1	0.95	0.95	0.95	0.9	7.2	8.6	51.7	72.3	122	43.9	
210 Min.	183	183	183	8.4	18.3	60.8	47.4			68.4	54.1	0.95	0.95	0.95	0.9	7.1	8.5	51.7	72.3	122	43.9	
225 Min.	180	180	180	8.4	18.0	60.8	47.2			68.4	54.1	0.95	0.95	0.95	0.9	7.1	8.4	51.7	72.3	122	43.9	
240 Min.	178	178	178	8.4	17.8	60.8	47.1			68.4	54.1	0.95	0.95	0.95	0.9	7.0	8.2	51.7	72.3	122	43.9	
300 Min.	178	178	178	8.1	17.8	60.8	47.1			68.4	54.1	0.95	0.95	0.95	0.9	6.9	8.1	51.7	72.3	122	43.9	
360 Min.	178	178	178	8.1	17.8	60.8	47.1			68.4	54.1	0.95	0.95	0.95	0.9	6.9	8.1	51.7	72.3	122	43.9	
Type Failure	C	C	C	C	C	C	C	C	C	C	C	C	C	C	C	C	C	C	C	C	C	C

NF - NO FAILURE
C - COHESIVE FAILURE
AM - ADHESIVE FAILURE TO PREVIOUSLY CURED MATERIAL
AX - ADHESIVE FAILURE TO METAL
PA - PARTIAL ADHESIVE FAILURE

4.7.2 Results and Discussion

Constant strain test results for the band specimens are shown in Table XXXVI. Stress relaxation versus time for typical specimens are shown in Figures 106 through 108. The greatest stress relaxation occurs during the first 2 minutes following loading. At room temperature, the adhesive materials show a total stress relaxation of approximately 5 to 10 percent. At -175°F , the stress relaxation is 70 to 90 percent, at -200°F , 50 to 60 percent, and at -270°F 5 to 10 percent. In general, the stress relaxation curves leveled approximately 1 hour after loading.

The results from the stacked specimens (Table XXXVII and Figures 109 through 111) although somewhat erratic show similar results. The inconsistencies in the stacked specimen results are believed to be due to problems encountered in obtaining uniform glue lines and parallel discs and the possibility of internal failures occurring during testing. These specimens were fabricated by bonding cured discs of adhesive between aluminum discs. In some of the failures, the MMC SLA-561 did not bond satisfactorily to itself. Also, several adhesive metal failures occurred with MMC SLA-561 and GE RTV-560. Partial adhesive failures (adhesive failures at the edges of the specimen) were also noted in the RTV-560/RL-1973 specimens. It is probable that these type of failures were also occurring internally in the specimen.

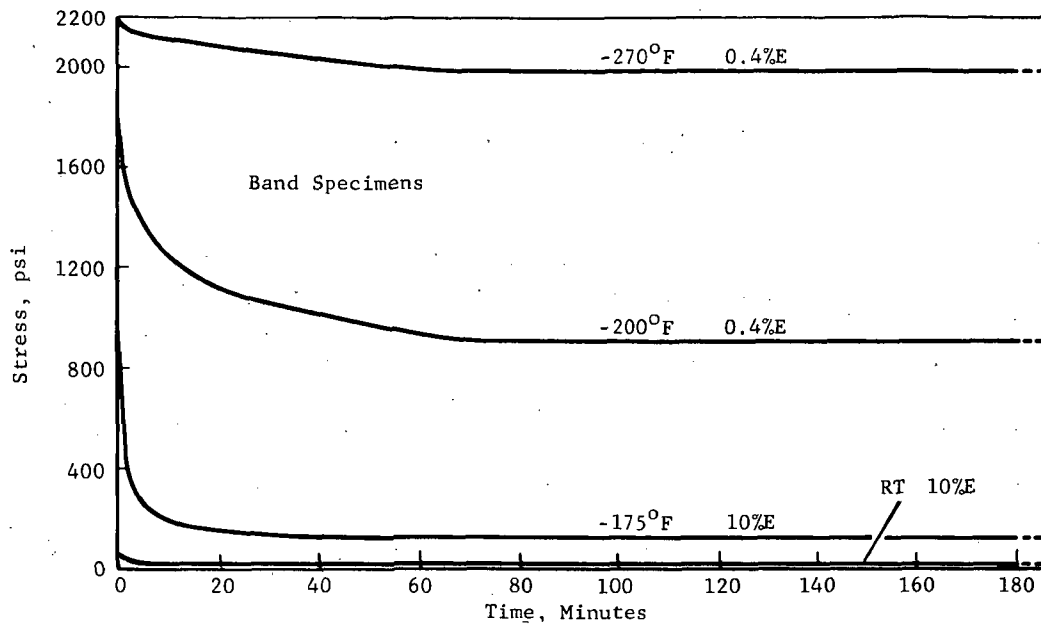


Figure 106 Stress Relaxation at Constant Strain, GE RTV-560, Band Specimens

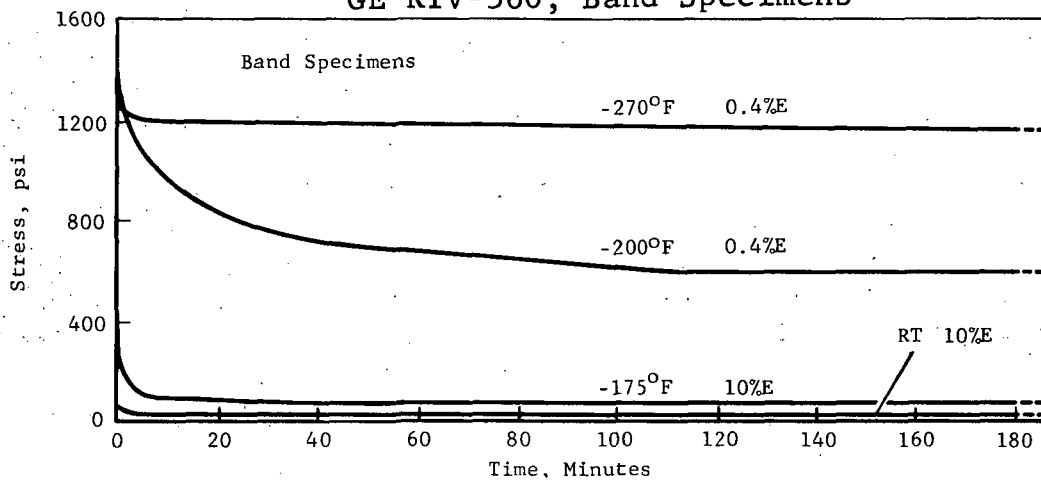


Figure 107 Stress Relaxation at Constant Strain, SLA-561, Band Specimens

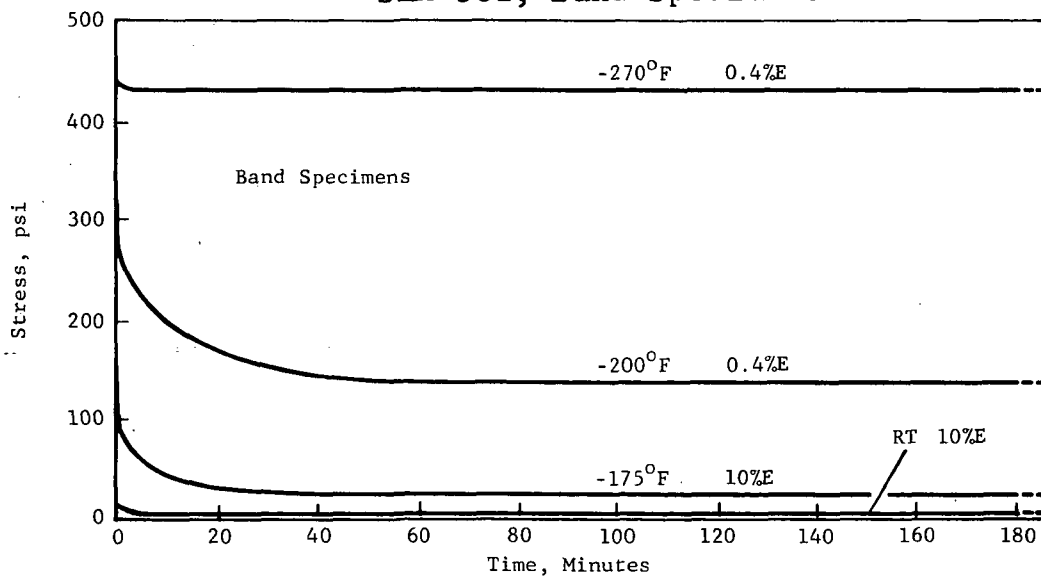


Figure 108 Stress Relaxation at Constant Strain, R/M RL-1973, Band Specimens

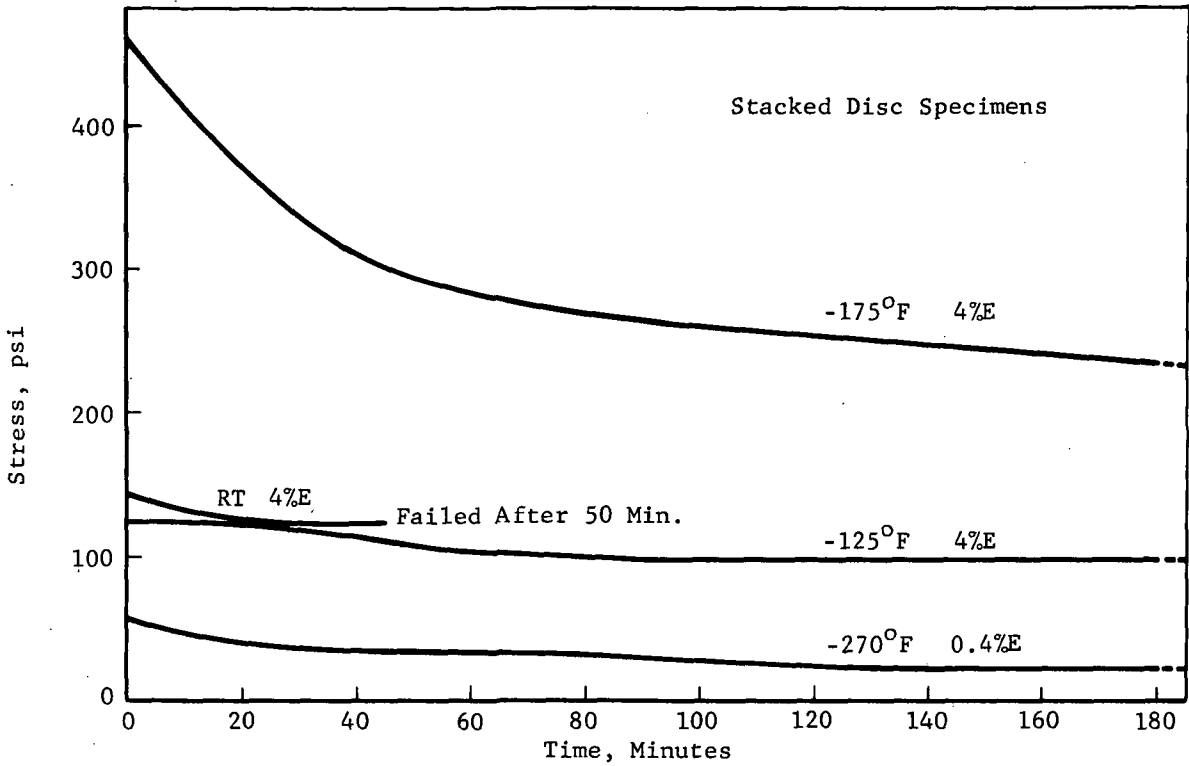


Figure 109 Stress Relaxation at Constant Strain, GE RTV-560, Stacked Disc Specimens

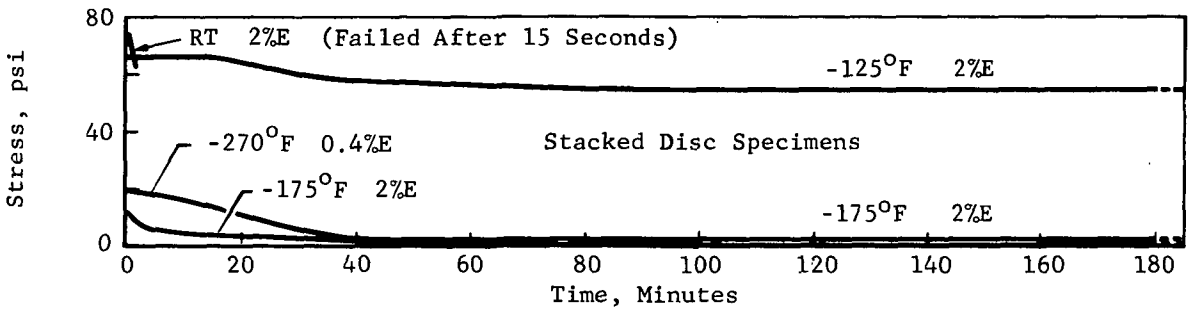


Figure 110 Stress Relaxation at Constant Strain, SLA-561, Stacked Disc Specimens

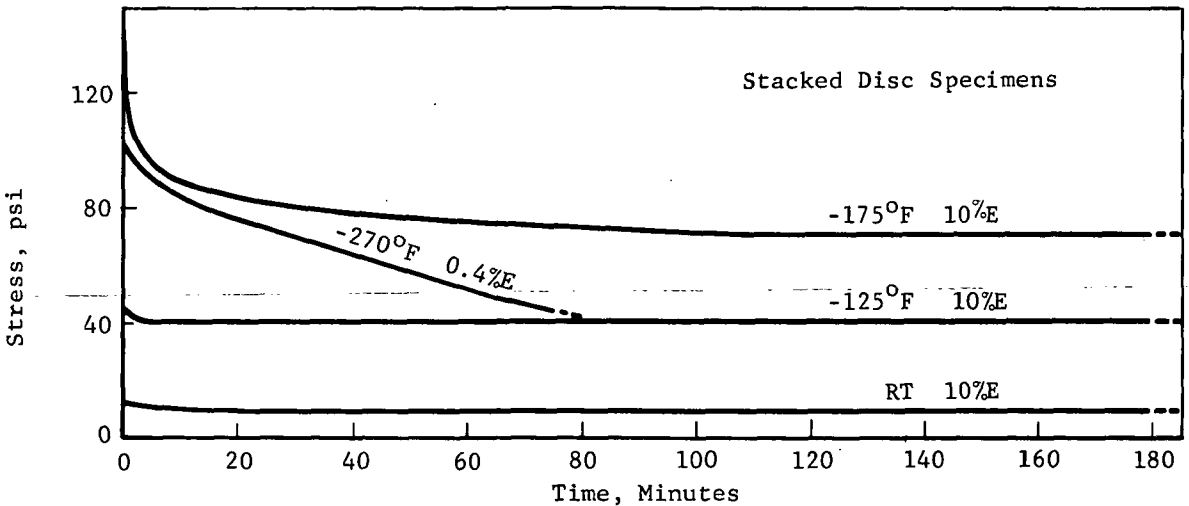


Figure 111 Stress Relaxation at Constant Strain, R/M RL-1973, Stacked Disc Specimens

SECTION 5
THERMAL PROPERTIES

S E C T I O N 5

T H E R M A L P R O P E R T I E S

5.1 THERMAL EXPANSION

The coefficient of linear thermal expansion is calculated by determining the change in length per unit length of the specimen and dividing that value by the magnitude of the temperature differential that produced the linear change.

5.1.1 Test Method

Linear thermal expansion determinations were conducted in accordance with ASTM E-228, Procedure B. Two linear voltage differential transformer (LVDT) dilatometer-type units were used. Both were calibrated with NBS standard specimens of fused silica and aluminum oxide.

5.1.1.1 Thermophysics Corporation Instrument

The initial measurements were made on the Thermophysics Corporation Model TE-3000L unit (Figure 112) which utilizes a 1/8- to 1/2-inch-diameter X 2-inch-long specimen (Figure 9, Section 2). The specimens were individually placed in the horizontally mounted fused silica dilatometer and precooled to approximately -300°F. Prior to the precooling operation, the environmental dome covering the furnace and dilatometer was evacuated by mechanical pump and back-filled with helium gas a minimum of three times. The cooling was accomplished by use of liquid nitrogen. Temperature and dilation of the specimen were monitored on an X-Y recorder. Specimens were stabilized at -300°F for 15 minutes.

A Thermac temperature controller/Data-Trak programming system was then used to raise the temperature of the specimen through 750°F at a rate of 8°F per minute. During the entire operation, the recorder maintained a plot of change in sample length (expansion or contraction) versus temperature. A run was terminated when deterioration, softening, and/or sagging was noted prior to achieving 750°F. A minimum of three specimens tested for each material.

The expansion of each specimen, as $\Delta L/L$ versus temperature, was then calculated, and the averages of the individual specimen values for each material were plotted. These data were normalized to 75°F. Calculation of the expansion coefficient between



Figure 112 Thermophysics Corp. Model TE-3000L Linear Thermal Expansion Unit

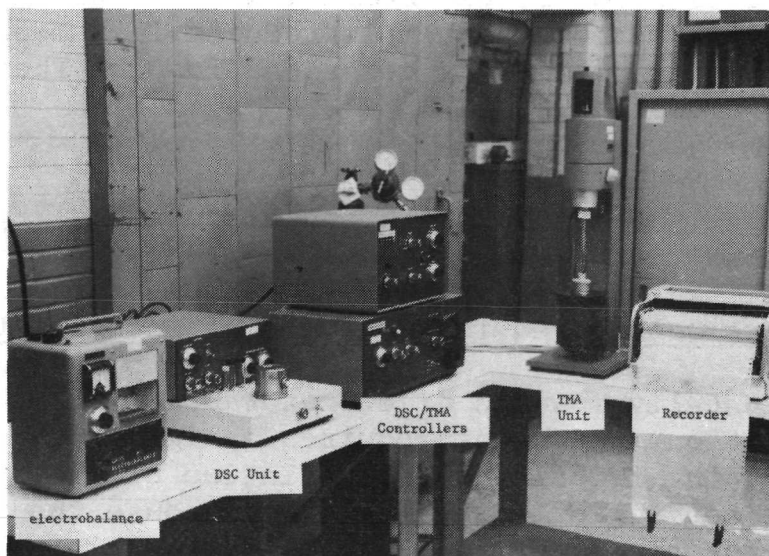


Figure 113 Perkin Elmer Differential Scanning Calorimeter/Thermomechanical Analyzer Unit

any temperatures, T_1 and T_2 , from the normalized values was then accomplished by use of the following formula:

$$\alpha T_1 \text{ to } T_2 = [(\Delta L/L)_{T_2} - (\Delta L/L)_{T_1}] - [T_2 - T_1].$$

5.1.1.2 Perkin Elmer Corporation Instrument

The Perkin Elmer Corporation Differential Scanning Calorimeter, model DSC-1B, with its accessory Thermomechanical Analyzer, model TMS-1, is shown in Figure 113. The TMS-1 uses a $\frac{1}{2}$ -inch-long by $\frac{1}{8}$ -to $\frac{1}{4}$ -inch-diameter sample. Each specimen was mounted vertically with the fused silica extensometer probe of the vertical dilatometer floating in a silicone liquid damper. Standard weights were added to the probe until a zero buoyancy or no-load condition existed on the material, thus minimizing the possibility of sample indentation by the probe.

The interior volume of the electrical furnace was continuously purged with helium gas, and the assembly was precooled to approximately -300°F by thermal transfer from a surrounding liquid nitrogen cooled dewar. Temperature and dilation were monitored continuously on an X-Y recorder. Specimens were stabilized at -300°F for 15 minutes, and the temperature was increased at a programmed rate ($2\text{-}5^\circ\text{F}/\text{min.}$) through 700°F or until the specimen exhibited signs of deterioration, softening, and/or sagging. The data were subsequently reduced in a manner identical to the one previously described for the Thermophysics Corporation instrument.

5.1.2 Results and Discussion

5.1.2.1 Factors Considered in Selection of Instrument

The horizontally mounted dilatometer used with the Thermophysics Corporation instrument requires a light load to be applied to overcome sliding friction during dilation of the specimen. Otherwise, the LVDT core is not heavy enough to cause the probe to "follow" or track the specimen when it contracts during the cooling cycle. This load has no adverse effect on the expansion/contraction/temperature profile of a material unless that material softens, sags, or deforms at some temperature within the desired expansion profile. When this occurs, the extensometer probe of the instrument begins to penetrate into the specimen and it appears on the X-Y plotter that expansion has ceased or that contraction has begun.

The initial runs on GE RTV-560 material with the Thermo-physics instrument revealed that the material softened between 350 to 400°F. Since this was not unexpected, no problem with the instrument was apparent until runs were attempted on the R/M RL-1973 sponge material. The pre-loading force on the dilatometer was sufficient to cause deformation on the sponge even at ambient room temperature. The pre-loading force could not be satisfactorily adjusted to a point where frictional force could be overcome without specimen deformation.

The Perkin Elmer instrument was found to offer an ideal solution to the problem since it contained the zero buoyancy or no-load capability and had no frictional component on the vertically mounted specimen. Comparison tests on the two instruments were made on the GE RTV-560 material, and the results are presented in Tables XXXVIII and XXXIX. The data from the two instruments are virtually identical throughout the temperature range. The coefficient of expansion for this material over the temperature range zero to 350°F has been reported by the vendor to be 11.4×10^{-5} inch/inch°F. This correlates well with the values of 11.0 and 11.58×10^{-5} inch/inch°F given in the sample calculations for that temperature range at the bottom of the tables.

Thermal expansion measurements were made with both instruments in accordance with ASTM E-228, Procedure B, with the exception that the specimen length for the Perkin Elmer instrument was less than the 2 inch minimum stipulated. This is considered acceptable practice since the data correlates well with (1) that reported by the vendor and (2) that generated on the Thermo-physics instrument, which uses a 2-inch-long specimen.

Based on the above information, the NASA, MSC technical monitor agreed to the use of the Perkin Elmer Model TMS-1 instrument in lieu of the Thermophysics Model TE-3000L instrument for the balance of the program.

5.1.2.2 Thermal Expansion of GE RTV-560

Expansion data for GE RTV-560 are given in the previously mentioned Table XXXIX. The expansion as $\Delta L/L$ versus temperature is also plotted in Figure 114. The radical change in expansion of RTV-560 near -175°F is attributed to a transition in the material. Penetration tests on a series of specimens pre-cooled to -270°F and allowed to warm up reveal that RTV-560 softens between -170° and -180°F.

TABLE XXXVIII
 SUMMARY OF LINEAR THERMAL EXPANSION DATA: RTV-560
 (NORMALIZED TO 75°F)

INSTRUMENT: THERMOPHYSICS CORPORATION MODEL TE-3000L,
 FUSED SILICA DILATOMETER
 PROCEDURE: ASTM E-228, PROCEDURE B

Temperature, °F	Expansion $\Delta L/L_{75^\circ F}$, Inch/Inch	Expansivity* $\alpha_{75^\circ F \text{ to } T^\circ F}$, Inch/Inch °F
-250	-27.65 X 10 ⁻³	8.51 X 10 ⁻⁵
-200	-25.92 X 10 ⁻³	9.43 X 10 ⁻⁵
-150	-23.04 X 10 ⁻³	10.24 X 10 ⁻⁵
-100	-18.30 X 10 ⁻³	10.46 X 10 ⁻⁵
- 50	-13.57 X 10 ⁻³	10.86 X 10 ⁻⁵
0	- 8.25 X 10 ⁻³	11.00 X 10 ⁻⁵
50	- 2.51 X 10 ⁻³	10.04 X 10 ⁻⁵
75	0	0
100	2.94 X 10 ⁻³	11.76 X 10 ⁻⁵
150	8.42 X 10 ⁻³	11.23 X 10 ⁻⁵
200	13.75 X 10 ⁻³	11.00 X 10 ⁻⁵
250	19.19 X 10 ⁻³	10.97 X 10 ⁻⁵
300	24.35 X 10 ⁻³	10.82 X 10 ⁻⁵
350	30.16 X 10 ⁻³	10.97 X 10 ⁻⁵
400**	36.00 X 10 ⁻³	11.08 X 10 ⁻⁵
450**	40.77 X 10 ⁻³	10.87 X 10 ⁻⁵
500**	44.48 X 10 ⁻³	10.47 X 10 ⁻⁵
600**	49.45 X 10 ⁻³	9.42 X 10 ⁻⁵

*Calculation of α from any T_1 through T_2 is accomplished by use of the following formula:

$$\alpha_{T_1 \text{ to } T_2} = [(\Delta L/L)_{T_2} - (\Delta L/L)_{T_1}] \div [T_2 - T_1]$$

Example: $\alpha_{0 \text{ to } 350^\circ F} = \frac{[30.16 - (-8.25)] \times 10^{-3}}{350} = 11.0 \times 10^{-5} \text{ in./in.}^\circ F$

**Specimens Sagged

TABLE XXXIX
SUMMARY OF LINEAR THERMAL EXPANSION DATA: RTV-560
(NORMALIZED TO 75°F)

INSTRUMENT: PERKIN ELMER CORPORATION, MODEL TMS-1
PROCEDURE: ASTM E-228, PROCEDURE B

Temperature, °F	Expansion $\Delta L/L_{75^\circ F}$, Inch/Inch	Expansivity* $\alpha_{75^\circ \text{ to } T^\circ F}$, Inch/Inch ^{°F}
-250	-30.72 X 10 ⁻³	9.45 X 10 ⁻⁵
-200	-28.80	10.47
-150	-25.56	11.36
-100	-20.22	11.55
- 50	-14.31	11.45
0	- 8.44	11.25
50	- 2.10 X 10 ⁻³	8.40 X 10 ⁻⁵
75	0	0
100	2.73 X 10 ⁻³	11.00 X 10 ⁻⁵
150	8.44	11.25
200	14.24	11.39
250	20.47	11.70
300	26.41	11.74
350	32.08	11.67
400	37.80	11.63
450	42.59	11.36
500	47.80 X 10 ⁻³	11.25 X 10 ⁻⁵

$$* \quad \alpha_{T_1 \text{ to } T_2} = \left[(\Delta L/L)_{T_2} - (\Delta L/L)_{T_1} \right] \div [T_2 - T_1]$$

Inch/Inch^{°F}

Example: $\alpha_{0 \text{ to } 350^\circ F} = \frac{[32.08 - (-8.44)]}{350} \times 10^{-3} = 11.58 \times 10^{-5}$

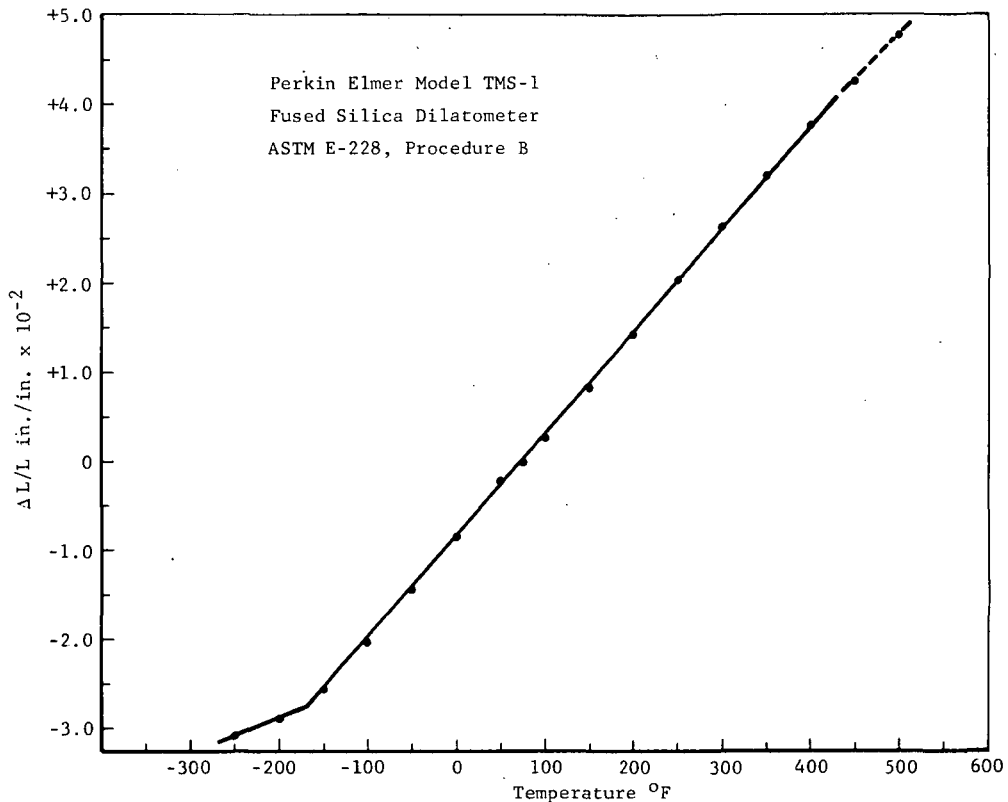


Figure 114 | Linear Thermal Expansion Vs. Temperature, RTV-560

The data presented in Table XXXIX and Figure 114 represent the average expansion of 5 to 9 specimens. All of these eventually sagged at temperatures ranging from 330°F to above 500°F, depending on the "time-at-temperature" history of the specimen. It should be noted that the expansion below the softening transition point (α -250°F to -200°F = 3.84×10^{-5} inch/inch°F) is approximately 1/3 of the expansion above that point (α -150°F to 400°F = 11.52×10^{-5} inch/inch°F), as calculated by the formula given in Table XXXIX.

5.1.2.3 Thermal Expansion of DC 93-046

Expansion data for DC 93-046 are given in Table XL and plotted as $\Delta L/L$ versus temperature in Figure 115. Penetration tests on 93-046 reveal it undergoes a softening transition in the -45°F to -60°F temperature range. Sag temperatures occur at 400°F and above.

TABLE XL
SUMMARY OF LINEAR THERMAL EXPANSION DATA: DC 93-046
(NORMALIZED TO 75°F)

INSTRUMENT: PERKIN ELMER CORPORATION, MODEL TMS-1
PROCEDURE: ASTM E-228, PROCEDURE B

Temperature °F	Expansion $\Delta L/L$ 75°F, Inch/Inch	Expansivity* $\alpha_{75^\circ \text{ to } T^\circ\text{F}}$, Inch/Inch°F
-250	-39.8×10^{-3}	12.25×10^{-5}
-200	-37.7	13.71
-150	-34.2	15.20
-100	-29.5	16.86
- 50	-21.2	16.96
- 25	-13.2	13.20
0	-10.0	13.33
50	- 3.6	14.40
75	0	0
100	3.8×10^{-3}	15.20×10^{-5}
150	10.7	14.27
200	17.3	13.84
250	24.4	13.94
300	31.5	14.00
350	38.4	13.96
400	45.8	14.09
450	51.2	13.65
500	47.3	11.13
550	>100	>21.05

$$* \alpha_{T_1 \text{ to } T_2} = \left[(\Delta L/L)_{T_2} - (\Delta L/L)_{T_1} \right] \div [T_2 - T_1]$$

Inch/Inch°F

Example: $\alpha_{0 \text{ to } 350^\circ\text{F}} = \frac{[38.4 - (-10.0)] \times 10^{-3}}{350} = 13.83 \times 10^{-5}$

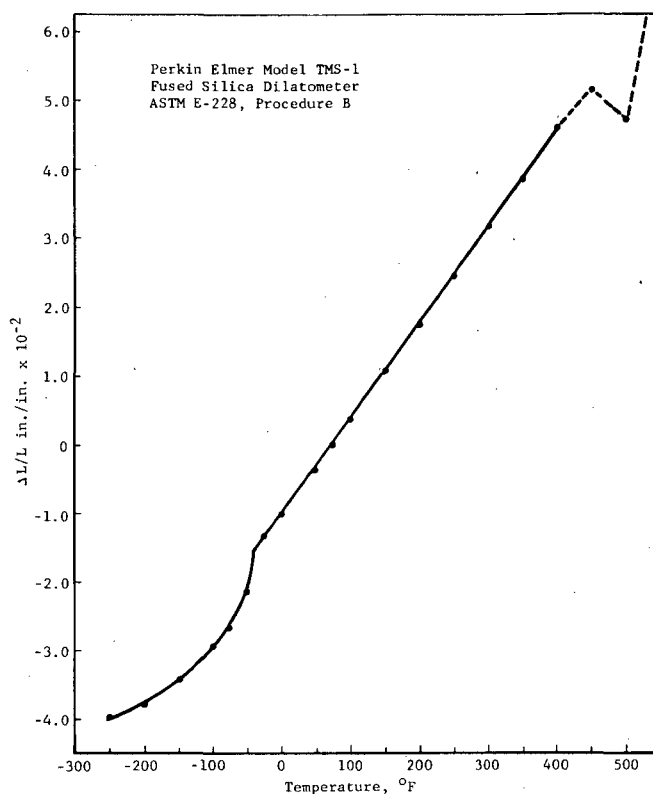


Figure 115 Linear Thermal Expansion Vs. Temperature, DC 93-046

The expansion of DC 93-046 above its softening transition point (α -25°F to 400°F = 13.88×10^{-5} inch/inch°F) is slightly higher than that of GE RTV-560 above its transition temperature. Expansion of 93-046 below the transition point does not appear constant and increases rapidly as it approaches the transition temperature.

5.1.2.4 Thermal Expansion of MMC SLA-561

Expansion data for MMC SLA-561 are summarized in Table XLI and plotted as $\Delta L/L$ versus temperature in Figure 116. Penetration tests on SLA-561 reveal that it undergoes its softening transition in the -175°F to -185°F temperature range. Sag temperatures were noted to be in the 685°F to 740°F range.

The expansion of SLA-561 below its softening transition temperature (α -275 to -175°F = 4.7×10^{-5} inch/inch°F) is approximately one-third of that between the softening point and 400°F (α -175°F to 400°F = 15.1×10^{-5} inch/inch°F), but decreases again above 400°F through its degradation temperature (α 400 to 700°F = 10.86×10^{-5} inch/inch°F).

TABLE XLI

SUMMARY OF LINEAR THERMAL EXPANSION: MMC SLA-561
(NORMALIZED TO 75°F)

INSTRUMENT: PERKIN ELMER CORPORATION, MODEL TMS-1
PROCEDURE: ASTM E-228, PROCEDURE B

Temperature °F	Expansion $\Delta L/L_{75^\circ F}$, inch/inch	Expansivity* $\alpha_{75^\circ \text{ to } T^\circ F}$, inch/inch ^{°F}
-275	-4.44×10^{-2}	12.69×10^{-5}
-250	-4.35	13.38
-225	-4.24	13.83
-200	-4.10	14.91
-175	-3.97	15.88
-150	-3.61	16.04
-100	-2.79	15.94
- 50	-1.94	15.52
0	-1.18	15.75
50	-0.38×10^{-2}	15.20×10^{-5}
75	0	0
100	0.37×10^{-2}	14.80×10^{-5}
150	1.13	15.07
200	1.84	14.72
250	2.59	14.80
300	3.31	14.71
350	4.06	14.76
400	4.71	14.49
450	5.31	14.16
500	5.87	13.81
550	6.42	13.52
600	6.92	13.18
650	7.50	13.04
700**	7.97×10^{-2}	12.75×10^{-5}

$$* \alpha_{T_1 \text{ to } T_2} = \left[\frac{(\Delta L/L)_{T_2}}{T_2} - \frac{(\Delta L/L)_{T_1}}{T_1} \right] \div [T_2 - T_1]$$

$$\text{Example: } \alpha_{0 \text{ to } 350^\circ F} = \left\{ \left[\frac{(4.06) - (-1.18)}{350} \right] \times 10^{-2} \right\} \div 350$$

$$= 14.97 \times 10^{-5} \text{ inch/inch}^\circ F.$$

**Specimens sagged in 685 to 740°F range.

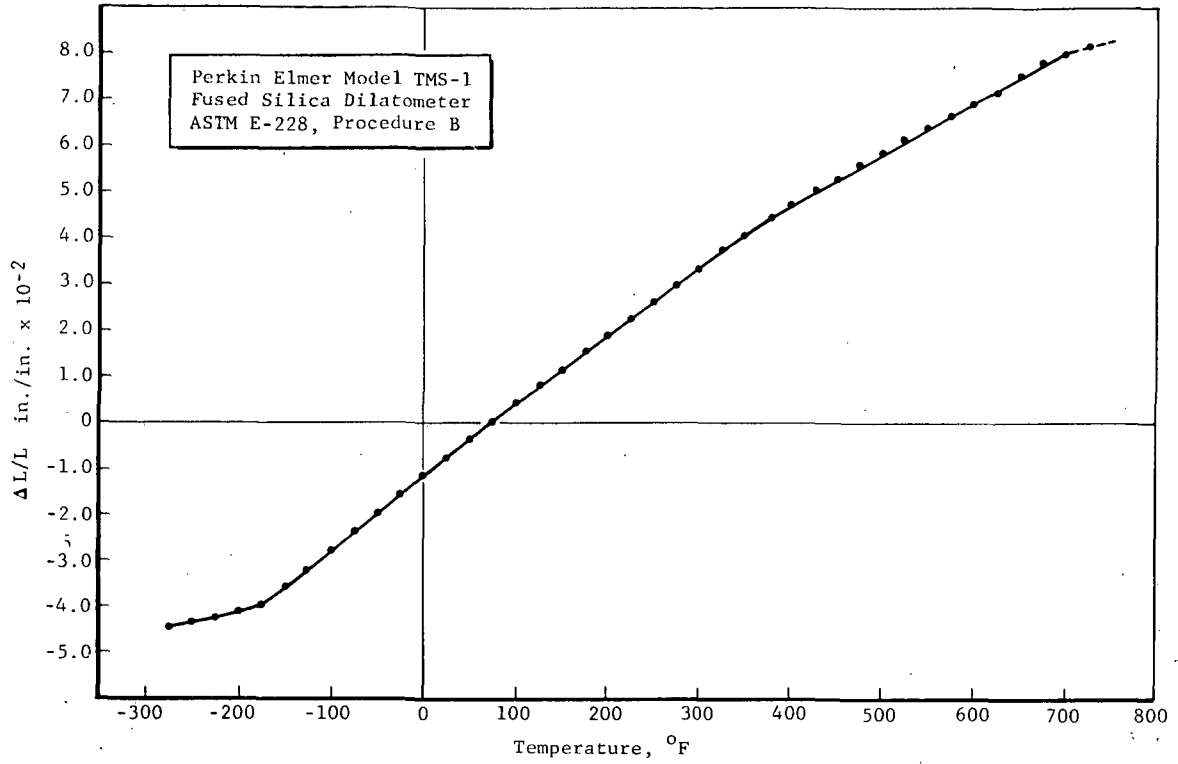


Figure 116 Linear Thermal Expansion Vs. Temperature, SLA 561

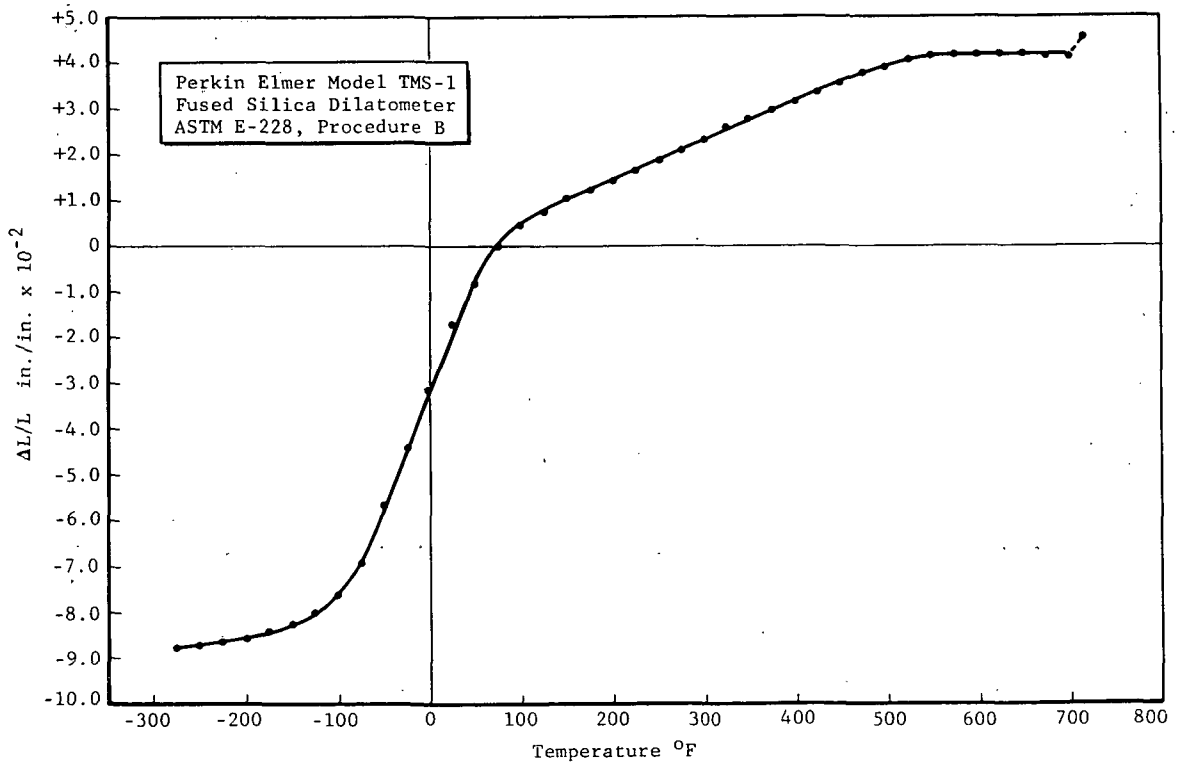


Figure 117, Linear Thermal Expansion Vs. Temperature RM/RL-1973

5.1.2.5 Thermal Expansion of R/M RL-1973

Expansion data for R/M RL-1973 sponge are summarized in Table XLII and plotted as $\Delta L/L$ versus temperature in Figure 117. Penetration tests on this material reveal its softening transition temperature range is between -175°F and -185°F . No sag temperature as such could be detected below 700°F , although the expansion appeared to level off between 550°F and 700°F this indicated that deformation might be occurring in that temperature range.

Three slopes are apparent in the thermal expansion curves for the RL-1973 sponge. The value is typically low below the softening transition (α -275 to $-200^{\circ}\text{F} = 2.4 \times 10^{-5}$ inch/inch $^{\circ}\text{F}$), increases rapidly through ambient temperature (α -75 to $50^{\circ}\text{F} = 48.6 \times 10^{-5}$ inch/inch $^{\circ}\text{F}$), and then decreases again through 500°F (α 100 to $500^{\circ}\text{F} = 8.65 \times 10^{-5}$ inch/inch $^{\circ}\text{F}$).

5.1.2.6 Comparison of Four Materials

The overall thermal expansions of the various adhesive systems can be compared in Figure 118.

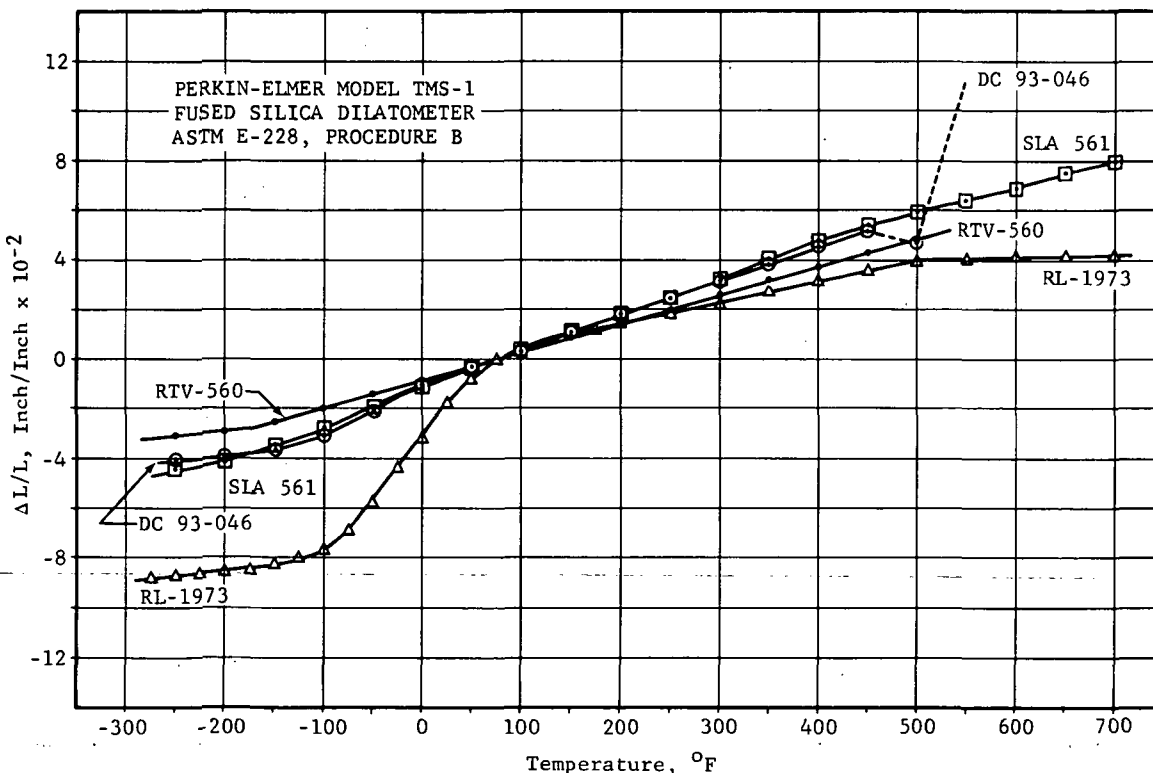


Figure 118 Linear Thermal Expansion Vs. Temperature

TABLE XLII

SUMMARY OF LINEAR THERMAL EXPANSION: R/M RL-1973 SPONGE
(Normalized to 75°F)

INSTRUMENT: PERKIN-ELMER CORPORATION MODEL TMS-1
PROCEDURE: ASTM E-228, PROCEDURE B

Temperature, °F	Expansion $\Delta L/L$ 75°F, inch/inch	Expansivity* α 75°F to T°F, inch/inch°F
-275	-8.79×10^{-2}	25.11×10^{-5}
-250	-8.73	26.86
-225	-8.65	28.83
-200	-8.61	31.31
-175	-8.47	33.88
-150	-8.23	36.58
-125	-7.99	39.95
-100	-7.65	43.71
-75	-6.91	46.07
-50	-5.67	45.36
-25	-4.40	44.00
0	-3.18	42.40
25	-1.71	34.20
50	-0.83×10^{-2}	33.20×10^{-5}
75	0	0
100	0.45×10^{-2}	18.00×10^{-5}
125	0.76	15.20
150	1.01	13.47
175	1.21	12.10
200	1.42	11.36
225	1.64	10.93
250	1.85	10.57
275	2.07	10.35
300	2.31	10.27
325	2.53	10.12
350	2.75	10.00
375	2.96	9.87
400	3.19	9.82
425	3.37	9.63
450	3.55	9.47
475	3.73	9.33
500	3.91×10^{-2}	9.20×10^{-5}

TABLE XLII (Continued)
 SUMMARY OF LINEAR THERMAL EXPANSION: R/M RL-1973 SPONGE
 (Normalized to 75°F)

Temperature, °F	Expansion $\Delta L/L_{75^\circ F}$, inch/inch	Expansivity* $\alpha_{75^\circ \text{ to } T^\circ F}$, inch/inch °F
525	4.05×10^{-2}	9.00×10^{-5}
550	4.12	8.67
575	4.16	8.32
600	4.17	7.94
625	4.17	7.58
650	4.17	7.25
675	4.11	6.85
700	4.11	6.58
725	4.11	6.32
740	4.63×10^{-2}	6.96×10^{-5}

$$* \alpha_{T_1 \text{ to } T_2} = \left[(\Delta L/L)_{T_2} - (\Delta L/L)_{T_1} \right] \div [T_2 - T_1]$$

Example: $\alpha_{0 \text{ to } 350^\circ F} = \left\{ \left[(2.75) - (-3.18) \right] \times 10^{-2} \right\} \div 350$
 $= 16.94 \times 10^{-5} \text{ inch/inch } ^\circ F$

5.2 THERMAL CONDUCTIVITY

Thermal conductivity of a material is measured by determining time rate of heat transfer by conduction through a unit thickness, across a unit area, for a unit difference in temperature.

5.2.1 Test Method

Thermal conductivity was determined throughout a mean temperature range of -300°F to $+500^{\circ}\text{F}$ by the guarded hot-plate method specified in ASTM C-177. One matched pair of specimens was used for each material. The specimens were 12 inches square by $\frac{1}{4}$ inch thick (Figure 9, Section 2). The central 8-by-8-inch area represented the test section, and the remainder of the specimen (2-inch-wide band around outer edge) comprised the guard section. The test and guard heaters of the hot-plate were of identical dimension, and a differential thermopile was used to maintain the guard section at the same temperature as the test section.

One specimen was placed on each side of the hot plate's heater and sandwiched between two 12-by-12-inch cold plates through which a coolant could be circulated. Six hot face side, six cold face side, and four guard zone thermocouples were used to monitor temperatures on a precision potentiometer equipped with a multipoint selector switch for establishing equilibrium conditions.

The entire hot plate/specimen/cold plate sandwich was mechanically locked in position in such a manner that the specimen faces were in intimate contact with the heater and cold plates but were under no compressive loading. This package was then lightly wrapped with foam insulation prior to the test run. The electrical input to the heater and the type and flow rate of the coolant through the cold plates were adjusted to provide mean temperatures of -300°F to $+500^{\circ}\text{F}$. Water, methanol, and liquid nitrogen were used as cooling media. In Figure 119, the guarded hot plate is shown in operation with a liquid nitrogen dewar cart as the coolant source.

The thermal conductivity was calculated from data taken at equilibrium conditions by using the following equation:

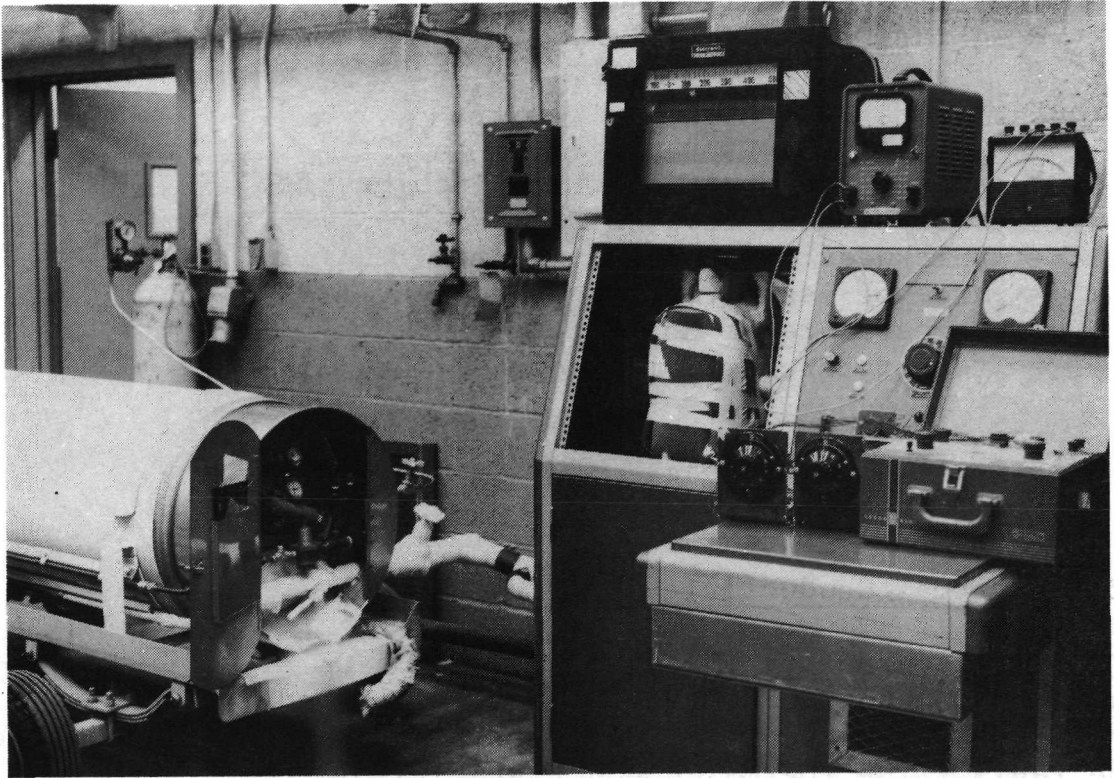


Figure 119 Liquid Nitrogen being Flowed through ASTM-C-177 Thermal Conductivity Tester

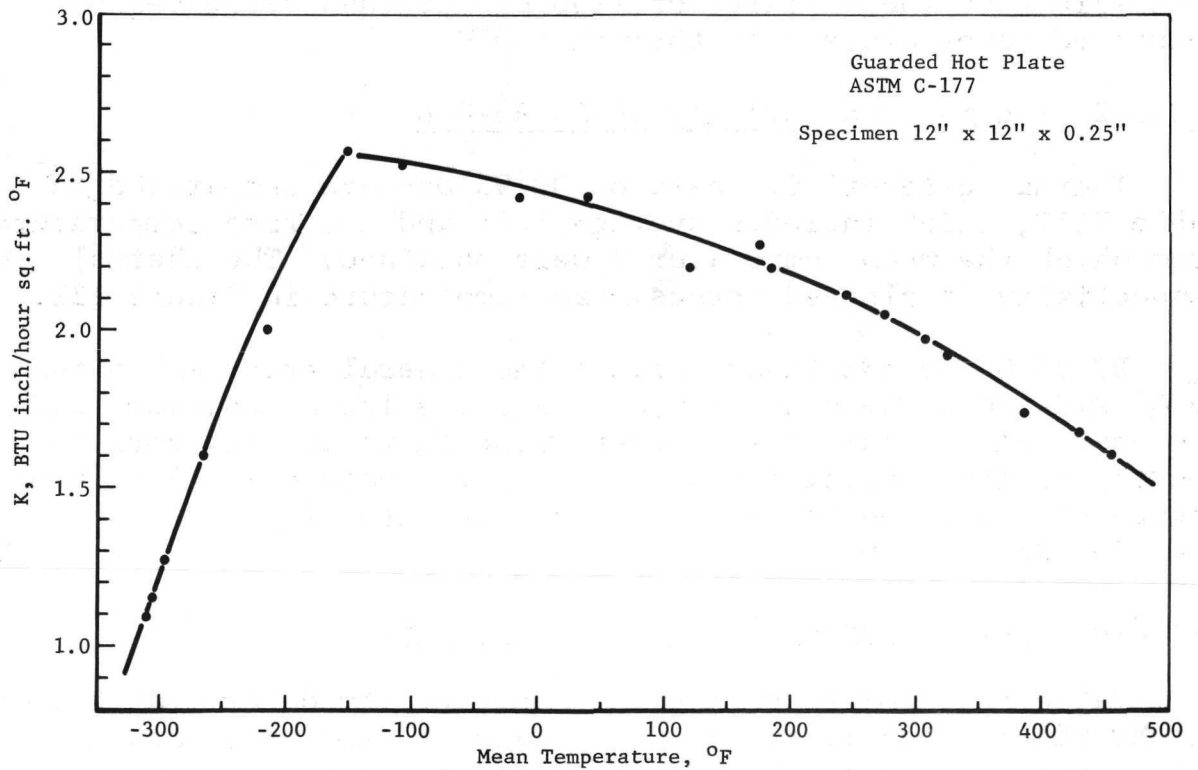


Figure 120 Thermal Conductivity Vs. Mean Temperature, RTV-560

$$k = qL/A(T_1 - T_2)$$

where:

- k = thermal conductivity, BTU inch/hr. ft.²°F
- q = rate of heat flow, BTU/hr
- L = thickness of specimen, inches
- A = area of isothermal test section, ft.²
- T₁ = temperature of hot face, °F
- T₂ = temperature of cold face, °F

5.2.2 Results and Discussion

5.2.2.1 Thermal Conductivity of GE RTV-560

Thermal conductivity determinations on GE RTV-560 are summarized in Table XLIII. The average cold and hot face temperatures from which the data were generated are also listed in the table. The thermal conductivity is plotted versus mean temperature in Figure 120.

The conductance increases sharply as the temperature rises from -310°F to the vicinity of -150°F. It then decreases on continued temperature rise through 450°F.

5.2.2.2 Thermal Conductivity of DC 93-046

Thermal conductivity data on DC 93-046 are summarized in Table XLIV, which includes average cold and hot face temperatures from which the mean temperatures were obtained. The thermal conductivity is plotted versus mean temperature in Figure 121.

DC 93-046 conductance follows the general trend exhibited by GE RTV-560. The conductance values are lower, however, and the peak value occurs at a higher temperature closely corresponding to the softening transition of the material. A greater degree of reversion in the test zone was noted for DC 93-046 than for GE RTV-560.

5.2.2.3 Thermal Conductivity of MMC SLA-561

Table XLV summarizes thermal conductivity determinations on MMC SLA-561 and lists face temperatures from which mean values were obtained. The thermal conductivity versus mean temperature for this material is plotted in Figure 122.

TABLE XLIII
THERMAL CONDUCTIVITY TEST RESULTS

Sample RTV-560

Procedure ASTM C-177

Thickness 0.25"

Average Cold Side Temp. °F	Average Hot Side Temp. °F	Mean T. °F	K $\left(\frac{\text{BTU-in.}}{\text{°F-ft.}^2\text{-hr.}}\right)$ *
-319	-300	-310	1.09
-321	-288	-305	1.15
-311	-280	-296	1.27
-315	-216	-265	1.60
-311	-121	-216	2.00
-159	-145	-152	2.56
-132	- 87	-110	2.52
- 32	+ 2	- 15	2.42
- 5	+ 82	+ 39	2.42
+ 94	+146	+120	2.20
+150	+199	+175	2.27
+133	+233	+183	2.20
+192	+296	+244	2.11
+248	+301	+275	2.05
+279	+334	+307	1.97
+297	+353	+325	1.92
+355	+417	+386	1.74
+397	+461	+429	1.68
+422	+489	+456	1.60

*In all thermal conductivity tests the BTU quantity was obtained from readings of precision electrical meters connected in the heater circuit.

TABLE XLIV

THERMAL CONDUCTIVITY TEST RESULTS

Sample DC 93-046Procedure ASTM C-177Thickness 0.25"

Average Cold Side Temp. °F	Average Hot Side Temp. °F	Mean T. °F	K $\left(\frac{\text{BTU-in.}}{\text{°F-ft}^2\text{-hr.}} \right)$
-311	-262	-287	0.18
-309	-183	-246	0.30
-296	- 70	-183	0.42
-272	+ 12	-131	0.65
-239	+ 43	- 98	0.80
-226	+ 66	- 80	0.94
-208	+109	- 50	1.07
- 34	- 19	- 27	1.40
- 29	- 5	- 17	1.41
- 17	+ 15	- 1	1.45
- 5	+ 26	+ 10	1.49
+ 7	+ 50	+ 29	1.52
+ 19	+ 85	+ 52	1.45
+ 69	+133	+101	1.51
+140	+242	+191	1.41
+164	+319	+242	1.41
+296	+402	+349	1.37
+335	+384	+360	1.37
+405	+457	+431	1.33
+436	+493	+465	1.23

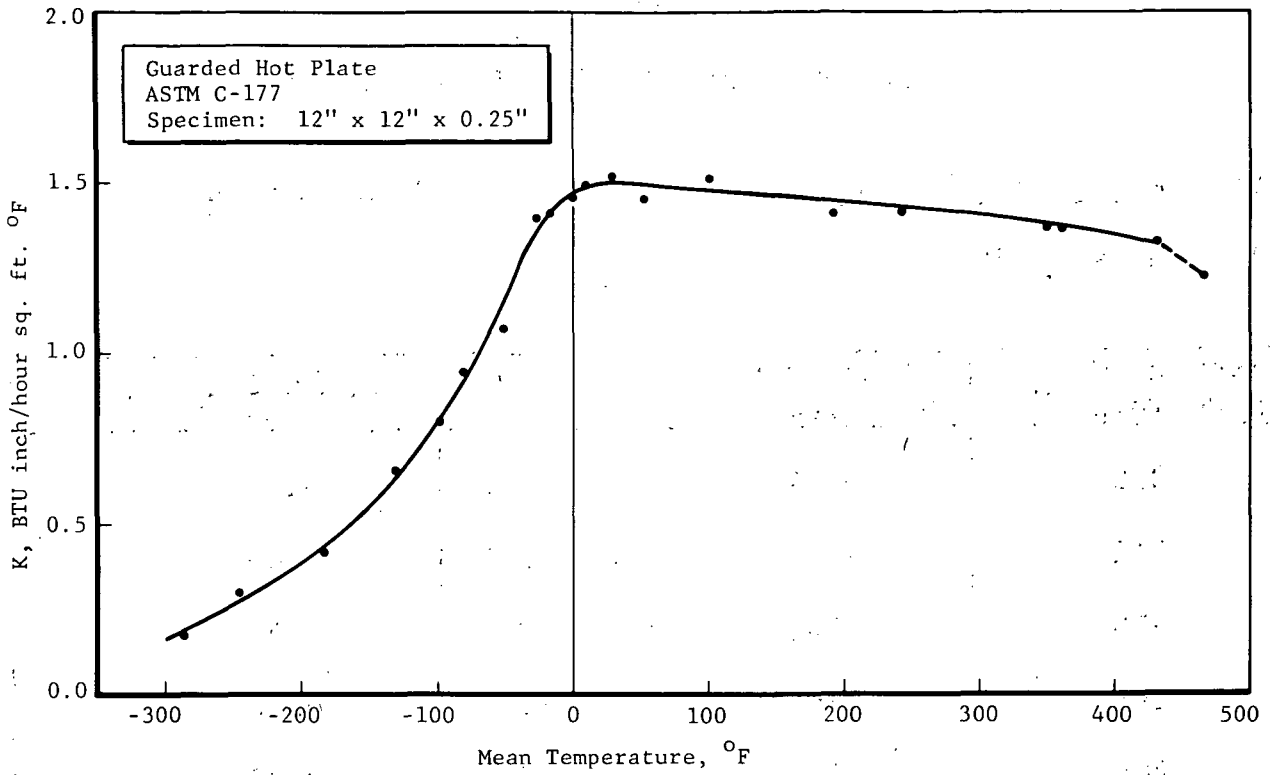


Figure 121 Thermal Conductivity Vs. Mean Temperature, DC 93-046

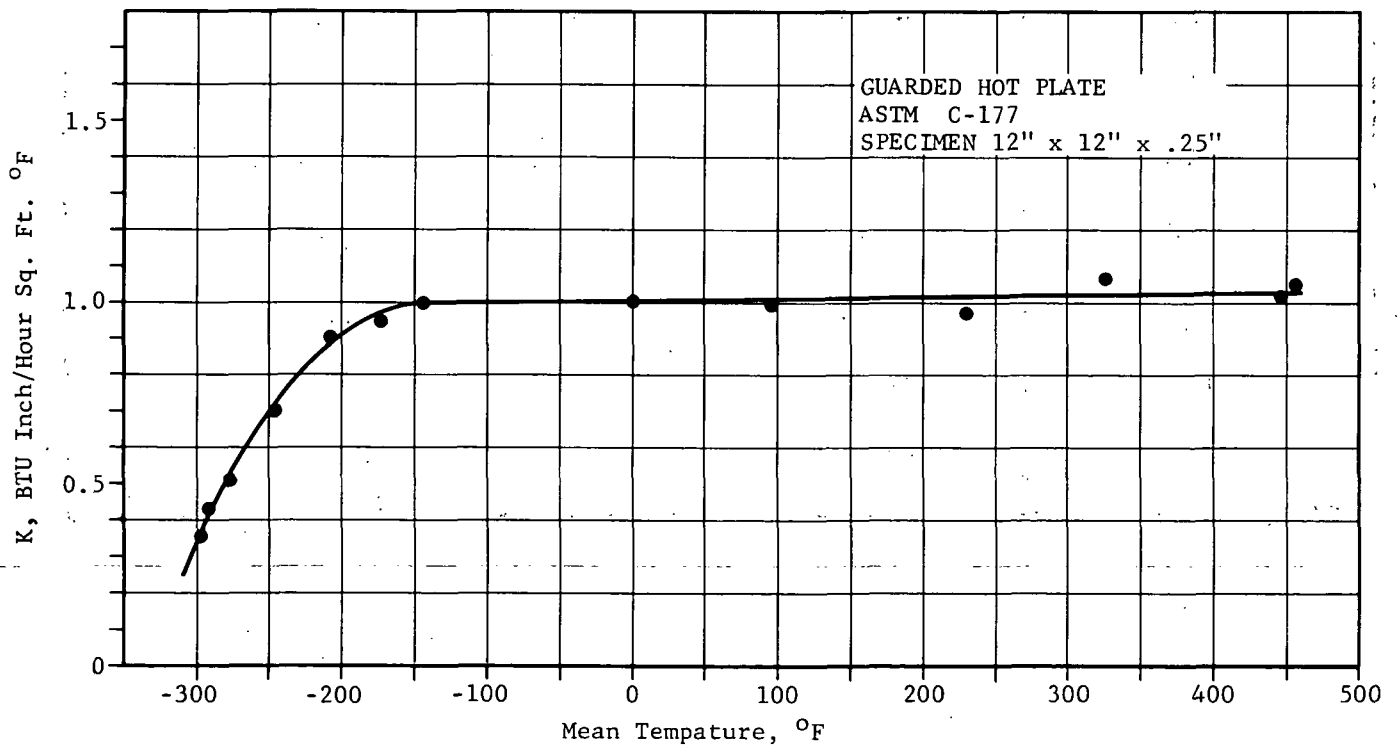


Figure 122 Thermal Conductivity Vs. Mean Temperature, SLA-561

TABLE XLV

THERMAL CONDUCTIVITY TEST RESULTS

Sample MMC-SLA-561Procedure ASTM C-177Thickness 0.25

Average Cold Side Temp. °F	Average Hot Side Temp. °F	Mean T. °F	K $\left(\frac{\text{BTU-in.}}{\text{°F-ft}^2\text{-hr.}} \right)$
-310	-281	-296	0.36
-312	-267	-290	0.43
-310	-240	-275	0.51
-298	-195	-247	0.70
-286	-127	-207	0.90
-253	- 90	-172	0.95
-236	- 44	-141	1.00
- 17	+ 19	+ 1	1.00
+ 45	+151	+ 98	1.00
+180	+280	+230	0.97
+288	+364	+326	1.07
+415	+479	+447	1.02
+421	+491	+456	1.05

Conductance of SLA-561 increases from -296°F through the materials softening transition temperature; then, conductance appears to remain constant from the softening temperature through 450°F . The thermal conductance of SLA-561 is considerably below that of RTV-560 throughout the temperature range -300 to 450°F ; however, at temperatures below -100°F , the conductance of SLA-561 is greater than that of 93-046, whereas at -50°F and above, SLA-561 exhibits less thermal conductance than 93-046.

5.2.2.4 Thermal Conductivity of RM/RL-1973

Thermal conductivity determinations on RM/RL-1973 sponge are summarized in Table XLVI and are plotted in Figure 123. Some fluctuation in data reproducibility was noted on the sponge. The data show slight variations in conductance values when the material is retested at some previously used temperature. Slight shrinkage was also noted in the specimen upon completion of the test. The RL-1973 sponge generally exhibited the lowest thermal conductance throughout the overall temperature range.

5.2.2.5 Comparison of Four Materials

Thermal conductivity versus mean temperature curves for the four adhesive systems are plotted for comparison in Figure 124.

5.3 SPECIFIC HEAT

Specific heat is determined by measuring the quantity of heat necessary to raise a unit mass of a material a unit temperature interval. Specific heat was determined in accordance with Perkin Elmer Corporation Instruction 900-9547 to be used with their Model DSC-1B differential scanning calorimeter (DSC).

5.3.1 Test Method

Specific heat was determined on the DSC unit previously shown in Figure 113. The tests were conducted from -130°F to 600°F on triplicate samples of each material. Liquid nitrogen was used as the coolant. Sample weight varied from 15 to 100 milligrams. Four sapphire discs (NBS standards) of known weight and specific heat at the temperatures of interest were used as comparison standards.

TABLE XLVI THERMAL CONDUCTIVITY TEST RESULTS

Sample Raybestos RL 1973 Silicone Sponge Procedure ASTM C-177Thickness 0.25" (See Note)

Average Cold Side Temp. °F	Average Hot Side Temp. °F.	Mean T. °F	K $\left(\frac{\text{BTU-in.}}{\text{°F-ft}^2\text{-hr}}\right)$
-308	-277	-293	0.12
-302	-262	-282	0.26
-303	-227	-265	0.32
-297	-197	-247	0.38
-254	-107	-180	0.47
- 23	+ 16	- 4	0.50
+ 97	+131	+114	0.56
+182	+213	+208	0.69
+323	+385	+355	0.62
+395	+482	+439	0.73
+415	+502	+460	0.76
(Decreasing Temp.)			
+359	+448	+404	0.74
+192	+262	+227	0.76
+145	+201	+173	0.72
Heater Off Overnight - Restarted in Morning			
+115	+163	+135	0.63
+152	+302	+227	0.68
+206	+458	+252	0.70
(Decreasing Temp.)			
+111	+167	+139	0.75

NOTE: At completion of test, sample dimensions had changed from 12" by 12" by 0.25" to 11½" by 11½" by 0.24" at room temperature.

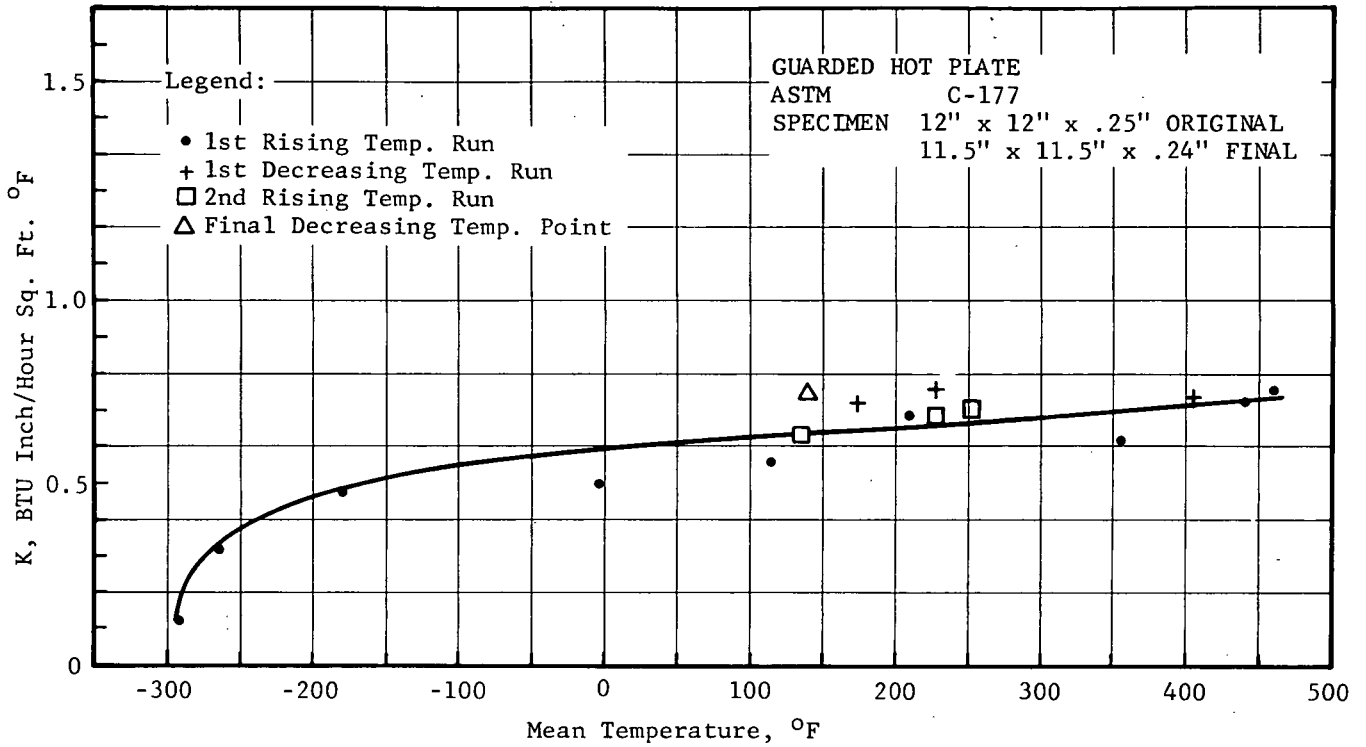


Figure 123 Thermal Conductivity Vs. Mean Temperature, R/M RL-1973 Sponge

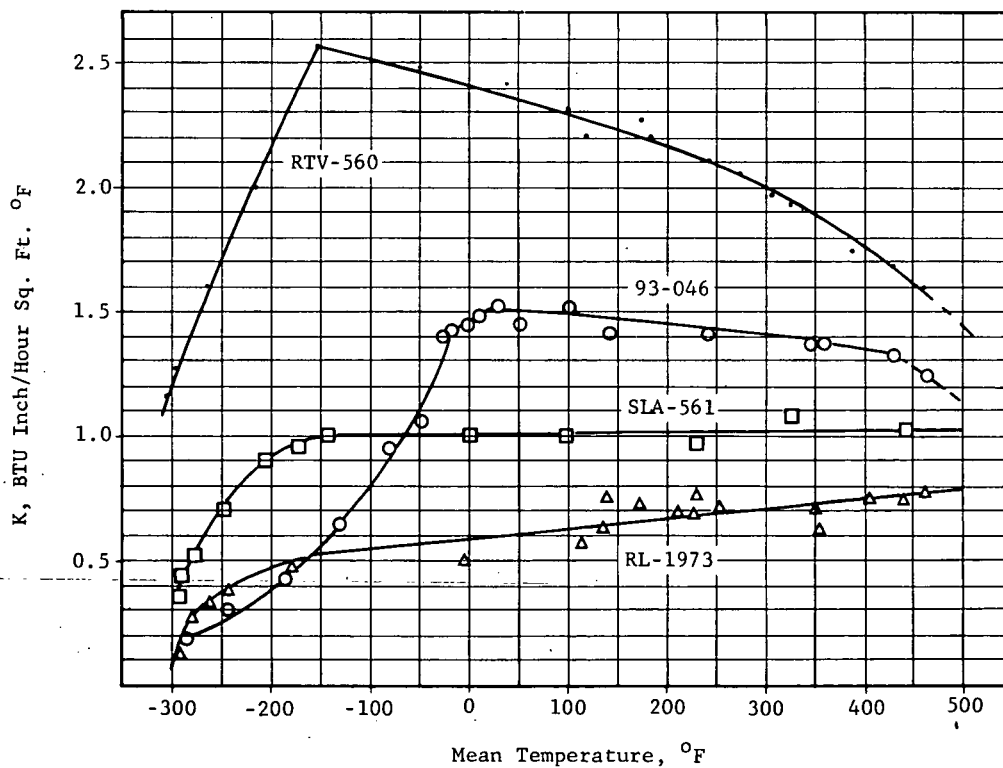


Figure 124 Thermal Conductivity Vs. Mean Temperature

The method involved scanning the sapphire standard at a rate of 18°F per minute over a 20°F temperature range with the test temperature at mid range, making a blank determination, and scanning the sample over the same range under identical conditions. The DSC readout was on recorder chart paper reading directly in calories per second. The sapphire and sample chart deflections were corrected for the blank deflection to obtain the amplitude of sapphire and sample. The specific heat (at temperature T) of the test sample was calculated as follows:

$$\text{Sp.ht.}_{x@T} = \frac{A_x W_s}{A_s W_x} \times \text{Sp.ht.}_{s@T}$$

where:

- Sp.ht._{x@T} = specific heat sample at temp., Cal./gm.°K
- Sp.ht._{s@T} = specific heat sapphire at temp., Cal./gm.°K
- A_x = amplitude of sample, Cal./sec.
- A_s = amplitude of sapphire, Cal./sec.
- W_x = weight of sample, grams
- W_s = weight of sapphire, grams

5.3.2 Results and Discussion

5.3.2.1 Establishment of Minimum Temperature Limit

The procedure described above requires that the temperature of the specimen and reference be programmable over a narrow 20°F band that straddles the desired test temperature. Liquid nitrogen temperatures had been achieved with this instrument in thermal expansion and penetration tests on the thermomechanical analyzer (TMA) accessory because the specimen temperature could be monitored directly by use of a thermocouple located at the base of the sample. However, in DSC runs no thermocouple exists in the sample cell compartment, and the temperature programmer is calibrated by use of various metal standards which melt at known temperatures. While liquid nitrogen temperatures could be achieved on the DSC, a programmable temperature scan could not be made at temperatures below -130°F. The limiting lower temperature of -130°F for specific heat measurements was reported to the NASA, MSC technical monitor, and he granted approval for Convair Aerospace to conduct specific heat tests between -130°F and 600°F.

5.3.2.2 Specific Heats of Four Adhesive Systems

The specific heats of the various adhesive systems are summarized in Table XLVII. The data reported for DC 93-046 at -65°F was erratic and not reproducible. This is not unusual since the test temperature is in the fringe of the glass transition for DC 93-046. An extra series of determinations was made on each side of the transition fringe (at -100°F and at -25°F) to provide additional check points.

The specific heats of all four adhesive systems are of the same order of magnitude over the temperature range investigated; the specific heats are generally between 0.2 and 0.4 calories/gram^oK.

5.4. THERMAL CYCLING

Tensile strength, tensile modulus, ultimate elongation, adhesion in tension, shear strength, and shear modulus were determined at room temperature before and after exposure to each series of thermal cycles listed below. Time at temperature was 5 minutes and three specimens were tested at each condition. Specimens were allowed to return to room temperature before a subsequent temperature exposure.

Thermal Cycle Temperatures

Series 1. R.T., -290°F , R.T. ($77^{+2^{\circ}}\text{F}$)

Series 2. R.T., $+500^{\circ}\text{F}$, R.T.

Series 3. R.T., -290°F , $+500^{\circ}\text{F}$, R.T.

Series 4. R.T., $+350^{\circ}\text{F}$, R.T.

Series 5. R.T., -290°F , $+350^{\circ}\text{F}$, R.T.

5.4.1 Band-Shaped Specimens

Tensile tests were conducted using molded band specimens with an inside diameter of 4.0 inches and a cross-section dimension of 0.125 inch thickness x 0.25 inch width (Figure 10, Section 2). Sponge specimens were cut with a fabricated "cookie" cutter type tool.

TABLE XLVII
SUMMARY OF SPECIFIC HEAT VERSUS TEMPERATURE
SPACE SHUTTLE ADHESIVES

INSTRUMENT: PERKIN-ELMER CORPORATION MODEL DSC-1B
PROCEDURE: PERKIN-ELMER INSTRUTION 900-9547 (SPECIFIC HEAT)

TEMPERATURE			SPECIFIC HEAT, CALORIES/GRAM °K			
°K	°C	°F	GE RTV-560	DC 93-046	MMC SLA-561	RMC RL-1973
183	-90	-130	0.23	0.27	0.30	0.22
200	-73.3	-100	-	0.28	-	-
219	-54	- 65	0.24	* 0.34-0.38	0.32	0.27
241	-32	- 25	-	0.31	-	-
300	27	80.6	0.27	0.32	0.34	0.28
422	149	300	0.32	0.38	0.39	0.32
450	177	350	0.34	0.38	0.39	0.31
561	288	550	0.33**	0.45**	0.41	0.33

* -65°F IS IN FRINGE OF A TRANSITION ZONE FOR DC93-046.
SPECIFIC HEAT ERRATIC AND NOT REPRODUCIBLE AT THIS TEMPERATURE.

** MATERIAL UNDERGOING THERMAL DEGRADATION DURING MEASUREMENTS AT
550°F. THESE VALUES ARE QUESTIONABLE.

5.4.1.1 Test Method

Tests were conducted according to ASTM-D-1414 Section 7 specified for O-rings, except the strain rate was 0.4 inch/inch/minute (Figure 125). Testing was conducted at room temperature.

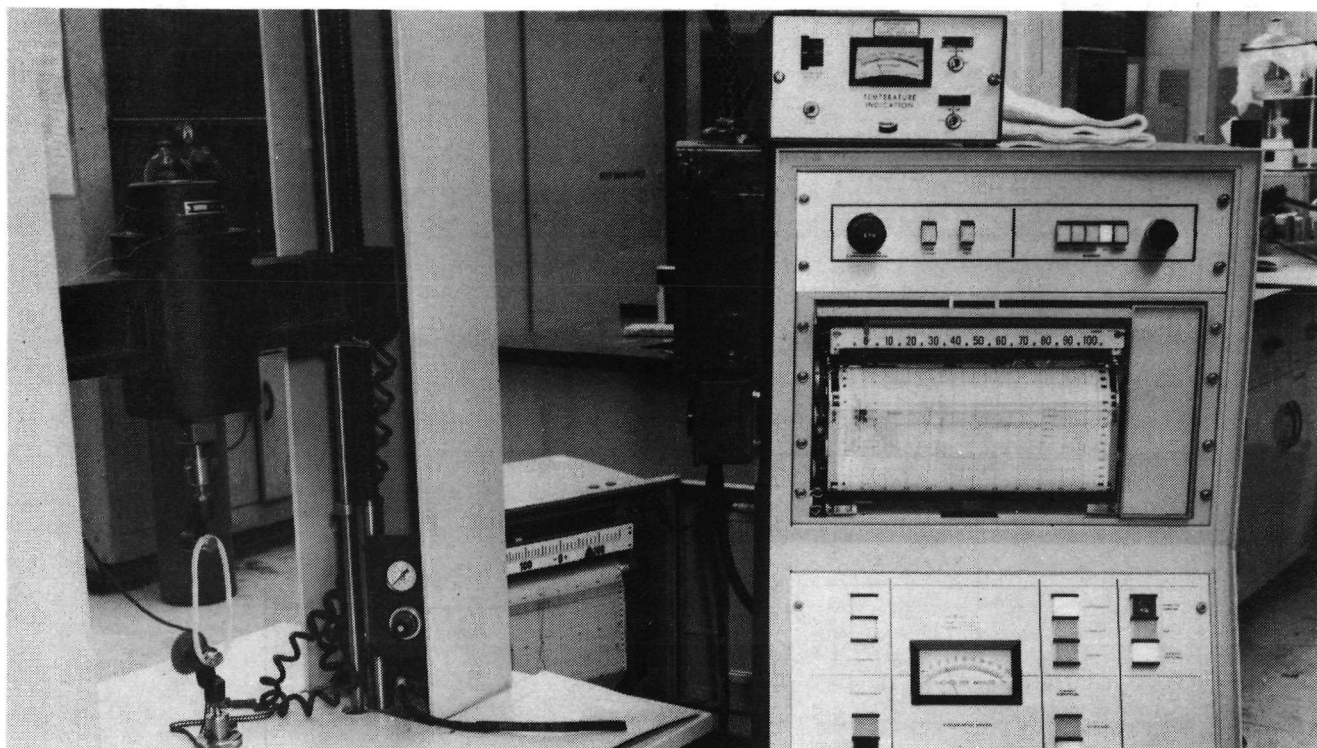


Figure 125 Band-Shaped Specimen in Test on CRE-2K Bendix Scott Test Machine

5.4.1.2 Effect on Tensile, Elongation, and Tensile Modulus

Ultimate tensile strength, percent elongation, and initial tensile modulus values were calculated from the data obtained from the band specimens. These values are shown in Table XLVIII. In general, GE RTV-560 exhibits a slight increase in tensile and elongation and a decrease in modulus whereas DC 93-046 exhibits a decrease in all properties. A decrease in properties is exhibited by MMC SLA-561 when exposed to environments requiring 500^oF exposure, but a slight increase is exhibited when exposed to the other conditions. RM/RL-1973 experiences a decrease in tensile and elongation properties under all conditions but modulus values are essentially unchanged.

5.4.2 Torsional Shear Specimens

Shear specimens were standard double overlap specimens

Table XLVIII ULTIMATE SHEAR STRENGTH AND ELONGATION AFTER ENVIRONMENTAL CONDITIONING OF BAND SHAPED SPECIMENS

Environmental Conditions	GE RTV-560			DC 93-046			MMC SLA 561			RM/RL 1973		
	Tensile psi	Ultimate Elong. %	Tensile Modulus, psi	Tensile psi	Ultimate Elong. %	Tensile Modulus, psi	Tensile psi	Ultimate Elong. %	Tensile Modulus, psi	Tensile psi	Ultimate Elong. %	Tensile Modulus, psi
Control	165	45	307	204	267	177	77	74	154	52	215	24
	164	45	312	277	370	194	98	94	160	52	195	31
	173	45	314	249	333	183	51	45	144	51	209	25
	167	45	311	243	323	185	75	71	152	52	206	27
RT, -290°F, RT	194	49	311	155	196	181	111	106	160	33	783	21
	215	54	317	232	298	192	98	81	168	37	167	24
	141	41	301	162	206	178	84	76	160	48	207	23
	183	48	309	183	233	184	98	88	163	39	186	23
RT, 500°F, RT	203	62	215	211	326	102	41	42	117	37	169	27
	230	67	209	219	347	93	31	31	112	39	175	26
	159	52	214	148	256	93	31	36	115	38	151	30
	197	61	213	193	310	96	36	36	115	38	165	28
RT, -290°F, 500°F, RT	218	62	236	222	329	96	68	80	112	49	188	27
	158	52	210	150	247	106	103	99	124	45	196	26
	175	53	238	195	297	113	50	48	125	38	175	21
	183	56	228	189	291	105	74	76	120	44	186	24
RT, 350°F, RT	213	54	297	213	259	180	114	84	167	37	164	27
	244	58	308	139	181	161	77	57	168	42	168	28
	202	55	271	195	254	170	78	57	168	40	159	25
	220	56	292	182	231	170	90	66	168	40	164	27
RT, -290°F, 350°F, RT	183	49	301	270	341	170	79	54	184	39	173	24
	220	56	299	199	246	174	95	68	181	43	186	27
	259	64	288	232	281	179	75	51	180	37	130	36
	221	56	296	234	290	175	83	56	182	40	163	29

(Figure 5, Section 2) with a bond line thickness of 0.100 inch.

5.4.2.1 Test Method

Shear modulus was determined in torsion at room temperature with the specimen loaded to 25 percent failing load as determined on three nontemperature-cycled control specimens. The test method was the same as that described in Section 4, Shear Modulus.

5.4.2.2 Effect on Torsional Shear Modulus

Shear modulus values are shown in Table XLIX. All materials experience a decrease in modulus after exposure to environmental conditions requiring exposure to 500^oF. When exposed to the other environmental conditions, the modulus of all materials except DC 93-043 is essentially unchanged. DC 93-046 experiences a decrease in modulus after all environmental conditions.

5.4.3 Shear Strength at Failure

Test specimens were as described above in 5.4.2 and this test was conducted on those specimens previously loaded to 25 percent of failure in torsion shear. However, in this test of shear strength, specimens were loaded longitudinally, which resulted in a tension-shear to failure arrangement. It could also be described as a double lap shear ultimate for the material.

5.4.3.1 Test Method

Test specimen load holes on the specimen ends were drilled out to 1/4-inch diameter to allow the use of stronger 3/16-inch pins, which would not bend under load. A clevis fitting was used to remove all slack in linkage. The strain rate was 0.4 in./in./min.

5.4.3.2 Effect on Shear Strength to Failure

Shear strengths before and after environmental conditioning are shown in Table XLIX. All materials exhibit a decrease in shear strength after exposure to environmental conditions requiring exposure to 500^oF and a slight increase in strength after

Table XLIX ULTIMATE SHEAR STRENGTH AND TORSIONAL SHEAR MODULUS AFTER ENVIRONMENTAL CONDITIONING OF DOUBLE LAP SHEAR SPECIMENS

Environmental Conditions	GE RTV 560		DC 93-046		MMC SLA 561		RM/RL 1973	
	Shear, psi	Shear* Modulus, psi	Shear psi	Shear* Modulus, psi	Shear, psi	Shear* Modulus, psi	Shear, psi	Shear* Modulus, psi
1	146	76	79	76	37	69	54	30
	144	92		72		74	54	22
	140	108	87	80	38	70	54	37
	143	92	78	76	38	71	54	29
Series 1 RT, -290°F, RT	171	107	40	50	44	85	82	23
	154	109	44	54	35	78	64	27
	167	55	47	58	37	73	66	26
	164	90	44	54	39	79	67	26
Series 2 RT, 500°F, RT	98	57	Failed in torsion below 25% of expected	7	30	51	57	25
	107	50		10	38	57	43	26
	84	43		7	30	55	35	25
	96	50		8	33	54	45	25
Series 3 RT, -290°F, 500°F, RT	92	50	32	27	23	38	56	20
	104	43	55	23	32	45	42	18
	114	48	47	24	31	46	52	26
	103	47	45	24	29	43	50	21
Series 4 RT, 350°F, RT	176	71	118	65	46	82	76	34
	167	110	100	64	43	79	72	29
	165	104	71	69	42	91	70	33
	169	95	96	66	44	84	73	32
Series 5 RT, -290°F, 350°F, RT	157	65	66	62	42	88	68	33
	161	61	74	63	44	85	70	34
	158	107	57	65	50	86	68	28
	159	78	66	64	45	86	69	32

*Determined at 25 Percent of Ultimate Shear Strength.

exposure to the other environments. It should be noted that the effect of 500^oF exposure on DC 93-046 was so severe that the specimens failed during the torsional shear test. This test required that the specimens be loaded in torsion to 25 percent of the average failing load of an unaged specimen before being tested in shear.

5.4.4 Tensile (Spool) Specimen

Flatwise tension specimens of 1.125 inch diameter, shown in Figure 2 of Section 2, with a 0.060 inch glueline of the candidate test materials were exposed to the five series of thermal environments.

5.4.4.1 Test Method

Specimens were tested in tension at room temperature at a strain rate of 0.4 inch/inch/minute as described in Section 4. Adhesion in Tension.

5.4.4.2 Effects on Tension and Elongation

As shown in Table L, all materials experience a decrease in tensile strength after exposure to environmental conditions requiring 500^oF exposure. A decrease in elongation is also exhibited by GE RTV-560 when exposed to this environment, but an increase in elongation occurs with DC 93-046 and MMC SLA-561. The elongation of RTV-560/RL-1973 is essentially unchanged.

After exposure to the other three environmental conditions, the tensile and elongation properties of GE RTV-560 and RTV-560/RL-1973 are essentially unchanged, whereas DC 93-046 exhibits a decrease in tensile strength and an increase in elongation. MMC SLA-561 exhibits an increase in tensile strength after exposure to -290^oF, but it is essentially unaffected by the other test environments.

Table L ADHESION IN TENSION AFTER ENVIRONMENTAL CONDITIONING OF CYLINDRICAL FLATWISE TENSION SPECIMENS

Environmental Conditions	GE RTV-560			DC 93-046			MMC SIA-561			RM/RL 1973		
	Tensile, psi	Ultimate Elong. %	Cohesive Failure, %	Tensile, psi	Ultimate Elong. %	Cohesive Failure, %	Tensile, psi	Ultimate Elong. %	Cohesive Failure, %	Tensile, psi	Ultimate Elong. %	Cohesive Failure, %
Control												
1	170	12	25	85	59	90	85	7	100	86	77	40
2	140	14	25	80	32	85	96	7	100	86	86	100
3	208	18	40	94	42	95	80	9	100	83	80	100
AVG	173	15	30	86	44	90	87	8	100	85	81	80
RT, -290°F, RT												
1	212	18	50	48	155	85	116	11	100	74	94	80
2	205	16	40	50	147	80	126	8	100	90	91	96
3	138	11	33	50	144	85	112	14	100	67	57	50
AVG	185	15	33	49	149	83	118	11	100	77	81	75
RT, 500°F, RT												
1	70	25	95	24	176	65	69	14	95	42	76	100
2	93	22	95	20	119	80	62	18	100	40	76	100
3	120	24	96	36	136	98	67	14	100	48	79	100
AVG	94	24	95	27	144	81	66	15	98	43	77	100
RT, -290°F, 500°F, RT												
1	109	19	98	16	166	80	59	14	100	49	91	100
2	120	25	98	20	173	80	60	20	100	56	93	100
3	124	24	99	16	198	98	65	14	100	46	71	100
AVG	117	23	98	17	179	86	61	16	100	50	85	100
RT, 350°F, RT												
1	195	22	93	51	114	75	99	16	100	82	77	100
2	192	17	98	48	143	80	80	10	100	64	65	10
3	185	23	100	62	139	60	81	11	100	73	76	95
AVG	190	21	97	54	132	72	87	13	100	73	72	68
RT, -290°F, 350°F, RT												
1	190	25	95	59	205	90	63	14	100	77	80	100
2	160	18	100	54	204	65	76	6	100	82	77	100
3	120	20	80	52	198	60	89	11	100	77	76	100
AVG	157	21	92	55	202	72	76	11	100	79	78	100

SECTION 6

BEHAVIOR OF
SILICONE RUBBER ADHESIVES
AT AND BELOW
THEIR GLASS TRANSITION
TEMPERATURES

S E C T I O N 6

B E H A V I O R O F S I L I C O N E R U B B E R A D H E S I V E S B E L O W T H E I R G L A S S - T R A N S I T I O N P O I N T S

Techniques used to test elastomeric materials for modulus and Poisson's ratio at temperatures above their glass transition points are not suitable for testing these same properties at temperatures below their glass transition points. In the rubbery state, the materials have high elongations and are usually tested at relatively high loading rates to minimize effects of stress relaxation. Because of the high elongations, minor errors in measurement of elongation as a function of applied stresses are inconsequential. In contrast, at glass transition temperatures and below these materials become hard and brittle thus have high moduli. Deformation caused by stress is small and optical techniques used for measurement of deformation at temperatures above the glass transition are no longer accurate enough to produce reproducible data. Loading rates must also be reduced by at least one order of magnitude in an attempt to obtain deformation measurements at incremental stress points. Conventional strain gauges cannot be used on rubber and extensometers tend to ice and freeze, which leads to slow testing and questionable test results.

6.1 OBSERVATION OF SPECIMENS AT AND BELOW GLASS TRANSITION TEMPERATURE

In testing the silicone based adhesives in this program, it was observed that at temperatures below their glass transition points, specimen were prone to shrink when initially subjected to stress. Pictures taken of the 10-inch-long, 2½-inch-wide and 0.10-inch-thick tensile strap specimens during loading showed this shrinkage, which resulted in negative deformations under initial loading conditions. This same phenomenon manifested itself in the compression tests of the 1.5-by 1.5-by 4-inch high molded blocks. At temperatures below the specimen's glass transition temperature, the test machine would

start the loading then load would be lost momentarily due to shrinkage of the specimen. As in the case of the tension specimen, this resulted in negative values in both the axial and transverse load directions.

The exact cause of the observed phenomenon described here was not determined. Nevertheless, three theories have been proposed to explain the unusual behavior. One is that the materials are supercooled and when axial load is applied molecular structure changes and shrinkage occur. Secondly, it is possible that a loose lattice formed during cool down prevents maximum shrinkage but when load is applied the lattice or restraining mechanism is broken thus allowing additional shrinkage to occur. A third theory is that the phenomenon is a results of the Joule Effect. The Joule Effect in rubber is that when it is placed under stress and subjected to heat the rubber specimen shrinks rather than expands (Ref. 2).

It is possible that when the specimens in this program are cooled below their glass transition temperature, stresses are set up in the polymer chains. Then, when low loads are introduced, the heat produced causes the Joule Effect to occur; hence, the specimen shrinks.

6.2 LITERATURE SURVEY REGARDING LOW TEMPERATURE PROPERTIES OF SILICONE RUBBER

Extensive work has been conducted by Polmanteer and associates at Dow Corning Corporation, Reference 3 and 4. He reports that silicone rubbers do supercool and the degree of supercooling is a function of quenching rates. Also he reports that two types of crystals form in polydimethylsiloxane.

Silicone rubber containing phenyl or diphenyl siloxane as a copolymer with the methyl or dimethyl siloxane, as exemplified by GE RTV-560, SLA-561 and RL-1973, are reported not to crystallize at low temperatures. The large phenyl side groups on the polymer chains tend to prevent the formation of crystalline patterns. The polymers get stiff and brittle at low temperature but do not crystallize as do the dimethyl siloxanes as exemplified by DC 93-046.

6.3 STRESS RELAXATION OF POLYMERS AT LOW TEMPERATURE

Mark and Tobolsky (Ref. 5) report some interesting points on the viscoelastic nature of polymers at low temperature as follows:

"The viscoelastic properties of substances in their glassy state have not been investigated extensively. Studies of stress relaxation in polyisobutylenes of different molecular weights and of Butyl rubber indicated that at sufficiently low temperatures the viscoelastic properties are independent of molecular weight and are also practically independent of the presence of cross linkages. The stress decay curves at low temperatures are of quite different shape from the curves obtained at high temperatures and the apparent activation energy of stress relaxation is very much higher in the glassy state than in the rubbery state."

"These results indicate that the instantaneous "modulus" of polymers stretched in their glassy state arises from a shift in short range interatomic distances rather than from the long range configurational changes that occur when these same substances are stretched in their "rubbery" state above the glass transition temperature. The force resisting stretching in the glassy state should probably be regarded as arising from a change in internal energy rather than from a change of entropy. Relaxation of stress is very rapid in the region of transition because only small range atomic movements are required to release distortion. Also, the change of viscoelastic properties with temperature here is not easily described as due to a simple translation of the relaxation time spectrum along the log time axis."

"An indication that the mechanism of stretching is completely different in the glassy state from that in the rubbery state is obtained by simultaneous measurements of stress and birefringence. The ratio, which is a constant in the rubbery range of temperature, changes very markedly in the region of the glass transition, there occasionally being a reversal of the sign of this quantity at the transition temperature."

Tobolsky's findings reported here may account for the rapid

stress relaxation of the silicone adhesives tested under constant strain and reported in Section 4.

S E C T I O N 7

C O N C L U S I O N S

A N D

R E C O M M E N D A T I O N S

7.0 CONCLUSIONS

AND

RECOMMENDATIONS

7.1 CONCLUSIONS

Conclusions drawn from this extensive development and testing work are:

1. An adhesive system comprised of a closed-cell silicone rubber sponge bonded to substrates with thin bond lines of GE RTV-560 exhibits density and modulus values approximately one-third that of the solid RTV silicone adhesives.
2. Utilization of glass or phenolic microballoons as fillers in RTV silicone adhesives reduce density but increase modulus of the vulcanized materials.
3. Mechanical properties of GE RTV-560, DC 93-046, SLA-561 and RL-1973/GE RTV-560 were determined. Data obtained over the temperature range of -175°F (-65°F for DC-93-046) to 350°F proved to be very reliable and suitable for establishing design allowables data curves. At temperatures below -175°F (-65°F for DC 93-046), the adhesives became stiff and brittle. Strains caused by stress are extremely small; therefore, methods of measuring strains at temperature above the glass transition temperatures are inadequate and do not provide the accuracy needed to establish reliable design allowables for temperatures below the glass transition points. Moreover, it was discovered that at these low temperatures, the silicone adhesives exhibit a phenomenon of shrinkage when initially subjected to loading conditions. This phenomenon causes aberrations in data such as modulus and Poisson's ratio derived from measurements of deformation. At test temperatures of 550 and 660°F , the silicone adhesives are in a transient state of deterioration; therefore, mechanical properties determined at these temperatures are low and variable.
4. Thermal cycling of the silicone adhesives to -270°F

causes no noticeable effects in mechanical properties subsequently tested at room temperature. Cycling to 350°F caused no significant changes but, cycling to 500°F is reflected in permanent reductions in mechanical properties.

5. Constant-strain/stress-relaxation tests produce interesting data in that stress relaxation is most pronounced near the glass transition temperature. GE RTV-560, SLA-561, and RL-1973 silicone rubber sponge exhibit approximately 10-percent relaxation at room temperature under a constant 10-percent strain. Under a 0.4-percent constant strain at -270°F there is a 3-to 5-percent stress relaxation in the first 5 minutes followed by a stabilization.

In contrast, at a test temperature of -175°F and 0.4-percent constant strain, there is approximately 90 percent stress relaxation. At -200°F under the same conditions, there is an approximately 50-percent stress relaxation. The majority of the stress relaxation occurs in the first 10 to 15 minutes of the test conditions.

6. The three solid adhesives (GE RTV-560, DC 93-046 and MMC SLA-561) exhibit virtually the same thermal expansion characteristics over the temperature range of -270 to 500°F. RM/RL -1973 sponge follows the same curve as the solids down to 75°F; then, it exhibits a greater rate of contraction.
7. GE RTV-560 has the highest thermal conductivity and RM/RL-1973 has the lowest. This is to be expected because of density difference and the air space in the closed-cell construction of the sponge.
8. Glass transition points (T_g) of the four adhesives are shown by breaks in both the thermal expansion and thermal conductivity curves; however, effects of T_g are more pronounced in thermal conductivity curves.

7.2 RECOMMENDATIONS

During the course of work described herein, it has become apparent that additional investigations and work are warranted. The following investigations are recommended:

1. Exploratory research should be conducted to fully characterize the silicone adhesive in their glass transition range and at temperatures down to -270°F .
2. Reserach and development should be conducted to provide a silicone rubber sponge that will exhibit a low modulus at temperatures down to -270°F .
3. Tests of candidate adhesives should be conducted to determine the effects of more severe thermal cycling than those to which the silicone adhesives were subjected in this program.
4. Research and development should be conducted to develop test techniques and instrumentation to accurately measure the minute deformations experienced by elastomeric materials subjected to loading conditions at extreme low temperature. These measurements should be recorded on a real-time basis.

A P P E N D I C E S

A P P E N D I X I

QUALITY CONTROL DOCUMENTS RECEIVED FOR
TEST CANDIDATE MATERIALS

The quality control documents shown here were received with the adhesives tested in this program. They verify that accompanying materials meet vendor quality control specifications.

Raybestos **R/M** Manhattan

Date June 12, 1972

CERTIFICATION OF COMPLIANCE

To: GENERAL DYNAMICS
P. O. BOX 748
FORT WORTH, TEXAS 76101

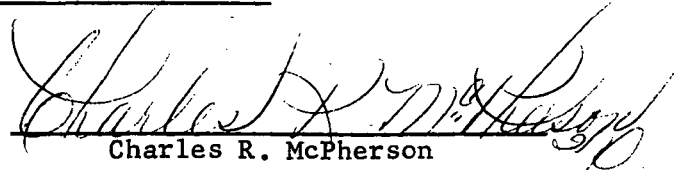
Contract No.: _____
P. O. No.: 542676
R/M Reg. No.: 21596
Quantity: see below *

This is to certify that the material identified as R/M RL-1973 Silicone Rubber
Sponge,

meets and complies with the following specifications R/M RL-1973

Compliance for quality assurance has been determined by testing and/or inspection
in accordance with the applicable specifications and/or Quality Control Standards,
the results of which are on file and are available to the Buyer and the Government.
Test results are attached hereto or may be obtained by referencing Quality Control
Report No. 780, dated June 12, 1972.

- 3 Pcs. - 23" x 23" x 1/4"
- 2 Pcs. - 16" x 24" x 1/4"
- 1 Pc. - 22" x 22" x 1/4"
- 1 Pc. - 22" x 22" x .100"/.126" thk.
- 1 Pc. - 14" x 22" x .100"/.126" thk.


Charles R. McPherson
Manager, Quality Assurance

Raybestos **R/M** Manhattan

Date July 11, 1972

CERTIFICATION OF COMPLIANCE

To: GENERAL DYNAMICS CONVAIR
AEROSPACE DIVISION
GRANTS LANE
FR. WORTH, TEXAS 76101

Contract No.: _____

P. O. No.: 079071

R/M Reg. No.: 22664

Quantity: 4 Sq/ Ft.

This is to certify that the material identified as R/M RL-1973 Silicone Sponge,
.060" thk.

meets and complies with the following specifications R/M RL-1973

Compliance for quality assurance has been determined by testing and/or inspection
in accordance with the applicable specifications and/or Quality Control Standards,
the results of which are on file and are available to the Buyer and the Government.
Test results are attached hereto or may be obtained by referencing Quality Control
Report No. 917, dated July 11, 1972.


Charles R. McPherson
Manager, Quality Assurance

Raybestos ^{R/M} Manhattan

Date March 28, 1972

CERTIFICATION OF COMPLIANCE

To: GENERAL DYNAMICS
CONVAIR AEROSPACE DIVISION
FT. WORTH, TEXAS 76101

Contract No.: _____

P. O. No.: 525068

R/M Reg. No.: 17926-1

Quantity: 15 Sq. Ft.-0.10" thk.
4 Sq. Ft.-0.030" thk.

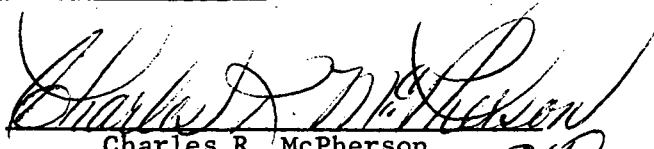
Attention: Mr. A. E. McDonald
Bldg. 80, Dept. 064-6

This is to certify that the material identified as R/M RL-1973 Silicone Sponge
Grey,

meets and complies with the following specifications R/M RL-1973 & R/M Factory
Specification 857 Sh. 1.

Compliance for quality assurance has been determined by testing and/or inspection
in accordance with the applicable specifications and/or Quality Control Standards,
the results of which are on file and are available to the Buyer and the Government.

Test results are attached hereto or may be obtained by referencing Quality Control
Report No. 428, dated March 28, 1972.


Charles R. McPherson
Manager, Quality Assurance

Raybestos **Manhattan**

Date February 18, 1972

CERTIFICATION OF COMPLIANCE

To: GENERAL DYNAMICS
CONVAIR AEROSPACE DIVISION
FT. WORTH, TEXAS

Contract No.: _____

P. O. No.: 525068

R/M Reg. No.: 17926

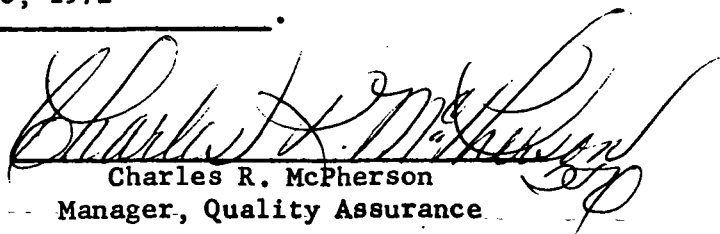
Quantity: see below *

Attn.: Mr. A. E. McDonald
Bldg. 80, Dept. 064-6

This is to certify that the material identified as R/M RL-1973 Silicone Sponge
Sheets, 1.5" thk.; .250" thk.; .060" thk. - each sheet 4 Sq. Ft.

meets and complies with the following specifications R/M RL-1973 & R/M Factory
Specification 857 Sh. 1

Compliance for quality assurance has been determined by testing and/or inspection
in accordance with the applicable specifications and/or Quality Control Standards,
the results of which are on file and are available to the Buyer and the Government.
Test results are attached hereto or may be obtained by referencing Quality Control
Report No. 245, dated February 18, 1972.


Charles R. McPherson
Manager, Quality Assurance

- * 4 Sq. Ft. - 1.5" thk. - Grey - Cure Date - 13 Oct. 1971
- 8 Sq. Ft. - .250" thk. - Green - Cure Date - 15 Nov. 1971
- 4 Sq. Ft. - .060" thk. - Green - Cure Date - 15 Nov. 1971

MARTIN MARIETTA DENVER DIVISION

Nº 44294

SHIP REQUEST/PACKING SHEET
FORM DEN 614780 (3-69)

DATE 9 June 1972	CHARGE TO BUILD ACCT NO. 204460-03890-00002	SHIPPING REGISTER NO. 72-05604	CONTRACT NO. SHIPPED FROM N/A
CI. FOR SHIPPING DOCUMENT, <input type="checkbox"/> DD-250 (FOR DELIVERABLE ITEM) <input checked="" type="checkbox"/> PACKING SHEET <input type="checkbox"/> DD-1140 (FOR GOVERNMENT-OWNED ITEM)	DIRECTIVE DOCUMENT IF ANY Customer Request	PRIORITY	SHEET 1 OF 1
	PURCHASE ORDER NO. FOR SHIP TO SUBCONTRACTOR PR No. 079054	MAT'L PROPERTY CONTROL NO. N/A	TRANSPORTATION CHARGE <input checked="" type="checkbox"/> COLLECT <input type="checkbox"/> PREPAID
	CREDIT VOUCHER NO. FOR DD1149 N/A	AUTHORITY FOR DD1149 N/A	EXPLOSIVE OR HAZARDOUS SHIP CLASS Corrosive
TRANSPORTATION CHARGE <input checked="" type="checkbox"/> COLLECT <input type="checkbox"/> PREPAID	SHIP VIA MARTIN MARIETTA TRUCK	COMMERCIAL AIR XX	OTHER, EXPLAIN

SHIP TO (INCLUDE MARKINGS, CONTRACT NO., BEING SHIPPED TO, AFN ACCT'BLE OFFICE AS APPLICABLE)

General Dynamics
Convair Aerospace Division
Fort Worth Operations
Fort Worth, Texas

Attn: A.E. McDonald (Bld'g 80; Dept. 064-b)

ITEM NO.	PART NO.	DESCRIPTION (INCLUDING SERIAL NO., CONTROL PT, ETC)	UNIT OF MEAS.	QUANTITY	VALUE
1	N/A	M&C 31A-51 Adhesive, Part A, Lot 306	Gal	1	
	N/A	Part B, Lot 306	Pt	1	

SHIPMENT REQUESTED BY THOMAS	PHONE 2979	MAIL I-1631	QUALITY APPROVAL OF ITEMS N/A	AUTHORIZED BY A.C. Thomas	PHONE 2979
RECEIVED	CHECKED BY 24003	CHARGE TO PACK & SHIP ACCT NO. 204460-03890-00002	QUALITY APPROVAL FOR PACKAGING 15-2-1-72	PACKAGES 1	GROSS WT 12.5
AL FOR SHIPMENT M 3210 6/15/72	AIR FORCE Q.C. N/A	DATE SHIPPED 6-15-72	SHIPPED VIA R & A Air Express	BOX SIZE 12x16x4	PACKED BY 2979
				S/L OR MANIFEST 42-16-90	

MARTIN MARIETTA DENVER DIVISION

Nº 42780

SHIP REQUEST/PACKING SHEET

FORM DEN 814780 (3-69)

DATE 17 March 1972	CHARGE TO BUILD ACCT NO. 204460-03890-00001	SHIPPING REGISTER NO. 72-04043	CONTRACT NO. SHIPPED FROM
CHI <input type="checkbox"/> DR SHIPPING DOCUMENT, <input type="checkbox"/> DD-250 (FOR DELIVERABLE ITEM) <input checked="" type="checkbox"/> PACKING SHEET <input type="checkbox"/> DD-1149 (FOR GOVERNMENT-OWNED ITEM)	DIRECTIVE DOCUMENT IF ANY Customer Request	PRIORITY	SHEET 1 OF 1
	PURCHASE ORDER NO. FOR SHIP TO SUBCONTRACTOR PR No. 525157	MAT'L PROPERTY CONTROL NO.	TRANSPORTATION CHARGE <input checked="" type="checkbox"/> COLLECT <input type="checkbox"/> PREPAID
	CREDIT VOUCHER NO. FOR DD1149	AUTHORITY FOR DD1149	EXPLOSIVE OR HAZARDOUS SHIP CLASS Corrosive
TRANSPORTATION CHARGE <input checked="" type="checkbox"/> COLLECT <input type="checkbox"/> PREPAID	SHIP VIA MARTIN MARIETTA TRUCK	COMMERCIAL AIR XX	OTHER, EXPLAIN

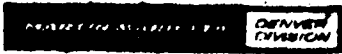
SHIP TO (INCLUDE MARKINGS, CONTRACT NO. BEING SHIPPED TO, AFM ACCT'BLE OFFICE AS APPLICABLE)

General Dynamics
Convair Aerospace Division
Fortworth Operations
Fortworth, Texas

Attn: K. L. Brooks

ITEM NO.	PART NO.	DESCRIPTION (INCLUDING SERIAL NO., CONTROL PT, ETC)	UNIT OF MEAS.	QUANTITY	VALUE
1	N/A	MMC SLA 561 Adhesive, Part A, Lot 306	Gal	3	
2	N/A	Part B, Lot 306	lt	3	

SHIPMENT REQUESTED BY D. A. Thomas	PHONE 2979	MAIL I-163	QUALITY APPROVAL OF ITEMS N/A	AUTHORIZED BY <i>[Signature]</i>	PHONE 2979
DATE -20-72	CHECKED BY 36051	CHARGE TO PACK & SHIP ACCT NO. 204460-03500-00001	QUALITY APPROVAL FOR PACKAGING	PACKAGES 1	GROSS WT. 52#
DATE SHIPPED 3/21/72	AIR FORCE Q.C. N/A	DATE SHIPPED 2-21-72	SHIPPED VIA Darruff	BOX SIZE 14x14x8	PACKED BY 4127
QUALITY APPROVAL FOR SHIPMENT <i>[Signature]</i>			B/L OR MANIFEST 002 Allen 0446-2200		



Nº 41019

SHIP REQUEST/PACKING SHEET

FORM DEN 814780 (2-69)

DATE: 08/16/72	CHARGE TO BUOLD ACCT NO. 204460-03890-00003	SHIPPERS REGISTER NO. 75-04173	CONTRACT NO. SHIPPED FROM N/A
CHECK FOR SHIPPING DOCUMENT, <input type="checkbox"/> DD-250 (FOR DELIVERABLE ITEM) <input checked="" type="checkbox"/> PACKING SHEET <input type="checkbox"/> DD-1148 (FOR GOVERNMENT-OWNED ITEM)	DIRECTIVE DOCUMENT IF ANY Customer Request	PRIORITY	SHEET 1 OF 1
	PURCHASE ORDER NO. FOR SHIP TO SUBCONTRACTOR P.R. 545734	MAT'L PROPERTY CONTROL NO. N/A	TRANSPORTATION CHARGE <input checked="" type="checkbox"/> COLLECT <input type="checkbox"/> PREPAID
	CREDIT VOUCHER NO. FOR DD1148 N/A	AUTHORITY FOR DD1148 N/A	EXPLOSIVE OR HAZARDOUS SHIP CLASS N/A
TRANSPORTATION CHARGE <input checked="" type="checkbox"/> COLLECT <input type="checkbox"/> PREPAID	SHIP VIA <input checked="" type="checkbox"/> AIR <input type="checkbox"/> TRUCK	OTHER, EXPLAIN	SAFETY APPROVAL N/A

SHIP TO (INCLUDE MARKINGS, CONTRACT NO. BEING SHIPPED TO, APO ACCT'BLE OFFICE AS APPLICABLE)

General Dynamics
Convair Aerospace Division
Fort Worth Operations
Fort Worth, Texas

Attn: A. E. McDonald
Bldg. 80, DeOt. 064-6
X-4700

ITEM NO.	PART NO.	DESCRIPTION (INCLUDING SERIAL NO., CONTROL PT, ETC)	UNIT OF MEAS.	QUANTITY	VALUE
1	N/A	MMC SLV 561 Adhesive, Part A, Lot BC312	Gal	1	
2	N/A	Part B, Lot BC312	Pt	1	

SHIP REQUESTED BY D. A. Thomas	PHONE 2979	MAR I-1631	QUALITY APPROVAL OF ITEMS <i>[Signature]</i>	AUTHORIZED BY J. L. Mascarenas	PHONE 5271
DATE RECEIVED 8-16-72	CHECKED BY 59272	CHARGE TO BUOLD & SHIP ACCT NO. 204460-03890-00003	QUALITY APPROVAL FOR SHIPMENT <i>[Signature]</i>	PACKAGES 1	GROSS WT 7#
QUALITY APPROVAL FOR SHIPMENT <i>[Signature]</i>			DATE SHIPPED 8/16/72	BOX SIZE 12x10x8	PACKED BY 52989
				B/L OR MANIFEST 4-2-15-04	

REQUEST/PACKING SHEET
FORM DEN 614/80 (3.64)

10 February 1972	CHARGE TO BUILD ACCT NO. 204460-03890-00001	SHIPPING REGISTER NO. 72-03362	CONTRACT NO. SHIPPED FROM N/A
SHIPPING DOCUMENT, 250 FOR DELIVERABLE ITEM)	DIRECTIVE DOCUMENT IF ANY Customer Request	PRIORITY	SHEET 1 OF 1
	PURCHASE ORDER NO. FOR SHIP TO SUBCONTRACTOR PR No. 525157	MATERIAL PROPERTY CONTROL NO. N/A	
PACKING SHEET 15-1149 FOR GOVERNMENT-OWNED ITEM)	CREDIT VOUCHER NO. FOR DD1149 N/A	EXPLOSIVE OR HAZARDOUS SHIP CLASS Red Label	
	AUTHORITY FOR DD1149 N/A	SAFETY APPROVAL See General Dynamics	
STATION CHARGE LECT <input type="checkbox"/> PREPAID	SHIP VIA <input checked="" type="checkbox"/> TRUCK	COMMERCIAL AIR XX	OTHER, EXPLAIN

INCLUDE MARKINGS, CONTRACT NO. BEING SHIPPED TO, AFN ACCT'BLE OFFICE AS APPLICABLE

General Dynamics
Convair Aerospace Division
Fortworth Operations
Fortworth, Texas

Attn: K. L. Brooks

PART NO.	DESCRIPTION (INCLUDING SERIAL NO., CONTROL PT, ETC)	UNIT OF MEAS.	QUANTITY	VALUE
N/A	MMC SLV 561 Adhesive, Part A, Lot 304 305 306	Gal	3	
N/A	Part B, Lot 304 305 306	Pt	3	

INT REQUESTED BY D. A. Thomas	PHONE 2979	MAIL H631	QUALITY APPROVAL OF ITEMS N/A	AUTHORIZED BY D.A. Thomas	PHONE 8979
RECEIVED	CHECKED BY 1-72 04003	CHARGE TO PACK & SHIP ACCT NO. 204460-03500-00001	QUALITY APPROVAL FOR PACKAGING 2/11/72	PACKAGES 3	GROSS WT 33
SAFETY APPROVAL FOR SHIPMENT 2/11/72		AIR FORCE Q.C. N/A	DATE SHIPPED 2-12-72	SHIPPED VIA Manifest	BOX SIZE 12x8x8
				PACKED BY 4127	B/L OR MANIFEST 002 Rev 0446-2916

MATERIAL CERTIFICATION

DATE June 28, 1972

General Dynamics

Ft. Worth, Texas

SUBJECT YOUR ORDER # 542689

FOR MATERIAL RTV 560 Gallon

OUR BATCH # BB619

DATE OF MFG. 6-21-72

SHELF LIFE Six months

Gentlemen:

The material supplied on your order as indicated above, was made in accordance with General Electric Company procedures. A final sample taken from this batch was tested, obtaining test results which meet General Electric Silicone Products Department control specifications.

Regards,

LAWRENCE ELECTRONIC COMPANY

M. H. Bonte

LAWRENCE ELECTRONIC COMPANY
P.O. Box 1038
921 North Bowser Road
Richardson, Texas 75080
Telephone: 235-5606

Dow Corning CORPORATION



ENGINEERING PRODUCTS DIVISION

ELIZABETHTOWN PLANT • ELIZABETHTOWN, KENTUCKY 42701

CERTIFICATE OF COMPLIANCE

SHIPPED TO

**General Dynamics Corporation
Convair Aerospace Division
Benbrook, Texas 76126**

DATE 2/17/72

cc: **Purchasing Department**

CUSTOMER P. O. NO. 52 6639	DOW CORNING INV. NO. DA794520E1	CUSTOMER SPECIFICATION None
PRODUCT	LOT NUMBER	QUANTITY
DOW CORNING® 93-046 aerospace sealant	203136	4 x 10 lb.
DOW CORNING® 93-046 catalyst	201136	

Extrusion Rate, Gms/Min	30
Tack Free Time	5 1/2 Hrs.
Snap Time	4 Hrs.
Cure Time 7 Days/RT	
Specific Gravity	1.09
Durometer	34
Tensile, psi	440
Elongation, %	580

Mfg. Date - February, 1972
Shelf Life-3 Months from Receipt
Store Below 90F.

It is hereby certified that the articles listed above comply with all applicable specification requirements. Test reports are on file-subject to examination.

DOW CORNING CORPORATION

NOTARY *Michael C. Adams*
MY COMMISSION EXPIRES

James C. ...
INSPECTOR, QUALITY CONTROL

12/4/74 187

DOW CORNING

REGMATEDDA

SHIP TO

D.C. ORDER NO. → DAB17437E1

CUSTOMER ORDER NO.

076922

3094324
GENERAL DYNAMICS CORP
CONVAIR AEROSPACE DIV
BENBROOK, TX 76126
!

CERTIFICATE OF COMPLIANCE

IT IS HEREBY CERTIFIED THAT THE ARTICLES LISTED BELOW COMPLY WITH ALL APPLICABLE SPECIFICATION REQUIREMENTS.

TEST REPORTS ARE ON FILE SUBJECT TO EXAMINATION.

BY *A. B. Lewis*

A. B. LEWIS
MANAGER, CORPORATE QUALITY CONTROL

QUANTITY	CONTAINER SIZE	PRODUCT DESCRIPTION			DOW CORNING LOT NO.	FREIGHT CLASS	WARNING CODE
000001	10 LB	7786917	93-046 SEALANT	15	103231		
	EA	0001102	HANDLING CHARGE				

FRIGHT RECEIVED
THE UNDERSIGNED HAS RECEIVED THE ABOVE DESCRIBED GOODS AND IS SATISFIED WITH THE SAME.

R. G. Vansumeren
R. G. VANSUMEREN

SEND ALL INQUIRIES REGARDING THIS SHIPMENT TO:
YOUR NEAREST DOW CORNING CUSTOMER SERVICE CENTER

OR TO:

DOW CORNING CORPORATION
P.O. BOX 1592
MIDLAND, MICHIGAN 48640, U.S.A.

INT NO.	PACKED BY	DATE	CHECKED BY	DATE		
9122230	<i>F.V.</i>	4/25/72				
CONTAINERS						
10						
GROSS WEIGHT						
14#						

DC 300/R-10-70

3 188
PACKING SLIP

A P P E N D I X I I

SUMMARY OF REGRESSION ANALYSIS AND TOLERANCE LIMIT TECHNIQUES USED IN DATA REDUCTION

The methods of regression analysis and tolerance limits used in data reduction of both flatwise tensile and single overlap shear results are well documented in the literature. The purpose of this appendix is to summarize the methods and the equations used in calculating statistical parameters and coefficients for convenient reference.

Regression Analysis

Application of regression analysis requires the assumption of a mathematical relationship between the variables being studied. In this case, the variables were stress versus strain and strength versus temperature. The best-fitting mathematical models for all analyses performed for the data on this program were forms that could be transformed to linear relationships; hence, the special case of multiple regression analyses, i.e. linear regression analysis, was used for all the data reduction that provided design allowables.

Mathematical Models

Three math models were used to represent stress-strain data. The models are

$$\epsilon = A \sigma^B \quad (1)$$

$$\epsilon = A e^{B \sigma} \quad (2)$$

$$\text{and } e^\epsilon = A \sigma^B \quad (3)$$

where ϵ = strain, in./in.

σ = stress, psi

A, B = constants.

The three models were transformed to the linear forms used for regression

$$\ln \epsilon = \ln A + B \ln \sigma \quad (4)$$

$$\ln \epsilon = \ln A + B \sigma \quad (5)$$

$$\text{and } \epsilon = \ln A + B \ln \sigma. \quad (6)$$

The strength-temperature data was found to be represented by a single math model, i.e.

$$\sigma = Ae^{BT} \quad (7)$$

where σ = strength, psi

T = absolute temperature, degrees R

A, B = constants.

It was generally necessary to determine a best-fitting form of Model (7) for strength-temperature data below the glass-transition temperature and a different best-fitting form of Model (7) for data above the glass-transition temperature. The linear form of Model (7) was used for regression analysis, i.e.

$$\ln \sigma = \ln A + BT. \quad (8)$$

Best-Fitting Equation

The math models selected for analysis are each of the form

$$\tilde{y}_i = \alpha + \beta x_i. \quad (9)$$

The best-fitting equation to the test data is determined by minimizing the sum of the squares of the differences between the model (\tilde{y}_i) and the data set (y_i) to obtain estimates of the constants α and β . The procedure is outlined briefly as follows.

$$\text{Let } Q = \sum_i^n (y_i - \tilde{y}_i)^2 = \sum_i^n (y_i - \alpha - \beta x_i)^2 \quad (10)$$

Minimizing Q by

$$\frac{\partial Q}{\partial \alpha} = 0 \text{ and } \frac{\partial Q}{\partial \beta} = 0 \text{ gives two equations}$$

$$\begin{bmatrix} n & \sum X_i \\ \sum X_i & \sum X_i^2 \end{bmatrix} \begin{bmatrix} \alpha \\ \beta \end{bmatrix} = \begin{bmatrix} \sum Y_i \\ \sum Y_i X_i \end{bmatrix} \quad (11)$$

which may be solved to give α and β

$$\begin{bmatrix} \alpha \\ \beta \end{bmatrix} = \begin{bmatrix} C \end{bmatrix} \begin{bmatrix} \Sigma Y_i \\ \Sigma Y_i X_i \end{bmatrix} \quad (12)$$

$$\text{where } \begin{bmatrix} C \end{bmatrix} = \begin{bmatrix} n & \Sigma X_i \\ \Sigma X_i & \Sigma X_i^2 \end{bmatrix}^{-1}$$

The general equations above are applicable to the four models presented in the previous discussion, Equations (4) through (6) and Equation (8), and they may be used by direct substitution. For example, in solving for Equation (8), Equation (12) is re-written to give

$$\begin{bmatrix} \ln A \\ B \end{bmatrix} = \begin{bmatrix} C \end{bmatrix} \begin{bmatrix} \Sigma \ln \sigma_i \\ \Sigma T_i \ln \sigma_i \end{bmatrix} \quad (13)$$

$$\text{where } \begin{bmatrix} C \end{bmatrix} = \begin{bmatrix} n & \Sigma T_i \\ \Sigma T_i & \Sigma T_i^2 \end{bmatrix}^{-1}$$

Confidence Limits

The estimated standard deviation between the best-fitting equation and the data is given by

$$S_{y.x} = \left[\frac{\Sigma (Y_i - \tilde{Y}_i)^2}{u} \right]^{1/2} \quad (14)$$

where $u = \text{degrees of freedom} = (n-3)$
in this case.

(Note that the units of $S_{y.x}$ are identical to the units of Y_i .)

The confidence limits are determined from

$$\begin{matrix} Y_{\text{upper}} \\ \text{lower} \end{matrix} = \tilde{Y} \pm (t_{u, .95} S_{y.x} U_x) \quad (15)$$

where

$$U_x = \begin{bmatrix} 1 & X_i \end{bmatrix} \begin{bmatrix} C \end{bmatrix} \begin{bmatrix} 1 \\ X_i \end{bmatrix} \quad (16)$$

$t_u, .95$ = 95-percentile of the statistical t-distribution.

Correlation Coefficient

Regression analyses that are performed on finite sample sizes result in estimates of the parameters of the mathematical model selected as the "best-fitting" relationship between the variables. In the limiting case, variables can be classified as being either "independent" or "nonindependent," but for finite estimates a measure of the "degree of correlation" between variables is necessary. A quantity designated as a "correlation coefficient" has been defined by statisticians to permit comparing the results of a correlation of variables based on a finite sample to the limiting cases.

The correlation coefficient (for two random variables) is defined by

$$\rho_{yx} = \frac{\text{covariance } (X, y)}{\sigma_x \sigma_y} = \frac{\sigma_{yx}}{\sigma_x \sigma_y} \quad (17)$$

where x, y are random variables

σ_x is standard deviation of x

σ_y is standard deviation of y .

The values of the correlation coefficient for the cases of "nonindependent" and "independent" variables are ± 1 and 0, respectively.

In application, a sample correlation coefficient is calculated; this coefficient is an estimate of the population coefficient defined by Equation (17). The sample correlation coefficient for the linear model is given by

$$r_{yx} = \frac{n \sum(Y_i X_i) - \sum Y_i \sum X_i}{n^2 S_y S_x} \quad (18)$$

where S_y = estimate of standard deviation of Y_i data

S_x = estimate of standard deviation of X_i data.

Confidence limits may be determined for values of r_{xy} by using a transformation equation

$$z = \frac{1}{2} \ln \frac{1+r}{1-r} = \tanh^{-1}(r) \quad (19)$$

The 95-percent confidence limits for z are calculated by

$$\begin{matrix} Z \text{ upper} \\ Z \text{ lower} \end{matrix} = Z \pm \frac{t_{u, .95}}{\sqrt{n-3}} \quad (20)$$

and then retransformed to give

$$\begin{matrix} r \text{ upper} \\ r \text{ lower} \end{matrix} = \tanh \begin{Bmatrix} Z \text{ upper} \\ Z \text{ lower} \end{Bmatrix} \quad (21)$$

Values of r may approach the limiting values of ρ . In general, values of $r > 0.9$ indicate good correlation. A plot of data pairs for which r is as low as 0.7 generally shows little visual relationship between variables.

One-Sided Tolerance Limits

Equation (15) gives a lower bound on "typical" values based on a 95-percent confidence level that the regression equation adequately represents the true equation. Design allowables for strength versus temperature are reduced values based on the lower confidence limit determined by Equation (15). The reduction is obtained in a manner analogous to the method used to determine A- and B-basis allowables as defined in MIL-HDBK-5A. The variation in this case is to use the statistical t-distribution percentil points rather than the so called "K-factors" used for A and B allowables. Equations (23) are used for calculation of allowables.

$$\begin{aligned} B' - \text{allowable} &= Y_{\text{lower}} - t_{u, .90} \left(\text{Sy.x} \right) \\ A' - \text{allowable} &= Y_{\text{lower}} - t_{u, .99} \left(\text{Sy.x} \right) \end{aligned} \quad (23)$$

The terms in Equation (23) have been defined previously.

A P P E N D I X I I I

COMPILATION OF STRESS-STRAIN CALCULATIONS

Stress-strain calculations based on discrete values read from continuous load deflection curves taken for specimens loaded in flatwise tension and overlap shear are summarized in this appendix. Tensile stress-strain data is included in Tables LI through LIX. Shear stress-strain data is included in Tables LX through LXVIII. In each of the tables the values of ultimate strength and strain are shown as the highest load level.

Table L11 TENSILE STRESS-STRAIN RESULTS, -200°F

Material	Specimen Number	Glue Line Thickness (Inch)	Property (1)	Load Level										Average Ultimate Strength	Average Ultimate Strain			
				#1	#2	#3	#4	#5	#6	Ultimate								
RTV-560	1	0.084	Stress	250	500	750	1,000	1,500	1,750									
			Strain	0.219	0.303	0.354	0.393	0.456	0.480									
	2	0.064	Stress	250	500	750	1,000	1,500	1,750									
			Strain	0.260	0.302	0.374	0.433	0.524	0.564	0.598								
	3	0.070	Stress	250	500	750	1,000											
			Strain	0.216	0.328	0.407	0.472											
	SIA-561	1	0.066	Stress	200	500	1,000	2,000	3,000	4,000								
				Strain	0.134	0.307	0.407	0.545	0.557	0.566	0.580							
		2	0.066	Stress	200	500	1,000	2,000	3,000									
Strain				0.134	0.257	0.409	0.648	0.818	0.849									
3		0.067	Stress	200	500	1,000	2,000	3,000	4,000									
			Strain	0.143	0.224	0.291	0.347	0.360	0.363	0.329(2)								
DC 93-046	1	0.080	Stress	250	500	1,000	1,500	1,750	2,000									
			Strain	0.171	0.255	0.356	0.420	0.450	0.472	0.529								
	2	0.072	Stress	250	500	1,000	1,500	1,750	2,000									
			Strain	0.079	0.141	0.230	0.291	0.315	0.340	0.445								
	3	0.090	Stress	250	500	1,000	1,500	1,750	2,000									
			Strain	0.065	0.128	0.203	0.256	0.278	0.298	0.319								
RTV 560/RL1973	1	0.080	Stress	50	100	200	400	600										
			Strain	0.227	0.270	0.304	0.351	0.433	0.465									
	2	0.084	Stress	50	100	200	400	600										
			Strain	0.316	0.370	0.432	0.498	0.543	0.601									
	3	0.087	Stress	50	100	200	400	600										
			Strain	0.255	0.293	0.340	0.415	0.491	0.516									

Note: (1) Values of stress in psi units; strain in in/in units
 (2) Data includes decrease in strain for corresponding increase in stress.

Table LIV TENSILE STRESS-STRAIN RESULTS, -150°F

Material	Specimen Number	Glueline Thickness (Inch)	Property (1)	Load Level										Average Ultimate Strength	Average Ultimate Strain
				#1	#2	#3	#4	#5	#6	Ultimate					
RTV-560	1	0.070	Stress	50	100	200	300	400	500	670					
			Strain	0.095	0.147	0.233	0.310	0.508	0.897	1.55					
			Stress	50	100	200	300	400	500	510					
	2	0.074	Stress	50	100	200	300	400	500	556					
				Strain	0.190	0.154	0.213	0.259	0.305	0.364			0.381		
				Stress	50	100	200	300	400	500			556		
	3	0.078	Stress	50	100	200	300	400	500	556					
				Strain	0.175	0.265	0.383	0.501	0.646	1.50			2.14		
				Stress	20	50	100	150	200	296			1.36		
SIA-561	0.062	Stress	0.081	0.138	0.196	0.271	0.288	0.535							
			Strain	20	50	100	150	200			300	410			
			Stress	0.139	0.181	0.215	0.237	0.264			0.312	0.385			
DC 93-046	0.062	Stress	20	50	100	150	200	300	364						
			Strain	0.118	0.183	0.236	0.271	0.307	0.360			0.470			
			Stress	250	500	1,000	1,500	1,750	2,000			2,040			
RTV 560/RL1973	0.080	Stress	0.118	0.178	0.253	0.304	0.329	0.351	0.369						
			Strain	250	500	800						940			
			Stress	0.237	0.336	0.408						0.446			
RTV 560/RL1973	0.079	Stress	250	500	1,000	1,500			1,560						
			Strain	0.206	0.277	0.358	0.413					0.428			
			Stress	25	50	100	150	200	250			291			
RTV 560/RL1973	0.080	Stress	0.208	0.262	0.371	0.554	0.800	1.036	1.272						
			Strain	25	50	100	150	200	250			270			
			Stress	0.240	0.296	0.428	0.649	0.885	1.134			1.287			
RTV 560/RL1973	0.082	Stress	25	50	100	150	200	250	283						
			Strain	0.214	0.258	0.355	0.527	0.761	0.988			1.175			
			Stress	281	1,513	0.432	0.463	0.432	0.432			0.432			

Note: (1) Values of stress in psi units; strain in in/in units

Table LV TENSILE STRESS-STRAIN RESULTS, -65°F

Material	Specimen Number	Glue-line Thickness (Inch)	Property (1)	Load Level							Average Ultimate Strength	Average Ultimate Strain		
				#1	#2	#3	#4	#5	#6	Ultimate				
RTV-560	1	0.074	Stress	20	50	100	150	200	300	388	387	0.563		
			Strain	0.057	0.119	0.180	0.225	0.266	0.356	0.581				
	2	0.074	Stress	20	50	100	150	200	300	358				
			Strain	0.072	0.138	0.195	0.234	0.272	0.358	0.537				
	3	0.078	Stress	20	50	100	150	200	300	415				
			Strain	0.077	0.139	0.200	0.236	0.273	0.357	0.570				
	SIA-561	1	0.060	Stress	20	50	100	150	200	245			232	0.325
				Strain	0.116	0.162	0.203	0.242	0.282	0.398				
		2	0.080	Stress	20	50	100	150	200	226				
Strain				0.087	0.114	0.144	0.165	0.214	0.266					
3		0.066	Stress	20	50	100	150	200	224					
			Strain	0.064	0.104	0.152	0.180	0.248	0.312					
DC 93-046		1	0.072	Stress	50	100	150	200	300	420	164	1.42(2)		
				Strain	0.148	0.257	0.439	0.828	1.31	1.80				
		2	0.070	Stress	50	100	150	200	248					
	Strain			0.141	0.261	0.616	1.24	1.71	1.71					
	3	0.081	Stress	(Stress-strain curve not obtained)									110	
			Strain	(Stress-strain curve not obtained)									-	
	RTV 560/RL1973	1	0.080	Stress	25	50	100	150	159	164			1.42(2)	
				Strain	0.381	0.583	0.964	1.30	1.416					
		2	0.081	Stress	(Stress-strain curve not obtained)									171
Strain	(Stress-strain curve not obtained)							-						
3	0.079	Stress	25	50	100	150	161	164	1.42(2)					
		Strain	0.401	0.600	0.976	1.316	1.428							

Note: (1) Values of stress in psi units; strain in in/in units
 (2) Average of two tests.

Table LVII TENSILE STRESS-STRAIN RESULTS, 3000F

Material	Specimen Number	Glue/line Thickness (Inch)	Property (1)	Load Level						Average Ultimate Strength	Average Ultimate Strain					
				#1	#2	#3	#4	#5	#6			Ultimate				
RTV-560	1	0.080	Stress	10	50	100	150				193	191	0.187			
			Strain	0.017	0.053	0.084	0.112				0.145					
	2	0.076	Stress	10	50	100	150				190					
			Strain	0.065	0.091	0.122	0.153				0.181					
	3	0.066	Stress	10	50	100	150				190					
			Strain	0.076	0.127	0.164	0.197				0.235					
	SLA-561	1	0.071	Stress	20	50	100							121	130	0.253
				Strain	0.142	0.192	0.292							0.299		
		2	0.066	Stress	20	50	100							132		
Strain				0.114	0.150	0.198					0.215					
3		0.064	Stress	20	50	100					138					
			Strain	0.113	0.157	0.216					0.246					
DC 93-046		1	0.066	Stress	5	10	30					39	57	1.024		
				Strain	0.090	0.407	0.579					0.622				
		2	0.080	Stress	5	10	30	40	50			60				
	Strain			0.335	0.618	0.706	0.729	0.784			1.24					
	3	0.076	Stress	5	10	30	40	50	60	71						
			Strain	0.088	0.392	0.472	0.512	0.573	0.738	1.21						
	RTV 560/RL1973	1	0.087	Stress	5(2)	10	15	20	30	40	52				48	0.615
				Strain	0.034	0.154	0.192	0.285	0.373	0.469	0.593					
		2	0.083	Stress	5(2)	10	15	20	30	40	53					
Strain				0.072	0.185	0.300	0.340	0.426	0.513	0.646						
3		0.080	Stress	5(2)	10	15	20	30	38							
			Strain	0.085	0.243	0.378	0.420	0.519	0.607							

Note: (1) Values of stress in psi units; strain in in/in units
 (2) Data not used in regression analysis

Table LVIII TENSILE STRESS-STRAIN RESULTS, 350°F

Material	Specimen Number	Glue Line Thickness (Inch)	Property (1)	Load Level											Average Ultimate Strength	Average Ultimate Strain				
				#1	#2	#3	#4	#5	#6	Ultimate										
RTV-560	1	0.080	Stress	10	50	100	150													
			Strain	0.096	0.137	0.171	0.211													
																				184
	2	0.074	Stress	10	50	100	150													
			Strain	0.127	0.189	0.224	0.261													
																				186
	3	0.088	Stress	10	50	100	150													
			Strain	0.044	0.082	0.117	0.148													
																				160
SLA-561	1	0.079	Stress	20	50															
			Strain	0.063	0.097															
																				97
	2	0.068	Stress	20	50	100														
			Strain	0.131	0.168	0.225														
																				107
	3	0.066	Stress	20	50	100														
			Strain	0.076	0.116	0.164														
																				110
DC 93-046	1	0.074	Stress	5	10	15	20	25	30											
			Strain	0.076	0.307	0.356	0.372	0.400	0.472	0.527										
																				32.5
	2	0.068	Stress	5	10	15	20	25	30											
			Strain	0.191	0.319	0.338	0.357	0.372	0.391	0.941										
																				51
	3	0.082	Stress	5	10	15	20	25	30											
			Strain	0.089	0.324	0.379	0.394	0.404	0.420	0.977										
																				73
RTV 560/RL1973	1	0.085	Stress	5(2)	10	15	20	30	40											
			Strain	0.034	0.154	0.192	0.285	0.373	0.469	0.593										
																				52
	2	0.083	Stress	5(2)	10	15	20	30	40											
			Strain	0.072	0.185	0.300	0.340	0.426	0.513	0.646										
																				53
	3	0.084	Stress	5(2)	10	15	20	30	40											
			Strain	0.085	0.243	0.378	0.420	0.519	0.607											
																				38
																		48		

Note: (1) Values of stress in psi units; strain in in/in units
(2) Data not used in regression analysis

TABLE LIX
 ULTIMATE TENSILE STRENGTH AND ELONGATION
 AT 550°F AND 600°F

Test Temperature and Spec. No.	GE RTV-560		DC 93-046		MMC SLA561		RTV-560/RL-1973	
	psi	%E	psi	%E	psi	%E	psi	%E
550°F								
1	33	4	0	0	47	13	14	56
2	16	4	0	0	51	11	16	46
3	29	14	0	0	44	20	14	60
Avg.	26	7	0	0	47	15	15	54
600°F								
1	2	30	0	0	33	25	4	26
2	2	19	0	0	33	14	2	17
3	2	28	0	0	28	22	3	22
Avg.	2	26	0	0	31	20	3	22

Table LX SHEAR STRESS-STRAIN RESULTS, -2700F

Material	Specimen Number	Glue/line Thickness (Inch)	Property (1)	Load Level										Average Ultimate Strength	Average Ultimate Strain
				#1	#2	#3	#4	#5	#6	Ultimate					
RTV-560	1	0.060	Stress	51	102	204	306	408	510	622					
	Strain		.079	0.108	0.129	0.147	0.151	0.144	0.143						
	2	0.060	Stress	(Stress-strain curve not obtained)										345	
SLA-561	3	0.050	Stress	49	98	196	294	392	490	593					
	Strain		0.05	0.055	0.065	0.060	0.046	0.035	0.026						
	1	0.065	Stress	99	198	495	990	1,485					520	0.146(2)	
DC 93-046	2	0.062	Strain	0.026	0.036	0.020	-0.057	-0.127							
	Stress		99	198	495	990	1,485								
	3	0.064	Strain	0.027	0.028	0.004	-0.064	-0.145							
RTV 560/RL1973	1	0.069	Stress	99	198	495	990	1,485							
	Strain		0.026	0.027	0.039	-0.039	-0.129								
	2	0.064	Stress	(Stress-strain curve not obtained)										500	
RTV 560/RL1973	3	0.069	Strain	(Stress-strain curve not obtained)										460	
	Stress		48	97	146	194	388	582	650						
	1	0.060	Strain	0.221	0.252	0.271	0.275	0.284	0.271	0.272					
RTV 560/RL1973	2	0.058	Stress	48	95	143	190	381	571	637					
	Strain		0.056	0.081	0.098	0.1076	0.1144	0.1162	0.110						
	3	0.061	Stress	48	97	146	194	388	485	575					
			Strain	0.223	0.263	0.296	0.320	0.361	0.364	0.370					

Note: (1) Values of stress in psi units; strain in in/in units
 (2) Data includes decreases in strain for corresponding increases in stress

Table LX1 SHEAR STRESS-STRAIN RESULTS, -200°F

Material	Specimen Number	Glue/line Thickness (Inch)	Property (1)	Load Level										Average Ultimate Strength	Average Ultimate Strain					
				#1	#2	#3	#4	#5	#6	Ultimate										
RTV-560	1	0.060	Stress	51	101	202	303	404												
			Strain	0.079	0.111	0.142	0.152	0.165												
	2	0.060	Stress	51	101	202	303	404	505	606										
			Strain	0.065	0.091	0.119	0.130	0.133	0.141	0.132										
	3	0.060	Stress	50	100	200	500	700	900	1,290										
			Strain	0.165	0.215	0.262	0.346	0.351	0.355	0.419										
	SLA-561	1	0.074	Stress	100	200	500	1,000	1,500	2,000	2,200(2)									
				Strain	0.027	0.084	0.074	0.0067	-0.042	0.070	0.591									
		2	0.071	Stress	100	200	500	1,000	1,500	2,000	2,200(2)									
Strain				0.138	0.151	0.151	0.051	0.011	0.141	0.879										
3		0.067	Stress	100	200	500	1,000	1,500	2,000	2,320										
			Strain	0.097	0.104	0.086	0.019	-0.042	0.057	0.876										
1	0.068	Stress	(Stress-strain curve not obtained)										922							
		Strain																		
DC 93-046	2	0.069	Stress	48	97	194	485	680	874	971										
			Strain	0.141	0.159	0.188	0.251	0.220	0.174	0.127										
	3	0.069	Stress	49	98	196	490	686	843											
			Strain	0.080	0.109	0.119	0.145	0.127	0.132											
	1	0.062	Stress	48	95	143	190	381	476	581										
			Strain	0.255	0.297	0.323	0.346	0.369	0.379	0.398										
2	0.063	Stress	48	96	144	192	385	481	580											
		Strain	0.200	0.240	0.255	0.271	0.296	0.295	0.320											
3	0.062	Stress	48	96	144	192	385	481	591											
		Strain	0.259	0.289	0.303	0.312	0.328	0.341	0.394											

Note: (1) Values of stress in psi units; strain in in/in units
 (2) Specimen failed in metal
 (3) Data includes decreases in strain for corresponding increases in stress

Table LXII SHEAR STRESS-STRAIN RESULTS, -175°F

Material	Specimen Number	Glue Line Thickness (Inch)	Property (1)	Load Level										Average Ultimate Strength	Average Ultimate Strain
				#1	#2	#3	#4	#5	#6	Ultimate					
RTV-560	1	0.055	Stress	48	97	194	291	388	485	738					
			Strain	0.250	0.309	0.398	0.472	0.590	0.736	1.27					
	2	0.060	Stress	51	102	204	306	408	510	719					
			Strain	0.172	0.235	0.317	0.390	0.483	0.578	1.00					
	3	0.060	Stress	50	99	198	297	396	495	693					
			Strain	0.087	0.113	0.172	0.238	0.333	0.442	1.01					
	SLA-561	1	0.072	Stress	49	98	196	290	387	483	680	717	1.09		
				Strain	0.076	0.101	0.149	0.206	0.271	0.346	0.421	0.496	0.571		
		2	0.072	Stress	49	98	196	290	387	483	680	717	1.09		
Strain				0.035	0.092	0.149	0.206	0.271	0.346	0.421	0.496	0.571			
3		0.074	Stress	49	98	196	290	387	483	680	717	1.09			
			Strain	0.058	0.1182	0.177	0.235	0.304	0.373	0.442	0.511	0.580			
DC 93-046		1	0.065	Stress	49	98	196	290	387	483	680	717	1.09		
				Strain	0.131	0.130	0.135	0.119	0.095	0.062	0.021				
		2	0.068	Stress	48	97	193	283	373	463	553	643	733	823	913
	Strain			-	-	0.061	0.043	0.023	-0.004	-0.004					
	3	0.069	Stress	50	100	200	300	400	500	600	700	800	900	1,000	
			Strain	0.091	0.116	0.127	0.117	0.098	0.083	0.093					
	RTV 560/RL1973	1	0.060	Stress	49	98	147	196	294	392	490	588	686	784	882
				Strain	0.079	0.138	0.231	0.377	0.654	0.948	1.029				
		2	0.060	Stress	48	97	146	194	291	386	481	576	671	766	861
Strain				0.061	0.105	0.149	0.263	0.660	0.955	1.039					
3		0.062	Stress	48	96	144	192	288	385	480	575	670	765	860	
			Strain	0.159	0.231	0.242	0.290	0.532	0.806	1.095					

Note: (1) Values of stress in psi units; strain in in/in units
(2) Data includes negative values of strain; therefore, no average calculated.

Table LXIII SHEAR STRESS-STRAIN RESULTS, -150°F.

Material	Specimen Number	Glue Line Thickness (Inch)	Property (1)	Load Level									Average Ultimate Strength	Average Ultimate Strain
				#1	#2	#3	#4	#5	#6	Ultimate				
RTV-560	1	0.055	Stress	49	98	196	490	686	882	1,078				
			Strain	0.455	0.702	0.915	1.53	1.81	2.10	2.64				
	2	0.055	Stress	50	100	200	500	700	900	1,190				
			Strain	0.483	0.716	1.03	1.60	1.89	2.34	2.81				
	3	0.055	Stress	49	99	198	495	693	891	1,213				
			Strain	0.455	0.716	1.01	1.58	1.84	2.12	2.69				
	SIA-561	1	0.072	Stress	50	99	198	297			384			
				Strain	0.705	1.163	1.664	1.983			2.38			
		2	0.072	Stress	49	98	196	295			375			
Strain				0.810	1.334	1.92	2.31			2.78				
3		0.072	Stress	49	98	196	294			382				
			Strain	0.824	1.351	1.945	2.36			2.86				
DC 93-046		1	0.063	Stress	49	98	196	490	686	882	1,098			
				Strain	0.018	0.025	0.023	-0.008	-0.040	-0.071	-0.092			
		2	0.060	Stress	50	99	198	495	693	891	1,416			
	Strain			0.029	0.021	0.039	-0.008	-0.037	-0.070	-0.126				
	3	0.066	Stress	49	98	196	491	687	883	1,319		(2)		
			Strain	0.049	0.064	0.083	0.072	0.046	0.018	-0.017				
	RTV 560/RL1973	1	0.065	Stress	49	98	147	196	245	281	281			
				Strain	0.531	0.928	1.211	1.453	1.668	1,856				
		2	0.064	Stress	49	98	147	196	245	285	285			
Strain				0.622	1.066	1.384	1.662	1.898	2.145					
3		0.064	Stress	49	98	147	196	245	271	271				
			Strain	0.623	1.094	1.417	1.703	1.949	2.116					
										1,278		(2)		
											279		2.04	

Note: (1) Values of stress in psi units; strain in in/in units
 (2) Data includes negative values of strain; therefore, no average calculated.

Table LXIV SHEAR STRESS-STRAIN RESULTS, -65°F

Material	Specimen Number	Glueline Thickness (Inch)	Property (1)	Load Level										Average Ultimate Strength	Average Ultimate Strain	
				#1	#2	#3	#4	#5	#6	Ultimate						
RTV-560	1	0.060	Stress	47	94	188	283	377	471	520						
			Strain	0.685	0.993	1.34	1.60	1.82	2.09	2.28						
	2	0.060	Stress	50	99	198	297	396	495	522						
			Strain	0.747	1.07	1.41	1.65	1.86	2.12	2.26						
	3	0.060	Stress	47	93	187	280	373	467	511						
			Strain	0.672	0.983	1.34	1.58	1.83	2.07	2.28						
	SLA-561	1	0.062	Stress	20	50	75				80					
				Strain	0.374	0.911	1.275				1.381					
		2	0.065	Stress	20	49	74				79					
Strain				0.345	0.865	1.239				1.351						
3		0.065	Stress	20	49	74				85						
			Strain	0.345	0.858	1.193				1.419						
DC 93-046		1	0.084	Stress	49	98	196	294	392	491	513					
				Strain	0.940	1.42	1.65	1.78	1.92	2.10	2.18					
		2	0.072	Stress	49	98	196	294	392	490	538					
	Strain			1.19	1.63	1.83	1.96	2.11	2.30	2.49						
	3	0.075	Stress	50	100	199	298	398	498	607						
			Strain	0.569	0.973	1.22	1.36	1.47	1.62	1.91						
	RTV 560/RL1973	1	0.066	Stress	24	49	73	98			140					
				Strain	1.003	1.422	1.704	1.935			2.375					
		2	0.066	Stress	24	49	73	98			140					
Strain				0.964	1.379	1.647	1.877			2.338						
3		0.065	Stress	24	49	73	98			139						
			Strain	0.931	1.347	1.638	1.861			2.336						

Note: (1) Values of stress in psi units; strain in in/in units

Table LXV SHEAR STRESS-STRAIN RESULTS, 80°F

Material	Specimen Number	Glue Line Thickness (Inch)	Property (1)	Load Level											Average Ultimate Strength	Average Ultimate Strain		
				#1	#2	#3	#4	#5	#6	Ultimate								
				Stress	Strain	Stress	Strain	Stress	Strain	Stress	Strain	Stress	Strain	Stress			Strain	
RTV-560	1	0.050	Stress	19	48	95	143	191	238	286								
			Strain	0.449	0.785	1.15	1.39	1.61	1.81	2.06								
	2	0.055	Stress	20	50	100	150	200	250	270								
			Strain	0.612	0.921	1.29	1.53	1.73	1.93	2.04								
	3	0.060	Stress	19	47	94	142	189	236	288								
			Strain	0.249	0.570	0.863	1.07	1.25	1.39	1.67	281							1.92
	SLA-561	1	0.064	Stress	19	47												
				Strain	0.264	0.803												
		2	0.064	Stress	20	50												
Strain				0.323	0.824													0.976
3		0.063	Stress	20	50													
			Strain	0.356	0.878													53
DC 93-046		1	0.081	Stress	(Stress-strain curve not obtained)											175		
				Strain														
		2	0.083	Stress	20	51	102	152										
	Strain			0.514	1.304	2.316	3.13											
	3	0.072	Stress	20	50	101	151											
			Strain	0.437	1.116	2.013	2.78											186
	RTV 560/RL1973	1	0.064	Stress	10	19	29	38	48	67	93							
				Strain	0.462	0.757	0.981	1.17	1.33	1.64	2.06							
		2	0.065	Stress	10	20	30	40	50	70	87							
Strain				0.505	0.833	1.06	1.25	1.416	1.713	2.09								
3		0.065	Stress	11	21	32	42	53	74	91								
			Strain	0.508	0.812	1.032	1.21	1.37	1.761	2.05								90

Note: (1) Values of stress in psi units; strain in in/in units
 (2) Average of two specimens

Table LXVI SHEAR STRESS-STRAIN RESULTS, 300°F

Material	Specimen Number	Glue Line Thickness (Inch)	Property (1)	Load Level										Average Ultimate Strength	Average Ultimate Strain					
				#1	#2	#3	#4	#5	#6	Ultimate										
RTV-560	1	0.055	Stress	25	50	76														
			Strain	0.281	0.485	0.666								101						
	2	0.050	Stress	25	50	76														
			Strain	0.40	0.629	0.839														
	3	0.060	Stress	25	50	75	100													
			Strain	0.320	0.517	0.688	0.871													
SIA-561	1	0.066	Stress	20	49															
			Strain	0.488	0.954															
	2	0.068	Stress	20	50															
			Strain	0.352	0.747															
	3	0.066	Stress	20	50															
			Strain	0.590	0.981															
DC 93-046	1	0.067	Stress	20	49	74														
			Strain	0.689	1.71	2.47														
	2	0.076	Stress	19	49	73														
			Strain	0.582	1.60	2.35														
	3	0.078	Stress	19	49	68														
			Strain	0.965	2.21	3.09														
RTV 560/RL1973	1	0.061	Stress	5	11	16	21	32	42											
			Strain	0.026	0.407	0.587	0.747	1.008	1.25	1.372										
	2	0.061	Stress	5	11	16	21	32	42											
			Strain	0.222	0.557	0.723	0.873	1.13	1.41	1.50										
	3	0.062	Stress	5	10	15	20	31	41											
			Strain	0.282	0.590	0.745	0.882	1.15	1.37	1.57										

Note: (1) Values of stress in psi units; strain in in/in units

Table LXVII SHEAR STRESS-STRAIN RESULTS, 350°F

Material	Specimen Number	Glue Line Thickness (Inch)	Property (1)	Load Level						Average Ultimate Strength	Average Ultimate Strain	
				#1	#2	#3	#4	#5	#6			Ultimate
RTV-560	1	0.060	Stress	25	50	75	100				120	
			Strain	0.28	0.479	0.662	0.853					1.00
	2	0.060	Stress	25	50	76	101				121	
			Strain	0.275	0.482	0.695	0.888					1.04
	3	0.060	Stress	25	50	76	101				126	
			Strain	0.161	0.389	0.572	0.755					0.970
	SLA-561	1	0.068	Stress	20	39						50
				Strain	0.427	0.693						0.872
		2	0.069	Stress	20	40						49
			Strain	0.445	0.712						0.841	
DC 93-046	3	0.069	Stress	20	40						51	
			Strain	0.491	0.742							0.940
	1	0.082	Stress	20	51						53	
			Strain	0.819	2.35						2.83	
RTV 560/RL1973	2	0.081	Stress	20	51						64	
			Strain	0.675	1.90							2.56
	3	0.079	Stress	20	49						54	
			Strain	0.911	2.42						2.72	
RTV 560/RL1973	1	0.062	Stress	5(2)	10	15	20	31			41	
			Strain	0.239	0.586	0.747	0.887	1.127				1.402
	2	0.069	Stress	5(2)	10	14	19	29			38	
			Strain	0.243	0.581	0.728	0.853	1.061				1.327
	3	0.065	Stress	5(2)	10	14	19	29			38	
			Strain	0.328	0.677	0.830	0.960	1.182				1.494
										41		
										57		
										50		
										0.884		

Note: (1) Values of stress in psi units; strain in in/in units
(2) Not included in regression analysis

TABLE LXVIII
 SINGLE OVERLAP SHEAR STRENGTH
 AT 550°F AND 600°F

Test Temp., & Spec. No.	GE RTV-560		DC 93-046		MMC SLA 561		RTV-560/RL-1973	
	psi	% Coh. Failure	psi	% Coh. Failure	psi	% Coh. Failure	psi	% Coh. Failure
550°F	20	100			22	100	4.3	100
	23	100	Deteriorated		26	100	4.4	100
	22	100			19	100	4.3	100
	22	100			22	100	4.3	100
600°F	8	100			18	100		
	12	100	Deteriorated		10	100		
	5	100			15	100		
	8	100			14	100	Not Tested	

A P P E N D I X I V

SUMMARY OF STRAIN CONFIDENCE LIMITS FOR BEST FITTING REGRESSION EQUATION TO STRESS-STRAIN DATA

The strain confidence limits for discrete values of stress corresponding to the best-fitting equation to stress-strain data for each material and test condition are summarized in this Appendix. Flatwise tensile strain confidence limits are given in Tables LXIX through LXXVI. Over lap shear strain confidence limits are given in Tables LXXVII through LXXXIV.

Table LXIX SUMMARY OF TENSILE STRAIN CONFIDENCE LIMITS AT -270°F

Material	Property	Load Levels						Math Model (4)
		#1	#2	#3	#4	#5	#6	
RTV-560	σ	250	500	750	1,000	1,500	1,750	(a)
	$\bar{\epsilon}$	0.167	0.246	0.308	0.362	0.454	0.495	
	ϵ upper	0.188	0.266	0.328	0.386	0.492	0.541	
	ϵ lower	0.146	0.226	0.288	0.338	0.416	0.449	
SIA-561	σ	(5)						
	ϵ upper							
	ϵ lower							
DC 93-046	σ	250	500	1,000	1,500	1,750	2,000	(a)
	$\bar{\epsilon}$	0.080	0.139	0.242	0.334	0.378	0.420	
	ϵ upper	0.102	0.165	0.276	0.389	0.444	0.500	
	ϵ lower	0.058	0.113	0.207	0.280	0.311	0.340	
RTV-560/RL-1973	σ	50	100	200	400	600	800	(a)
	$\bar{\epsilon}$	0.200	0.241	0.290	0.349	0.389	0.421	
	ϵ upper	0.273	0.309	0.353	0.424	0.485	0.537	
	ϵ lower	0.126	0.172	0.227	0.274	0.294	0.305	

Notes:

- (1) σ = stress, psi
- (2) $\bar{\epsilon}$ = strain, in./in.
- (3) $\bar{\epsilon}$ upper, lower = 95-percent confidence limits
- (4) Math models for regression analysis:
 - (a) $\ln \bar{\epsilon} = \ln A + B \ln \sigma$
 - (b) $\bar{\epsilon} = \ln A + B \ln \sigma$
 - (c) $\ln \bar{\epsilon} = \ln A + B\sigma$
- (5) Regression analysis not conducted

Table LXX SUMMARY OF TENSILE STRAIN CONFIDENCE LIMITS AT -200°F

Material	Property	Load Levels						Math Model (4)
		#1	#2	#3	#4	#5	#6	
RTV-560	σ	250	500	750	1,000	1,500	1,750	1,900
	$\bar{\epsilon}$	0.205	0.321	0.388	0.436	0.504	0.529	0.543
	ϵ upper ϵ lower	0.241 0.169	0.343 0.299	0.406 0.371	0.454 0.418	0.527 0.480	0.556 0.503	0.571 0.515
SLA-561	σ	(5)						
	$\bar{\epsilon}$							
	ϵ upper ϵ lower							
DC 93-046	σ	250	500	1,000	1,500	1,750	2,000	2,500
	$\bar{\epsilon}$	0.103	0.158	0.242	0.312	0.343	0.372	0.428
	ϵ upper ϵ lower	0.127 0.078	0.184 0.131	0.272 0.213	0.353 0.271	0.391 0.294	0.429 0.316	0.502 0.353
RTV-560/RL-1973	σ	50	100	200	400	600	800	
	$\bar{\epsilon}$	0.257	0.307	0.367	0.439	0.487	0.524	
	ϵ upper ϵ lower	0.290 0.224	0.336 0.279	0.393 0.341	0.470 0.403	0.534 0.439	0.583 0.465	

Notes:

- (1) σ = stress, psi
- (2) $\bar{\epsilon}$ = strain, in./in.
- (3) ϵ upper, lower = 95-percent confidence limits
- (4) Math models for regression analysis:
 - (a) $\ln \bar{\epsilon} = \ln A + B \ln \sigma$
 - (b) $\bar{\epsilon} = \ln A + B \ln \sigma$
 - (c) $\ln \bar{\epsilon} = \ln A + B \sigma$
- (5) Regression analysis not conducted.

Table LXXI SUMMARY OF TENSILE STRAIN CONFIDENCE LIMITS AT -175°F

Material	Property	Load Levels						Match Model (4)
		#1	#2	#3	#4	#5	#6	
RTV-560	σ	100	300	400	500	700	900	1.000
	$\bar{\epsilon}$	0.106	0.218	0.247	0.270	0.304	0.329	0.340
	ϵ upper	0.170	0.250	0.276	0.298	0.337	0.368	0.382
	ϵ lower	0.414	0.185	0.218	0.241	0.271	0.291	0.299
SLA-561	σ	(5)						
	$\bar{\epsilon}$							
	ϵ upper							
	ϵ lower							
DC 93-046	σ	250	500	1,000	1,500	1,750	2,000	2,500
	$\bar{\epsilon}$	0.131	0.192	0.280	0.350	0.381	0.410	0.463
	ϵ upper	0.154	0.214	0.304	0.382	0.418	0.453	0.519
	ϵ lower	0.109	0.170	0.257	0.318	0.344	0.366	0.407
RTV-560/RL-1973	σ	50	100	150	200	250	300	400
	$\bar{\epsilon}$	0.263	0.308	0.360	0.421	0.492	0.575	0.785
	ϵ upper	0.289	0.333	0.385	0.451	0.532	0.631	0.895
	ϵ lower	0.238	0.283	0.334	0.391	0.452	0.518	0.676

Notes:

- (1) σ = stress, psi
- (2) $\bar{\epsilon}$ = strain, in./in.
- (3) $\bar{\epsilon}$ upper, lower = 95-percent confidence limits
- (4) Math models for regression analysis:
 - (a) $\ln \bar{\epsilon} = \ln A + B \ln \sigma$
 - (b) $\bar{\epsilon} = \ln A + B \ln \sigma$
 - (c) $\ln \bar{\epsilon} = \ln A + B \sigma$
- (5) Regression analysis not conducted.

Table LXXII SUMMARY OF TENSILE STRAIN CONFIDENCE LIMITS AT -150°F

Material	Property	Load Levels								Math Model (4)
		#1	#2	#3	#4	#5	#6			
RTV-560	σ	50	100	200	300	400	500	650	(a)	
	ξ	0.101	0.180	0.321	0.450	0.572	0.689	0.857		
	ϵ upper lower	0.140 0.063	0.230 0.130	0.388 0.254	0.546 0.354	0.709 0.434	0.874 0.503	1.12 0.594		
SLA-561	σ	20	50	100	150	200	300	400	(a)	
	ξ	0.108	0.163	0.223	0.268	0.306	0.367	0.418		
	ϵ upper lower	0.124 0.092	0.179 0.147	0.240 0.206	0.290 0.247	0.332 0.279	0.406 0.328	0.469 0.367		
DC 93-046	σ	250	500	1,000	1,500	1,750	2,000	(a)		
	ξ	0.195	0.249	0.318	0.367	0.387	0.406			
	ϵ upper lower	0.242 0.149	0.289 0.210	0.362 0.274	0.429 0.304	0.460 0.314	0.488 0.323			
RTV-560/RL-1973	σ	50	100	150	200	250	300	(c)		
	ξ	0.273	0.384	0.540	0.760	1.07	1.50			
	ϵ upper lower	0.290 0.257	0.402 0.366	0.563 0.518	0.795 0.724	1.13 1.00	1.62 1.38			

Notes:

- (1) σ = stress, psi
- (2) ξ = strain, in./in.
- (3) ϵ upper, lower = 95-percent confidence limits
- (4) Math models for regression analysis:
 - (a) $\ln \xi = \ln A + B \ln \sigma$
 - (b) $\xi = \ln A + B \ln \sigma$
 - (c) $\ln \xi = \ln A + B \sigma$

Table LXXIII SUMMARY OF TENSILE STRAIN CONFIDENCE LIMITS AT -65°F

Material	Property	Load Levels						Math Model (4)
		#1	#2	#3	#4	#5	#6	
RTV-560	σ	20	50	100	150	200	300	400
	$\bar{\epsilon}$	0.067	0.122	0.191	0.248	0.299	0.389	0.469
	ϵ upper lower	0.075 0.060	0.131 0.113	0.202 0.180	0.262 0.234	0.318 0.280	0.419 0.359	0.511 0.427
SLA-561	σ	20	50	100	150	200	245	
	$\bar{\epsilon}$	0.081	0.128	0.179	0.219	0.252	0.278	
	ϵ upper lower	0.098 0.065	0.143 0.111	0.198 0.161	0.244 0.193	0.286 0.218	0.320 0.237	
DC 93-046	σ	50	100	150	200	300	400	
	$\bar{\epsilon}$	0.132	0.333	0.574	0.843	1.45	2.13	
	ϵ upper lower	0.171 0.092	0.388 0.268	0.671 0.476	1.00 0.687	1.80 1.10	2.75 1.52	
RTV-560/RL-1973	σ	25	50	100	150	200		
	$\bar{\epsilon}$	0.380	0.614	0.992	1.31	1.60		
	ϵ upper lower	0.399 0.360	0.634 0.594	1.02 0.963	1.36 1.26	1.67 1.53		

Notes:

- (1) σ = stress, psi
- (2) $\bar{\epsilon}$ = strain, in./in.
- (3) $\bar{\epsilon}$ upper, lower = 95-percent confidence limits
- (4) Math models for regression analysis:
 - (a) $\ln \bar{\epsilon} = \ln A + B \ln \sigma$
 - (b) $\bar{\epsilon} = \ln A + B \ln \sigma$
 - (c) $\ln \bar{\epsilon} = \ln A + B \sigma$

Table LXXIV SUMMARY OF TENSILE STRAIN CONFIDENCE LIMITS AT 80°F

Material	Property	Load Levels						Math Model (4)
		#1	#2	#3	#4	#5	#6	
RTV-560	σ	20	50	100	150	200	250	280
	$\bar{\epsilon}$	0.058	0.100	0.151	0.192	0.228	0.260	0.278
	ϵ upper lower	0.064 0.053	0.106 0.094	0.158 0.144	0.201 0.183	0.240 0.216	0.276 0.244	0.296 0.260
SLA-561	σ	20	50	100	120	140		
	$\bar{\epsilon}$	0.038	0.066	0.101	0.113	0.124		
	ϵ upper lower	0.044 0.032	0.072 0.060	0.112 0.090	0.127 0.098	0.141 0.107		
DC 93-046	σ	10	30	40	50	80	90	130
	$\bar{\epsilon}$	0.046	0.370	0.489	0.560	0.710	0.747	0.864
	ϵ upper lower	0.290 -0.198	0.553 0.241	0.647 0.330	0.728 0.391	0.918 0.501	0.968 0.526	1.13 0.599
RTV-560/RL-1973	σ	25	50	75	100	150		
	$\bar{\epsilon}$	0.300	0.542	0.766	0.980	1.38		
	ϵ upper lower	0.318 0.282	0.560 0.524	0.792 0.741	1.02 0.938	1.47 1.30		

Notes:

- (1) σ = stress, psi
- (2) $\bar{\epsilon}$ = strain, in./in.
- (3) $\bar{\epsilon}$ upper, lower = 95-percent confidence limits
- (4) Math models for regression analysis:
 - (a) $\ln \bar{\epsilon} = \ln A + B \ln \sigma$
 - (b) $\bar{\epsilon} = \ln A + B \ln \sigma$
 - (c) $\ln \bar{\epsilon} = \ln A + B\sigma$

Table LXXV SUMMARY OF TENSILE STRAIN CONFIDENCE LIMITS AT 300°F

Material	Property	Load Levels						Math Model (4)
		#1	#2	#3	#4	#5	#6	
RTV-560	σ	10	50	100	200			
	$\tilde{\epsilon}$	0.042	0.090	0.125	0.174			
	ϵ_{upper}	0.059	0.110	0.154	0.225			(a)
	ϵ_{lower}	0.026	0.070	0.097	0.123			
SIA-561	σ	20	50	100	120	140		
	$\tilde{\epsilon}$	0.121	0.174	0.228	0.245	0.260		
	ϵ_{upper}	0.142	0.191	0.254	0.276	0.297		(a)
	ϵ_{lower}	0.101	0.156	0.201	0.213	0.222		
DC 93-046	σ	5	10	30	40	50	60	
	$\tilde{\epsilon}$	0.186	0.289	0.583	0.700	0.807	0.907	
	ϵ_{upper}	0.251	0.365	0.704	0.862	1.01	1.16	(a)
	ϵ_{lower}	0.120	0.213	0.461	0.538	0.601	0.655	
RTV-560/RL-1973	σ	10	15	20	30	40	50	60
	$\tilde{\epsilon}$	0.157	0.216	0.270	0.371	0.464	0.553	0.638
	ϵ_{upper}	0.180	0.238	0.294	0.403	0.514	0.624	0.731
	ϵ_{lower}	0.134	0.193	0.247	0.339	0.415	0.482	0.544

Notes:

- (1) σ = stress, psi
- (2) $\tilde{\epsilon}$ = strain, in./in.
- (3) $\tilde{\epsilon}$ upper, lower = 95-percent confidence limits
- (4) Math models for regression analysis:
 - (a) $\ln \tilde{\epsilon} = \ln A + B \ln \sigma$
 - (b) $\tilde{\epsilon} = \ln A + B \ln \sigma$
 - (c) $\ln \tilde{\epsilon} = \ln A + B\sigma$

Table LXXVI SUMMARY OF TENSILE STRAIN CONFIDENCE LIMITS AT 350°F

Material	Property	Load Levels						Math Model (4)
		#1	#2	#3	#4	#5	#6	
RTV-560	σ	10	50	100	150	185		(a)
	$\bar{\epsilon}$	0.078	0.136	0.173	0.199	0.213		
	ϵ upper	0.104	0.161	0.206	0.243	0.265		
	ϵ lower	0.052	0.111	0.139	0.154	0.162		
SIA-561	σ	20	40	50	100			(a)
	$\bar{\epsilon}$	0.084	0.116	0.129	0.178			
	ϵ upper	0.108	0.138	0.151	0.218			
	ϵ lower	0.060	0.094	0.106	0.138			
DC 93-046	σ	5	10	20	30	50		(a)
	$\bar{\epsilon}$	0.137	0.229	0.381	0.513	0.748		
	ϵ upper	0.168	0.262	0.425	0.585	0.892		
	ϵ lower	0.107	0.196	0.337	0.441	0.603		
RTV-560/RL-1973	σ	10	15	20	30	40	50	(a)
	$\bar{\epsilon}$	0.207	0.271	0.328	0.428	0.517	0.599	
	ϵ upper	0.235	0.297	0.353	0.463	0.571	0.674	
	ϵ lower	0.179	0.245	0.302	0.392	0.464	0.524	

Notes:

- (1) σ = stress, psi
- (2) $\bar{\epsilon}$ = strain, in./in.
- (3) $\bar{\epsilon}$ upper, lower = 95-percent confidence limits
- (4) Math models for regression analysis:
 - (a) $\ln \bar{\epsilon} = \ln A + B \ln \sigma$
 - (b) $\bar{\epsilon} = \ln A + B \ln \sigma$
 - (c) $\ln \bar{\epsilon} = \ln A + B \sigma$

Table LXXVII SUMMARY OF SHEAR STRAIN CONFIDENCE LIMITS AT -270°F

Material	Property	Load Levels							Math Model (4)
		#1	#2	#3	#4	#5	#6		
RTV-560	σ	(5)							
	$\bar{\epsilon}$								
	ϵ upper lower								
SLA-561	σ	(5)							
	$\bar{\epsilon}$								
	ϵ upper lower								
DC 93-046	σ	(5)							
	$\bar{\epsilon}$								
	ϵ upper lower								
RTV-560/RL-1973	σ	40	70	100	150	200	400	700	(a)
	$\bar{\epsilon}$	0.150	0.164	0.175	0.187	0.196	0.221	0.243	
	ϵ upper	0.214	0.221	0.225	0.233	0.242	0.283	0.331	
	ϵ lower	0.085	0.108	0.124	0.141	0.151	0.159	0.155	

Notes:

- (1) σ = stress, psi
- (2) $\bar{\epsilon}$ = strain, in./in.
- (3) $\bar{\epsilon}$ upper, lower = 95-percent confidence limits
- (4) Math models for regression analysis:
 - (a) $\ln \bar{\epsilon} = \ln A + B \ln \sigma$
 - (b) $\bar{\epsilon} = \ln A + B \ln \sigma$
 - (c) $\ln \bar{\epsilon} = \ln A + B\sigma$
- (5) Regression analysis not conducted

Table LXXVIII SUMMARY OF SHEAR STRAIN CONFIDENCE LIMITS AT -200°F

Material	Property	Load Levels						Meth Model (4)
		#1	#2	#3	#4	#5	#6	
RTV-560	σ	(5)						
	$\bar{\epsilon}$							
	ϵ upper lower							
SLA-561	σ	(5)						
	$\bar{\epsilon}$							
	ϵ upper lower							
DC 93-046	σ	(5)						
	$\bar{\epsilon}$							
	ϵ upper lower							
RTV-560/RL-1973	σ	40	80	100	150	200	400	600
	$\bar{\epsilon}$	0.235	0.262	0.272	0.290	0.303	0.338	0.361
	ϵ	0.260	0.282	0.289	0.305	0.318	0.360	0.390
	ϵ upper							
	ϵ lower							
		0.210	0.243	0.254	0.274	0.288	0.317	0.332

Notes:

- (1) σ = stress, psi
- (2) $\bar{\epsilon}$ = strain, in./in.
- (3) $\bar{\epsilon}$ upper, lower = 95-percent confidence limits
- (4) Math models for regression analysis:
 - (a) $\ln \bar{\epsilon} = \ln A + B \ln \sigma$
 - (b) $\bar{\epsilon} = \ln A + B \ln \sigma$
 - (c) $\ln \bar{\epsilon} = \ln A + B \sigma$
- (5) Regression analysis not conducted

Table LXXIX SUMMARY OF SHEAR STRAIN CONFIDENCE LIMITS AT -175°F

Material	Property	Load Levels						Math Model (4)
		#1	#2	#3	#4	#5	#6	
RTV-560	σ	50	100	200	300	400	500	700
	$\bar{\epsilon}$	0.027	0.217	0.408	0.520	0.598	0.660	0.752
	ϵ upper	0.221	0.351	0.505	0.618	0.709	0.785	0.903
	ϵ lower	-0.168	0.084	0.311	0.421	0.488	0.535	0.601
SLA-561	σ	(5)						
	ϵ							
	ϵ upper							
	ϵ lower							
DC 93-046	σ	(5)						
	ϵ							
	ϵ upper							
	ϵ lower							
RTV-560/RL-1973	σ	40	80	100	150	200	400	600
	$\bar{\epsilon}$	0.058	0.130	0.169	0.270	0.377	0.842	1.35
	ϵ upper	0.075	0.156	0.198	0.308	0.430	1.013	1.69
	ϵ lower	0.042	0.105	0.140	0.232	0.324	0.671	1.00

Notes:

- (1) σ = stress, psi
- (2) $\bar{\epsilon}$ = strain, in./in.
- (3) $\bar{\epsilon}$ upper, lower = 95-percent confidence limits
- (4) Math models for regression analysis:
 - (a) $\ln \bar{\epsilon} = \ln A + B \ln \sigma$
 - (b) $\bar{\epsilon} = \ln A + B \ln \sigma$
 - (c) $\ln \bar{\epsilon} = \ln A + B \sigma$
- (5) Regression analysis not conducted.

Table LXXX SUMMARY OF SHEAR STRAIN CONFIDENCE LIMITS AT -150°F

Material	Property	Load Levels								Math Model (4)
		#1	#2	#3	#4	#5	#6			
RTV-560	σ	50	100	200	500	700	800			
	$\bar{\epsilon}$	0.474	0.686	0.994	1.62	1.94	2.09			1.000
	ϵ upper	0.495	0.708	1.02	1.66	2.00	2.15			2.35
	ϵ lower	0.453	0.664	0.970	1.58	1.89	2.03			2.43
SLA-561	σ	50	100	200	300	380				
	$\bar{\epsilon}$	0.815	1.22	1.83	2.31	2.65				(a)
	ϵ upper	0.890	1.29	1.92	2.46	2.86				
	ϵ lower	0.740	1.15	1.73	2.16	2.45				
DC 93-046	σ	(5)								
	$\bar{\epsilon}$									
	ϵ upper									
	ϵ lower									
RTV-560/RL-1973	σ	50	100	150	200	250	300			
	$\bar{\epsilon}$	0.617	1.00	1.33	1.62	1.90	2.16			(a)
	ϵ upper	0.667	1.05	1.38	1.70	2.00	2.29			
	ϵ lower	0.567	0.954	1.28	1.55	1.80	2.02			

Notes:

- (1) σ = stress, psi
- (2) $\bar{\epsilon}$ = strain, in./in.
- (3) ϵ upper, lower = 95-percent confidence limits
- (4) Math models for regression analysis:
 - (a) $\ln \bar{\epsilon} = \ln A + B \ln \sigma$
 - (b) $\bar{\epsilon} = \ln A + B \ln \sigma$
 - (c) $\ln \bar{\epsilon} = \ln A + B \sigma$
- (5) Regression analysis not conducted

Table LXXXI SUMMARY OF SHEAR STRAIN CONFIDENCE LIMITS AT -65°F

Material	Property	Load Levels						Math Model (4)
		#1	#2	#3	#4	#5	#6	
RTV-560	σ	50	100	200	300	400	500	600
	$\bar{\epsilon}$	0.723	1.00	1.39	1.69	1.93	2.15	2.34
	ϵ upper	0.745	1.02	1.41	1.71	1.97	2.19	2.40
	ϵ lower	0.702	0.984	1.37	1.66	1.90	2.10	2.29
SLA-561	σ	20	50	75	80			
	$\bar{\epsilon}$	0.358	0.863	1.28	1.36			
	ϵ upper	0.374	0.882	1.31	1.40			
	ϵ lower	0.342	0.844	1.24	1.32			
DC 93-046	σ	50	100	200	300	400	500	600
	$\bar{\epsilon}$	0.938	1.19	1.50	1.72	1.89	2.04	2.17
	ϵ upper	1.11	1.34	1.64	1.89	2.11	2.30	2.48
	ϵ lower	0.763	1.03	1.35	1.55	1.68	1.78	1.86
RTV-560/RL-1973	σ	20	25	50	70	100	150	
	$\bar{\epsilon}$	0.880	0.983	1.39	1.64	1.95	2.39	
	ϵ upper	0.910	1.01	1.41	1.66	1.99	2.45	
	ϵ lower	0.851	0.955	1.36	1.61	1.92	2.33	

Notes:

- (1) σ = stress, psi
- (2) $\bar{\epsilon}$ = strain, in./in.
- (3) $\bar{\epsilon}$ upper, lower = 95-percent confidence limits
- (4) Math models for regression analysis:
 - (a) $\ln \bar{\epsilon} = \ln A + B \ln \sigma$
 - (b) $\bar{\epsilon} = \ln A + B \ln \sigma$
 - (c) $\ln \bar{\epsilon} = \ln A + B \sigma$

Table LXXXI | SUMMARY OF SHEAR STRAIN CONFIDENCE LIMITS AT 80°F

Material	Property	Load Levels						Math Model (4)
		#1	#2	#3	#4	#5	#6	
RTV-560	σ	20	50	100	140	200	300	(a)
	$\bar{\epsilon}$	0.442	0.733	1.08	1.29	1.58	1.97	
	ϵ_{upper}	0.524	0.821	1.17	1.42	1.75	2.24	
	ϵ_{lower}	0.360	0.645	0.975	1.17	1.40	1.70	
SLA-561	σ	20	40	50	60			(a)
	$\bar{\epsilon}$	0.317	0.685	0.878	1.07			
	ϵ_{upper}	0.350	0.728	0.943	1.17			
	ϵ_{lower}	0.284	0.642	0.813	0.979			
DC 93-046	σ	20	50	100	150	200		(a)
	$\bar{\epsilon}$	0.489	1.13	2.12	3.07	3.98		
	ϵ_{upper}	0.545	1.20	2.25	3.31	4.34		
	ϵ_{lower}	0.434	1.05	1.99	2.83	3.63		
RTV-560/RL-1973	σ	10	20	30	40	50	70	(a)
	$\bar{\epsilon}$	0.494	0.772	1.00	1.21	1.39	1.73	
	ϵ_{upper}	0.512	0.789	1.02	1.23	1.42	1.77	
	ϵ_{lower}	0.477	0.755	0.985	1.19	1.37	1.69	

- Notes:
- (1) σ = stress, psi
 - (2) $\bar{\epsilon}$ = strain, in./in.
 - (3) $\bar{\epsilon}$ upper, lower = 95-percent confidence limits
 - (4) Math models for regression analysis:
 - (a) $\ln \bar{\epsilon} = \ln A + B \ln \sigma$
 - (b) $\bar{\epsilon} = \ln A + B \ln \sigma$
 - (c) $\ln \bar{\epsilon} = \ln A + B \sigma$

Table LXXXIII SUMMARY OF SHEAR STRAIN CONFIDENCE LIMITS AT 300°F

Material	Property	Load Levels										Math Model (4)	
		#1	#2	#3	#4	#5	#6						
RTV-560	σ	25	50	75	100								(a)
	$\tilde{\epsilon}$	0.325	0.545	0.736	0.911								
	ϵ upper lower	0.367 0.283	0.586 0.504	0.794 0.678	1.00 0.818								
SLA-561	σ	20	40	50	60								(a)
	$\tilde{\epsilon}$	0.467	0.766	0.899	1.02								
	ϵ upper lower	0.572 0.362	0.871 0.661	1.04 0.759	1.21 0.836								
DC 93-046	σ	20	50	75	90								(a)
	$\tilde{\epsilon}$	0.764	1.87	2.78	3.32								
	ϵ upper lower	0.923 0.605	2.09 1.65	3.19 2.37	3.88 2.76								
RTV-560/RL-1973	σ	5	10	15	20	30	40	50					(a)
	$\tilde{\epsilon}$.305	.495	.657	.804	1.07	1.31	1.53					
	ϵ upper lower	.314 .295	.505 .485	.666 .648	.813 .795	1.08 1.06	1.32 1.29	1.55 1.50					

Notes:

- (1) σ = stress, psi
- (2) $\tilde{\epsilon}$ = strain, in./in.
- (3) ϵ upper, lower = 95-percent confidence limits
- (4) Math models for regression analysis:
 - (a) $\ln \tilde{\epsilon} = \ln A + B \ln \sigma$
 - (b) $\tilde{\epsilon} = \ln A + B \ln \sigma$
 - (c) $\ln \tilde{\epsilon} = \ln A + B \sigma$

Table LXXXIV SUMMARY OF SHEAR STRAIN CONFIDENCE LIMITS AT 350°F

Material	Property	Load Levels						Math Model (4)
		#1	#2	#3	#4	#5	#6	
RTV-560	σ	25	50	75	100	120		(a)
	ϵ	0.232	0.442	0.642	0.839	0.993		
	ϵ_{upper}	0.267	0.482	0.695	0.924	1.11		
	ϵ_{lower}	0.197	0.402	0.589	0.754	0.877		
SLA-561	σ	20	30	40	50			(a)
	ϵ	0.452	0.603	0.741	0.869			
	ϵ_{upper}	0.483	0.629	0.774	0.918			
	ϵ_{lower}	0.421	0.577	0.708	0.819			
DC 93-046	σ	20	40	50	60			(a)
	ϵ	0.803	1.75	2.25	2.77			
	ϵ_{upper}	0.956	1.96	2.54	3.19			
	ϵ_{lower}	0.650	1.55	1.96	2.34			
RTV-560/RL-1973	σ	10	15	20	30	40	50	(a)
	ϵ	0.617	0.777	0.916	1.154	1.360	1.544	
	ϵ_{upper}	0.654	0.809	0.947	1.199	1.429	1.640	
	ϵ_{lower}	0.581	0.746	0.885	1.109	1.291	1.449	

Notes:

- (1) σ = stress, psi
- (2) ϵ = strain, in./in.
- (3) ϵ_{upper} , lower = 95-percent confidence limits
- (4) Math models for regression analysis:
 - (a) $\ln \bar{\epsilon} = \ln A + B \ln \sigma$
 - (b) $\bar{\epsilon} = \ln A + B \ln \sigma$
 - (c) $\ln \bar{\epsilon} = \ln A + B \sigma$

A P P E N D I X V

SUMMARY OF STRENGTH CONFIDENCE LIMITS FOR BEST FITTING REGRESSION EQUATION TO STRENGTH-TEMPERATURE DATA

The strength confidence limits for discrete values of temperature corresponding to the best-fitting equation to strength-temperature data for each material are summarized in Tables LXXXV and LXXXVI for flatwise tension and overlap shear tests, respectively.

Table LXXXV SUMMARY OF TENSILE STRENGTH CONFIDENCE LIMITS AND STRENGTH ALLOWABLES

Material	Temp °F	Ultimate Strength Values/Allowables (psi)									
		-200	-175	-150	-65	80	300	350			
RTV-560	σ upper	1,707	999	585	376	287	191	174			
	σ lower	3,370	1,993	1,224	404	301	201	184			
	B' allow.	864	501	280	351	274	181	164			
	A' allow.	625	363	203	313	244	161	146			
		482	280	156	287	224	148	132			
SLA-561	σ upper	5,046	1,353	363	200	161	115	107			
	σ lower	15,514	4,230	1,226	247	184	135	128			
	B' allow.	1,641	433	107	162	140	98	89			
	A' allow.	478	126	31	114	99	69	63			
		177	47	11	89	77	54	49			
DC 93-046	σ upper	3,348	2,062	1,270	208	123	56	46			
	σ lower	4,922	2,797	1,661	317	162	77	68			
	B' allow.	2,277	1,520	971	136	93	40	32			
	A' allow.	1,065	710	454	65	45	19	15			
		613	409	261	38	26	11	9			
RTV-560/RL-1973	σ upper	512	401	314	158	104	55	48			
	σ lower	591	468	374	175	112	59	53			
	B' allow.	433	334	254	141	96	51	43			
	A' allow.	292	224	168	108	75	39	33			
		230	178	130	94	66	34	29			

Notes:

- (1) σ = A exp (BT) where T is in degrees R
- (2) σ upper, lower = 95-percent confidence limits
- (3) A', B' allow. = allowable strength values

Table LXXXVI SUMMARY OF SHEAR STRENGTH CONFIDENCE LIMITS AND STRENGTH ALLOWABLES

Material	Temp °F	Ultimate Strength Values/Allowables (psi)						
		-200	-175	-150	-65	80	300	350
RTV-560	σ upper	906	819	741	525	292	120	98
	σ lower	1,102	985	882	608	337	151	126
	B' allow.	745	681	622	453	254	96	76
	A' allow.	446	408	373	272	152	57	46
SLA-561	σ upper	320	292	267	195	109	41	33
	σ lower	3,985	1,229	379	73	65	53	51
	B' allow.	4,387	1,355	420	85	71	60	58
	A' allow.	3,620	1,115	341	63	59	48	45
DC 93-046	σ upper	3,459	1,065	326	37	35	28	26
	σ lower	3,334	1,027	314	25	23	19	18
	B' allow.	1,158	1,010	880	551	248	74	56
	A' allow.	1,369	1,182	1,021	625	280	90	70
RTV-560/RL-1973	σ upper	980	862	758	487	220	61	45
	σ lower	633	557	489	314	142	39	29
	B' allow.	476	419	368	236	107	30	22
	A' allow.	589	407	281	139	91	47	41
RTV-560/RL-1973	σ upper	622	426	301	142	93	48	42
	σ lower	546	388	261	136	89	46	40
	B' allow.	465	334	222	129	85	44	38
	A' allow.	423	306	202	126	83	43	37

Notes:

- (1) σ = A exp (BT) where T is in degrees R
- (2) σ upper, lower = 95-percent confidence limits
- (3) A', B' allow. = allowable strength values

A P P E N D I X V I

TENSILE MODULUS, POISSON'S RATIO, LEAST SQUARE COMPUTATIONS

METHOD FOR COMPUTING MATERIAL CONSTANTS

The test specimen is marked with 0.02-inch-diameter dots applied with a template at the corners of a 5-by 2-inch rectangle; then, a series of increasing loads were applied. Photographs were taken of the dots at these various loads. This report concerns the analysis of those photographs.

The (X, Y) coordinates of each of the dots were measured on the Oscillogram Analyzer and Reader (OSCAR) interfaced to a Hewlett-Packard model 2116A digital computer. Digital counts were converted from the various positions of potentiometers in each of the horizontal and vertical axes. The program provides for calibration and scaling of these counts to inches.

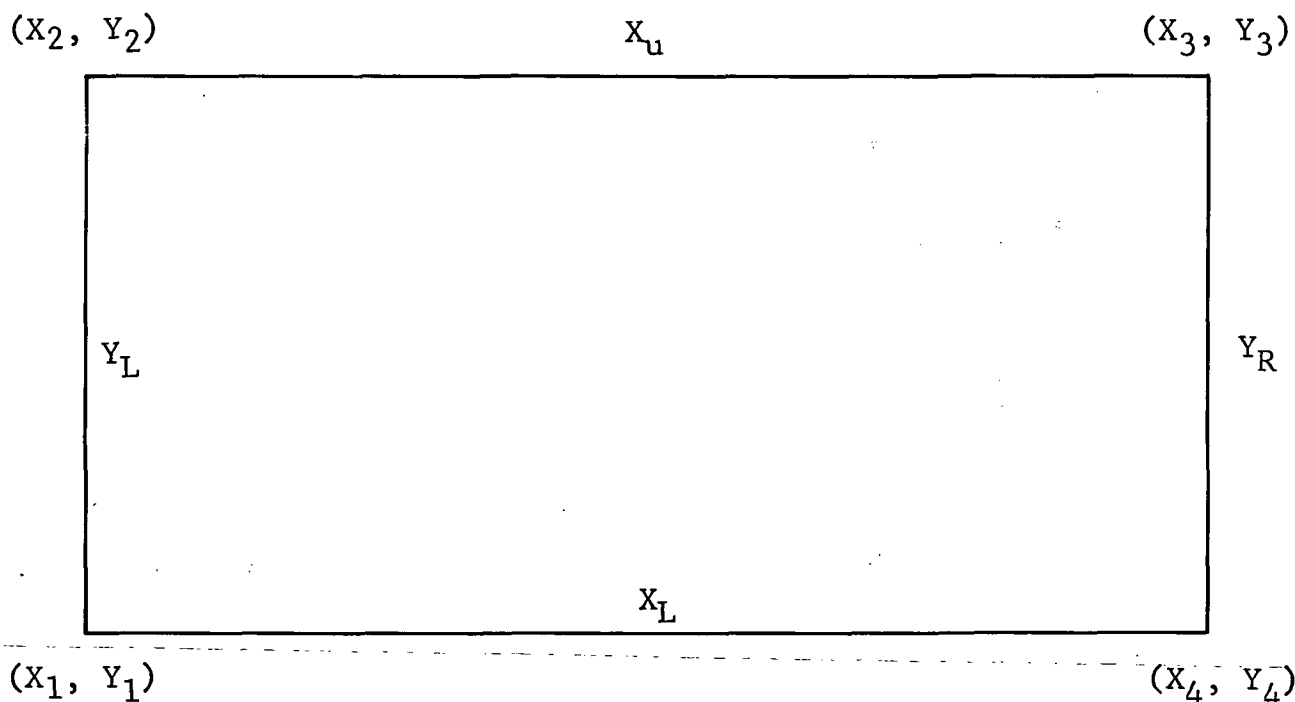


Figure 126 Test Area for Tensile Modulus and Poisson's Ratio

As shown in Figure 126, the four lengths of the quadrilateral are determined as follows:

$$Y_L = \sqrt{(X_2 - X_1)^2 + (Y_2 - Y_1)^2} \quad (\text{Left})$$

$$X_u = \sqrt{(X_3 - X_2)^2 + (Y_3 - Y_2)^2} \quad (\text{Upper})$$

$$Y_R = \sqrt{(X_3 - X_4)^2 + (Y_3 - Y_4)^2} \quad (\text{Right})$$

$$X_L = \sqrt{(X_4 - X_1)^2 + (Y_4 - Y_1)^2} \quad (\text{Lower})$$

The first measurement was taken at no load, and the four original lengths X_{L0} , X_{u0} , Y_{L0} , Y_{R0} were determined. At any load, the two axial (A) strains and the two transverse (T) strains were computed from

$$A_L = \frac{X_L - X_{L0}}{X_{L0}}$$

$$A_u = \frac{X_u - X_{u0}}{X_{u0}}$$

$$T_L = \frac{Y_L - Y_{L0}}{Y_{L0}}$$

$$T_R = \frac{Y_R - Y_{R0}}{Y_{R0}}$$

Then, the average axial and average transverse strains were calculated by

$$A = \frac{1}{2} (A_L + A_u)$$

and

$$T = \frac{1}{2} (T_L + T_R)$$

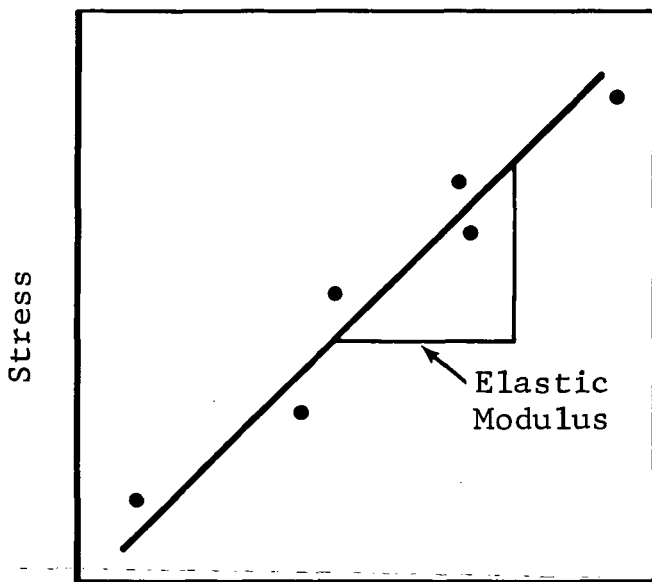
The original cross-sectional area was entered into the computer from the keyboard, as was each load P_i . Then, for each load,

$$\text{STRESS}_i = \frac{P_i}{\text{AREA}}$$

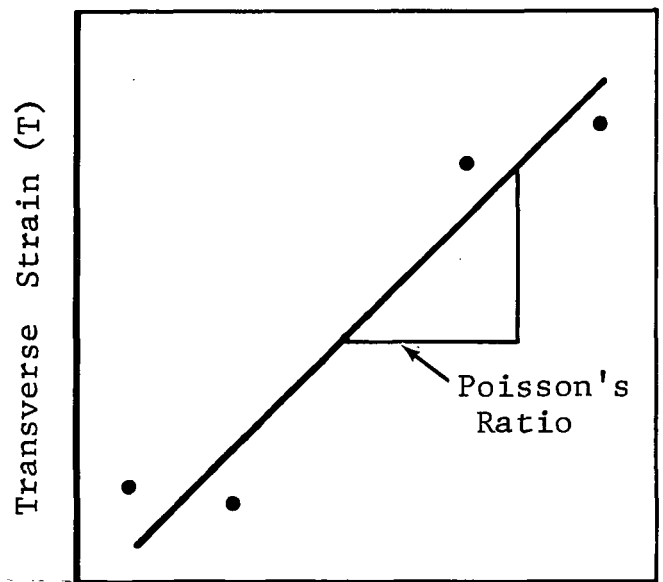
$$\text{ELASTIC MODULUS} = \frac{\text{STRESS}_i}{A_i}$$

$$\text{POISSON'S RATIO} = \left| \frac{T_i}{A_i} \right|$$

The computer then determined the least squares, best-fit straight line from the points STRESS_i versus A_i (Figure 127). The slope of this line is the least squares elastic modulus. The slope of the T_i versus A_i line is the least squares Poisson's ratio.



Axial Strain (A)



Axial Strain (A)

Figure 127 Least Squares Elastic Modulus and Poisson's Ratio

The least squares line for N points Y_i versus X_i is the line such that the mean square error between the line and the points is a minimum. It is described completely by the Y-intercept and the slope.

$$Y_0 = \frac{\sum Y_i \sum X_i^2 - \sum X_i Y_i \sum X_i}{N \sum X_i^2 - (\sum X_i)^2}$$

and

$$\text{SLOPE} = \frac{N \sum X_i Y_i - \sum X_i \sum Y_i}{N \sum X_i^2 - (\sum X_i)^2}$$

where all summations are $i = 1$ to N .

R E F E R E N C E S

1. S. Timoshenko, et al., Theory of Elasticity, Second Ed., Mc Graw-Hill, N.Y., (1951).
2. "Facts About Neoprene for the Engineer," Elastomers Div., E. I. Dupont de Nemours and Company, Inc., No. A-8746-65M-12-54m10553, Wilmington, Delaware, December 1954.
3. K. E. Polmanteer, et al., "Low Temperature Behavior of Silicone and Organic Rubber," Industrial and Engineering Chemistry, Vol. 44, p. 1576, July 1952.
4. J. D. Helmer and K. E. Polmanteer, "Supercooling of Polydimethylsiloxane," Journal of Applied Polymer Sc., Vol. 13, pp. 2113-2118. (1969).
5. H. Mark and A. V. Tobolsky, Physical Chemistry of High Polymeric Systems, Second Edition, Interscience Publishers, Inc., N.Y., pp. 347-348, (1950).

Page Intentionally Left Blank